

BENDING FEEDBACK CONTROL FINAL REPORT

GPO PRICE \$ _____

CFSTI PRICE(S) \$ _____

DOUGLAS REPORT **JUNE 1966**
DAC-59275

Hard copy (HC) _____

Microfiche (MF) _____

653 July 65

FACILITY FORM 602

N66 32120

(ACCESSION NUMBER)

304

(PAGES)

OK-76557

(NASA CR OR TMX OR AD NUMBER)

(THRU)

(CODE)

10

(CATEGORY)

BENDING FEEDBACK CONTROL FINAL REPORT

JUNE 1966
DOUGLAS REPORT DAC-59275

PREPARED BY:
W.K. WAYMEYER,
PROGRAM DIRECTOR
I.R. BLACKBURN,
PRINCIPAL INVESTIGATOR
M.G. CURRIE
R.T. STEFANI
ADVANCE FLIGHT MECHANICS DEPARTMENT



APPROVED BY:
J.C. WALKER
ACTING CHIEF ENGINEER
ADVANCE FLIGHT MECHANICS DEPARTMENT

ABSTRACT

32120

The results of a 12-month study of the application of quadratic optimal control, least squares state, and parameter estimation to the stability and control problem of the flexible launch vehicle are presented. The feasibility of using optimal control on a few states of a high-order system to control the damping in the bending modes is demonstrated. State estimation (Kalman) filters are shown to be capable of stabilizing the higher-order bending modes. Combined state and parameter estimation is shown to be straightforward, although rather complex in mechanization. A set of control gains and filters is derived for a particular model vehicle provided by NASA-MFSC. This model, based on the general characteristics of Saturn V, is specifically tailored to make it difficult to stabilize. It is shown that the methods described can stabilize this model at three sample flight conditions which represent the extremes in the environment. A set of design guides, or principles, for the application of these techniques is presented. It is suggested that these techniques raise the capacity of the control system designer to the consideration of better and higher-order systems than have been readily tractable heretofore.

author

FOREWORD

The work was conducted under Contract NAS8-20087. The study directors for NASA-MSFC were R. Lewis and B. Davis, Control Theory Section, R-AERO-D, Marshall Space Flight Center, Huntsville, Alabama. It was administered under the direction of R. W. Hallet, Jr., Director of Research and Development, Douglas Missile and Space Systems Division. Dr. D. R. Vaughan and (later) W. K. Waymeyer were the study directors and T. R. Blackburn was the principal investigator. The following personnel contributed substantially to the study effort.

C. G. Cheronis
M. G. Currie
Dr. J. M. Mendel
W. C. Nowak
R. J. Stefani
Dr. A. R. Stubberud

BLANK PAGE

CONTENTS

Section 1	SUMMARY	1
Section 2	INTRODUCTION	3
	2.1 Scope of Work	3
	2.2 Report Format	4
	2.3 Related Work in the Literature	5
	2.4 Background Theory	6
	2.5 Methods of Investigation	10
Section 3	SYSTEM DEFINITION	13
	3.1 System Equations	13
	3.2 System Parameters	20
	3.3 Low Order Study Models	26
Section 4	QUADRATIC OPTIMAL CONTROL	37
	4.1 Basic Approach	38
	4.2 The Optimal Control Problem, Basic Equations	39
	4.3 Root Location	41
	4.4 Selection of the Cost Ratio	44
	4.5 Cost Selection for Rigid Body States	44
	4.6 Cost Selection for Body Bending States	48
	4.7 Optimal Control Designs	49
Section 5	STATE ESTIMATION	57
	5.1 System Observability	57
	5.2 Some Useful Theorems	59
	5.3 A Small System Study	63
	5.4 Filter Dimension Reduction	74
	5.5 Conventional Analysis Techniques	87
	5.6 Filter Development Experiments Performed	95

Section 6	COMBINED ESTIMATION	139
6.1	Introduction	139
6.2	Combined Estimation Via Continuous Kalman Filtering	140
6.3	Simulation of Combined Estimation; Sixth-Order Plant with Two Unknown Parameters	153
Section 7	COMPUTATIONAL PROBLEMS	169
7.1	Solution of the Riccati Equation	169
7.2	System Pole-Zero Solution	174
Section 8	CONCLUSIONS	179
8.1	Design Requirements	179
8.2	Response to Commands	180
8.3	Response to Winds	180
8.4	Stability	181
8.5	Simplicity	182
8.6	Complexity of Plant	182
8.7	Integration	183
Section 9	SYMBOLS	185
Section 10	REFERENCES	191
Appendix A	COMPUTER ROUTINES	193
Appendix B	21-DIMENSION SYSTEM MATRIXES	231

FIGURES

2-1	Closed-Loop System Block Diagram	9
2-2	System Guidance Command Response	9
3-1	F Matrix	17
3-2	Apr Matrix	17
3-3	C Matrix and D Matrix	19
4-1	Closed-Loop Poles Opposed to Cost for Rigid Body States θ and $\dot{\theta}$ with Zero Cost on $\dot{\theta}$, Increasing Cost on θ	45
4-2	Closed-Loop Poles Opposed to Cost for Rigid Body States θ and $\dot{\theta}$, Constant Cost on $\dot{\theta}$, Increasing Cost on θ	46
4-3	Closed-Loop Poles Opposed to Cost for Body Bending States \dot{A} and A , with Zero Cost on A , Increasing Cost on \dot{A}	50
4-4	Closed-Loop Poles Opposed to Cost for Body Bending States on A and \dot{A} , with Increasing Cost on A	50
4-5	Root Square Locus of System Roots for System 4-1	53
5-1	System 4-1, Symbolic Version	57
5-2	System Reduction by Theorem 1	61
5-3	4-D Study System	63
5-4	Kalman Gain Transient Solutions	64
5-5	Steady-State Kalman Gains Versus Q/R	65
5-6	Plant Filter Combination Rearranged	66
5-7	Body Response Curves, System 4-2	67
5-8	Sensor Bode Responses to Commands	68
5-9	Kalman Filter Bode Gains	69

5-10	Low-Noise System Bode Gains	70
5-11	High-Noise System Bode Gains	71
5-12	Systems Block Diagram Rearranged for Root Locus Analysis	72
5-13	Study System Root Locus Plots	73
5-14	System Block Diagram with Reduced Order Filter	75
5-15	Kalman Filter with High-Order Steady- State Assumption	77
5-16	System Block Diagram, $A_{21} = A_{12} = 0$	78
5-17	Block Diagram of States To Be Rejected	79
5-18	Equivalent Discrete System Block Diagram	81
5-19	Closed-Loop System	88
5-20	Modified Closed-Loop System	89
5-21	Pole-Zero Printout Format	91
5-22	Nyquist Diagram--Ideal System	92
5-23	Nyquist Diagram--Suboptimal System	94
5-24	Analysis Method--Block Diagram	96
5-25	Attitude Gyro	98
5-26	Rate Gyro Response to 1.5×10^4 Wind	98
5-27	Roots, Plant 6-4 with Fourth-Order Filter 4-3	104
5-28	System Roots for Varying Noise Level	108
5-29	Attitude Response to a Step Wind Input	109
5-30	Engine Deflection Response to a Step Wind Input	110
5-31	Parameter Mismatch Stability ($C = 10^{-5}$)	111
5-32	Parameter Mismatch Stability ($C = 10^{-3}$)	112
5-33	Parameter Mismatch Stability ($C = 10^{-1}$)	113
5-34	Parameter Mismatch Stability ($C = 10$)	114
5-35	System Roots (88 Sec, Cases 4, 5, and 6)	119
5-36	System Roots (150 Sec, Cases 4, 5, and 6)	120
5-37	System Roots (24 Sec)	121
5-38	System Roots (88 Sec, Cases 1, 2, and 3)	122
5-39	System Roots (150 Sec, Cases 1, 2, and 3)	123

5-40	Transient Responses (Filter Model 6-4, $C = 10^2$)	124
5-41	Transient Responses (Filter Model 6-4, $C = 10^0$)	125
5-42	Transient Responses (Filter Model 6-4, $C = 10^{-2}$)	126
5-43	Parameter Mismatch Stability	127
5-44	Parameter Mismatch Stability	128
5-45	Transient Responses (Filter Model 6-5, $C = 10^0$)	129
5-46	Transient Responses (Filter Model 6-5, $C = 10^2$)	130
5-47	Parameter Mismatch Stability	131
5-48	Parameter Mismatch Stability	132
5-49	Transient Responses (Filter Model 6-6, $C = 10^2$)	133
5-50	Parameter Mismatch Stability	134
5-51	Parameter Mismatch Stability	135
5-52	Colored Noise Stability	138
6-1	Block Diagram for Kalman Filter for Adjoined State	152
6-2	Block Diagram for Solving Matrix Riccati Equation for Covariance of Estimation Error	152
6-3	Block Diagram for Simulation of Combined Estimation Equations	153
6-4	Nominal Q_a , Except $Q_{55} = 2.5 \times 10^7$ and $Q_{66} = 2.85 \times 10^8$, $R = 10^{-2}$, S1 Sinusoidal with 10-sec Period and 10% of Nominal Amplitude	159
6-5	Nominal Q_a , Except $Q_{55} = 2.5 \times 10^7$ and $Q_{66} = 2.85 \times 10^8$, $R = 10^{-1}$, S1 Sinusoidal with 10-sec Period and 10% of Nominal Amplitude	160
6-6	Nominal Q_a , Except $Q_{55} = Q_{66} = 0$, $R 10^{-1}$, S1 Constant	161
6-7	Nominal Q_a , Except $Q_{55} = Q_{66} = 0$, $R 10^{-1}$, S1 Constant, and No 3rd Bending Mode in Plant	162

6-8	Nominal Q_a , Except $Q_{55} = 2.5 \times 10^7$ and $Q_{66} = 2.85 \times 10^8$, $R = 10^{-1}$, S1 Sinusoidal with 10-sec Period and 10% of Nominal Amplitude, and No 3rd Bending Mode in Plant	163
6-9	$Q_{55} = 5 \times 10^7$, $Q_{66} = 4 \times 10^6$, All Other Entries of Q_a Are Zero, $R = 10^{-3}$, S1 Constant, No 3rd Bending Mode in Plant	165
6-10	$Q_{55} = 5 \times 10^7$, $Q_{66} = 4 \times 10^6$, All Other Entries of Q_a Are Zero, $R = 10^{-3}$, S1 Constant, Initial Condition on Estimate of S1 is 90% S1, and No 3rd Bending Mode in Plant	166
6-11	$Q_{55} = 5 \times 10^7$, $Q_{66} = 4 \times 10^6$, All Other Entries of Q_a Are Zero, $R = 10^{-3}$, S1 Constant, Initial Condition on Estimate of S1 is 90% S1, and No 1st Bending Mode in Plant	167

TABLES

3-1	System Parameters	22
3-2	Plant Poles	25
4-1	Optimal Control Gains and Closed-Loop Poles for Systems 4-1, 4-2, 4-3, 6-4, 6-5, and 6-6	52
5-1	Wind Response Kalman Gain Values	100
5-2	System Roots, Filter Designed on Disturbance Transfer Function = ϕ/V_w	101
5-3	Kalman Gains, Command Response	102
5-4	System Roots, Filter Designs Based on Command Response	103
5-5	Kalman Gains, 6-D Filter	105
5-6	System Roots, 6-D Filter	106
5-7	Max-Q and Burnout, 6-D Kalman Gains	115
5-8	Kalman Gains, Correlated Noise, 4-D Filter, $t = 24$ -Sec Plant	117
5-9	Kalman Gains, Correlated Noise, 6-D Filter	118
5-10	Colored Noise Kalman Gains	137
A-1	Documentation of Term Definitions Used in Program H266	199
A-2	Definition of Symbols Not Defined in Program H266 List	203
A-3	Program Matrixes	204

BLANK PAGE

Section 1 SUMMARY

This report presents the results of study that has demonstrated the feasibility of a design approach for launch vehicle stabilization and control systems. This approach combines the method of quadratic optimal control and least square estimation, and was applied particularly to a launch vehicle similar to Saturn V.

An experimental descriptive model (Model No. 2) with low-frequency bending modes was furnished by NASA-Marshall Space Flight Center (MSFC). This model exhibits lateral translation, rotation, three sloshing modes, four bending modes, and a third-order actuator. A systematic method for developing the optimal control cost coefficients is used to develop a low-order control law. Several methods for the design of the satisfactory low-order Kalman filter are presented. The design can be carried out by following the design procedure stated in Section 8.

The resultant design, demonstrating feasibility with Model No. 2 (Figures 35 through 41) incorporates sixth-order filter-control combinations. Stability, excellent bending mode vibration suppression, good insensitivity to parameter variation, and response characteristics are shown.

The necessity for adaptivity or parameter identification was not shown, but parameter identification was accomplished. The first bending mode frequency and gain (or influence coefficient) were successfully estimated, using a parameter estimation augmentation to the Kalman filter. This was accomplished using a lower-order model in the filter than in the approximation to Model No. 2.

Demonstration of the feasibility of this method is significant in three ways:

1. The method extends the conceptual range of the designer toward the synthesis of higher-dimensional optimal control systems which strain the more conventional intuitive analysis procedures.
2. The system synthesis need not be carried to full plant-dimensioned optimality. The resultant system can be mechanized (if not synthesized) in relatively conventional ways.
3. The method provides for escalation to tighter and hence more sophisticated adaptive control systems, should the need exist.

Section 2 INTRODUCTION

2.1 SCOPE OF WORK

This report summarizes the work performed and the conclusions drawn under National Aeronautics and Space Administration Contract NAS8-20087, Bending Feedback Control. The contract period was 25 June 1965 to 25 June 1966. The fundamental objectives of this research have been to develop methods for the design of autopilots for rocket vehicles similar to the Saturn V and to demonstrate their feasibility.

The following paragraph is quoted verbatim from the contract and constitutes the entire Statement of Work.

"B. STATEMENT OF WORK

The control problem for study is the "stability problem" or the bending feedback control problem. A model vehicle of the Saturn class will be furnished as a study model. This model exhibits severe control characteristics. The rigid body performance specifications may be such that control frequency to fundamental bending mode frequency is a ratio of 1:2. Assumptions for the study may be made (1) that the bending mode data is virtually unknown except for the range of the variable parameters or (2) that the bending mode data is accurate to within only ± 10 percent. These two assumptions specify distinctions which must be an integral part of the control design philosophy or ground rules. In the first case in-flight identification might be required as well as a control system which readily adapts to the changing flight conditions; in the second case, identification and/or a nonconventional control system might be necessary. The solution may mean active control of the modes. The latest control theory techniques may be employed in searching for a solution to the problem, or it may be desirable to use a conventional

engineering approach. Although the study will be analytical, the control system proposed must lead to a design which can eventually be mechanized in the near future."

Douglas formally proposed and was thereby committed to attack the problem with a combination of quadratic optimal control and Kalman filter theory. The scope of subsequent research has been limited to this combination.

In early conversations with R. Lewis and M. Rheinfurth of NASA-MSFC, the following significant additional information was obtained:

1. MSFC was interested in suppressing bending mode motion for pilot comfort and reduced structural stress.
2. They were interested in Kalman filters but were concerned that their order might be too large for them to be mechanized as airborne equipment.
3. Assumption (a) of the Work Statement, assuming no knowledge of the bending mode shapes, was somewhat excessive, because one can guess, from experience, their approximate shape and frequency.

2.2 REPORT FORMAT

The remainder of this section is devoted to a discussion of closely related control work on launch vehicles (subsection 2.3), introductions to the concepts of quadratic optimal control and Kalman filtering (subsection 2.4), and the methods of analysis used in the study (subsection 2.5).

The nature of the design approach has led to (1) development of the optimal control gains based on the defined low-order linear system, (2) development of a filter based on the same order system, and (3) the study of parameter estimation. Sections 3, 4, 5, and 6 are therefore arranged in this order. Each section is somewhat dependent on the preceding sections but relatively independent of those following. Section 3 describes the interpretations made of the mode system furnished for analysis by NAS-MSFC (Model Specification No. 2), the reduction of this model to state space form, and the simplifying assumptions made. Section 4 includes studies of the model system roots as they were located by quadratic control cost weighting. Section 5 includes three methods for the interpretation of noise in defining Kalman's

filters and summarizes the experiments made with the optimal controls combined with the several Kalman filters. Section 5 also presents most of the final system results. Section 6 discusses the augmentation of the filtering to render the system adaptive and presents the experiments made to develop this capability.

As the work was performed, a large portion of the difficulties involved computer operations on the large-dimension system matrixes. Section 7 is devoted to a discussion of these computing difficulties and their resolution. Section 8 summarizes the findings of the study and relates them to the original problem. Problem areas and opportunities for future work are discussed. Section 9 defines terms used, and Section 10 lists references. Appendix A contains listings of selected computer routines developed for the purposes of the contract study; those included are considered to be of enduring value.

2.3 RELATED WORK IN THE LITERATURE

Quadratic optimal control has received considerable interest for application to system control problems because it leads to linear control, which is usually well behaved.

Rynaski has done considerable work in refining the criterion for a design method (References 1 and 2). He has also applied the method to a simplified boost vehicle. He assumes vehicle states are available and shows that one gets no control gains for unobservable states.

Fisher (Reference 3) applied quadratic control to a somewhat more sophisticated model, with three bending modes, but no sloshing or engine dynamics. He obtains a 9-dimensional system and suggests using 9 sensor signals and solving algebraically for the 9 unknown states. He further shows experimental results indicating the number of sensors in an axis can be reduced to 6. But, since states come in pairs (i. e., a state and its derivative), one needs only half as many sensors as there are elements in the state vector. One merely obtains the remaining states by differentiating. He defines a

vehicle with rigid body rotation and two bending modes and develops control with three sensors. He suggests that perhaps other states can be ignored.

The fundamental contribution supplementing this earlier work and summarized in this report is the application of least squares estimation of vehicle states from a small number of sensor signals. Also, quadratic control is developed to a stage close to the real-world engineering problem. Feasibility is demonstrated with a high level of certainty with a 20-dimensional vehicle model, including four bending modes, three sloshing modes, third-order actuator dynamics, and vehicle translation and rigid body rotation. One of the major design problems, that of parameter uncertainty, is also considered at length. The problems of angle of attack disturbance sensitivity and engine deflection limits are considered indirectly through transient response studies.

2.4 BACKGROUND THEORY

Given a linear system whose equations of motion are expressed in the state-space form

$$\dot{\underline{x}} = \underline{A}\underline{x} + \underline{B}\underline{u} + \underline{G}\underline{\xi} \quad (2-1)$$

$$\underline{z} = \underline{H}\underline{x} + \underline{v} \quad (2-2)$$

the quadratic performance criterion produces control such that the functional

$$E \left\{ \underline{x}'(T) \lambda_1 \underline{x}(T) + \int_0^T \left[\underline{x}'(t) \lambda_2 \underline{x}(t) + \underline{u}'(t) \lambda_3 \underline{u}(t) \right] dt \right\} \quad (2-3)$$

is minimized. λ_3 is a continuous positive definite matrix and λ_2 is a continuous non-negative definite matrix. It is shown by Schultz (Reference 4) that this performance index is minimized with the linear control

$$\underline{u}(t) = -\lambda_3^{-1} \underline{B}' \underline{P} \underline{\hat{x}} \quad (2-4)$$

where

$$\frac{dP}{dt_1} = -PA - A'P + PB\lambda_3^{-1}B'P - \lambda_2 \quad (2-5)$$

$$P_{(T)} = \lambda \quad (2-6)$$

This is elaborated upon somewhat by Potter (Reference 5) who shows that the separation principle proposed by Gunkel and Joseph (References 6 and 7) for discrete systems also applies to corresponding continuous systems. This separation principle states that the minimum value of the cost functional (Equation 2-3) can be achieved by developing the control (Equation 2-4), assuming $\hat{x} = x$, and then independently developing the least squares estimation filter. It can be seen that the optimal control is a linear operation on the state estimate, which will henceforth be written

$$\underline{u} = \Delta \hat{\underline{x}} \quad (2-7)$$

The most convenient form of least squares filtering was presented by Kalman (Reference 8) and bears his name. His basic filter equations are

$$\dot{\hat{\underline{x}}} = A\hat{\underline{x}} + B\underline{u} + K(z - H\hat{\underline{x}}) \quad (2-8)$$

$$K = (PH' + GC) R^{-1} \quad (2-9)$$

$$\dot{P} = AP + PA' - (PH' + GC) R^{-1} (PH' + GC)' + GQG' \quad (2-10)$$

based on the assumptions that

1. The plant (Equation 2-1) is linear.
2. The disturbance (ξ) and noise (v) are white, gaussian, and of zero mean.

The white disturbance and noise assumptions are not as restrictive as they may seem. Gaussian stochastic processes with arbitrary spectral densities continuous infrequency can be approximated to an arbitrary level of accuracy

by n^{th} order Markov processes. These processes in turn can be expressed as white disturbances passing through linear filters. The linear filtering can be interpreted as an uncontrollable augmentation to the plant, with transfer matrix A . These equations are expanded by Kumar (Reference 9) to include least squares estimation of parameters for the special case of Kalman's equations with $C = 0$.

Equations 2-1, 2-2, 2-7, and 2-8 can be combined in a block diagram to show the resulting closed-loop system, as shown in Figure 2-1.

Figure 2-1 is supplemented with an external command channel (u_c), which for this application would be guidance commands to the plant. It is interesting to note that the response to u_c is dependent only on A , B , and Δ and is independent of the filter. This can be shown by dropping the inputs ξ and v from Figure 2-1. The block diagram will then reduce to Figure 2-2.

Theoretically, with the gaussian and linear assumptions, Kalman filtering contains all the information possible. However, the resulting filtering has been limited in its use because of two basic assumptions:

1. The dimensions of the filter is the same as that of the plant.
2. It is assumed that the plant parameters contained in A , B , and G are known exactly.

Assumption (1) leads to exorbitantly large filters for large dimensional systems such as a flexible launch vehicle. Assumption (2) is somewhat unrealistic because the plant parameters are never exactly known. Augmentation of the filtering for parameter identification is practical for a limited number of parameters only. The matrices become exorbitantly large as an increasing number of parameters are estimated. Experiments with Kalman filtering in navigation applications have shown that in many cases the plant model can be simplified to contain only a few of the lowest frequency states, without significant deterioration of filter performance. This experience offered the hope that the filtering for the flexible launch vehicle application could be simplified to dimensions practical for mechanization. It also suggested the

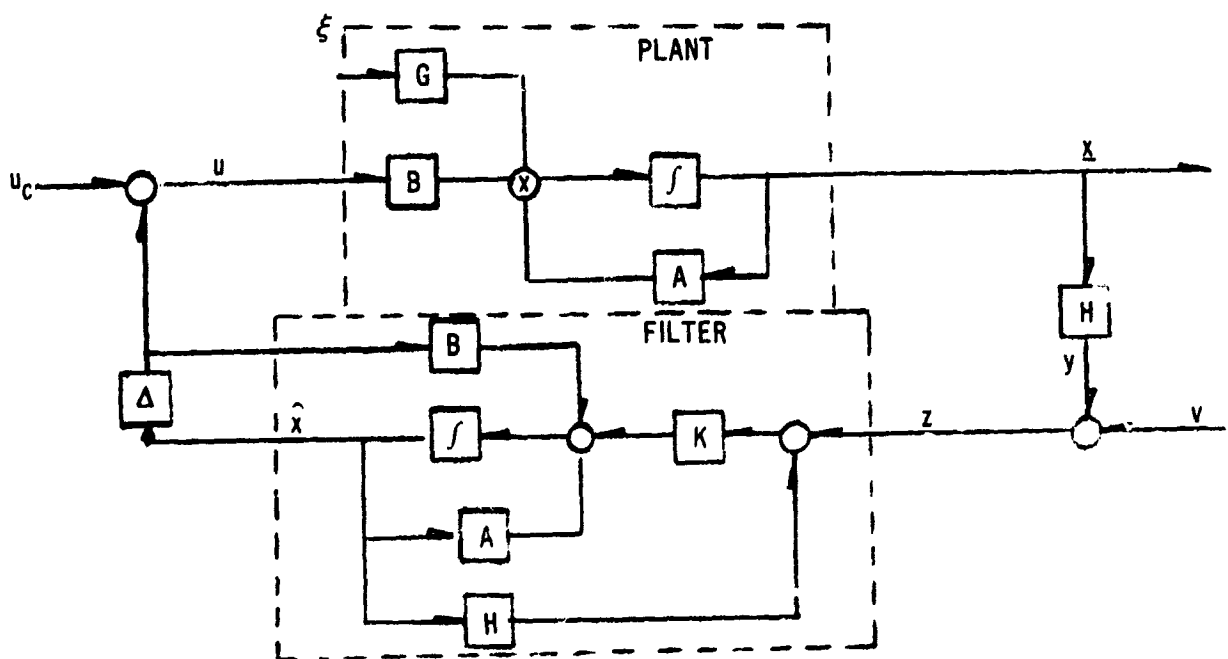


Figure 2-1. Closed Loop System Block Diagram

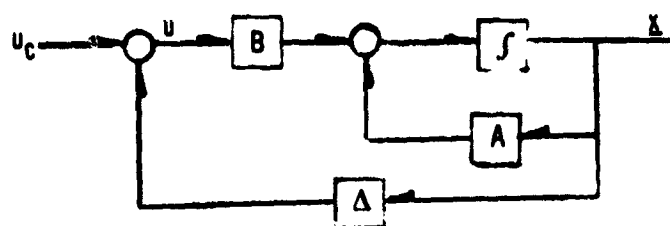


Figure 2-2. System Guidance Command Response

following design procedure as an upper limit on what might be achieved in terms of control simplification.

1. Define the system in state space form and determine system poles corresponding to the various state values. Determine which poles must be moved to achieve satisfactory stability characteristics.
2. Define a low-order plant model containing only the states whose poles it has been determined must be moved. Develop optimal control gains and Kalman filtering for this system.
3. Insert this filtering and control in the system.

The hoped-for result will be a minimum of coupling with the higher-order states, with little movement of their closed-loop poles from their open-loop positions. In addition, it is hoped that the poles and zeros of the states included in the filter will remain where they were positioned by the optimal control defined for the simplified plant. Also, it is hoped that the response characteristic would not be sensitive to differences between estimated parameter values in the low-order model and the corresponding parameters in the plant. If the above procedure could be accomplished, the objections to Kalman filtering would be completely overcome. It cannot be expected that the procedure suggested will work exactly; however, a compromise filter somewhere between this lower dimension limit and one of the same dimension as the plant will yield satisfactory performance; this filter will have to be augmented to estimate only a practical number of parameters to achieve satisfactory parameter insensitivity. The exploration of this compromise has been the main object in this contract.

2.5 METHODS OF INVESTIGATION

The general form of the quadratic control can be simplified somewhat for this application. The optimal control is to be applied to a launch situation, remote in time from any guidance-critical terminal time. This allows setting λ_1 to zero and making λ_2 and λ_3 constant in time in the performance index (Equation 2-3). This also allows the use of the steady-state solution of the Riccati equation (Equation 2-5) and leads to optimal control gains (Δ) constant in time. The assumption of a launch situation has similarly allowed the use of steady-state solutions to the Kalman filter equations

(Equations 2-8, 2-9, and 2-10). (The related studies of parameter estimation did not utilize this assumption.)

In reality, the plant matrixes A , B , H , A , and R change with time. It has been assumed in this work that they change slowly enough with time so they may be assumed constant about a particular flight time of interest, and optimal steady-state control and filter gains prepared. This is a reasonable approach, used extensively in the past for launch vehicle autopilot design, which greatly reduces the demand on vehicle home control equipment. Even in this ground-based study, the assumption has been necessary because of the storage limitations of the IBM 7094 computer. The use of a steady-state Kalman gain matrix may not apply, however, with the filter augmented for parameter estimation. In this work this year, the transient solution of the Riccati equation has been computed. (Removal of this difficulty is a subject for future study.)

An investigator has a choice when beginning a study on quadratic control: whether to conduct the investigation using the discrete or continuous versions of the control and filter equations. The continuous approach was adopted for this study primarily because experience has shown that pole-zero system analysis is more useful and straightforward in continuous systems than in discrete systems. Also, the continuous version describes the limit that is approached as the time interval in the discrete version approaches zero.

As stated in the quoted Statement of Work, this study was oriented toward development and evaluation of system stability. A review of available methods of defining or determining system stability led to the conclusion that closed-loop poles, or eigenvalues, of the system with parameters frozen to time invariance would yield the most stability information. System poles and step transient response studies have formed the methods of evaluating systems, exclusive of the parameter estimation work. For complete autopilot evaluation, it is standard procedure to simulate vehicle attitude and engine deflection response through various wind profiles or flight histories.

Such extensive evaluation was beyond the scope of this contract, but a fairly good idea of the vehicle characteristic response to wind, can be inferred from vehicle response to a simple unit step wind input. For systems with rapidly varying parameters (i. e., the parameter estimating system), stability is a more obscure concept; pole-zero analysis loses its applicability. In the parameter estimation system, stability is inferred from inspection of the error signal time histories resulting from various disturbance inputs.

Both the optimal control and the Kalman filtering require the steady-state solution of a matrix Riccati equation. A number of methods were investigated but virtually all of the solutions used in the various experiments were obtained with the Automatic Synthesis Program (ASP) (Reference 10) developed at the Research Institute of Advanced Studies.

Section 3 SYSTEM DEFINITION

3.1 SYSTEM EQUATIONS

As was intended, equations and parameter values for a hypothetical launch vehicle system were furnished by NASA-MSFC. This information was titled Model Specification No. 2 (unpublished). The equations listed were reduced to the following set for the purposes of this study.

Translation

$$\ddot{Z} = -\frac{N'}{mV} \dot{Z} + \left(\frac{N'}{m} + \frac{F - X}{m} \right) \phi - \frac{1}{m} \sum_j m_{S_j} \ddot{Z}_{S_j} - \frac{F}{m} \sum_K Y'_K (X_\beta) \eta_K + \frac{R'}{m} \beta + \frac{N'}{mV} V_w \quad (3-1)$$

Rotation

$$\ddot{\phi} = \frac{C_1}{V} \dot{Z} - C_1 \phi_R - \frac{C_1}{V} V_w - C_2 \beta \quad (3-2)$$

j^{th} sloshing mode

$$\ddot{Z}_{S_j} = \left(\frac{F - X}{m} \right) \phi - \omega_{S_j}^2 Z_{S_j} - \left(\frac{F - X}{m} \right) \sum_K Y'_K (X_{S_j}) \eta_K - \ddot{Z} + l_{S_j} \ddot{\phi} - \sum_K Y_K (X_{S_j}) \ddot{\eta}_K \quad (3-3)$$

i^{th} bending mode

$$\begin{aligned}
 \ddot{\eta}_i = & -\frac{G_i}{V} \dot{Z} + G_i \phi - \frac{1}{m_i} \left(\frac{F - X}{m} \right) \sum_j m_{S_j} Y_i'(X_{S_j}) Z_{S_j} - \omega_i^2 \eta_i \\
 & - \frac{R_i'}{m_i} Y_i(X_\beta) \sum_K Y_K'(X_\beta) \eta_K - 2\xi\omega_i \dot{\eta}_i + \frac{R_i'}{m_i} Y_i(X_\beta) \beta_R + \frac{G_i}{V} V_w \\
 & + \frac{1}{m_i} \left[S_E Y_i(X_\beta) + I_E Y_i'(X_\beta) \right] \ddot{\beta} - \frac{1}{m_i} \sum_j m_{S_j} Y_i(X_{S_j}) \ddot{Z}_{S_j} \\
 & - \frac{1}{m_i} \sum_j \left[S_E Y_i(X_\beta) + I_E Y_i'(X_\beta) \right] \eta_j
 \end{aligned} \tag{3-4}$$

where

$$G_i = q \frac{A}{m_i} \int_0^{l_{\partial C_Z}} \frac{\partial}{\partial X} Y_i(X) dX$$

Engine/actuator

$$\ddot{\beta} = C_{\dot{\beta}} \dot{\beta} + C_{\beta} \beta - C_{\beta} u \tag{3-5}$$

The above equations are arranged in order of increasing frequency of the dominant roots and constitute the system dynamical equations. In an effort to reduce the dimension of the system state vector, the dynamic phenomena with break frequencies above 6 cps were discarded. This in effect gave all the sensors the attribute of instantaneous response. It was learned from MSFC that the equations in Model Specification No. 2 had been extracted from Reference 11. Since this handbook derives the equations and is available for general use, the equation notation was altered slightly from that in Model Specification No. 2 to bring it into line with this handbook.

The following assumptions were incorporated in the dynamical equations:

1. Sensor response was assumed instantaneous.

2. Aerodynamic lift and moment coefficients were made linear with angle of attack.
3. The angle of attack was assumed constant over the entire vehicle surface and was referenced to rigid body attitude. This means that vehicle bending is not included in the angle of attack determination and that a transverse wind affects all stations of the vehicle simultaneously, rather than traveling progressively aft across the vehicle surface.
4. Actuator dynamics are related only to engine deflection (β).
5. Longitudinal acceleration (\ddot{x}) is zero.

Assumption 3 masks any usefulness of forward mounting the sensors to receive earlier indication of angle of attack. Assumption 5 causes a hangoff in the steady-state response to attitude commands. Normally, the steady-state attitude response of the stable, closed-loop system to attitude commands would be unity. With Assumption 5, the response is slightly less than unity (about 0.9).

In addition to these equations, a first-order Markov wind was added to the system equations

$$\dot{V}_w = -a_w V_w + \xi_w \quad (3-6)$$

In all, the system states include lateral velocity (1), rigid body rotation (2), three sloshing modes (6), four bending modes (8), a third-order actuator (3), and wind (1), constituting a 21-dimensional system.

Model Specification No. 2 contained sensor signal equations for an attitude gyro, rate gyro, accelerometer, and an angle of attack meter. NASA-MSFC personnel indicated in discussions that they were not much interested in the angle of attack meter during this study, and it was not considered further. The following are the sensor signal equations used.

$$Y_{AG} = \phi - \sum_i Y'_i(X_{AG})\eta_i \quad (3-7)$$

$$Y_{RG} = \dot{\phi} - \sum_i Y'_i(X_{RG})\dot{\eta}_i \quad (3-8)$$

$$Y_{AC} = -l_A \ddot{\phi} + \sum_i Y_i(X_{AC}) \ddot{\eta}_i - \left(\frac{F - X}{m} \right) \phi + \frac{F - X}{m} \sum_i Y_i'(X_A) \dot{\eta}_i \quad (3-9)$$

Equations 3-10 through 3-19 are grouped in the state-space equations, in the same order.

$$F \dot{\underline{X}} = A_{pr} \underline{X} + B_{pr} u + G_{pr} \underline{\xi} \quad (3-10)$$

$$\underline{Y} = C \dot{\underline{X}} + D \underline{X} \quad (3-11)$$

where

$$\underline{X} = [\dot{Z} \phi \dot{\phi} Z_{S_1} \dot{Z}_{S_1} Z_{S_2} \dot{Z}_{S_2} Z_{S_3} \dot{Z}_{S_3} \eta_1 \dot{\eta}_1 \eta_2 \dot{\eta}_2 \eta_3 \dot{\eta}_3 \beta \dot{\beta} \ddot{\beta} v_w]' \quad (3-12)$$

$$\underline{Y} = [Y_{AG}, Y_{RG}, Y_{AC}]' \quad (3-13)$$

$$B_{pr} = [0 \ 0 \ \dots \ 0 \ C_\beta \ 0]' \quad (3-14)$$

The matrixes F , A_{pr} , C , and D are shown in Figures 3-1 through 3-3. Equation 3-10 can be rewritten

$$\dot{\underline{X}} = F^{-1} A_{pr} \underline{X} + F^{-1} B_{pr} u + F^{-1} G_{pr} \underline{\xi} \quad (3-15)$$

$$\dot{\underline{X}} = A \underline{X} + B u + G \underline{\xi} \quad (3-16)$$

Substituting Equation 3-16 into 3-11 gives

$$\underline{Y} = [CA + D] \underline{X} + C B u + C G \underline{\xi} \quad (3-17)$$

because of zero terms in the matrixes many of the terms in Equation 3-17 drop out, leaving

$$\underline{Y} = [CA + D] \underline{X} \quad (3-18)$$

z	$\dot{\theta}_R$	$\ddot{\theta}_R$	\dot{z}_{1S}	\ddot{z}_{1S}	\dot{z}_{2S}	\ddot{z}_{2S}	\dot{z}_{3S}	\ddot{z}_{3S}	\dot{n}_1	\ddot{n}_1
1				$\frac{M_{S1}}{m}$		$\frac{M_{S2}}{m}$		$\frac{M_{S3}}{m}$		
	1									
		1								
			1							
1		$-l_{S1}$		1						$Y_1(X_{S1})$
					1					
1		$-l_{S2}$				1				$Y_1(X_{S2})$
							1			
1		$-l_{S3}$						1		$Y_1(X_{S3})$
									1	
				$\frac{1}{M_1} m_{S1} Y_1(X_{S1})$		$\frac{1}{M_1} m_{S2} Y_1(X_{S2})$		$\frac{1}{M_1} m_{S3} Y_1(X_{S3})$		$1 + \frac{1}{M_1} [S_E Y_1(X_{\beta}) + I_E Y_1'(X_{\beta})] Y_1'(X_{\beta})$
				$\frac{1}{M_2} m_{S1} Y_2(X_{S1})$		$\frac{1}{M_2} m_{S2} Y_2(X_{S2})$		$\frac{1}{M_2} m_{S3} Y_2(X_{S3})$		$\frac{1}{M_2} [S_E Y_2(X_{\beta}) + I_E Y_2'(X_{\beta})] Y_2'(X_{\beta})$
				$\frac{1}{M_3} m_{S1} Y_3(X_{S1})$		$\frac{1}{M_3} m_{S2} Y_3(X_{S2})$		$\frac{1}{M_3} m_{S3} Y_3(X_{S3})$		$\frac{1}{M_3} [S_E Y_3(X_{\beta}) + I_E Y_3'(X_{\beta})] Y_3'(X_{\beta})$
				$\frac{1}{M_4} m_{S1} Y_4(X_{S1})$		$\frac{1}{M_4} m_{S2} Y_4(X_{S2})$		$\frac{1}{M_4} m_{S3} Y_4(X_{S3})$		$\frac{1}{M_4} [S_E Y_4(X_{\beta}) + I_E Y_4'(X_{\beta})] Y_4'(X_{\beta})$

Figure 3-1. F Mat

17-1

[illegible]

BLANK PAGE

\dot{z}	$\dot{\phi}_R$	$\dot{\phi}_R$	z_{1S}	\dot{z}_{1S}	z_{2S}	\dot{z}_{2S}	z_{3S}	\dot{z}_{3S}	n_1	\dot{n}_1
$\frac{-N}{mv}$	$\frac{N}{m} + \frac{F-X}{m}$								$-\frac{F}{m} Y_1'(x_p)$	
		1								
$\frac{c_1}{V}$	$-c_1$									
				1						
$\frac{F-X}{m}$			$-\omega_1^2$	$-2\zeta_1 \omega_1$					$\left(\frac{F-X}{m}\right) Y_1'(x_{s_1})$	
						1				
$\frac{F-X}{m}$					$-\omega_2^2$	$-2\zeta_2 \omega_2$			$-\left(\frac{F-X}{m}\right) Y_1'(x_{s_2})$	
								1		
$\frac{F-X}{m}$							$-\omega_3^2$	$-2\zeta_3 \omega_3$	$-\left(\frac{F-X}{m}\right) Y_1'(x_{s_3})$	
										1
$\frac{c_1}{V}$	c_1		$\frac{1}{M_1} \left(\frac{F-X}{m}\right) m_{s_1} Y_1'(x_{s_1})$		$\frac{1}{M_1} \left(\frac{F-X}{m}\right) m_{s_2} Y_1'(x_{s_2})$		$\frac{1}{M_1} \left(\frac{F-X}{m}\right) m_{s_3} Y_1'(x_{s_3})$		$-\omega_1^2 - \frac{R_1'}{M_1} Y_1'(x_p) Y_1'(x_p)$	$-2\zeta_1 \omega_1$
$\frac{c_2}{V}$	c_2		$\frac{1}{M_2} \left(\frac{F-X}{m}\right) m_{s_1} Y_2'(x_{s_1})$		$\frac{1}{M_2} \left(\frac{F-X}{m}\right) m_{s_2} Y_2'(x_{s_2})$		$\frac{1}{M_2} \left(\frac{F-X}{m}\right) m_{s_3} Y_2'(x_{s_3})$		$-\frac{R_2'}{M_2} Y_2'(x_p) Y_2'(x_p)$	
$\frac{c_3}{V}$	c_3		$\frac{1}{M_3} \left(\frac{F-X}{m}\right) m_{s_1} Y_3'(x_{s_1})$		$\frac{1}{M_3} \left(\frac{F-X}{m}\right) m_{s_2} Y_3'(x_{s_2})$		$\frac{1}{M_3} \left(\frac{F-X}{m}\right) m_{s_3} Y_3'(x_{s_3})$		$-\frac{R_3'}{M_3} Y_3'(x_p) Y_3'(x_p)$	
$\frac{c_4}{V}$	c_4		$\frac{1}{M_4} \left(\frac{F-X}{m}\right) m_{s_1} Y_4'(x_{s_1})$		$-\frac{1}{M_4} \left(\frac{F-X}{m}\right) m_{s_2} Y_4'(x_{s_2})$		$-\frac{1}{M_4} \left(\frac{F-X}{m}\right) m_{s_3} Y_4'(x_{s_3})$		$-\frac{R_4'}{M_4} Y_4'(x_p) Y_4'(x_p)$	

Figur

n_2	\dot{n}_2	n_3	\dot{n}_3	n_4	\dot{n}_4	\ddot{n}	\ddot{n}	\ddot{n}	V_W
$-\frac{F}{m}Y_2'(X_p)$		$-\frac{F}{m}Y_3'(X_p)$		$-\frac{F}{m}Y_4'(X_p)$		$\frac{R'}{E}$			$\frac{N}{V}$
						C_2			$\frac{C_1}{V}$
$-\left(\frac{F-X}{m}\right)Y_2'(X_{s_1})$		$-\left(\frac{F-X}{m}\right)Y_3'(X_{s_1})$		$-\left(\frac{F-X}{m}\right)Y_4'(X_{s_1})$					
$-\left(\frac{F-X}{m}\right)Y_2'(X_{s_2})$		$-\left(\frac{F-X}{m}\right)Y_3'(X_{s_2})$		$-\left(\frac{F-X}{m}\right)Y_4'(X_{s_2})$					
$-\left(\frac{F-X}{m}\right)Y_2'(X_{s_1})$		$-\left(\frac{F-X}{m}\right)Y_3'(X_{s_2})$		$-\left(\frac{F-X}{m}\right)Y_4'(X_{s_2})$					
$-\frac{R'}{M_1}Y_1(X_p)Y_2'(X_p)$		$\frac{R'}{M_1}Y_1(X_p)Y_3'(X_p)$		$\frac{R'}{M_1}Y_1(X_p)Y_4'(X_p)$		$\frac{R'}{M_1}Y_1(X_p)$		$\frac{1}{M_1}(S_E Y_1(X_p) + I_E Y_1'(X_p))$	$\frac{G_1}{V}$
$-\omega_2^2 - \frac{R'}{M_2}Y_2(X_p)Y_2'(X_p)$	$-2\omega_2$	$-\frac{R'}{M_2}Y_2(X_p)Y_3'(X_p)$		$-\frac{R'}{M_2}Y_2(X_p)Y_4'(X_p)$		$\frac{R'}{M_2}Y_2(X_p)$		$\frac{1}{M_2}(S_E Y_2(X_p) + I_E Y_2'(X_p))$	$\frac{G_2}{V}$
$-\frac{R'}{M_3}Y_3(X_p)Y_2'(X_p)$		$-\omega_3^2 - \frac{R'}{M_3}Y_3(X_p)Y_3'(X_p)$	$-2\omega_3$	$-\frac{R'}{M_3}Y_3(X_p)Y_4'(X_p)$		$\frac{R'}{M_3}Y_3(X_p)$		$\frac{1}{M_3}(S_E Y_3(X_p) + I_E Y_3'(X_p))$	$\frac{G_3}{V}$
$-\frac{R'}{M_4}Y_4(X_p)Y_2'(X_p)$		$-\frac{R'}{M_4}Y_4(X_p)Y_3'(X_p)$		$-\omega_4^2 - \frac{R'}{M_4}Y_4(X_p)Y_4'(X_p)$	$-2\omega_4$	$\frac{R'}{M_4}Y_4(X_p)$		$-\frac{1}{M_4}(S_E Y_4(X_p) + I_E Y_4'(X_p))$	$\frac{G_4}{V}$
						C_p	C_p	C_p	

3-2. APR Matrix

18-2

$$C = \begin{bmatrix} \ddot{Z} & \dot{\phi}_R & \ddot{\phi}_R & \dot{Z}_{1S} & \ddot{Z}_{1S} & \dot{Z}_{2S} & \ddot{Z}_{2S} \\ 0 & 0 & 0 & 0 & 0 & 0 & 0 \\ 0 & 0 & 0 & 0 & 0 & 0 & 0 \\ 1 & 0 & -l_A & 0 & 0 & 0 & 0 \end{bmatrix}$$

$$D = \begin{bmatrix} \dot{Z} & \phi_R & \dot{\phi}_R & Z_{1S} & \dot{Z}_{1S} & Z_{2S} & \dot{Z}_{2S} \\ 0 & 1 & 0 & 0 & 0 & 0 & 0 \\ 0 & 0 & 1 & 0 & 0 & 0 & 0 \\ 0 & -\frac{F-X}{m} & 0 & 0 & 0 & 0 & 0 \end{bmatrix}$$

\dot{z}_{3S}	\ddot{z}_{3S}	\dot{n}_1	\ddot{n}_1	\dot{n}_2	\ddot{n}_2	\dot{n}_3
0	0	0	0	0	0	0
0	0	0	0	0	0	0
0	0	0	$Y_1(X_A)$	0	$Y_2(X_A)$	0
\dot{z}_{3S}	\ddot{z}_{3S}	\dot{n}_1	\ddot{n}_1	\dot{n}_2	\ddot{n}_2	\dot{n}_3
0	0	$-Y_1'(X_{PG})$	0	$-Y_2'(X_{RG})$	0	$-Y_3'(X_{PG})$
0	0	0	$-Y_1'(X_{RG})$	0	$-Y_2'(X_{RG})$	0
0	0	0	$\left(\frac{F-X}{m}\right)Y_1'(X_A)$	0	$\left(\frac{F-X}{m}\right)Y_2'(X_A)$	0

Figure 3-3. C Matrix and D Matrix

19.2

\ddot{n}_3	\dot{n}_4	\ddot{n}_4	$\dot{\beta}$	$\ddot{\beta}$	$\ddot{\beta}$	\dot{V}_w
0	0	0	0	0	0	0
0	0	0	0	0	0	0
$Y_3(X_A)$	0	$Y_4(X_4)$	0	0	0	0

]

\dot{n}_3	n_4	\dot{n}_4	β	$\dot{\beta}$	$\ddot{\beta}$	V_w
0	$-Y_4'(X_{PG})$	0	0	0	0	0
$-Y_3'(X_{RG})$	0	$-Y_4'(X_{RG})$	0	0	0	0
$\left(\frac{F-X}{m}\right)Y_3'(X_Z)$	0	$\left(\frac{F-X}{m}\right)Y_4'(X_A)$	0	0	0	0

]

10-3

$$\underline{Y} \triangleq \underline{H}\underline{X} \quad (3-19)$$

Equations 3-16 and 3-19 serve as the state-space representation of the system. Because of their large dimension, it is a practical necessity to have them prepared by a computer program.

The program listed in Appendix A was prepared to perform this task. It takes as input a list of 96 numerical parameter values and generates the matrixes A, B, and H. Because of the Markov wind,

$$G = [0 \ 0 \ \dots \ 0 \ 1] \quad (3-20)$$

and need not be generated by computer program.

3.2 SYSTEM PARAMETERS

The 21-D system was derived for three flight conditions: 24, 80, and 155 sec. The 24-sec case represents conditions immediately after liftoff. T = 0 sec was not used because of the irrational angle of attack and lack of aerodynamic disturbance. This is the region where most parameter estimation will be performed. The 80-sec case represents the conditions when the dynamic pressure is a maximum (Max-q). The 155-sec case represents conditions just prior to burnout. These three cases represent the environmental extremes in a typical launch vehicle mission. Satisfactory control with these conditions will infer satisfactory control throughout the entire mission with a fairly great degree of certainty.

Model Specification No. 2 listed acceptable regions for instrument placement. It is desirable for disturbance suppression to mount sensors as far forward as possible; the attitude gyro and accelerometer were mounted at the avionics compartment, at Station 120M. Since the derivatives of the attitude gyro can be deduced by the Kalman filter, the mounting of a rate gyro in the same area would not furnish any extra information. It therefore was mounted further aft, at Station 80M.

BLANK PAGE

A spectral density for the wind was obtained from Bisplingoff (Reference 12) of

$$\Phi_{(\omega)} = \frac{0.06 u^2}{\omega^2 + 4 \times 10^{-6} u^2} \quad (3-21)$$

where u is the vehicle velocity. For the $t = 24$ sec case, u is 77.1 ft/sec, which makes Equation 3-21 equal

$$\Phi_{(\omega)} = \frac{357}{\omega^2 + 0.0238} \quad (3-22)$$

For most of the studies, a white noise approximation was used instead of Equation 3-22. This was obtained by setting Ω to zero,

$$\Phi_{(0)} \cong 1.5 \times 10^4 \quad (3-23)$$

and using this as the covariance matrix (Q) of the white disturbance. Although the Markov wind capability was built into the system model, it was never used in the study.

Table 3-1 lists the numerical values of the parameters used. The resulting A and H matrixes are listed in Appendix B. Table 3-2 lists the corresponding plant poles of these three flight conditions. These poles indicate the plant is stable except for rigid body rotation, as is typical for a launch vehicle of this type. These three system-state numerical solutions have formed the plant models for most of the experiments performed. Reduced state models have been formed by striking out the row and columns corresponding to the unwanted states.

Table 3-1
SYSTEM PARAMETERS (page 1 of 4)

Storage Location	Computer Symbol	Symbol	Flight Time			Units
			24 sec	80 sec	155 sec	
1	C1	$N'I_{CP}/I_{xx}$	-0.0085	-0.13089	0.000565	1/sec ²
2	C2	$R'I_{CG}/I_{xx}$	0.363	0.4735	2.161	1/sec ²
3	AN	N'	129,100	1,091,391	23,253	kg/rad
4	V	V	77.1	506.9	2,521	m/sec
5	FC	F	5,300,000	5,819,805	6,150,000	kg
6	EX	X	26,500	238,780	1,735	kg
7	ALW	aw	0.1194	0.1194	0.1194	rad/sec
8	RP	R'	2,650,000	909,903	3,075,000	kg
9	SE	S_E	1,111	1,111	1,111	kg-sec ²
10	AM	M	376,000	269,989	176,412	kg-sec ² /m
11	AMS(1)	M_{S_1}	11,200	11,612	338	kg-sec ² /m
12	AMS(2)	M_{S_2}	17,400	18,400	772	kg-sec ² /m
13	AMS(3)	M_{S_3}	11,170	11,170	11,170	kg-sec ² /m
14			0	0	0	
15	ALS(1)	I_{S_1}	24	31.04	60.96	m
16	ALS(2)	I_{S_2}	-1	10.12	42.36	m
17	ALS(3)	I_{S_3}	-22.7	-20.15	5.85	m
18			0	0	0	
19	YPB(1)	$Y'_1(X_\beta)$	0.0353	0.0357	0.021	1/m
20	YPB(2)	$Y'_2(X_\beta)$	0.0447	0.0476	0.0314	1/m
21	YPB(3)	$Y'_3(X_\beta)$	0.0545	0.0576	0.0509	1/m
22	YPB(4)	$Y'_4(X_\beta)$	0.0628	0.0636	0.1101	1/m
23	YB(1)	$Y_1(X_\beta)$	1	0.929	0.958	ND
24	YB(2)	$Y_2(X_\beta)$	1	0.905	0.938	ND
25	YB(3)	$Y_3(X_\beta)$	1	0.886	0.900	ND
26	YB(4)	$Y_4(X_\beta)$	1	0.871	0.787	ND
27						
28	Z(1)	ζ_1	0.005	0.005	0.005	ND

Table 3-1 (page 2 of 4)

Storage Location	Computer Symbol	Symbol	Flight Time			Units
			24 sec	80 sec	155 sec	
29	Z(2)	ξ_2	0.005	0.005	0.005	ND
30	Z(3)	ξ_3	0.005	0.005	0.005	ND
31	Z(4)	ξ_4	0.005	0.005	0.005	ND
32	W(1)	ω_1	2.21	2.314	2.91	rad/sec
33	W(2)	ω_2	5.17	5.62	6.59	rad/sec
34	W(3)	ω_3	8.79	9.15	11.71	rad/sec
35	W(4)	ω_4	12.46	12.49	24.85	rad/sec
36	YXS(1, 1)	$Y_1(X_{S_1})$	0.508	0.568	0.832	ND
37	YXS(1, 2)	$Y_2(X_{S_1})$	0.356	0.409	0.747	ND
38	YXS(1, 3)	$Y_3(X_{S_1})$	0.168	0.264	0.589	ND
39	YXS(1, 4)	$Y_4(X_{S_1})$	0.00115	0.14	0.11	ND
40	YXS(2, 1)	$Y_1(X_{S_2})$	-0.277	-0.125	0.418	ND
41	YXS(2, 2)	$Y_2(X_{S_2})$	-0.438	-0.419	0.152	ND
42	YXS(2, 3)	$Y_3(X_{S_2})$	-0.379	-0.552	-0.318	ND
43	YXS(2, 4)	$Y_4(X_{S_2})$	-0.116	-0.544	-1.508	ND
44	YXS(3, 1)	$Y_1(X_{S_3})$	-0.695	-0.838	-0.191	ND
45	YXS(3, 2)	$Y_2(X_{S_3})$	-0.00909	-0.171	-0.252	ND
46	YXS(3, 3)	$Y_3(X_{S_3})$	0.878	0.634	-0.0612	ND
47	YXS(3, 4)	$Y_4(X_{S_3})$	0.855	0.873	0.629	ND
48		q	353	3,856	93	kg/m ²
49	AIE	I_E	3,456	3,456	3,456	kg/m/sec ²
50	AIX	I_{xx}	0.277×10^9	0.2525×10^9	0.925×10^8	kg/m/sec ²
51	ZS(1)	ξ_{S_1}	0.005	0.005	0.005	ND
52	ZS(2)	ξ_{S_2}	0.005	0.005	0.005	ND
53	ZS(3)	ξ_{S_3}	0.005	0.005	0.005	ND
54	WS(1)	ω_{S_1}	2.32	2.76	3.58	rad/sec
55	WS(2)	ω_{S_2}	2.32	2.76	3.77	rad/sec
56	WS(3)	ω_{S_3}	2.32	2.76	4.71	rad/sec

Table 3-1 (page 3 of 4)

Storage Location	Computer Symbol	Symbol	Flight Time			Units
			24 sec	80 sec	155 sec	
57	YPS(1, 1)	$Y'_1(X_{S_1})$	0.0356	0.0366	0.0211	1/m
58	YPS(1, 2)	$Y'_2(X_{S_1})$	0.048	0.052	0.0318	1/m
59	YPS(1, 3)	$Y'_3(X_{S_1})$	0.0635	0.067	0.0519	1/m
60	YPS(1, 4)	$Y'_4(X_{S_1})$	0.0759	0.0798	0.1117	1/m
61	YPS(2, 1)	$Y'_1(X_{S_2})$	0.0278	0.0315	0.0198	1/m
62	YPS(2, 2)	$Y'_2(X_{S_2})$	0.00934	0.0228	0.0253	1/m
63	YPS(2, 3)	$Y'_3(X_{S_2})$	-0.0324	-0.00643	0.0319	1/m
64	YPS(2, 4)	$Y'_4(X_{S_2})$	-0.0702	-0.0487	0.0312	1/m
65	YPS(3, 1)	$Y'_1(X_{S_3})$	0.00676	0.00623	0.0114	1/m
66	YPS(3, 2)	$Y'_2(X_{S_3})$	-0.0462	-0.0447	-0.0168	1/m
67	YPS(3, 3)	$Y'_3(X_{S_3})$	-0.0363	-0.0155	-0.0827	1/m
68	YPS(3, 4)	$Y'_4(X_{S_3})$	0.0514	0.128	-0.147	1/m
69	BM(1)	M_1	186,700	171,690	17,867	kg-sec ² /m
70	BM(2)	M_2	144,000	116,484	29,068	kg-sec ² /m
71	BM(3)	M_3	163,500	101,071	169,960	kg-sec ² /m
72	BM(4)	M_4	530,000	602,613	203,336	kg-sec ² /m
73	G(1)	G_1	0.315	28.95	0.0443	kg
74	G(2)	G_2	0.171	4.73	0.0111	kg
75	G(3)	G_3	0.423	3.49	0.132	kg
76	G(4)	G_4	-0.1225	4.34	0.791	kg
77	YA(1)	$Y_1(X_A)$	1.928	1.767	0.413	ND
78	YA(2)	$Y_2(X_A)$	0.438	0.605	0.509	ND
79	YA(3)	$Y_3(X_A)$	-1.74	-0.013	-2.76	ND
80	YA(4)	$Y_4(X_A)$	4.119	4.37	0.65	ND
81	YPRG(1)	$Y'_1(X_{RG})$	-0.0165	-0.0132	0.0044	1/m
82	YPRG(2)	$Y'_2(X_{RG})$	-0.066	-0.0691	-0.0396	1/m
83	YPRG(3)	$Y'_3(X_{RG})$	0.0565	0.03104	-0.0969	1/m
84	YPRG(4)	$Y'_4(X_{RG})$	0.217	0.236	0.0729	1/m

Table 3-1 (page 4 of 4)

Storage Location	Computer Symbol	Symbol	Flight Time			Units
			24 sec	80 sec	155 sec	
85	YPMG(1)	$Y_1'(HIG)$	-0.1155	-0.1182	-0.0438	1/m
86	YPMG(2)	$Y_2'(HIG)$	0.142	0.129	0.066	1/m
87	YPMG(3)	$Y_3'(HIG)$	-0.107	-0.0702	-0.0355	1/m
88	YPMG(4)	$Y_4'(HIG)$	0.0083	0.0052	-0.622	1/m
89	X(89)	C_β	-31,100	-31,100	-31,000	1/sec ³
90	X(90)	$C_{\dot{\beta}}$	-3,059	-3,059	-3,059	1/sec ²
91	X(91)	$C_{\ddot{\beta}}$	-23.72	-23.72	-23.72	1/sec
92	ALA	l_A	-82.54	-79.54	-53.29	m
93	YPA(1)	$Y_1'(X_A)$	-0.1155	-0.1182	-0.0438	1/m
94	YPA(2)	$Y_2'(X_A)$	-0.142	0.129	0.066	1/m
95	YPA(3)	$Y_3'(X_A)$	-0.107	-0.0702	-0.0355	1/m
96	YPA(4)	$Y_4'(X_A)$	0.0083	0.0052	-0.622	1/m

Table 3-2
PLANT POLES

State Value	24 sec	80 sec	155 sec
Lateral velocity	-0.1419	+0.0413	+0.01127
Rigid body angular displacement	+0.069 ± j0.079	+0.389 -0.381	-0.00566 ± j0.0257
1st sloshing mode	-0.01142 ± j2.31	-0.0134 ± j2.741	-0.0137 ± j3.263
2nd sloshing mode	-0.01296 ± j2.43	-0.0182 ± j2.952	-0.0183 ± j3.652
3rd sloshing mode	-0.01475 ± j2.64	-0.0156 ± j3.082	-0.0198 ± j3.858
1st bending mode	-0.0094 ± j2.11	-0.0129 ± j2.285	-0.0252 ± j4.906
2nd bending mode	-0.0273 ± j5.36	-0.0306 ± j5.894	-0.0362 ± j7.069
3rd bending mode	-0.0483 ± j9.19	-0.053 ± j9.812	-0.0586 ± j11.75
4th bending mode	-0.0639 ± j12.60	-0.0653 ± j12.72	-0.129 ± j25.31
Engine dynamics	-6.53 ± j53.6	-6.53 ± j53.6	-6.53 ± j53.6
Engine dynamics	-10.65	-10.65	-10.65

3.3 LOW ORDER STUDY MODELS

A series of system models has been used during the program. To reduce confusion, a notation system for these models was developed as follows:

$$i - j$$

where i is an integer signifying the order of the model and j is an integer designating the particular model. For example, model No. 4-3 is a 4-dimensional model, the third one developed. The following are the definitions of these models.

4-1 is an early experimental model with little relation to Model Specification No. 2.

$$\begin{Bmatrix} \ddot{\phi} \\ \dot{\phi} \\ \ddot{\eta} \\ \dot{\eta} \end{Bmatrix} = \begin{bmatrix} 0 & 0 & 0 & 0 \\ 1 & 0 & 0 & 0 \\ 0 & 0 & -0.0221 & -4.88 \\ 0 & 0 & 1 & 0 \end{bmatrix} \begin{Bmatrix} \dot{\phi} \\ \phi \\ \dot{\eta} \\ \eta \end{Bmatrix} + \begin{bmatrix} 1.221 \\ 0 \\ 1.221 \\ 0 \end{bmatrix} u \quad (3-24)$$

$$\underline{Y} = [0 \ 1 \ 0 \ -0.5] \underline{X}$$

4-2 is a model approximating the Model Specification No. 2 system at $t = 24$ sec but with no coupling between the bending mode and rigid body rotation or aerodynamic influence.

$$\begin{Bmatrix} \dot{\phi} \\ \ddot{\phi} \\ \dot{\eta}_1 \\ \ddot{\eta}_1 \end{Bmatrix} = \begin{bmatrix} 0 & 1 & 0 & 0 \\ 0 & 0 & 0 & 0 \\ 0 & 0 & 0 & 1 \\ 0 & 0 & -4.88 & -0.0221 \end{bmatrix} \begin{Bmatrix} \phi \\ \dot{\phi} \\ \eta_1 \\ \dot{\eta}_1 \end{Bmatrix} + \begin{bmatrix} 0 \\ -0.363 \\ 0 \\ 14.2 \end{bmatrix} \beta + \begin{bmatrix} 0 \\ 1.114 \times 10^{-3} \\ 0 \\ 4.08 \times 10^{-3} \end{bmatrix} V_w$$

$$\begin{Bmatrix} Y_{AG} \\ Y_{RG} \end{Bmatrix} = \begin{bmatrix} 1 & 0 & 0.1189 & 0 \\ 0 & 1 & 0 & 0 \end{bmatrix} \underline{X} \quad (3-25)$$

4-3 is a model taken directly from Model Specification No. 2, 24-sec run, with no coupling terms omitted.

$$\begin{Bmatrix} \dot{\phi} \\ \ddot{\phi} \\ \dot{\eta}_1 \\ \ddot{\eta}_1 \end{Bmatrix} = \begin{bmatrix} 0 & 1.0 & 0 & 0 \\ 0.00858 & 0 & -0.272 \times 10^{-8} & -0.1029 \times 10^{-10} \\ 0 & 0 & 0 & 1.0 \\ 0.299 & 0 & -5.66 & -0.0234 \end{bmatrix} \begin{Bmatrix} \phi \\ \dot{\phi} \\ \eta_1 \\ \dot{\eta}_1 \end{Bmatrix} \quad (3-26)$$

$$+ \begin{bmatrix} 0 \\ -0.363 \\ 0 \\ 15.19 \end{bmatrix} \beta + \begin{bmatrix} 0 \\ 0.1113 \times 10^{-3} \\ 0 \\ 0.388 \times 10^{-3} \end{bmatrix} V_w$$

$$\begin{Bmatrix} Y_{AG} \\ Y_{RG} \\ Y_{AC} \end{Bmatrix} = \begin{bmatrix} 1 & 0 & 0.1155 & 0 \\ 0 & 1 & 0 & 0.0165 \\ -14.64 & 0 & -10.94 & 0.0702 \end{bmatrix} \underline{X} \quad (3-27)$$

4-4 is a model taken directly from Model Specification No. 2, 80 sec, Run 21-2, with no coupling terms omitted.

$$\begin{Bmatrix} \dot{\phi} \\ \ddot{\phi} \\ \dot{\eta}_1 \\ \ddot{\eta}_1 \end{Bmatrix} = \begin{bmatrix} 0 & 1 & 0 & 0 \\ 0.1309 & 0 & -0.657 \times 10^{-7} & -0.259 \times 10^{-9} \\ 0 & 0 & 0 & 1 \\ 31.0 & 0 & -6.33 & -0.0249 \end{bmatrix} \begin{Bmatrix} \phi \\ \dot{\phi} \\ \eta_1 \\ \dot{\eta}_1 \end{Bmatrix}$$

$$+ \begin{bmatrix} 0 \\ -0.472 \\ 0 \\ 17.6 \end{bmatrix} \beta + \begin{bmatrix} 0 \\ 0.258 \times 10^{-3} \\ 0 \\ 0.0611 \end{bmatrix} V_w \quad (3-28)$$

$$Y = \begin{bmatrix} 1 & 0 & 0.1182 & 0 \\ 0 & 1 & 0 & 0.01319 \\ 14.02 & 0 & -11.24 & 0.0736 \end{bmatrix} \underline{X}$$

4-5 is a model taken directly from Model Specification No. 2, 155 sec, near burnout, Run 21-3, with no coupling terms omitted.

$$\begin{Bmatrix} \dot{\phi} \\ \ddot{\phi} \\ \dot{\eta}_1 \\ \ddot{\eta}_1 \end{Bmatrix} = \begin{bmatrix} 0 & 1 & 0 & 0 \\ -0.565 \times 10^{-3} & 0 & -0.1682 \times 10^{-8} & -0.339 \times 10^{-11} \\ 0 & 0 & 0 & 1 \\ -0.0635 & 0 & -12.54 & -0.0305 \end{bmatrix}$$

$$x \begin{Bmatrix} \phi \\ \dot{\phi} \\ \eta_1 \\ \dot{\eta}_1 \end{Bmatrix} + \begin{bmatrix} 0 \\ -2.16 \\ 0 \\ 176.5 \end{bmatrix} \beta + \begin{bmatrix} 0 \\ -0.224 \times 10^{-6} \\ 0 \\ -0.252 \times 10^{-4} \end{bmatrix} V_w \quad (3-29)$$

$$Y = \begin{bmatrix} 1 & 0 & 0.0438 & 0 \\ 0 & 1 & 0 & -0.0044 \\ -34.7 & 0 & -5.55 & 0.031 \end{bmatrix} \underline{X}$$

6-1 is a model the same as 4-2, but with the third bending mode added.

Coupling between rigid body rotation and the bending modes, and aerodynamic moment are omitted.

$$\begin{Bmatrix} \dot{\phi} \\ \ddot{\phi} \\ \dot{\eta}_1 \\ \ddot{\eta}_1 \\ \dot{\eta}_3 \\ \ddot{\eta}_3 \end{Bmatrix} = \begin{bmatrix} 0 & 1 & 0 & 0 & 0 & 0 \\ 0 & 0 & 0 & 0 & 0 & 0 \\ 0 & 0 & 0 & 1 & 0 & 0 \\ 0 & 0 & -4.88 & -0.0221 & 0 & 0 \\ 0 & 0 & 0 & 0 & 0 & 1 \\ 0 & 0 & 0 & 0 & -78.2 & -0.0879 \end{bmatrix} \begin{Bmatrix} \phi \\ \dot{\phi} \\ \eta_1 \\ \dot{\eta}_1 \\ \eta_3 \\ \dot{\eta}_3 \end{Bmatrix}$$

$$+ \begin{bmatrix} 0 \\ -0.363 \\ 0 \\ 14.2 \\ 0 \\ 16.21 \end{bmatrix} \beta + \begin{bmatrix} 0 \\ 1.114 \times 10^{-3} \\ 0 \\ 4.08 \times 10^{-3} \\ 0 \\ 5.49 \times 10^{-3} \end{bmatrix} V_w$$

$$\begin{Bmatrix} Y_{AG} \\ Y_{RG} \end{Bmatrix} = \begin{bmatrix} 1 & 0 & 0.1189 & 0 & 0.1356 \\ 0 & 1 & 0 & 0 & 0 \end{bmatrix} \underline{X}$$

(3-30)

(3-31)

6-2 is a model the same as 4-2, but the second bending mode is added. It approximates $t = 24$ sec conditions, but coupling between the bending modes and aerodynamic moment are omitted.

$$\begin{Bmatrix} \dot{\phi} \\ \ddot{\phi} \\ \dot{\eta}_1 \\ \ddot{\eta}_1 \\ \dot{\eta}_2 \\ \ddot{\eta}_2 \end{Bmatrix} = \begin{bmatrix} 0 & 1 & 0 & 0 & 0 & 0 \\ 0 & 0 & 0 & 0 & 0 & 0 \\ 0 & 0 & 0 & 1 & 0 & 0 \\ 0 & 0 & -4.88 & -0.0221 & 0 & 0 \\ 0 & 0 & 0 & 0 & 0 & 0 \\ 0 & 0 & 0 & 0 & -26.7 & -0.0517 \end{bmatrix} \begin{Bmatrix} \phi \\ \dot{\phi} \\ \eta_1 \\ \dot{\eta}_1 \\ \eta_2 \\ \dot{\eta}_2 \end{Bmatrix}$$

$$+ \begin{bmatrix} 0 \\ -0.363 \\ 0 \\ 14.2 \\ 0 \\ 25.7 \end{bmatrix} \beta + \begin{bmatrix} 0 \\ 0.1113 \times 10^{-3} \\ 0 \\ 0.388 \times 10^{-2} \\ 0 \\ 0.233 \times 10^{-2} \end{bmatrix} V_w$$

(3-32)

$$\begin{Bmatrix} Y_{AG} \\ Y_{RG} \\ Y_{AC} \end{Bmatrix} = \begin{bmatrix} 1 & 0 & 0.1155 & 0 & -14.2 & 0 \\ 0 & 1 & 0 & 0.0165 & 0 & 0.0660 \\ -14.64 & 0 & -10.94 & 0.0702 & -13.56 & -0.1662 \end{bmatrix} \underline{X}$$

6-3 is a model taken from Model Specification No. 2, $t = 24$ sec computer solution, with no coupling terms omitted. It includes rigid body and first and third bending mode state values.

$$\begin{Bmatrix} \dot{\phi} \\ \ddot{\phi} \\ \dot{\eta}_1 \\ \ddot{\eta}_1 \\ \dot{\eta}_3 \\ \ddot{\eta}_3 \end{Bmatrix} = \begin{bmatrix} 0 & 1 & 0 & 0 & 0 & 0 \\ 0.00858 & 0 & -0.272 \times 10^{-8} & -0.1029 \times 10^{-13} & -0.959 \times 10^{-8} & -0.1023 \times 10^{-10} \\ 0 & 0 & 0 & 1 & 0 & 0 \\ 0.299 & 0 & -5.66 & -0.0234 & 1.277 & 0.266 \times 10^{-2} \\ 0 & 0 & 0 & 0 & 0 & 1 \\ 0.466 & 0 & -0.508 & 0.645 \times 10^{-3} & -84.8 & -0.0947 \end{bmatrix} \begin{Bmatrix} \phi \\ \dot{\phi} \\ \eta_1 \\ \dot{\eta}_1 \\ \eta_3 \\ \dot{\eta}_3 \end{Bmatrix}$$

$$+ \begin{bmatrix} 0 \\ -0.363 \\ 0 \\ 15.19 \\ 0 \\ 17.62 \end{bmatrix} \beta + [0 \quad 1.113 \times 10^{-4} \quad 0 \quad 3.88 \times 10^{-3} \quad 0 \quad 6.09 \times 10^{-3}]' V_w$$

(3-33)

$$\begin{Bmatrix} Y_{AG} \\ Y_{RG} \\ Y_{AC} \end{Bmatrix} = \begin{bmatrix} 1 & 0 & 0.1155 & 0 & 0.107 & 0 \\ 0 & 1 & 0 & 0.0165 & 0 & -0.0565 \\ -14.64 & 0 & -10.94 & 0.0702 & 140.3 & 0.268 \end{bmatrix} \underline{X}$$

6-4 is a model taken directly from Model Specification No. 2, $t = 24$ sec computer run, with no terms omitted. It includes rigid body rotation and first and second bending mode state values.

$$\begin{Bmatrix} \dot{\phi} \\ \ddot{\phi} \\ \dot{\eta}_1 \\ \ddot{\eta}_1 \\ \dot{\eta}_2 \\ \ddot{\eta}_2 \end{Bmatrix} = \begin{bmatrix} 0 & 1 & 0 & 0 & 0 & 0 \\ 0.00858 & 0 & -0.272 \times 10^{-8} & -0.1029 \times 10^{-10} & -0.677 \times 10^{-8} & -0.1024 \times 10^{-10} \\ 0 & 0 & 0 & 1.0 & 0 & 0 \\ 0.299 & 0 & -5.66 & -0.0234 & -1.232 & -0.1249 \times 10^{-2} \\ 0 & 0 & 0 & 0 & 0 & 1 \\ 0.1798 & 0 & -0.850 & -0.694 \times 10^{-3} & -28.5 & -0.0535 \end{bmatrix} \begin{Bmatrix} \phi \\ \dot{\phi} \\ \eta_1 \\ \dot{\eta}_1 \\ \eta_2 \\ \dot{\eta}_2 \end{Bmatrix} + \begin{bmatrix} 0 \\ -0.363 \\ 0 \\ 15.19 \\ 0 \\ 20.0 \end{bmatrix} \beta + [0 \quad 1.1113 \times 10^{-4} \quad 0 \quad 3.88 \times 10^{-8} \quad 0 \quad 2.33 \times 10^{-3}] \dot{V}_w$$

(3-34)

$$\begin{Bmatrix} Y_{AC} \\ Y_{RG} \\ Y_{AC} \end{Bmatrix} = \begin{bmatrix} 1 & 0 & 0.1155 & 0 & -0.142 & 0 \\ 0 & 1 & 0 & 0.0165 & 0 & 0.0660 \\ -14.64 & 0 & -10.94 & 0.0702 & -13.56 & -0.1662 \end{bmatrix} \underline{X}$$

6-5 is a model taken directly from Model Specification No. 2, $t = 80$ -sec (Max-q) computer run, with no terms omitted. It includes rigid body rotation, and first and second bending mode state values.

$$\begin{Bmatrix} \dot{\phi} \\ \ddot{\phi} \\ \dot{\eta}_1 \\ \ddot{\eta}_1 \\ \dot{\eta}_2 \\ \ddot{\eta}_2 \end{Bmatrix} = \begin{bmatrix} 0 & 1 & 0 & 0 & 0 & 0 \\ 0.1309 & 0 & -0.657 \times 10^{-7} & -0.259 \times 10^{-9} & 1.802 \times 10^{-8} & -1.963 \times 10^{-10} \\ 0 & 0 & 0 & 1 & 0 & 0 \\ 31.0 & 0 & -6.33 & -0.0249 & -1.737 & -1.868 \times 10^{-3} \\ 0 & 0 & 0 & 0 & 0 & 1 \\ 0.10 & 0 & -1.166 & -1.152 \times 10^{-3} & -34.4 & 10.0592 \end{bmatrix} \begin{Bmatrix} \phi \\ \dot{\phi} \\ \eta_1 \\ \dot{\eta}_1 \\ \eta_2 \\ \dot{\eta}_2 \end{Bmatrix} + \begin{Bmatrix} 0 \\ -0.472 \\ 0 \\ 17.6 \\ 0 \\ 25.7 \end{Bmatrix} \beta \quad (3-35)$$

$$\begin{Bmatrix} Y_{AG} \\ Y_{RG} \\ Y_{AC} \end{Bmatrix} = \begin{bmatrix} 1 & 0 & 0.1182 & 0 & -0.1293 & 0 \\ 0 & 1 & 0 & 0.01319 & 0 & 0.0691 \\ 14.02 & 0 & -11.24 & 0.0736 & -21.9 & -0.1664 \end{bmatrix} \underline{X}$$

6-6 is a model taken directly from Model Specification No. 2, $t = 155$ -sec (burnout) computer run, with no terms omitted. It includes rigid body rotation and first and second bending mode state values.

$$\begin{Bmatrix} \dot{\phi} \\ \ddot{\phi} \\ \dot{\eta}_1 \\ \ddot{\eta}_1 \\ \dot{\eta}_2 \\ \ddot{\eta}_2 \end{Bmatrix} = \begin{bmatrix} 0 & 1 & 0 & 0 & 0 & 0 \\ -0.565 \times 10^{-3} & 0 & -0.1682 \times 10^{-8} & -0.339 \times 10^{-11} & -0.606 \times 10^{-8} & -0.767 \times 10^{-11} \\ 0 & 0 & 0 & 1 & 0 & 0 \\ -0.0635 & 0 & -12.54 & -0.0305 & -7.4 & -0.00317 \\ 0 & 0 & 0 & 0 & 0 & 1 \\ -0.0649 & 0 & -2.46 & -0.866 \times 10^{-3} & -48.1 & -0.0682 \end{bmatrix} \begin{Bmatrix} \phi \\ \dot{\phi} \\ \eta_1 \\ \dot{\eta}_1 \\ \eta_2 \\ \dot{\eta}_2 \end{Bmatrix} + \begin{Bmatrix} 0 \\ -2.16 \\ 0 \\ 176.5 \\ 0 \\ 105.2 \end{Bmatrix} \underline{V_w} + \begin{bmatrix} 0 & -0.224 \times 10^{-6} & 0 & -0.252 \times 10^{-4} & 0 & -0.258 \times 10^{-4} \end{bmatrix} \underline{V_w} \quad (3-36)$$

$$\begin{Bmatrix} Y_{AG} \\ Y_{RG} \\ Y_{AC} \end{Bmatrix} = \begin{bmatrix} 1 & 0 & 0.0438 & 0 & -0.066 & 0 \\ 0 & 1 & 0 & -0.0044 & 0 & 0.0396 \\ -34.7 & 0 & -5.55 & 0.031 & -26.0 & -0.1014 \end{bmatrix} \underline{X}$$

6-7 is the colored noise system model prepared. The first four states are System 4-3 and the last two make up the 2-D colored noise.

$$\begin{Bmatrix} \dot{\phi} \\ \ddot{\phi} \\ \dot{\eta}_1 \\ \ddot{\eta}_1 \\ \dot{\lambda} \\ \ddot{\lambda} \end{Bmatrix} = \begin{bmatrix} 0 & 1.0 & 0 & 0 & 0 & 0 \\ 0.00858 & 0 & -0.272 \times 10^{-8} & -0.1029 \times 10^{-10} & 0 & 0 \\ 0 & 0 & 0 & 1.0 & 0 & 0 \\ 0.299 & 0 & -5.66 & -0.0234 & 0 & 0 \\ 0 & 0 & 0 & 0 & 0 & 1 \\ 0 & 0 & 0 & 0 & -25.0 & -1.0 \end{bmatrix} \begin{Bmatrix} \phi \\ \dot{\phi} \\ \eta_1 \\ \dot{\eta}_1 \\ \lambda \\ \dot{\lambda} \end{Bmatrix} \\
 + \begin{bmatrix} 0 \\ 0.363 \\ 0 \\ 14.2 \\ 0 \\ 0 \end{bmatrix} V_w + \begin{bmatrix} 0 & 1.114 \times 10^{-3} & 0 & 4.08 \times 10^{-3} & 0 & 0 \\ 0 & 0 & 0 & 0 & 0 & 25.0 \end{bmatrix}^T \begin{Bmatrix} V_w \\ \xi \end{Bmatrix} \quad (3-37)$$

$$\begin{Bmatrix} Y_{AG} \\ Y_{RG} \\ Y_{AC} \end{Bmatrix} = \begin{bmatrix} 1 & 0 & 0.1155 & 0 & 0.224 & 0 \\ 0 & 1 & 0 & 0.0165 & 0 & 1 \\ -14.64 & 0 & -10.94 & 0.0702 & 0.224 & 0 \end{bmatrix} \underline{X}$$

7-1, the seven-dimensional model, is the same as 4-2, with the third-order actuator included. Coupling between the bending modes and angle of attack is omitted.

$$\begin{Bmatrix} \dot{\phi} \\ \ddot{\phi} \\ \dot{\eta}_1 \\ \ddot{\eta}_1 \\ \dot{\beta} \\ \ddot{\beta} \\ \ddot{\beta} \end{Bmatrix} = \begin{bmatrix} 0 & 1 & 0 & 0 & 0 & 0 & 0 \\ 0 & 0 & 0 & 0 & -0.363 & 0 & 0 \\ 0 & 0 & 0 & 1 & 0 & 0 & 0 \\ 0 & 0 & -4.88 & -0.0221 & 14.2 & 0 & 0 \\ 0 & 0 & 0 & 0 & 0 & 1 & 0 \\ 0 & 0 & 0 & 0 & 0 & 0 & 1 \\ 0 & 0 & 0 & 0 & -0.311 \times 10^5 & -3059 & -23.7 \end{bmatrix} \begin{Bmatrix} \phi \\ \dot{\phi} \\ \eta_1 \\ \dot{\eta}_1 \\ \beta \\ \dot{\beta} \\ \ddot{\beta} \end{Bmatrix} + \begin{bmatrix} 0 \\ 0 \\ 0 \\ 0 \\ 0 \\ 0 \\ 0.311 \times 10^5 \end{bmatrix} u \quad (3-38)$$

$$y = [1 \quad 0 \quad 0.1189 \quad 0 \quad 0 \quad 0 \quad 0] \bar{X}$$

11-1, 11-2, and 11-3 systems are formed by striking wind and sloshing states out of 21-1, 21-2, and 21-3. They are not presented here because of their large size. The remaining state vector is

$$\underline{X}' = [\dot{z} \dot{\phi} \dot{\eta}_1 \dot{\eta}_1 \dot{\eta}_2 \dot{\eta}_2 \dot{\eta}_3 \dot{\eta}_3 \dot{\eta}_4 \dot{\eta}_4 \dot{\beta} \dot{\beta} \ddot{\beta}]' \quad (3-39)$$

21-1, 21-2, and 21-3 models are Model Specification No. 2 systems for $t = 24$ sec, 80 sec, and 155 sec. They are presented in Appendix B. Most of the low-order models have been formed by striking out rows and columns from these matrixes.

BLANK PAGE

Section 4

QUADRATIC OPTIMAL CONTROL

This section contains the basic equations involved in optimal control for an arbitrary system. The root-square locus approach is considered. This approach provides a simple way to evaluate those poles of a system which result from certain design considerations. It is shown that costs may be systematically chosen for the control and for the system states so as to achieve some desired bandwidth and damping for each of the controlled modes. In this particular case, the costs are chosen to attain a ratio of two to one on the first bending mode to the controlled rigid body mode, and to cause the bending modes transients to die out in about the same time interval as the rigid body transient.

Examples are presented where the control matrix is derived for typical fourth-, sixth-, and seventh-order systems to achieve desired pole configurations. The optimal gains for the above systems are calculated at specific points in flight (24 sec, maximum dynamic pressure, and burnout). While several of the optimal gains are nearly independent of the time of flight, some change considerably. Switching may be required for control over the entire flight. The switching logic may be activated by the parameter estimates, or simply time.

The issue of controllability is usually discussed in parallel with optimal control derivations. For many practical systems, including this one, the following simple statement adequately defines controllability. Those states to which a path may be traced through the system block diagram, from the control, are controllable. Wind disturbance states are therefore not controllable, but all other states in the typical launch vehicle plant are controllable.

4.1 BASIC APPROACH

In order to apply quadratic optimum control to a linearized system, that system is described by a set of n equations.

$$\dot{x} = Ax + Bu \quad (4-1)$$

Costs are chosen for the states of the system so as to achieve adequate control as follows:

1. Normalize B and the cost on control.
2. Set costs on θ by choosing a desired rigid body bar width.

$$L_2 = (\omega_{RB})^4 \quad (4-2)$$

3. Set costs for $\eta, \dot{\eta}_1$, etc., by choosing a desired closed loop body bending ratio.

$$\text{Cost} \approx \frac{\omega^4 [1 - (1 - 2\xi_{BB}^2)^2]}{(1 - 2\xi_{BB}^2)^2} \quad (4-3)$$

4. Find the left half plane roots of the Z matrix for the above conditions.

$$Z = \left[\begin{array}{c|c} -A & B\lambda_3^{-1}B' \\ \hline \lambda_2 & A' \end{array} \right] \quad (4-4)$$

5. If Equation 4-4 is acceptable, adjust the costs for the denormalized B matrix such that

$$\lambda_3' = 1$$

$$L_2' = \frac{L_2}{B_{PB}^2}$$

(4-5)

$$L_4' = \frac{L_4}{B_{BB}^2}$$

ETC.

6. Find the left half plane roots of the Z matrix for the dermalized B matrix using the costs in Equation 4-5.
7. If (6) is acceptable, solve the matrix Riccati equation to obtain the steady-state gains. If P(SS) is the steady-state solution to the Riccati equation, the gains are

$$K_{OPT} = -\lambda_3^{-1} B' P(SS) \quad (4-6)$$

8. Find the roots of

$$[A + BK_{OPT}] \quad (4-7)$$

and check against those found in step 6 above.

The above eight steps will achieve a stable system if all states are observable. If the control is suboptimal, trial and error will determine the minimum number of states for stable suboptimal control, assuming that Kalman filtering provided noise-free estimates of those states.

4.2 THE OPTIMAL CONTROL PROBLEMS, BASIC EQUATIONS

The goal of optimal control is to minimize the following performance index (PI).

$$PI = \int_0^{\infty} (x' \lambda_2 x + u' \lambda_3 u) dt \quad (4-8)$$

Care must be taken that other, more traditional indices are met (for example, adequate damping at some desired bandwidth).

The quantities which may be varied to achieve the above goals are the relative costs placed on the control and on the system states. The cost on control tends to suppress the control activity, with a corresponding sacrifice in speed of response.

The above PI is minimal if the linear control (References 1, 2) given by

$$u = -\lambda_3^{-1} B' P \hat{x} \quad (4-9)$$

is used. P is the solution to the matrix-Riccati equation

$$\dot{P} = -PA - A'P + PB\lambda_3^{-1}B'P - \lambda_2 \quad (4-10)$$

One method of solving the above is to perform a change of variables. Equation 4-10 is equivalent to

$$P = \overline{YX}^{-1} \quad (4-11)$$

where

$$\begin{bmatrix} \dot{\overline{X}} \\ \dot{\overline{Y}} \end{bmatrix} = \begin{bmatrix} -A & B\lambda_3^{-1}B' \\ \lambda_2 & A' \end{bmatrix} \begin{bmatrix} \overline{X} \\ \overline{Y} \end{bmatrix} = [Z] \begin{bmatrix} \overline{X} \\ \overline{Y} \end{bmatrix} \quad (4-12)$$

The equivalence of Equations 4-11 and 4-12 to Equation 4-10 may be demonstrated by taking the derivative of 4-11 and substituting Equation 4-12 into it. The 2^{nth} order linear first-order differential equation (4-12) has the solution

$$\begin{bmatrix} \overline{X}(t + \tau) \\ \overline{Y}(t + \tau) \end{bmatrix} = \begin{bmatrix} e^{Z\tau} \end{bmatrix} \begin{bmatrix} \overline{X}(t) \\ \overline{Y}(t) \end{bmatrix} \quad (4-13)$$

If the transition matrix is partitioned as follows

$$e^{Z\tau} = \left[\begin{array}{c|c} \theta_{11} & \theta_{12} \\ \hline \theta_{21} & \theta_{22} \end{array} \right] \quad (4-14)$$

it follows from Equations 4-11, 4-13, and 4-14 that

$$P(t + \tau) = [\theta_{21}X(t) + \theta_{22}\bar{Y}(t)] [\theta_{11}X(t) + \theta_{12}\bar{Y}(t)]^{-1} \quad (4-15)$$

Equation 4-15 may be simplified, since $\bar{Y}(t) = P(t)\bar{X}(t)$

$$P(t + \tau) = [\theta_{21} + \theta_{22}P(t)] [\theta_{11} + \theta_{12}P(t)]^{-1} \quad (4-16)$$

Equation 4-16 is used by the Automatic Synthesis Program (ASP) made available to Douglas for this study.

4.3 ROOT LOCATION

The transient characteristic of Equation 4-10 is clearly linked with Equation 4-14. It is reasonable, then, that the performance of the closed-loop system, where $u = \Delta x$, is also given by Equation 4-14 when the gains (Δ) are taken from the steady-state solution of Equation 4-16, where Δ is equal to $-(\lambda_3^{-1}B')$ times the steady-state solution to Equation 4-10. In fact, the $2n$ eigenvalues of

$$Z = \left[\begin{array}{cc} -A & B\lambda_3^{-1}B' \\ \lambda_2 & A' \end{array} \right] \quad (4-17)$$

consist of n left half plane roots and n right half plane roots reflected about the $j\omega$ axis. The n left half plane roots of Z consist of the closed-loop roots of

$$[A + B\Delta]$$

This powerful fact implies that one can change any parameter (an element of A or B), and any cost (an element of λ_2 or λ_3), and the roots of Z will indicate the corresponding effect on the closed-loop poles of the system without having to find the optimal gains corresponding to that condition. This fact has been used in choosing costs.

A simple example can illustrate several points. Consider the unstable first-order system. With zero input, one may write

$$\dot{x} = ax + bu \quad (4-18)$$

If we make the cost on $u = 1$ and the cost on $x = \lambda_2$ (the ratio of λ_2/λ_3 is important, not the absolute value of each), then Equation 4-17 becomes

$$Z = \begin{bmatrix} -a & b^2 \\ 1/2 & a \end{bmatrix} \quad (4-19)$$

Suppose we make $b = 1$, $a = 3$, $\lambda_2 = -7$; then

$$Z = \begin{bmatrix} -3 & 1 \\ 7 & 3 \end{bmatrix} \quad (4-20)$$

The eigenvalues of Z are given by solving for λ_i which satisfy

$$\text{Determinant } (\lambda I - Z) = 0 \quad (4-21)$$

Thus the eigenvalues are +4 and -4. One expects the closed-loop system to have a pole at $S = 4$. To verify this, the matrix Riccati equation (4-10) at steady state requires

$$0 = P^2 - 6P - 7 \quad (4-22)$$

This is satisfied by $P = +7$. Then

$$K_{OPT} = -\lambda_3^{-1} B'P = -7 \quad (4-23)$$

Or, in another way, one can show that e^{ZT} is given in closed form by

$$e^{ZT} = \begin{bmatrix} \left(\frac{1}{8} e^{4T} + \frac{7}{8} e^{-4T}\right) \left(\frac{1}{8} e^{4T} - \frac{1}{8} e^{-4T}\right) \\ \left(\frac{7}{8} e^{4T} - \frac{7}{8} e^{-4T}\right) \left(\frac{7}{8} e^{4T} + \frac{1}{8} e^{-4T}\right) \end{bmatrix} \quad (4-24)$$

Equation 4-24 may be substituted in 4-16. When time approaches infinity, one has

$$P(t + \tau) = \left[\frac{7}{8} e^{4T} + \frac{7}{8} e^{-4T} P(t) \right] \left[\frac{1}{8} e^{4T} + \frac{1}{8} e^{-4T} P(t) \right]^{-1} = 7 \quad (4-25)$$

Using either Equation 4-22 or 4-25, the optimal gain is -7, indicating negative feedback. Since $u = -7x$, Equation 4-18 becomes

$$\dot{x} = (3 - 7)x = -4x \quad (4-26)$$

Thus, the system has a root at $S = +4$, as predicted.

It is most important to notice that Equation 4-20 also has a root at -4 and that Equation 4-22 has a root at -1. If one should find e^{-ZT} by mistake and substitute into Equation 4-16, one would obtain the root of $P = -1$ at steady state. That would require an optimal gain of +7 and, consequently, the unstable root at -4 as predicted by Z . Care must be taken to make the proper definition of Z when the ASP program is used.

4.4 SELECTION OF THE COST RATIO

It is interesting to note that it is the ratio of the costs λ_2/λ_3 that is important rather than their individual values. (For a proof of the analogous statement for state estimation, see subsection 5.2, Theorem 2.)

A demonstration of the truth of this statement for the scalar case follows from Equation 4-17. Note that when Equation 4-17 contains only scalar quantities, the roots of Z are

$$1 \pm \sqrt{a^2 + b^2 \frac{\lambda_2}{\lambda_3}} \quad (4-27)$$

As expected, Equation 4-27 depends only on the ratio of λ_2/λ_3 for some system defined by a and b . Thus, for simplicity, λ_3 can be made equal to 1, with no loss in generality.

As outlined in subsection 4.1, the costs are first approximated by considering the rigid body and first bending dynamics independently. The roots of the combined system, coupled through the control, are evaluated and compared to the desired roots. The roots are then moved into conformance by trial and error adjustments on the costs.

4.5 COST SELECTION FOR RIGID BODY STATES

Consider a system with second-order rigid body dynamics and control applied using the states ϕ and $\dot{\phi}$. This system equation may be written

$$\begin{bmatrix} \ddot{\phi} \\ \dot{\phi} \end{bmatrix} = \begin{bmatrix} 0 & 0 \\ 0 & 1 \end{bmatrix} \begin{bmatrix} \dot{\phi} \\ \phi \end{bmatrix} + \begin{bmatrix} B \\ 0 \end{bmatrix} u \quad (4-28)$$

where

$$u = \begin{bmatrix} -K_1 & -K_2 \end{bmatrix} \begin{bmatrix} \dot{\phi} \\ \phi \end{bmatrix} \quad (4-29)$$

4.5.1 Results

A root square locus (Figure 4-1) was plotted to indicate the effect of changing the cost on ϕ while the cost on $\dot{\phi}$ is zero and the cost on control is constant. Note for increasing cost on θ that the damping ratio is constant but that the bandwidth increases.

A similar plot (Figure 4-2) was made by varying the cost on $\dot{\phi}$ while keeping the cost on control and on ϕ a constant. Note that the bandwidth remains nearly constant but that the damping ratio increases to unity and above as the cost on $\dot{\phi}$ increases. Thus the conclusion that the cost on $\dot{\phi}$ tends to fix the damping ratio while the cost on ϕ tends to fix the bandwidth. If a damping ratio of 0.707 is acceptable, then the cost on ϕ can be used to specify bandwidth.

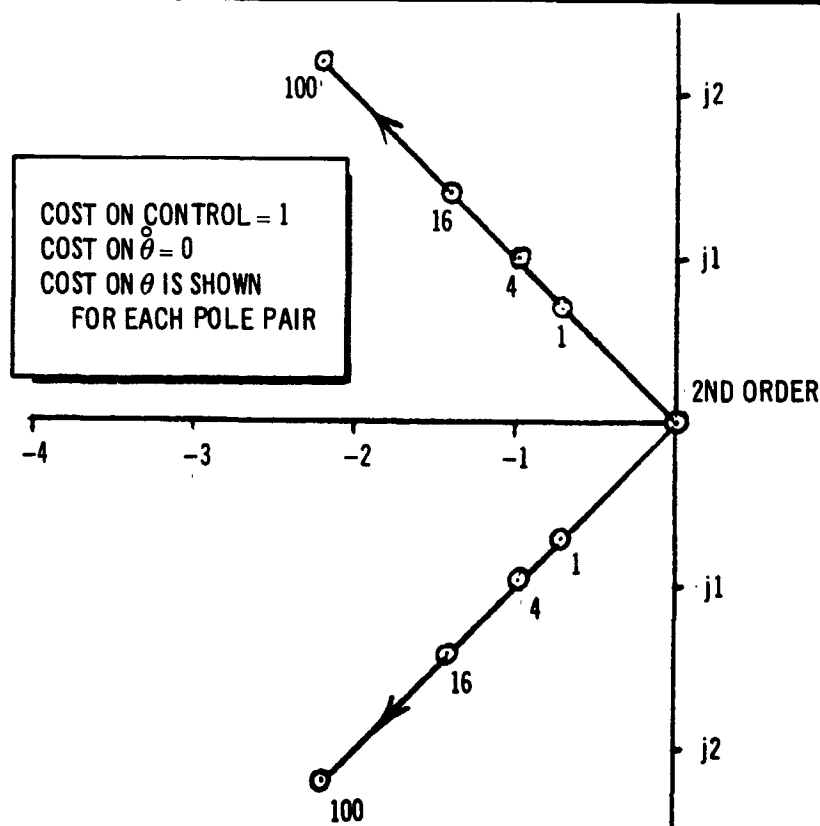


Figure 4-1. Closed-Loop Poles Opposed to Cost for Rigid Body States $\dot{\theta}$ and θ with Zero Cost on $\dot{\theta}$, Increasing Cost on θ

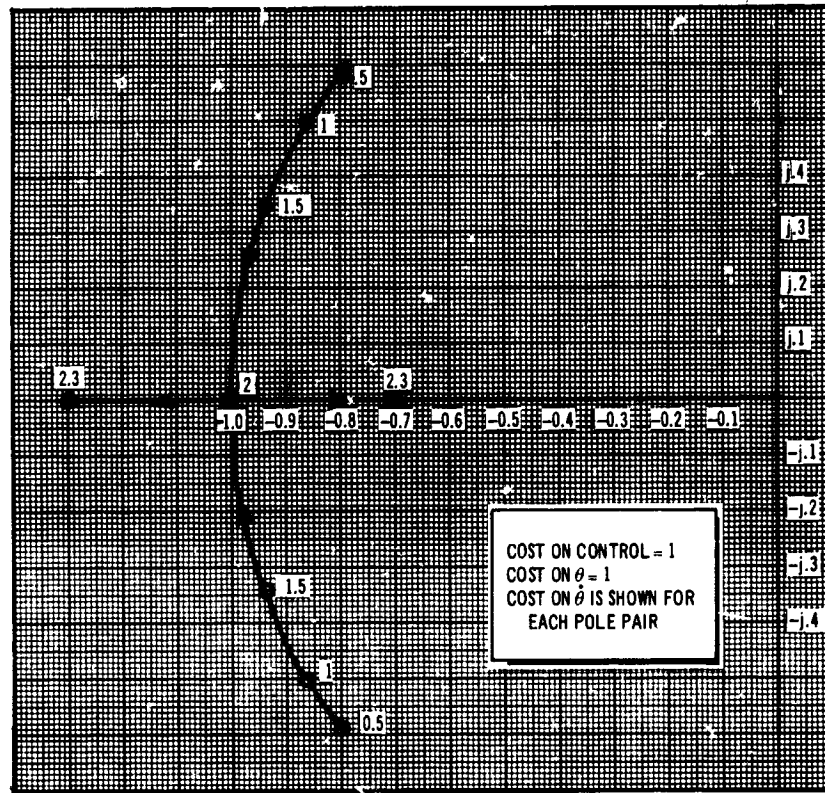


Figure 4-2. Closed-Loop Poles Opposed to Cost for Rigid Body States $\dot{\theta}$ and $\dot{\phi}$, Constant Cost on θ , Increasing Cost on $\dot{\theta}$

If $\lambda_3 = 1$, then the optimal gain (Equation 4-9) for the above case is

$$\Delta = [-BP_{11} \ -BP_{12}] = [-K_1 \ -K_2] \quad (4-30)$$

Suppose that the cost on $\dot{\phi}$ is set at zero and the cost on ϕ is L_2 . Then Equation 4-10 may be written as follows for steady state ($\dot{P} = 0$)

$$-P \begin{bmatrix} 0 & 0 \\ 1 & 0 \end{bmatrix} - \begin{bmatrix} 0 & 1 \\ 0 & 0 \end{bmatrix} P + P \begin{bmatrix} B^2 & 0 \\ 0 & 0 \end{bmatrix} P - \begin{bmatrix} 0 & 0 \\ 0 & L_2 \end{bmatrix} = \begin{bmatrix} 0 & 0 \\ 0 & 0 \end{bmatrix} \quad (4-31)$$

Since P is symmetrical, $P_{12} = P_{21}$. Equation 4-31 can be written as

$$\begin{aligned} B^2 P_{11}^2 - 2P_{12} &= 0 \\ B^2 P_{12}^2 &= L_2 \end{aligned} \quad (4-32)$$

Solving Equation 4-32, we obtain

$$\begin{aligned} BP_{12} &= K_2 = \sqrt{L_2} \\ BP_{11} &= K_1 = \sqrt{\frac{2\sqrt{L_2}}{B}} \end{aligned} \quad (4-33)$$

The transfer function of ϕ/u is easily found to be

$$\frac{\phi}{u} = \frac{B}{s^2 + K_1 s + K_2} \quad (4-34)$$

From Equations 4-33 and 4-34, the bandwidth and damping ratio can be found for the closed-loop rigid body system. The closed-loop rigid body bandwidth is

$$\begin{aligned} \omega_{RB} &= \sqrt[4]{L_2} \\ \text{or} \\ L_2 &= (\omega_{RB})^4 \end{aligned} \quad (4-35)$$

The closed-loop rigid body damping ratio is

$$\xi_{RB} = \frac{\sqrt{2}}{2} \sqrt{\frac{1}{B}} = 0.707 \sqrt{\frac{1}{B}} \quad (4-36)$$

By normalizing B to unity, note that the rigid body damping ratio is 0.707 when $\lambda_3 = 1$. By properly choosing L_2 , the rigid body bandwidth can be set to any desired value using Equation 4-35.

4.6 COST SELECTION FOR BODY BENDING STATES

A typical second-order body bending model is described by the following equation.

$$\begin{bmatrix} \ddot{\eta} \\ \dot{\eta} \end{bmatrix} = \begin{bmatrix} -2\xi\omega & -\omega^2 \\ 1 & 0 \end{bmatrix} \begin{bmatrix} \eta \\ \dot{\eta} \end{bmatrix} + \begin{bmatrix} B \\ 0 \end{bmatrix} u \quad (4-37)$$

where

$$u = [-K_3 \ -K_4] \begin{bmatrix} \dot{\eta} \\ \eta \end{bmatrix}$$

If $\lambda_3 = 1$, then the optimal gain (Equation 4-9) for the above case is

$$\Delta = [-BP_{11} \ -BP_{12}] = [-K_3 \ -K_4] \quad (4-38)$$

Suppose that the cost on $\dot{\eta}$ is equal to zero but the cost on η is equal to L_4 . The matrix Riccati equation (4-10) for steady state may be written as

$$\begin{aligned} B^2 P_{12}^2 + 2\omega^2 P_{12} - L_4 &= 0 \\ B^2 P_{11}^2 + 4\xi\omega P_{11} - 2P_{12} &= 0 \end{aligned} \quad (4-39)$$

The transfer function for this system is given by

$$\frac{\eta}{u} = \frac{1}{s^2 + (2\xi\omega + K_3)s + (\omega^2 + K_4)} \quad (4-40)$$

From Equations 4-38, 4-39, and 4-40, the bandwidth and damping ratio can be calculated for the typical closed-loop body bending system. For simplicity, B is normalized to unity. The closed-loop body bending bandwidth is

$$\omega_{BB} = \sqrt[4]{\omega^4 + L_4} \quad (4-41)$$

The closed-loop body bending damping ratio is

$$\xi_{BB} = \frac{1}{2} \sqrt{2 - \frac{2\omega^2(1 - 2\xi^2)}{\sqrt{\omega^2 + L_4}}}$$

or

$$L_4 = \frac{\omega^4[(1 - 2\xi^2)^2 - (1 - 2\xi_{BB}^2)^2]}{(1 - 2\xi_{BB}^2)^2} \quad (4-42)$$

Therefore, Equation 4-42 may be used to select a cost L_4 on η under the constraints that $\lambda_3 = 1$ and $B = 1$. The corresponding bandwidth for the selected L_4 can be calculated from Equation 4-41.

A root square locus (Figure 4-3) was plotted to indicate the effect of changing the cost on η while the cost on $\dot{\eta}$ is zero and the cost on control is constant. Note for increasing cost on η that the damping ratio and bandwidth both increase.

A similar plot (Figure 4-4) was made by varying the cost on $\dot{\eta}$ while keeping the cost on control and on η a constant. Note that the bandwidth remains nearly constant but that the damping ratio increases to unit and above as the cost on $\dot{\eta}$ increases. As a conclusion, a single cost on η is sufficient to set the bandwidth and damping ratios at a desired level.

4.7 OPTIMAL CONTROL DESIGNS

Consider the equations for System 4-1. This system contains two rigid body modes and two body bending modes. The open-loop bending mode has a frequency of 2.21 radians/sec with a damping ratio of 0.0050. It is desired to apply control so as to achieve closed-loop poles such that the time constant ($\xi\omega$) is about 0.75 for both rigid body and body bending modes.

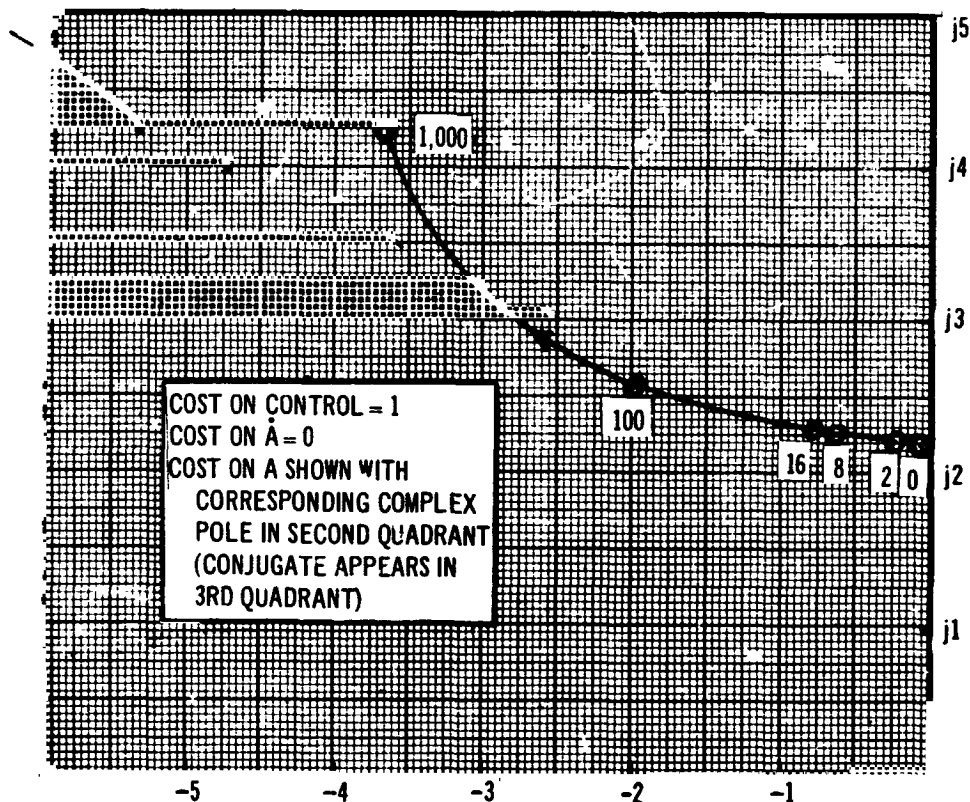


Figure 4-3. Closed-Loop Poles Opposed to Cost for Body Bending States \dot{A} and A , with Zero Cost on \dot{A} , Increase Cost on A

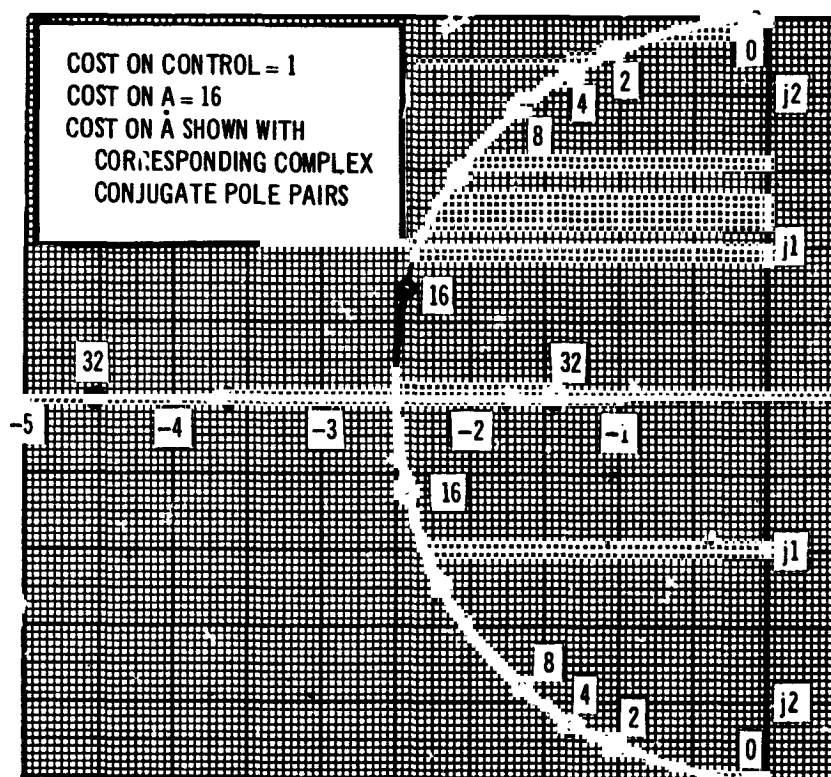


Figure 4-4. Closed-Loop Poles Opposed to Cost for Body Bending States A and \dot{A} , With Constant Cost on A , Increasing Cost on \dot{A}

$$\xi_{RB} = 0.7$$

$$\omega_{RB} \approx (1/2)(2.21 \text{ rad/sec}) = 1.105$$

$$\xi_{BB} = 0.3$$

$$\omega_{BB} \approx 2.5$$

(4-43)

Table 4-1 indicates the actual damping ratios and bandwidths for the combined fourth-order system as well as root locations. Note that when $L_2 = 1.5$ and $L_4 = 15$ the following parameters were realized for System 4-1 by using the steady-state gains

$$\xi_{RB} = 0.68$$

$$\omega_{RB} = 0.984$$

$$\xi_{BB} = 0.351$$

$$\omega_{BB} = 2.51$$

(4-44)

Figure 4-5 contains a plot of the roots for System 4-1 when the cost on η was varied and the cost on control and on ϕ was a constant. This plot may be compared with Figures 4-1 and 4-3. Note that increasing the cost on η while holding the cost on ϕ constant has the same effect on the rigid body poles as decreasing the cost on ϕ in Figure 4-1.

Note from Table 4-1 that the following parameters resulted for the denormalized uncoupled fourth-order system (4-2).

$$\xi_{RB} = 0.68$$

$$\omega_{RB} = 0.923$$

$$\xi_{BB} = 0.366$$

$$\omega_{BB} = 2.73$$

(4-45)

Table 4-1
OPTIMAL CONTROL GAINS AND CLOSED-LOOP POLES FOR
SYSTEMS 4-1, 4-2, 4-3, 6-4, 6-5, and 6-6

System	Cost Coefficients										Optimal Gain				Closed-Loop Poles									
	Control					ϕ					η_1				η_2				Rigid Body		First Bending		Second Bending	
	λ_3	ϕ	L_1	L_2	L_3	ϕ	K_2	ϕ	K_1	η_1	K_4	η_1	K_3	η_2	K_6	ξ_{RB}	ω_{RB}	ξ_{BB1}	ω_{BB1}	ξ_{BB2}	ω_{BB2}			
4-1	1	0	1.5	0	3	-1.7613	-1.2248	-0.4812	-1.3102			0.696	1.08	0.159	2.38									
4-1	1	0	1.5	0	15	-2.0120	-1.224	-0.95	-3.186			0.68	0.984	0.351	2.51									
4-1	1	0	1.5	0	150	-2.793	-1.225	-1.773	-11.537			0.606	0.606	0.594	3.59									
4-2	1	0	11	0	0.1	3.3166	5.6823	-0.2636	-1.0751			0.680	0.923	0.366	2.56									
4-3	1	0	11	0	0.1	3.3166	5.6823	-0.2636	-0.0757			0.705	0.940	0.346	2.73									
6-4	1	0	11	0	0.1	0	0.33	3.3730	5.7934	-0.2212	-0.1010	-0.3939	-0.0667	0.690	0.953	0.302	2.62	0.197	5.43					
6-5	1	0	11	0	0.1	0	0.33	5.651	6.907	-0.2704	-0.0753	-0.4195	-0.0552	0.80	1.12	0.312	2.86	0.205	6.17					
6-6	1	0	11	0	0	0	0.33	3.3133	4.2217	-0.3073	-0.0447	-0.5004	-0.0182	0.66	1.26	0.336	5.5	0.526	9.26					

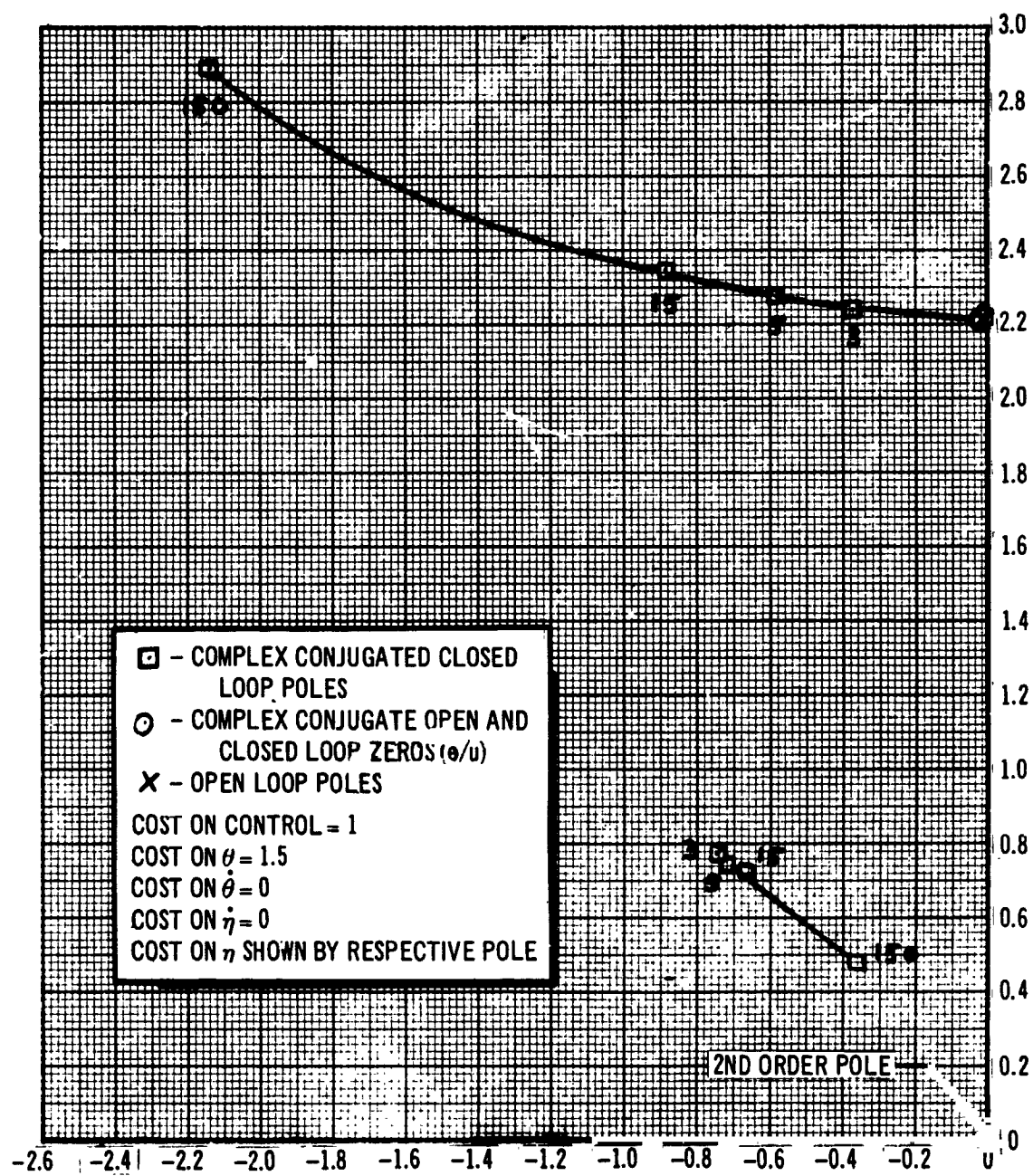


Figure 4-5. Root Square Locus of System Roots for System 4-1

Parameters (Equation 4-45) are sufficiently close to Equation 4-43 to be acceptable. The next application is to a coupled four-dimensional system (4-3). This system is merely System 4-2 with all coupling included between the rigid body states and the body bending states. The optimal steady-state gains from System 4-2 were used in conjunction with System 4-3. Note from Table 4-1 that the parameters changed somewhat (5 to 10%) but that the values are still acceptable.

Actuator dynamics added to System 4-3 result in the seventh-order system (7-1). The optimal gains for each state ($\phi, \dot{\phi}, \eta, \dot{\eta}, \beta, \dot{\beta}, \ddot{\beta}$) using costs (11, 0, 0.1, 0, 0, 0, 0) were respectively (+3.3165, +5, 9831, -0.2236, -0.0984, -0.3085, -0.0025, -0.0001). The rigid body and body bending parameters were

$$\begin{aligned}\xi_{RB} &= 0.684 \\ \omega_{RB} &= 0.948 \\ \xi_{BB} &= 0.360 \\ \omega_{BB} &= 2.54\end{aligned}\tag{4-46}$$

The actuator poles were at very nearly their open-loop values

$$\begin{aligned}-6.57 \pm j53.63 \\ -10.56\end{aligned}$$

As a result of the above, one may conclude that actuator dynamics are separable from the system's dynamics with little loss in accuracy. The reason is, of course, that actuator singularities are far removed from the systems natural frequencies.

Inclusion of higher bending modes is now considered. Systems 6-4, 6-5, and 6-6 include two rigid body states, two states for the first bending mode (as in 4-2 and 4-3), and two additional states for the second bending mode.

The desired bandwidth and damping ratios for the second bending mode are

$$\begin{aligned}\xi_{BB2} &= 0.2 \\ \omega_{BB2} &\approx 6\end{aligned}\tag{4-47}$$

The time constant ($\xi\omega$) is 1.2 and therefore the second bending mode signals will settle out faster than rigid body and first bending signals.

The costs shown in Table 4-1 were used for System 6-4. The cost L_6 was made equal to 0.33 to be an even multiple of all other costs. Note that the desired parameters of Equations 4-43 and 4-44 were met with reasonable accuracy.

System 6-4 and Systems 4-2 and 4-3 refer to conditions 24 sec into flight. The same costs were used for the sixth-order system at maximum dynamic pressure (6-5) and at burnout (6-6). Note that sufficient damping is in evidence for the first and second bending modes and that the rigid body damping and bandwidth are adequate. Optimum gain changes for different flight conditions would require selective switching of gains simply as a function of time or as certain values of the system parameters are estimated.

BLANK PAGE

Section 5

STATE ESTIMATION

The primary considerations in the state estimation filter design are reduced dimensionality, system stability, parameter insensitivity, and system response. For this application, the general form of filter Equations 2-9 and 2-10 can be reduced to

$$K = PH' R^{-1} \quad (5-1)$$

$$O = AP + PA' + PH'R^{-1}HP + GQG' \quad (5-2)$$

which uses the steady-state solution of the filtering. The system sensor noise is assumed uncorrelated with the plant disturbance, i. e., $C = 0$. The object of this filtering is to approximate the performance of the systems developed with optimal feedback gains (Section 4), using only the available sensor signal information.

5.1 SYSTEM OBSERVABILITY

An investigation was made early in the program to determine if any states were unobservable. Such states would cause divergence of the filter Riccati equation and frustrate any attempts to adjust their dynamic characteristics. A necessary and sufficient condition (Reference 13) for complete observability is that the matrix

$$[H^*, A^*H^*, \dots, A^{*n-1}H^*]$$

must have rank n , where n is the dimension of the system. To determine the observability problems which might be encountered, System 4-1 was set up in symbolic form, as shown in Figure 5-1. It includes rigid body rotation

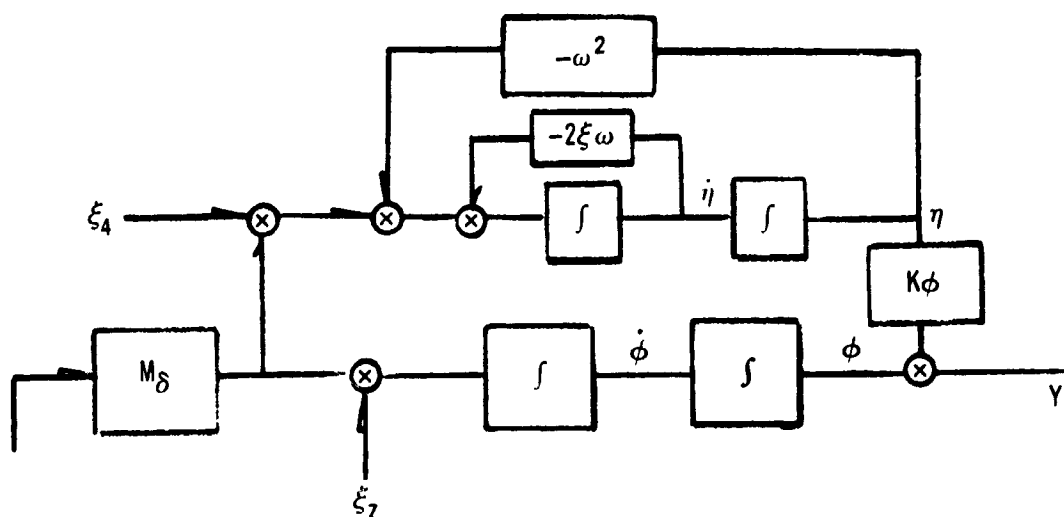


Figure 5-1. System 4-1, Symbolic Version

and a single bending mode. A single attitude gyro is assumed. The state equation can be written

$$\begin{Bmatrix} \dot{\phi} \\ \ddot{\phi} \\ \dot{\eta} \\ \ddot{\eta} \end{Bmatrix} = \begin{bmatrix} 0 & 1 & 0 & 0 \\ 0 & 0 & 0 & 0 \\ 0 & 0 & 0 & 1 \\ 0 & 0 & -\omega^2 & -2\xi\omega \end{bmatrix} \begin{Bmatrix} \phi \\ \dot{\phi} \\ \eta \\ \dot{\eta} \end{Bmatrix} + \begin{bmatrix} 0 \\ M_\delta \\ 0 \\ M_\delta \end{bmatrix} u + \begin{bmatrix} 0 \\ \xi_2 \\ 0 \\ \xi_4 \end{bmatrix} \quad (5-3)$$

$$Y = [1 \ 0 \ K_\phi \ 0] \{\phi \ \dot{\phi} \ \eta \ \dot{\eta}\}' \quad (5-3a)$$

Applying the observability criterion to this system, one obtains

$$\begin{bmatrix} 0 & 1 & 0 & 0 \\ 1 & 0 & 0 & 0 \\ 0 & K_{\phi} & -2\xi\omega K_{\phi} & \omega^2(4\xi^2 - 1)K_{\phi} \\ K_{\phi} & 0 & -\omega^2 K_{\phi} & 2\xi\omega^3 K_{\phi} \end{bmatrix} \quad (5-4)$$

which has a determinant equal to

$$\omega^4 K_{\phi}^2$$

which indicates the system is completely observable unless K_{ϕ} is zero. This would occur if the gyro were placed on the bending mode antinode. This will likely hold true for the system of Model Specification No. 2 as well, indicating all states are observable unless all sensors are on the antinodes of a dynamical mode.

5.2 SOME USEFUL THEOREMS

5.2.1 Theorem 1

Assuming no parameter errors in the Kalman filter, the system stability characteristics are identical with the corresponding completely observable system

Proof: repeating Equation 2-8

$$\dot{\underline{x}} = A\underline{x} + Bu + K(\underline{Z} - H\underline{x})$$

discarding the sensor noise input, since it has no effect on stability,

$$\dot{\underline{x}} = A\underline{x} + Bu + KH(\underline{x} - \hat{x}) \quad (5-5)$$

letting

$$\underline{\tilde{x}} \triangleq \underline{x} - \underline{\hat{x}} \quad (5-6)$$

then

$$\dot{\underline{\tilde{x}}} = \dot{\underline{x}} - \dot{\underline{\hat{x}}} \quad (5-7)$$

substituting in Equations 2-1 and 5-5 into 5-7 and solving for $\dot{\underline{\tilde{x}}}$

$$\dot{\underline{\tilde{x}}} = (A - KH)\underline{\tilde{x}} + G\dot{\underline{\xi}}$$

which has a time solution

$$\underline{\tilde{x}} = e^{(A-KH)t}\underline{\tilde{x}}_0 + \int_0^t e^{(A-KH)(t-\tau)} G\dot{\underline{\xi}}(\tau) d\tau \quad (5-8)$$

but the system driving functions do not affect stability so they can be zeroed in Equation 5-8. This leaves

$$\underline{\tilde{x}} = \underline{0} \quad (5-9)$$

Substituting Equations 5-9 and 5-6 into 5-5 gives

$$\dot{\underline{\hat{x}}} = A\underline{\hat{x}} + B\underline{u} \quad (5-10)$$

The time solution is

$$\underline{\hat{x}} = \int_0^t e^{A(t-\tau)} B \underline{u} d\tau \quad (5-11)$$

but, omitting the disturbance from Equation 2-1 gives

$$\underline{x} = \int_0^t e^{A(t-\tau)} B \underline{u} d\tau \quad (5-12)$$

comparing Equation 5-12 to 5-11 shows

$$\hat{x}(u) = x(u) \quad (5-13)$$

Therefore, if the system is shown as in Figure 5-2a, the identity of Equation 5-13 allows the reduction to Figure 5-2b.

It is interesting to note that the proof is not dependent on K. This K-matrix need not be the Kalman gain matrix. However, if it is not the Kalman gain, the filter may have some unexcited poles in the right half plane.

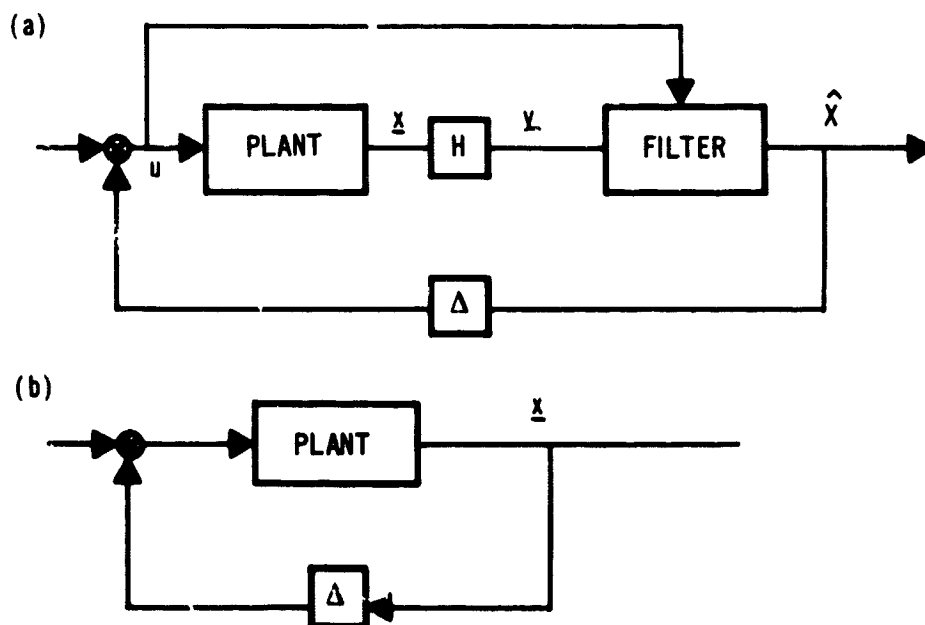


Figure 5-2. System Reduction by Theorem 1

5.2.2 Theorem 2

The Kalman filter is not dependent on the absolute values of the disturbance and noise levels, but only their ratio; i. e.,

$$K(Q, R) = K(CQ, CR) \quad (5-14)$$

Proof: referring to Equations 5-1 and 5-2, suppose CR is substituted for R and CQ for Q, where C is a scalar constant that controls the scaling of Q and R. C can be changed at will without the ratio

$$[CQ] [CR]^{-1}$$

changing. And, with these substitutions, suppose the dependent variables of Equations 5-1 and 5-2 are P^* and K^* ; then, these equations become

$$0 = -P^*A' - AP^* + P^*H' \frac{1}{C} R^{-1} HP^* - GCQG' \quad (5-15)$$

$$K^* = P^*H' \frac{1}{C} R^{-1} \quad (5-16)$$

for a trial solution of Equation 5-15,

$$P^* = CP \quad (5-17)$$

then Equation 5-14 becomes

$$f = -CPA' - ACP + CPH' \frac{1}{C} R^{-1} HCP - GCQG' \quad (5-18)$$

To verify Equation 5-17, f must be equal to zero. Since C is a scalar, it can be permuted with the matrixes to give

$$f = C[-PA' - AP + PH'R^{-1}HP - GQG'] \quad (5-19)$$

but the term in brackets is zero by Equation 5-1, so f is zero and Equation 5-17 is verified. Substituting Equation 5-17 into 5-16

$$K^* = CPH' \frac{1}{C} R^{-1} \quad (5-20)$$

$$K^* = PH'R^{-1} \quad (5-21)$$

Comparing Equation 5-21 with 5-1 shows $K^* = k$. Therefore the K matrix and the filter are independent of the scale factor C and the theorem is proved.

5.3 A SMALL SYSTEM STUDY

To gain insight into the workings of Kalman filtering, a small plant was set up and analyzed. (See Figure 5-3.)

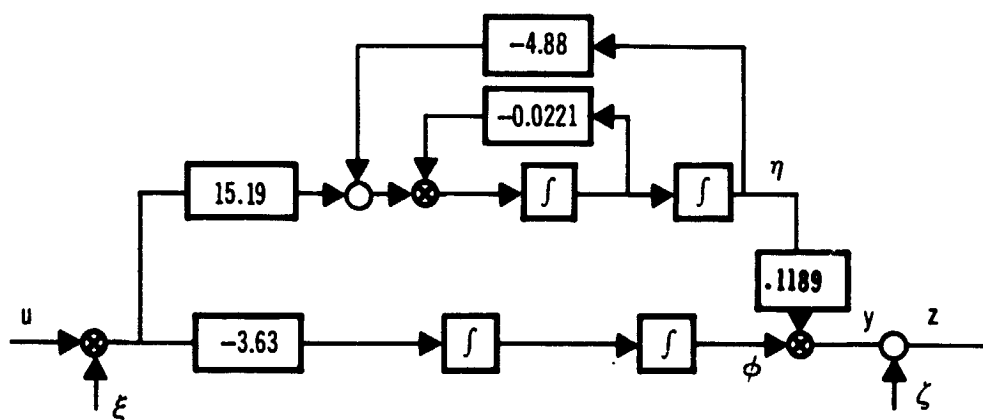


Figure 5-3. 4D Study System

This system was developed early in the work as an approximation of the system at $t = 24$ sec. It includes rigid body rotation and the first bending mode. Coupling terms between bending and rigid body rotation and aerodynamic moment are omitted. A single sensor, an attitude gyro at Station 120M, is assumed. This is System 4-2, presented in subsection 3.3. Figure 5-4 shows the transient solution of a typical set of Kalman gains for this system. The steady-state gains are plotted against the signal-to-noise ratio in Figure 5-5.

If the control loop in Figure 2-1 is opened, the block diagram can be arranged in the form shown in Figure 5-6.

Figure 5-16 illustrates the point that Kalman estimation is a blended combination of a modeling response $\underline{\hat{x}}_1/u$ and a filtered response to the sensor signals $\underline{\hat{x}}_2/y$. By Theorem 1 in subsection 5.2.1, the sum of the two parallel paths, $\underline{\hat{x}}_1/u + \underline{\hat{x}}_2/u$ must equal \underline{x}/u .

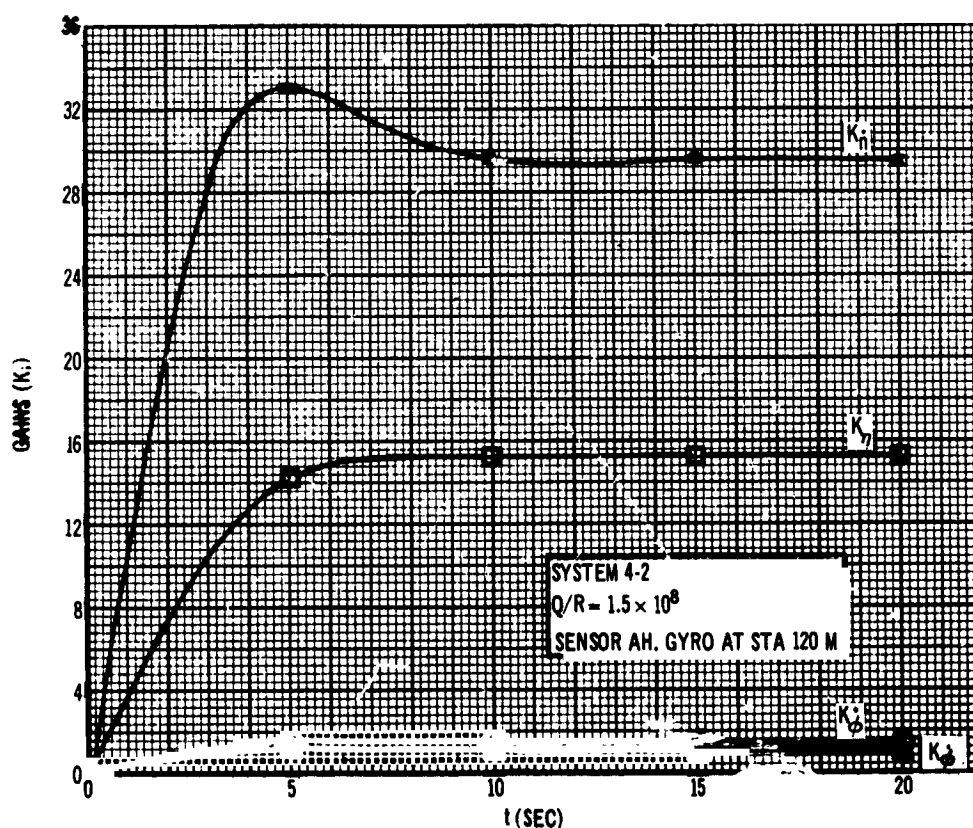


Figure 5-4. Kalman Gain Transient Solutions

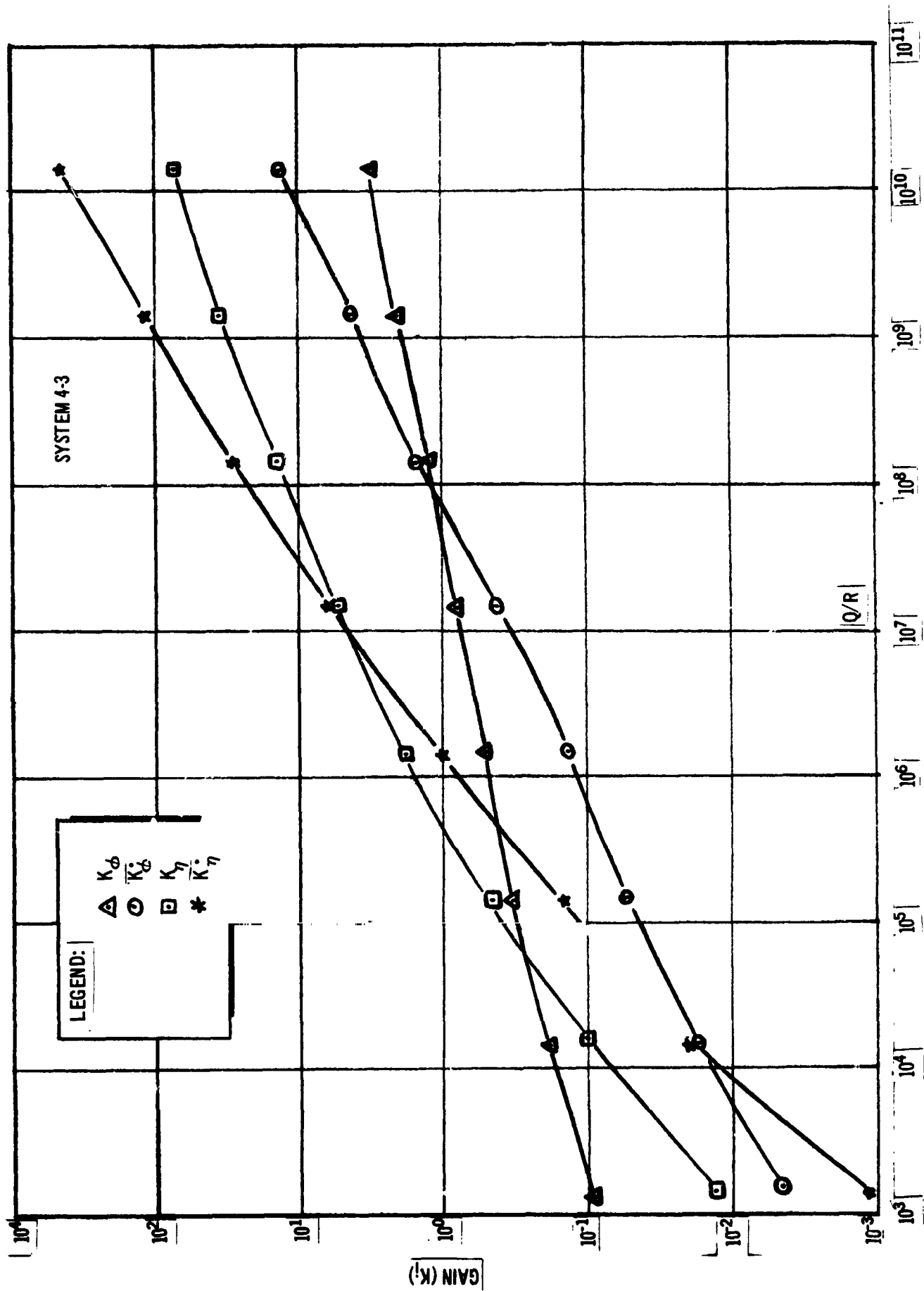


Figure 5-5. Steady-State Kalman Gains as a Function of Q/R

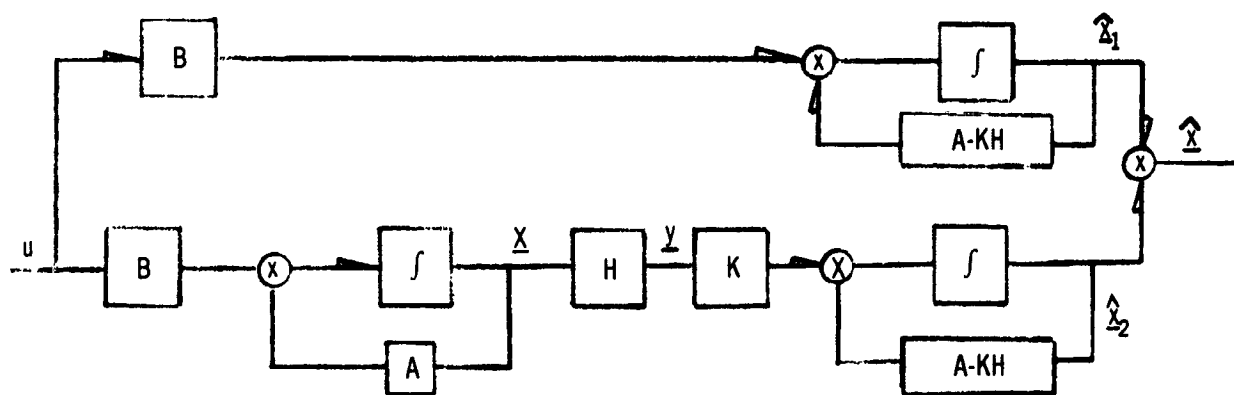


Figure 5-6. Plant Filter Combination Rearranged

Suppose one wishes to estimate ϕ in the system of Figure 5-3. Figure 5-7 shows the Bode gain and phase response curves of y_ϕ/β and y_η/β deviation. The Bode gain curves can be thought of as square roots of the spectral density curves with a unity amplitude white noise disturbance (ξ). Bode gains rather than spectral densities are used because phase is lost with spectral density. Figure 5-8 shows the Bode gain and phase of the total sensor signal response to β inputs. Figure 5-9 shows the gain and phase response curves of the filter response to sensor signals ($\hat{\phi}_2/y$). Comparing Figure 5-9 with the Bode gain in Figure 5-7 shows the filter gains are high, when the ϕ -signal is large compared to the η and v signals. Figures 5-10 and 5-11 show the total gain and phase for the upper and lower paths for the low noise ($Q/R = 7.5 \times 10^7$, slow filter) and high noise ($Q/R = 7.5 \times 10^5$, slow filter) cases.

Notice how in each case the model compensates for the attenuation on the signal of the sensor filter to reconstruct the true response to command signals.

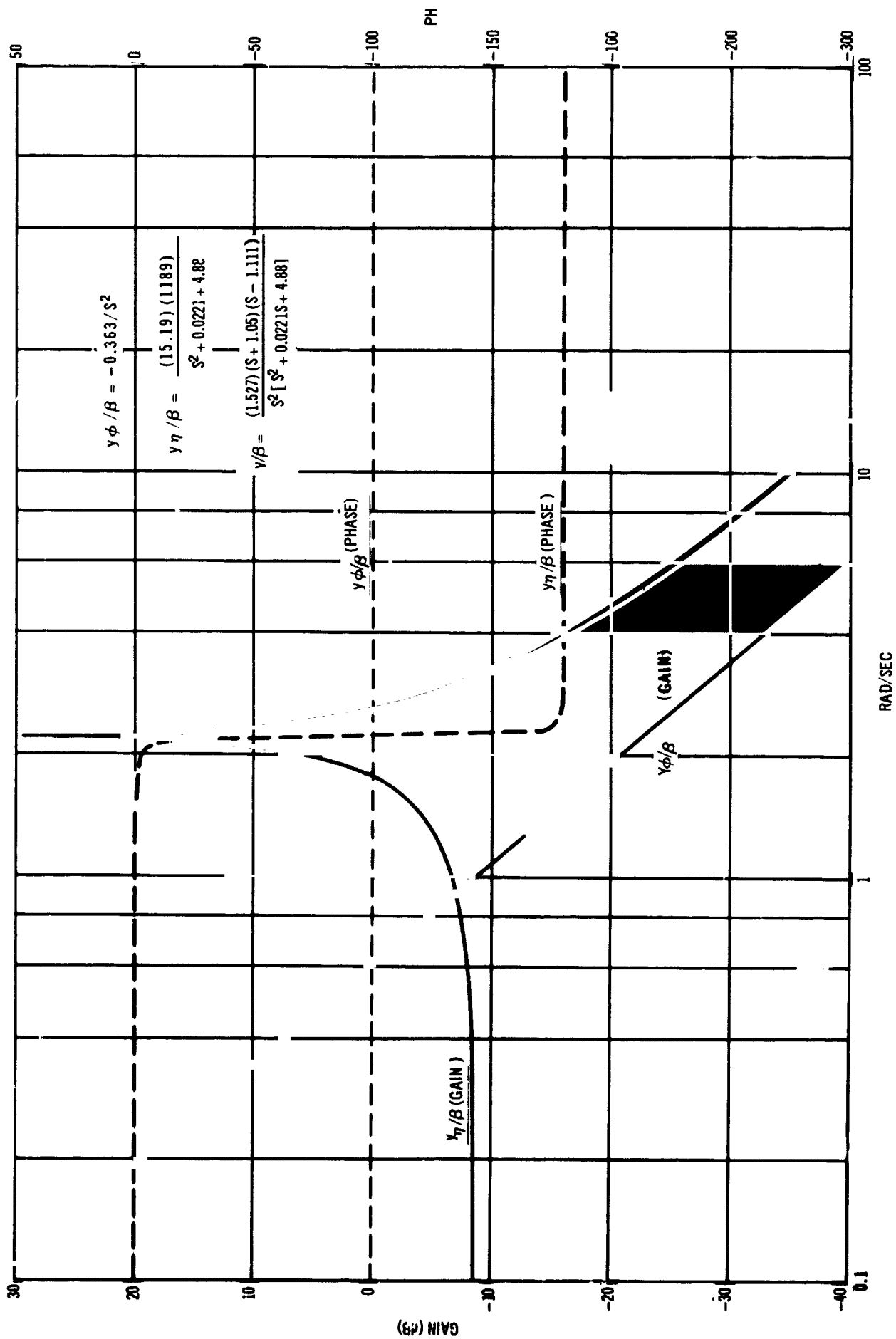


Figure 5-7. Body Response Curves, System 4-2

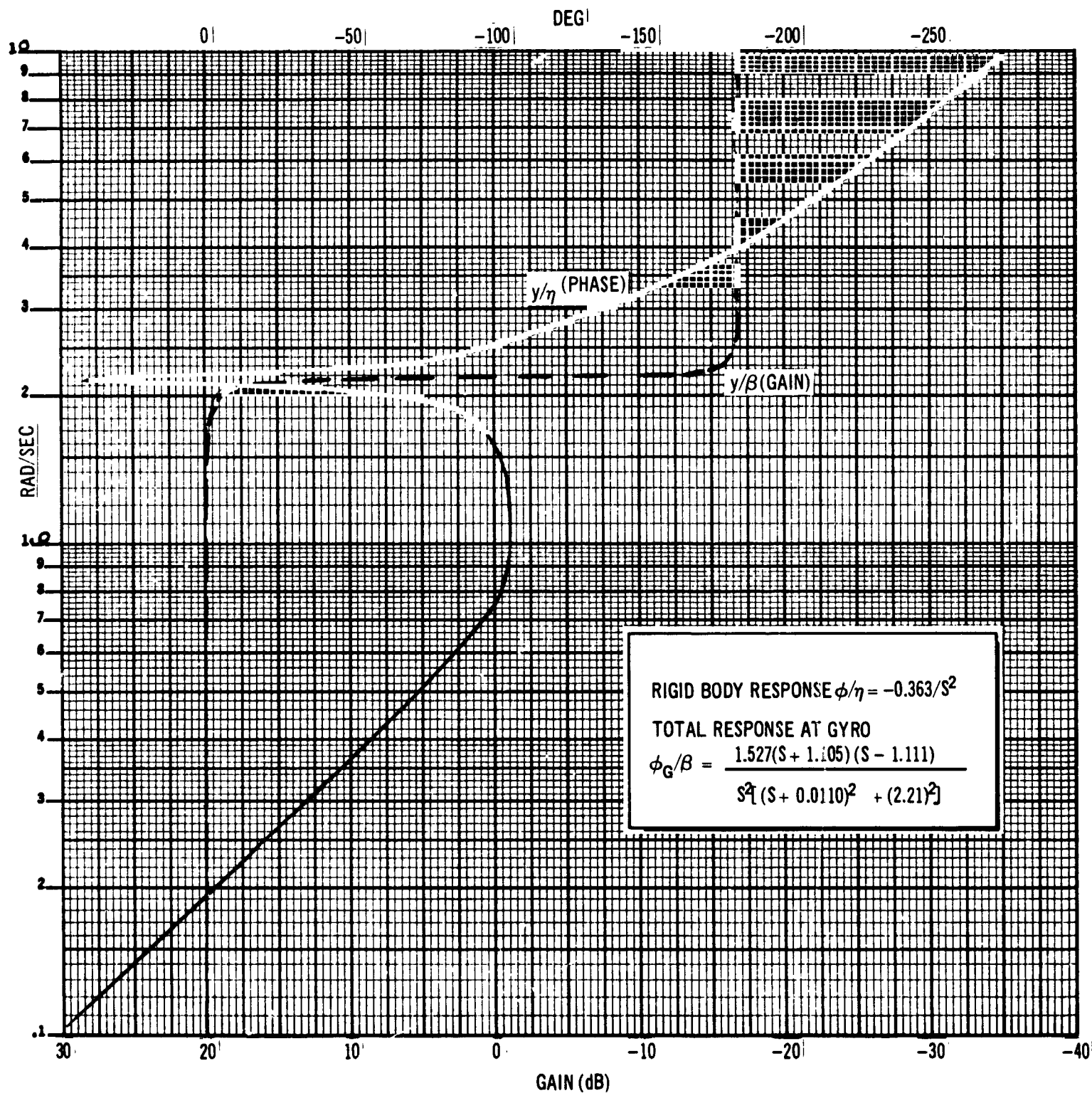


Figure 5-8. Sensor Bode Response to Commands

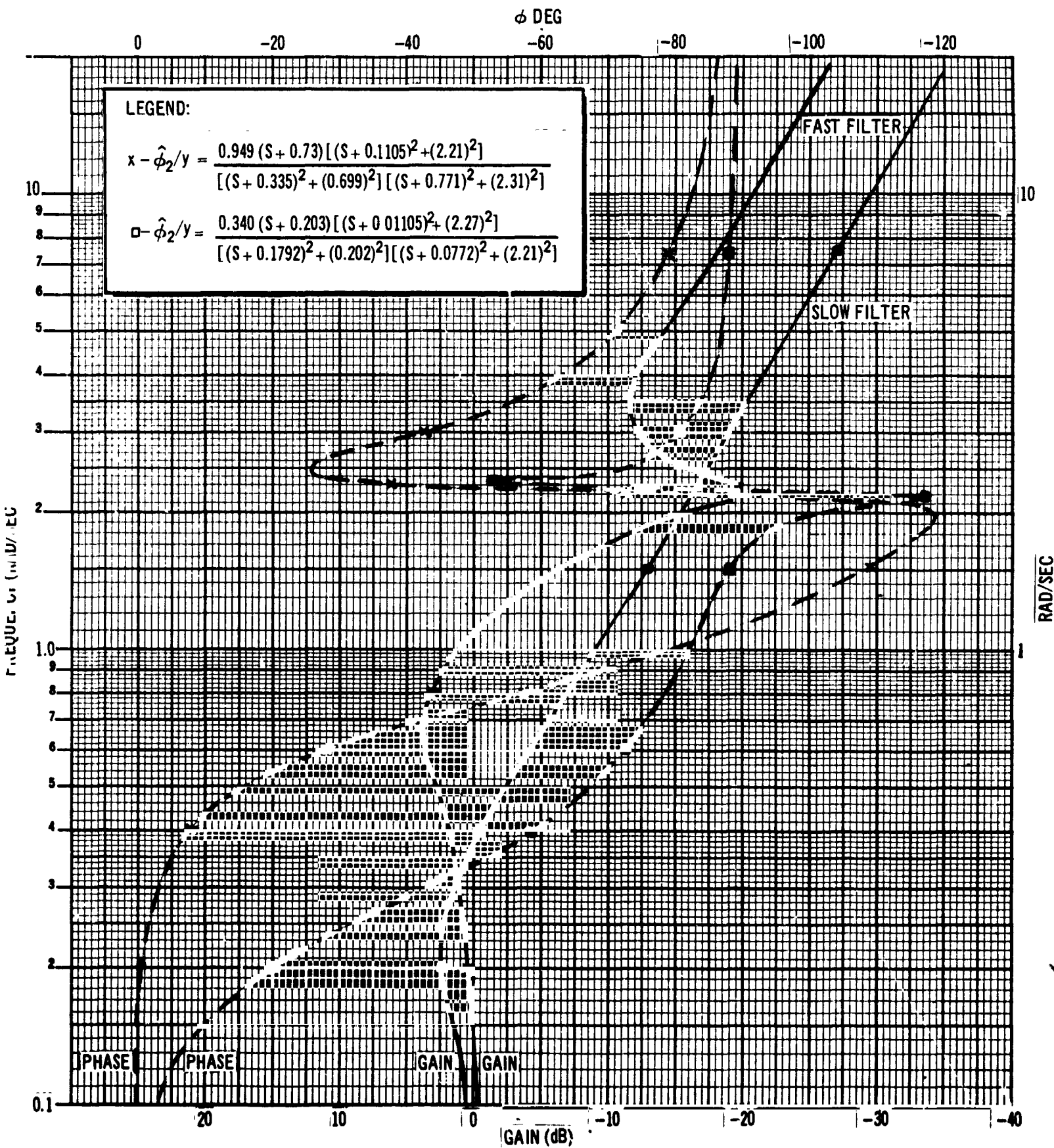


Figure 5-9. Kalman Filter Bode Gains

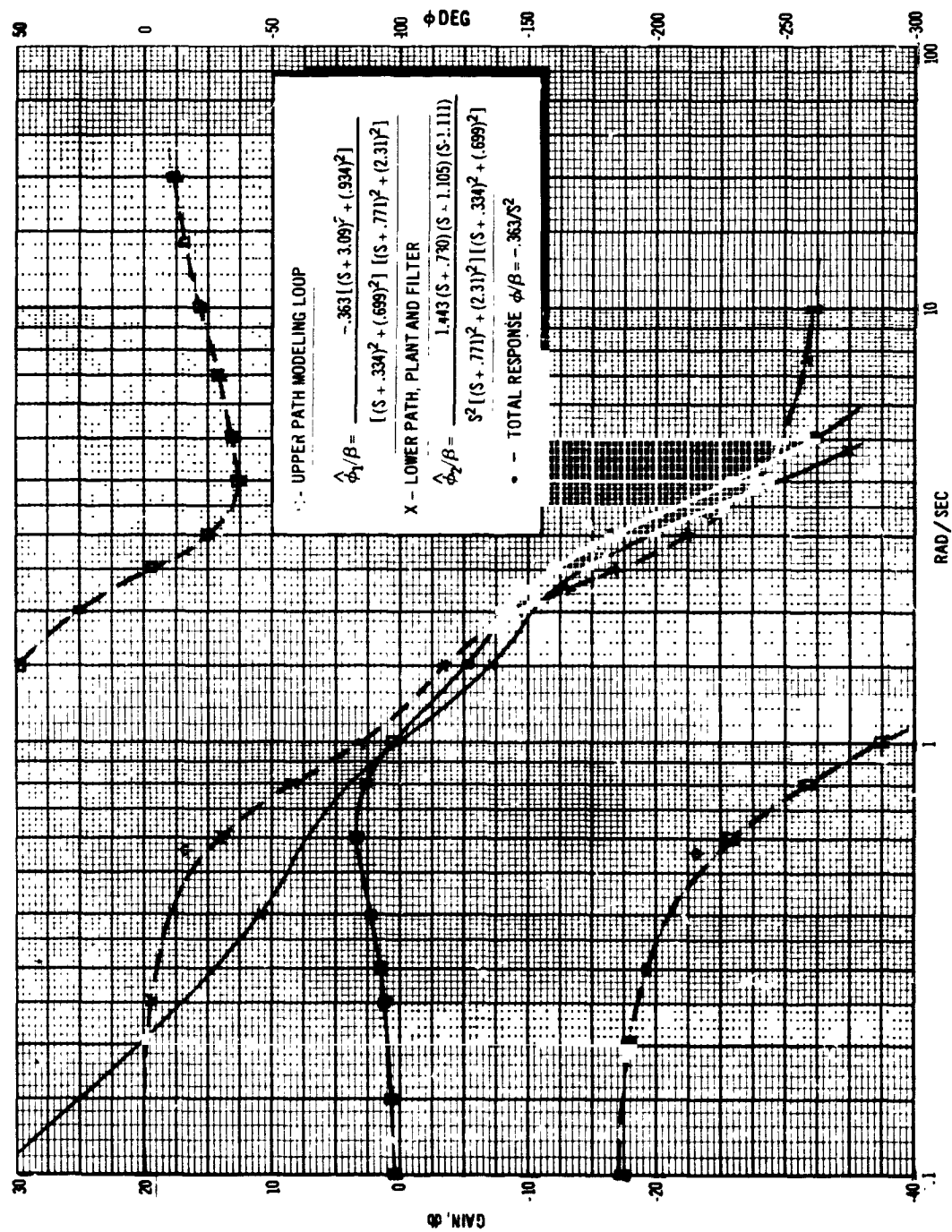


Figure 5-10. Low-Noise System Bode Gains

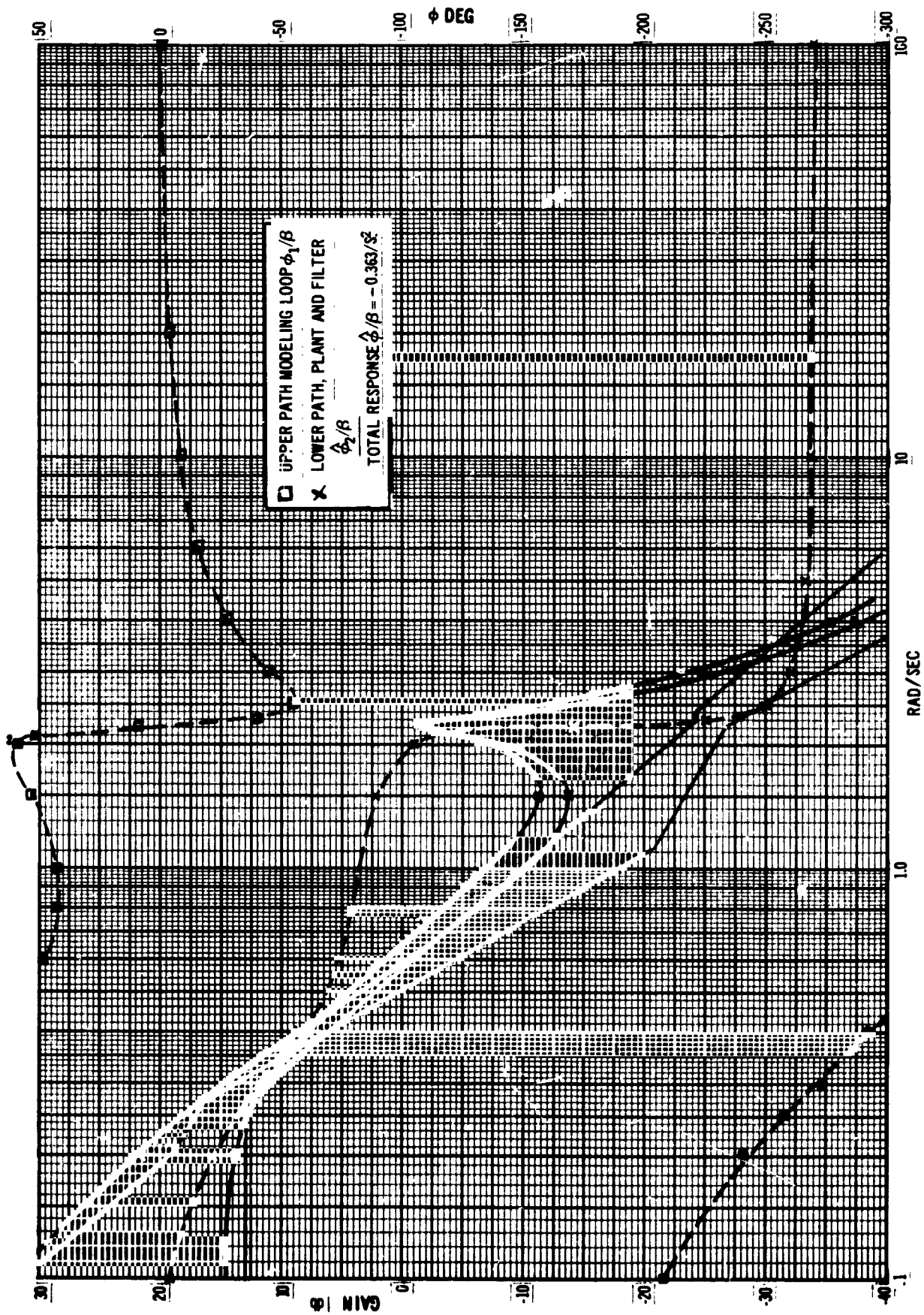


Figure 5-11. High-Noise System Bode Gains

This system, along with the corresponding optimal gains, was also considered in closed-loop form, setting the block diagram of Figure 2-1 up as shown in Figure 5-12.

The outside loop was broken and a root locus plot made using the Kalman gains for $Q/R = 7.5 \times 10^7$. This root locus plot is shown in Figure 5-13a. Notice that the closed-loop poles of this system are in the same place as those in Figure 4-5, as Theorem 2 dictates they must be.

To gain insight into the filter behavior with additional unknown states in the plant, a second bending mode was added to the model, forming System 6-2. The resulting root locus plot is shown in Figure 5-13b. The system is stable but some distortion of the rigid body and second bending closed-loop poles have taken place. Figure 5-13c is the plot for the same system but with the sign on the second bending mode influence coefficient at the sensor reversed. Again the system is stable. Figure 5-13d was made with a different set of control gains, i.e.,

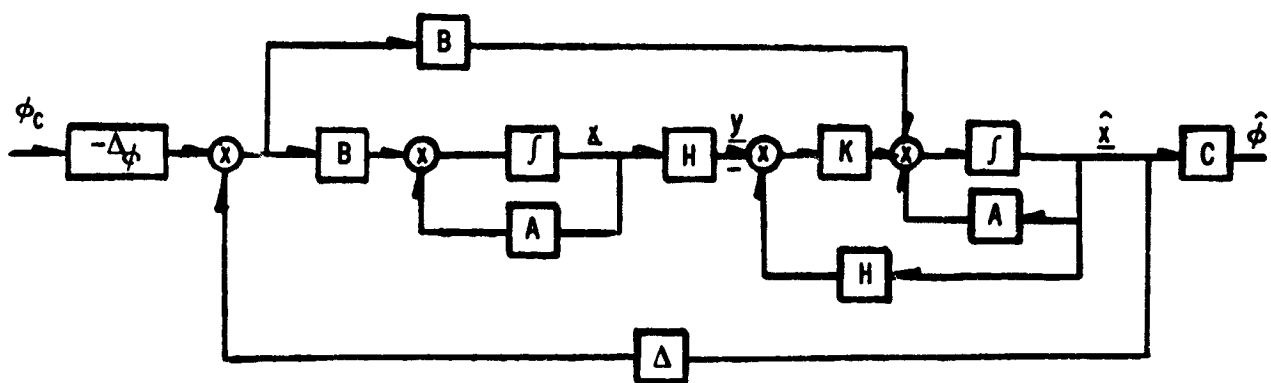


Figure 5-12. System Block Diagram Rearranged for Root Locus Analysis

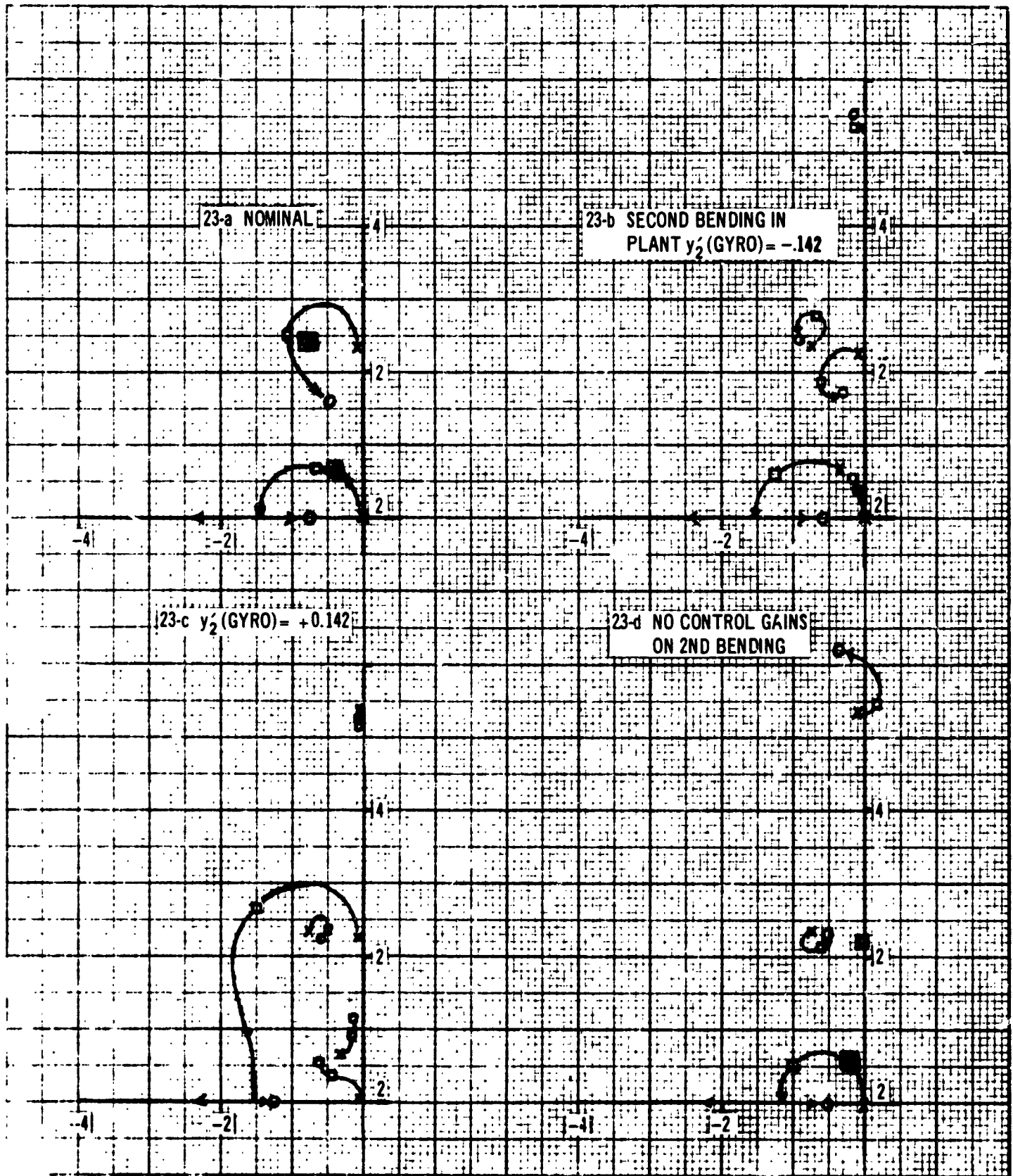


Figure 5-13. Study System Root Locus Plots

$$\beta = [2.51, 3.36, 0, 0]\underline{x} \quad (5-22)$$

which with complete observability would place the rigid body poles in the same place as they are in 5-13a but would merely open the loop on the first bending mode. Figure 5-13d shows the result with the 4-dimensional filter. The system is obviously unstable. In this system, putting a control gain on the first bending mode has aided stability with respect to the neglected states.

5.4 FILTER DIMENSION REDUCTION

Referring to the general system state Equation 2-1, let it be partitioned into two coupled subsystems, the 1-system containing the portion of the plant to be assumed by the filter and the 2-system to be neglected by the filter. Equation 2-1 can be partitioned as follows:

$$\begin{Bmatrix} \dot{\underline{x}}_1 \\ \dot{\underline{x}}_2 \end{Bmatrix} = \begin{bmatrix} A_{11} & A_{12} \\ A_{21} & A_{22} \end{bmatrix} \begin{Bmatrix} \underline{x}_1 \\ \underline{x}_2 \end{Bmatrix} + \begin{bmatrix} B_1 \\ B_2 \end{bmatrix} \underline{u} + \begin{bmatrix} G_1 \\ G_2 \end{bmatrix} \underline{\xi} \quad (5-23)$$

$$\underline{Z} = [H_1 \quad H_2] \underline{x} + \underline{v} \quad (5-23a)$$

The block diagram of Figure 2-1 will be somewhat altered because of the discrepancy between the plant and the plant model in the filter. This discrepancy is shown in Figure 5-14.

5.4.1 High-Frequency State, Steady-State Substitution

This approach assumes one can substitute the steady-state solution for the transient solution of the higher-order states. Inspection of the filter Bode gain plots for the 4-dimensional study system shown in Figure 5-7 shows that the filter cuts off the signal above the break frequency of the state in question. With this approach, it is assumed it does not matter what the high-frequency state gain and phase plots look like above the break frequencies of the low-frequency states. For the high-order bending modes, with their very low damping, and for the actuator, the phase lags are approximately

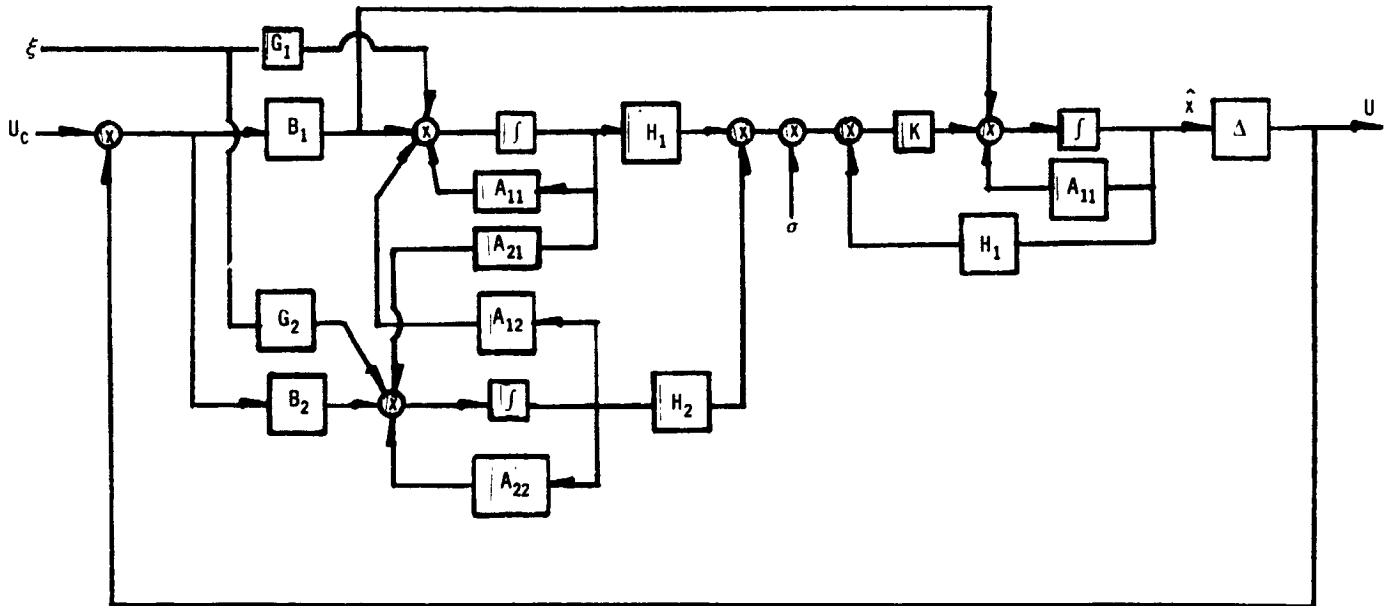


Figure 5-14. System Block Diagram with Reduced Order Filter

zero in the filter region of interest, reflecting the applicability of the steady-state solution.

From

$$\dot{\underline{x}}_2 = A_{21}\underline{x}_1 + A_{22}\underline{x}_2 + B_2\underline{u} + G_2\underline{\xi} \quad (5-24)$$

In Laplace form,

$$\underline{x}_2^s = A_{21}\underline{x}_1 + A_{22}\underline{x}_2 + B_2\underline{u} + G_2\underline{\xi} \quad (5-25)$$

or

$$\underline{x}_2 = [I_s - A_{22}]^{-1} [A_{21}\underline{x}_1 + B_2\underline{u} + G_2\underline{\xi}] \quad (5-26)$$

The question of whether A_{22} has an inverse has been checked. It apparently has whenever the state response is bounded with time, or is stable. This is true for both high-order bending modes and the engine. Substituting Equation 5-26 with $s = 0$ into Equations 5-23 and 5-23a gives

$$\dot{\underline{x}}_1 = \left[A_{11} - A_{12}A_{22}^{-1}A_{21} \right] \underline{x}_1 + \left[B_1 - A_{12}A_{22}^{-1}B_2 \right] u + \left[G_1 - A_{12}A_{22}^{-1}G_2 \right] \underline{\xi} \quad (5-27)$$

$$Z = \left[H_1 - H_2A_{22}^{-1}A_{21} \right] \underline{x} - H_2A_{22}^{-1}B_2u - H_2A_{22}^{-1}G_2\underline{\xi} + \underline{v} \quad (5-27a)$$

The system has now been reduced to the dimension of the 1-system. Notice, however, that $\underline{\xi}$ now appears as disturbance in Equation 5-27 and as noise in Equation 5-27a. Therefore, the correlation matrix C reappears

$$C = \begin{bmatrix} \left[H_2A_{22}^{-1}G_2Q \right]^T \\ 0 \end{bmatrix} \quad (5-28)$$

and R must include both $\underline{\xi}$ and \underline{v} covariances

$$R = \left[H_2A_{22}^{-1}G_2Q \left(H_2A_{22}^{-1}G_2 \right)^T + R \right] \quad (5-29)$$

The observation vector Z contains an extra term also

$$-H_2A_{22}^{-1}B_2u$$

The Kalman filter therefore takes on a slightly amended form, shown in Figure 5-15. Because $C \neq 0$ the general form of filter Equations 2-9 and 2-10 must be used, rather than Equations 5-1 and 5-6.

This approach is very promising, but it was developed too late in the program for experimental evaluation.

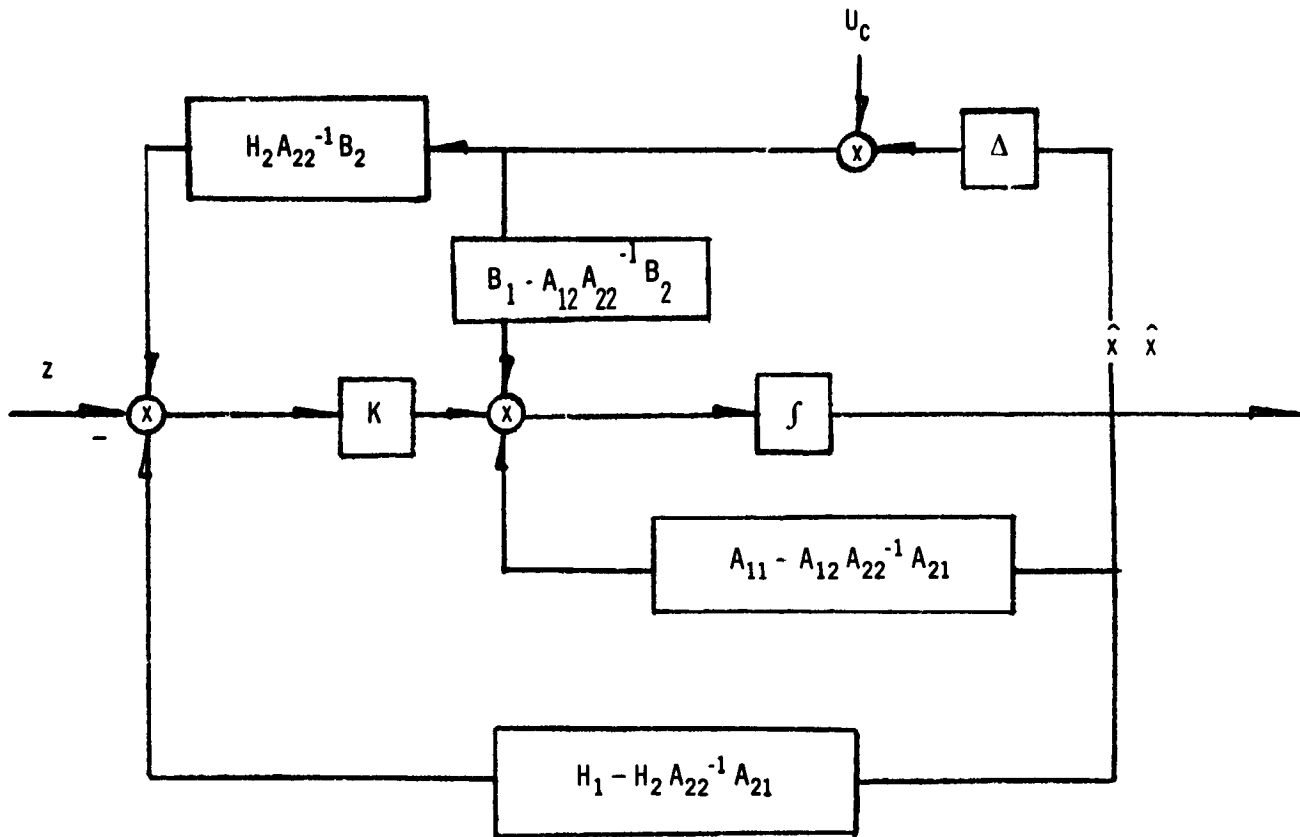


Figure 5-15. Kalman Filter with High-Order Steady State Assumption

5.4.2 Low-Order State Substitution, Colored Noise

The remainder of the approximations developed generally depend on the uncoupling of the 1- and 2- portions of the system, i.e., $A_{21} = A_{12} = 0$. This simplifies the block diagram of Figure 5-14 to the form shown in Figure 5-16. This approximation appears to be conservative for this system if the actuator dynamics are first excluded. Once this is done the bending and sloshing modes are generally in parallel with one another with a negligible amount of coupling between them. A_{12} and A_{21} can also be made perfectly equal to zero by diagonalizing the system.

One means of lowering the order of the filter is to substitute a low-order system for the 2-system, say

$$\begin{aligned}\underline{\lambda} &= \alpha \underline{\lambda} + \beta u + \gamma \xi \\ \underline{y} &= H \underline{\lambda}\end{aligned}\tag{5-30}$$

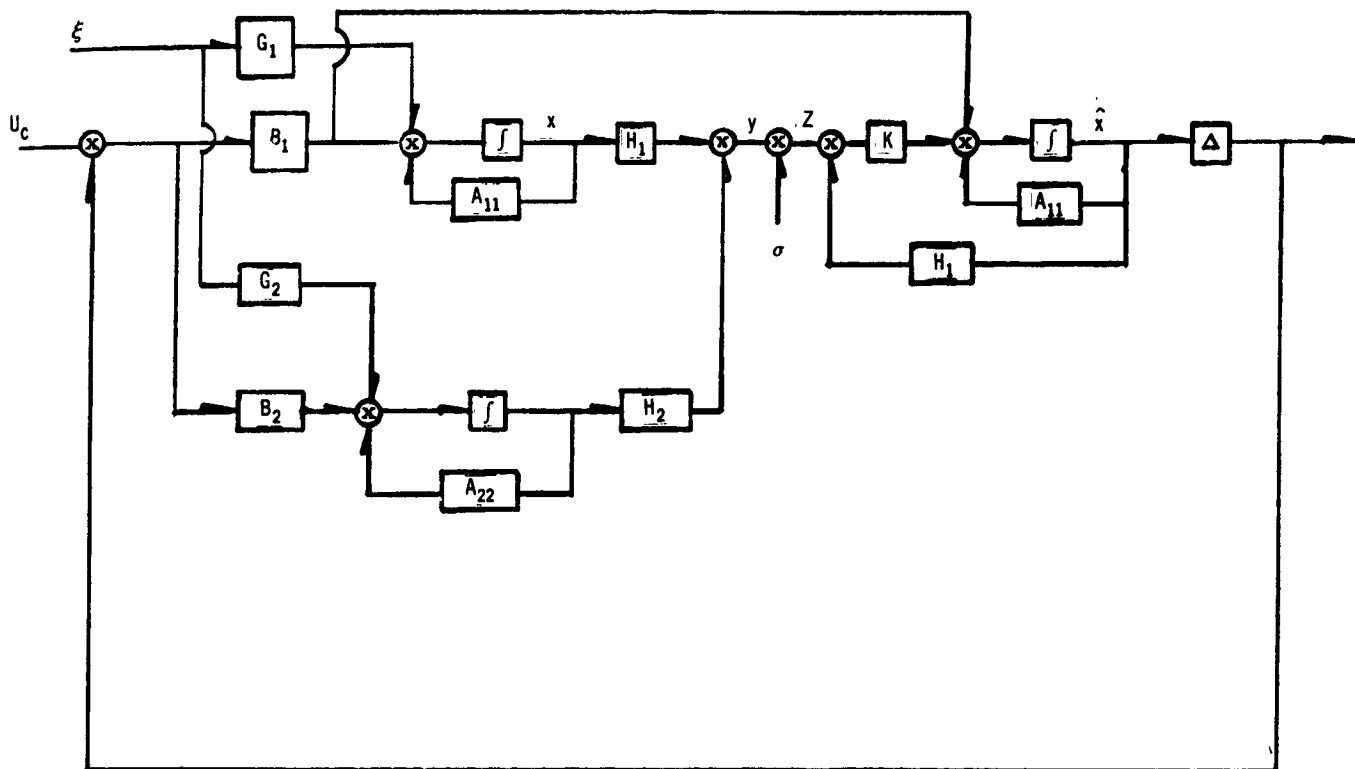


Figure 5-16. System Block Diagram, $A_{21} = A_{12} = 0$

and then substitute this back into the 1-system. This augments the 1-system.

The constraint on this low-order approximation to the 2-system is the gain and phase characteristics of the $y_1(u)$ of it must approximate those of the 2-system over the frequency range of the 1-system states. This approach in practice has proved to be virtually equivalent to transferring a state back into the 1-system if satisfactory performance cannot be achieved with it in the 2-portion of the system.

A successively greater simplification is to uncouple Equation 5-30 from the closed-loop commands and substitute an uncorrelated noise for the u -commands. This yields

$$\dot{\underline{\lambda}} = \alpha \underline{\lambda} + [\alpha \beta] \begin{bmatrix} \xi \\ \underline{u} \end{bmatrix} \quad (5-31)$$

which is equivalent to the filter assuming a colored or Markov noise in the system. This approach was tried and found to be of very little value. Once again, if a designer is going to raise the order of the filter to include the colored noise, he is usually much better off using the extra orders to simulate the troublesome state values.

5.4.3 White Noise Approximation

Figure 5-16 shows the output of the 2-portion of the plant entering the sensor signal beside the sensor white noise. If the white noise assumption in the derivation of the Kalman gain matrix can be made to represent a signal similar to the output of H_2 , then (supposedly) the filter would reject this signal as noise. Of the various approaches, this has been pursued the most extensively and experimental results indicate it is quite effective.

Breaking out the system to be approximated from Figure 5-16 produces Figure 5-17.

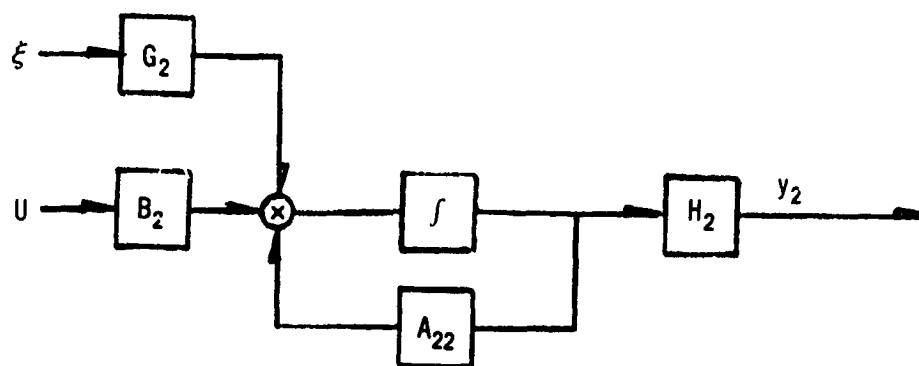


Figure 5-17. Block Diagram of States to be Rejected

Several approaches to developing a white noise approximating the spectral characteristics of Y_2 have been pursued. The first approach tried was to compute spectral density plots of $Y_i(\xi)$, assuming (ξ) was wind disturbance. Reflection on the results of the experiments conducted with this approach led to the speculation that, since the primary concern is stability, perhaps it would be better to compute R based on $\hat{Y}_i(u)$, where u is assumed to be white noise. This would make the filter more resistant to signals coming around the feedback loop. This was tried with somewhat improved results. The effort in both approaches has been to develop a white noise covariance matrix.

$$R = \begin{bmatrix} R_{11} & 0 & 0 \\ 0 & R_{22} & 0 \\ 0 & 0 & R_{33} \end{bmatrix} \quad (5-32)$$

The R_{ii} are set to assume a white noise with a power level approximately equal to the power level of the Y_i of the 2-system signals over the bandpass region of the lower state values. What is achieved are relative magnitudes between the R_{ii} . One has little to go on in setting Q . Families of runs were therefore made over ranges of Q/R , holding the ratios between the R_{ii} fixed.

In reality, the Y_i , since they have many common state values, will be correlated with one another. In an attempt to introduce the proper correlation terms, a differential equation for system variance was derived. Figure 5-18 shows a discrete system whose response characteristics will approach those of the corresponding continuous system as the sampling interval approaches zero time.

The discrete equivalent of continuous white noise with zero mean and variance $R\delta(\tau)$ is R/τ . The difference equation representing the system of Figure 5-18 is

$$\underline{x}_2(K+1) = \phi \underline{x}_2(K) + \chi G_2 \frac{r(K)}{v\tau} \quad (5-33)$$

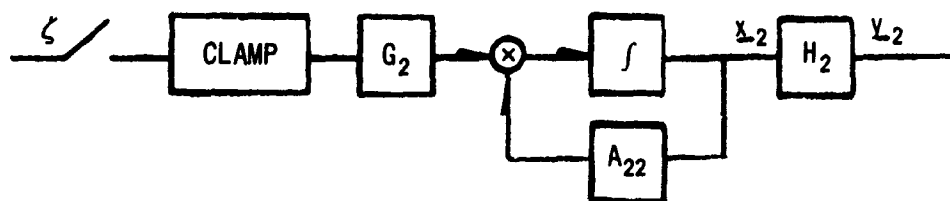


Figure 5-18. Equivalent Discrete System Block Diagram

where

$r(K)$ = a random gaussian sequence with zero mean and variance Q

$$\phi \triangleq I + A\tau + A^2 \frac{\tau^2}{2} + \dots \quad (5-34)$$

$$\chi \triangleq \tau + A \frac{\tau^2}{2} + A^2 \frac{\tau^3}{6} + \dots \quad (5-35)$$

now, dropping the 2-subscripts, let

$$S_{(K+1)} \triangleq E \left\{ \mathbf{x}_{(K+1)} \mathbf{x}'_{(K+1)} \right\} \quad (5-36)$$

$$= E \left\{ \left[\phi \mathbf{x}_{(K)} + \chi G \frac{\mathbf{r}(K)}{\sqrt{\tau}} \right] \left[\phi \mathbf{x}_{(K)} + \chi G \frac{\mathbf{r}(K)}{\sqrt{\tau}} \right]' \right\} \quad (5-37)$$

$$= \phi E \left[x_{(K)} x'_{(K)} \right] \phi^T + \frac{\phi}{\sqrt{\tau}} E \left[x_{(K)} r'_{(K)} \right] G' \chi' \quad (5-38)$$

$$+ \frac{\chi}{\sqrt{\tau}} G E \left[r_{(K)} x_{(K)} \right] \phi' + \frac{1}{\tau} \chi G E \left[r_{(K)} r'_{(K)} \right] \chi' G'$$

$$S_{(K+1)} = \phi S'_{(K)} \phi' + \frac{1}{\tau} \chi G Q G' \chi' \quad (5-39)$$

Substituting from Equations 5-34 and 5-35

$$S_{(K+1)} = S_{(K)} + A S_{(K)} \tau + S_{(K)} A' \tau + G Q G' \tau + o \tau^2 \quad (5-40)$$

Now

$$\frac{S_{(K+1)} - S_{(K)}}{\tau} = A S_{(K)} + S_{(K)} A' + G Q G' + o \tau \quad (5-41)$$

The derivative is defined

$$\dot{S} \triangleq \lim_{\tau \rightarrow 0} \frac{S_{(K+1)} - S_{(K)}}{\tau} \quad (5-42)$$

letting τ approach zero in Equation 5-41 gives

$$\dot{S} = A S + S A' + G Q G' \quad (5-43)$$

The observation vector is defined

$$y_2 = H_2 x_2 \quad (5-44)$$

The desired covariance is

$$R = E[y_2 y_2'] \quad (5-45)$$

$$= H_2 E[x_2 x_2'] H_2 \quad (5-46)$$

$$R = H_2 S_2 H_2' \quad (5-47)$$

Equation 5-43 is a special case of the Riccati equation and has been solved using the ASP computer program. This solution is substituted in Equation 5-47 for the desired covariance matrix. A number of runs have been made using Equation 5-47 as the white noise R matrix. However, it was not realized at the time that R from Equation 5-47 represents the areas under the spectral density curves, rather than the desired spectral levels. The resulting R matrixes are therefore too large. A possible method of resolving this is to solve the system of Figure 5-17 in Laplace form, giving

$$y_2(s) = C[Is - A]^{-1} B_2 G_2 \xi(s) \quad (5-48)$$

substituting ω for s and multiplying by the transpose

$$E[y_2(\omega) y_2'(\omega)] = E\left\{ C[I_\omega - A]^{-1} B_2 G_2 \xi(\omega) \xi'(\omega) G_2' B_2' [I_\omega - A]^{-1'} C' \right\} \quad (5-49)$$

letting

$$E[\xi(\omega) \xi'(\omega)] = I$$

$$R = C[I_\omega - A]^{-1} B_2 G_2 G_2' B_2' [I_\omega - A]^{-1'} C' \quad (5-50)$$

and, substituting a value for ω in the bandpass region of the 1-system, one has a covariance matrix (R) with approximately the correct signal levels.

In all these white noise approximation schemes it is difficult to approximate the spectral levels of the signals entering the rate gyro because they are not flat before the system fundamental break frequency is reached. All of these white noise substitution attempts cause the filter to assume the presence of white sensor noise of the approximate spectral levels as the extraneous state signals. There is no information about the correlation between these signals and the commands, and so information is lost. For this reason the steady-state approach of subsection 5.4.1 may be more effective.

5.4.4 Zero Noise Filtering

In reality, the instruments for measuring vehicle attitude, attitude rate, and acceleration produce almost noise-free signals. Taking the viewpoint that the observations are absolutely noise free allows the interpretation that the role of the Kalman filtering is not to filter out noise but rather to estimate a large number of states from a small number of sensor signals. However, the continuous Kalman filter was derived using the explicit assumption that R was positive definite. If one attempts the direct approach of, say, putting $R=0$ in the final form of Kalman equations, since the Kalman gain is

$$K = PH'R^{-1} \quad (5-51)$$

it appears to blow-up if $PH' \neq 0$.

The treatment of this situation suggested by Bryson and Johanssen was investigated at some length. They suggest applying a linear transformation to the state vector to form a new state vector, part of whose elements are the sensor signals and their noise-free derivatives. These state values are removed from the system differential equation. The derivatives of the sensor signals containing white noise are used as the sensor signals.

As an illustrative example, the technique can be applied to the system at Figure 5-1. The state equations are given by Equations 5-3 and 5-3a.

The derivatives of y are

$$\dot{y} = \dot{\phi} + K_{\phi\dot{\eta}} \quad (5-52)$$

$$\ddot{y} = \ddot{\phi} + K_{\phi\ddot{\eta}} \quad (5-53)$$

$$\ddot{y} = M_{\delta}u + \xi_2 + K_{\phi}(-\omega^2\eta - 2\xi\omega\dot{\eta} + M_{\delta}u + \xi_4) \quad (5-54)$$

$$\ddot{y} = [0 \ 0 \ -K_{\phi}\omega^2 \ -K_{\phi}2\xi\omega] \begin{Bmatrix} \phi \\ \dot{\phi} \\ \eta \\ \dot{\eta} \end{Bmatrix} + (1 + K_{\phi})M_{\delta}u + [0 \ 1 \ 0 \ K_{\phi}]\underline{\xi} \quad (5-55)$$

State elements can be made of y and \dot{y} . Choosing the remaining two signals arbitrarily

$$\begin{Bmatrix} x_1 \\ x_2 \\ y \\ \dot{y} \end{Bmatrix} = \begin{Bmatrix} x_1 \\ x_2 \\ x_3 \\ x_4 \end{Bmatrix} = \begin{bmatrix} 1 & 0 & -K_{\phi} & 0 \\ 0 & 1 & 0 & -K_{\phi} \\ 1 & 0 & K_{\phi} & 0 \\ 0 & 1 & 0 & K_{\phi} \end{bmatrix} \begin{Bmatrix} \phi \\ \dot{\phi} \\ \eta \\ \dot{\eta} \end{Bmatrix} \quad (5-56)$$

or

$$\underline{x} = M\underline{\theta} \quad (5-57)$$

differentiating

$$\dot{\underline{x}} = M\dot{\underline{\theta}} \quad (5-58)$$

solving for $\dot{\underline{\theta}}$

$$\dot{\underline{\theta}} = M^{-1}\dot{\underline{x}} \quad (5-59)$$

if the original state equation is

$$\dot{\underline{\theta}} = A\underline{\theta} + B\underline{u} + \underline{\xi} \quad (5-60)$$

one can multiply through by M

$$M\dot{\underline{\theta}} = MA\underline{\theta} + MB\underline{u} + M\underline{\xi} \quad (5-61)$$

substituting in Equations 5-58 and 5-59

$$\dot{\underline{x}} = \underline{M} \underline{A} \underline{M}^{-1} \underline{x} + \underline{M} \underline{B} \underline{u} + \underline{M} \underline{\xi} \quad (5-62)$$

If this is done to Equation 5-3a, one gets

$$\begin{Bmatrix} \dot{x}_1 \\ \dot{x}_2 \\ \dot{x}_3 \\ \dot{x}_4 \end{Bmatrix} = \begin{bmatrix} 0 & 1 & 0 & 0 \\ \omega^2/2 & -\xi_\omega & -\omega^2/2 & \xi_\omega \\ 0 & 0 & 0 & 1 \\ \omega^2/2 & \xi_\omega & -\omega^2/2 & -\xi_\omega \end{bmatrix} \begin{Bmatrix} x_1 \\ x_2 \\ x_3 \\ x_4 \end{Bmatrix} + \begin{bmatrix} 0 \\ 1 - K_\phi \\ 0 \\ 1 + K_\phi \end{bmatrix} u + \begin{bmatrix} 0 & 0 \\ 1 & -K_\phi \\ 0 & 0 \\ 1 & K_\phi \end{bmatrix} \begin{Bmatrix} \xi_2 \\ \xi_4 \end{Bmatrix} \quad (5-63)$$

since (x_3) and (x_2) are known, Equation 5-63 can be reduced to

$$\begin{Bmatrix} \dot{x}_1 \\ \dot{x}_2 \end{Bmatrix} = \begin{bmatrix} 0 & 1 \\ \omega^2/2 & -\xi_\omega \end{bmatrix} \begin{Bmatrix} x_1 \\ x_2 \end{Bmatrix} + \begin{bmatrix} 0 & 0 \\ \omega^2/2 & \xi_\omega \end{bmatrix} \begin{Bmatrix} x_3 \\ x_4 \end{Bmatrix} + \begin{bmatrix} 0 \\ 1 - K_\phi \end{bmatrix} u + \begin{bmatrix} 0 & 0 \\ 1 & -K_\phi \end{bmatrix} \begin{Bmatrix} \xi_2 \\ \xi_4 \end{Bmatrix} \quad (5-64)$$

and, from Equations 5-54 and 5-56

$$\ddot{y} = \left[\frac{\omega^2}{2} \xi_\omega - \frac{\omega^2}{2} - \xi_\omega \right] \underline{x} + M_\delta (1 + K_\phi) u + [1 \ K_\phi] \begin{Bmatrix} \xi_2 \\ \xi_4 \end{Bmatrix} \quad (5-65)$$

Equations 5-64 and 5-65 are in the proper form to apply Kalman filtering, Equations 2-8, 2-9, and 2-10.

The significant point to notice about the above development is that the order of Equation 5-64 is lower than the original system. Other studies have shown sloshing can be removed from the 20th order system, reducing it to 14th order. Then, by the above process, the order would be reduced, probably to 10. The potential drawback of the approach is that the methods developed so far to reduce the order of the filtering and to obtain parameter estimation error insensitivity have relied upon artificial levels of white sensor noise. The filter order reduction to 10 may solve the filter problem; this still leaves the parameter sensitivity problem an open question.

5.5 CONVENTIONAL ANALYSIS TECHNIQUES

This section discusses the use of Nyquist diagrams and root location displays in the evaluation of systems described in this report. These systems are characterized by vector state variables and suboptimal control and sub-optimal state estimation.

Were the methods of optimal control and optimal state estimation used, then the motivation to Nyquist functions and root display would be of lesser concern.

In the final analysis, there is little theoretical difference between root displays and Nyquist functions, both being used to display characteristics of the system in the frequency domain. In practice, however, each engineer's experience leads him to expect different insights from Nyquist functions than root displays. The term root displays (rather than root locus) is used purposely here, in that it may be much easier to get one or several sets of roots than a locus of roots.

5.5.1 Analysis by Nyquist Diagrams

The analysis of systems of this kind, characterized by high order and multiple vector variable looping, is a challenge. There are many loop functions to choose from. It would be desirable to break the loop and construct Nyquist diagrams which show both the cause of the unwanted shape of the Nyquist plot and the cure.

In the context of this research, the cause of the unwanted shape of the Nyquist diagram is the distortion of the ideal diagram by the presence of the higher bending modes, whose states are not included in the state estimator.

The cure for the undesired shape of the Nyquist plot, under the ground rules of this research, is the alteration of the gains in the filter. Therefore, an ideal Nyquist function would be constructed so that the effect of the higher bending modes could be identified explicitly, and so that the effect of changes in the filter gains would also be explicitly apparent. Because there are

several of these bending modes, and their states influence the measurements at several transducers, and since the gain matrix has a large number of elements, it seems impossible to define an ideal Nyquist function.

Examination of the vector-matrix block diagram (Figure 5-19) will clarify some of the difficulties. Numbers in parenthesis indicate typical dimensions of vectors and matrixes. As an example, consider breaking the loop in front of the gain matrix K . There are three variables at this location, and each of them affects the system performance and stability through six elements of the K matrix. Apparently, to study the effect of each element of the K matrix, one would have to develop 18 Nyquist functions.

A typical approach to Nyquist analysis for a conventional control system is to study each loop through a particular transducer. Consideration of this approach is facilitated through Figure 5-20. Figure 5-20 is easily derived from Figure 5-19 by block diagram manipulations. Since the control

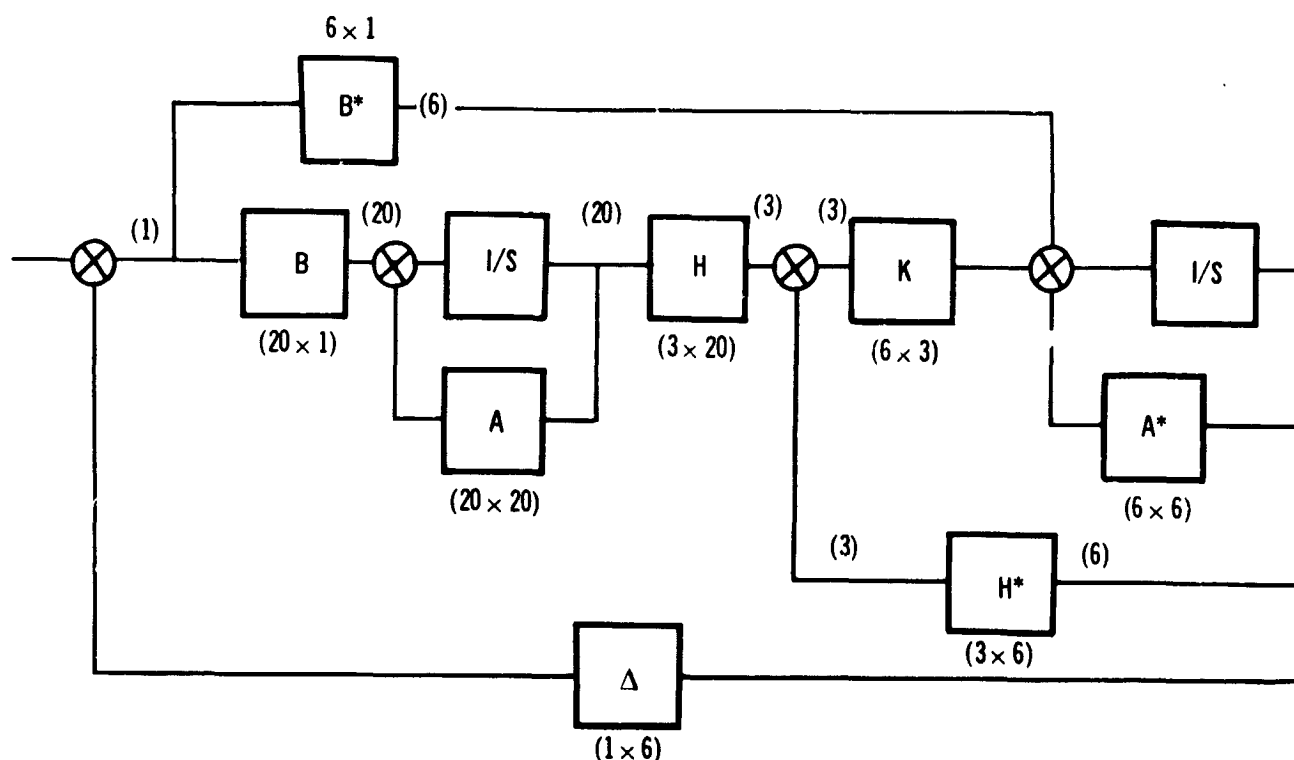


Figure 5-19. Closed-Loop System

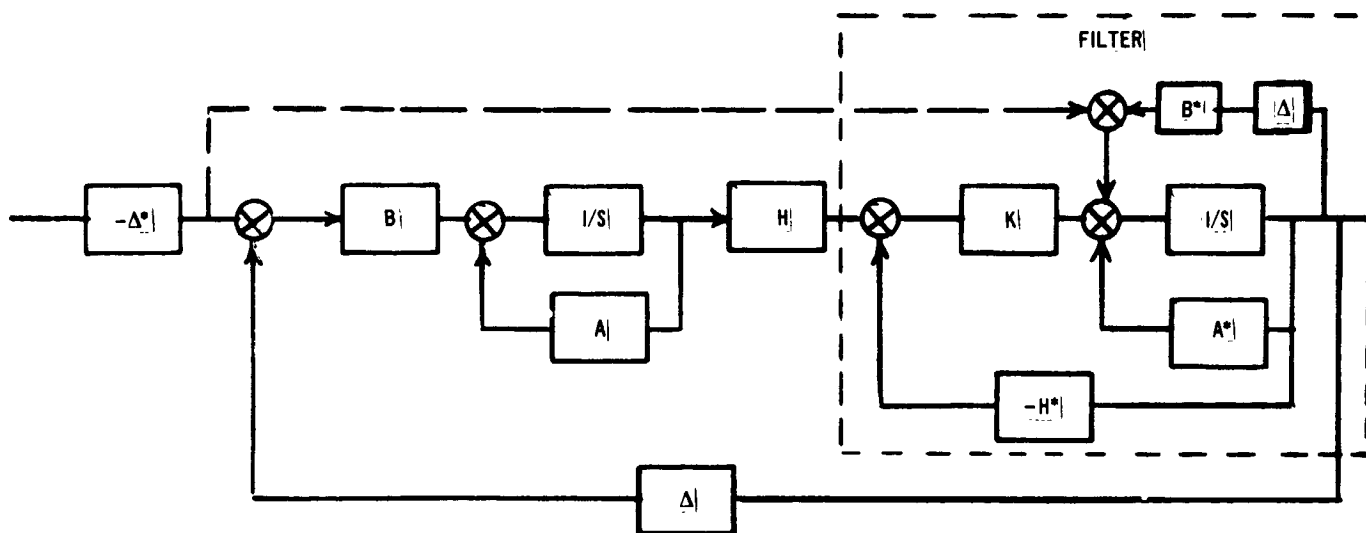


Figure 5-20. Modified Closed-Loop System

matrix Δ is considered fixed, it can be included in the definition of the filter(s) acting on the transducer signals. These signals are assembled through matrix H . Three Nyquist functions could be developed by breaking the loop at the control and tracing a loop through each transducer. This does not provide the insight in this case that it does in traditional design, because of the large amount of coupling in the filter. However, the approach should not be discarded, because it will provide interesting comparison data with conventional design methods.

The approach taken in this research has been to develop Nyquist functions similar to the traditional ones. However, instead of loops being traced through each transducer, loops are traced through the control resulting from the estimate of each generalized coordinate and its derivative. These Nyquist functions are thought to have more significance in this design approach. Because this approach concentrates on the state space and the state vector, it is more appropriate to develop Nyquist functions based on the states rather than the transducer information. Unfortunately, these functions do not expose explicitly the effect of the elements of the K matrix. At resonance, they effectively expose the influence of the higher bending modes on the system stability.

It is particularly interesting to compare these Nyquist functions for the suboptimum control, no-filter case with those for the suboptimum control filter case. Of the many possible Nyquist functions, the one defined below is considered to be among the most useful and has contributed to the insights gained in this study.

These particular Nyquist functions are clarified by examination of Figures 5-21a and 5-21c. Figure 5-21c shows the suboptimal closed loop system. The control matrix Δ is expressed as two matrixes, as shown, so that two scalar control variables, U_η and U_ϕ , are created. Their sum is, of course, the scalar control variable U . Typical Nyquist functions

$$\text{Bending} = \begin{bmatrix} 0 & 0 & \Delta_\eta & \Delta_\eta \end{bmatrix} [SI - A]^{-1} B$$

$$\text{Rigid body} = \begin{bmatrix} \Delta_\phi & \Delta_\phi & 0 & 0 \end{bmatrix} [SI - A]^{-1} B$$

and

$$\text{Total} = [\Delta] [SI - A]^{-1} B$$

are plotted in Figure 5-22 and discussed in another context in subsection 5.6.

Figure 5-21c shows the suboptimal closed loop system with suboptimal state estimation. Control variables similar to the previous case are developed. Typical Nyquist functions

$$\text{Bending} = \begin{bmatrix} 0 & 0 & \Delta_\eta & \Delta_\eta \end{bmatrix} [\Omega]$$

$$\text{Rigid body} = \begin{bmatrix} \Delta_\phi & \Delta_\phi & 0 & 0 \end{bmatrix} [\Omega]$$

and

$$\text{Total} = \begin{bmatrix} \Delta_\phi & \Delta_\phi & \Delta_\eta & \Delta_\eta \end{bmatrix} [\Omega]$$

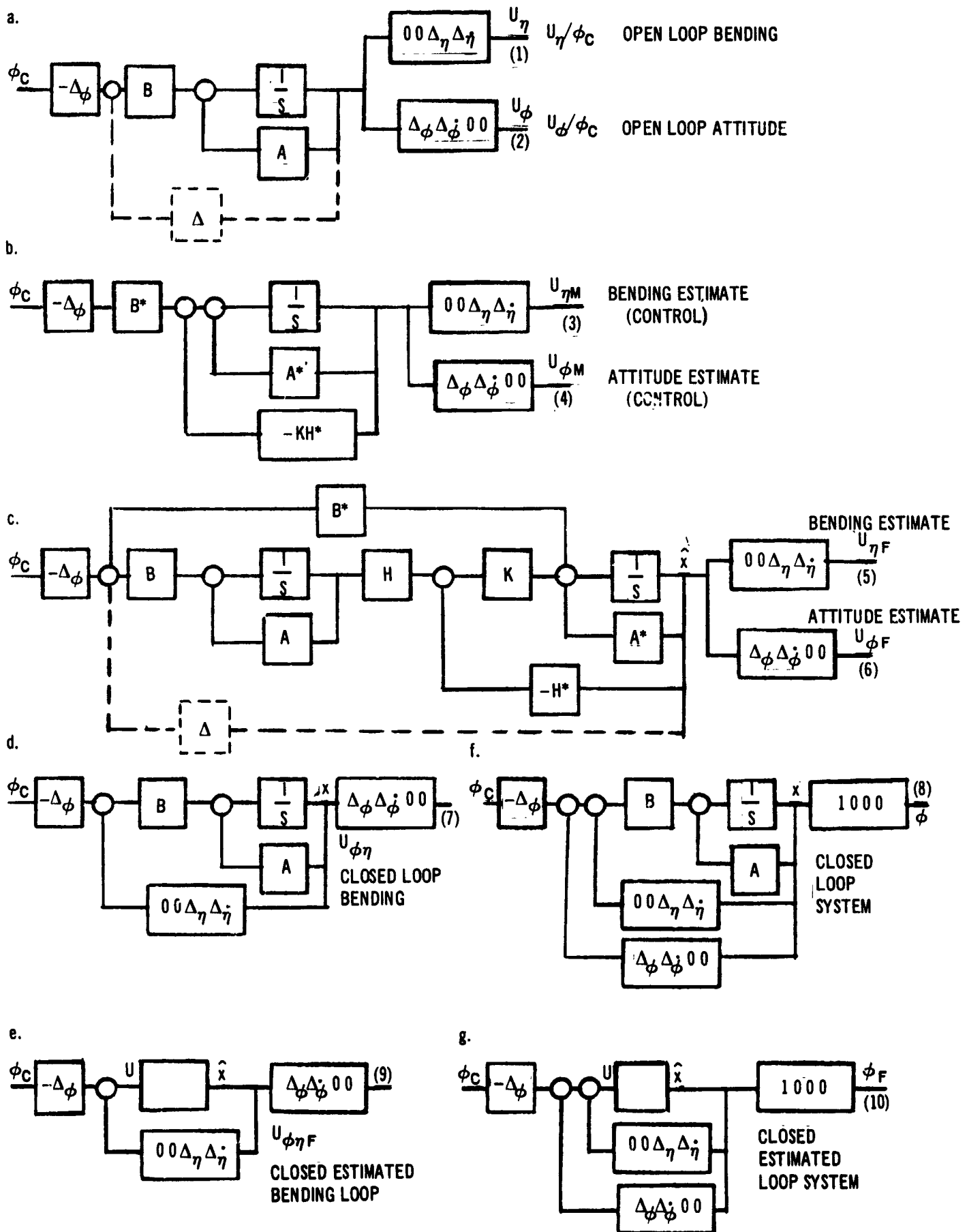


Figure 5-21. Pole-Zero Printout Format

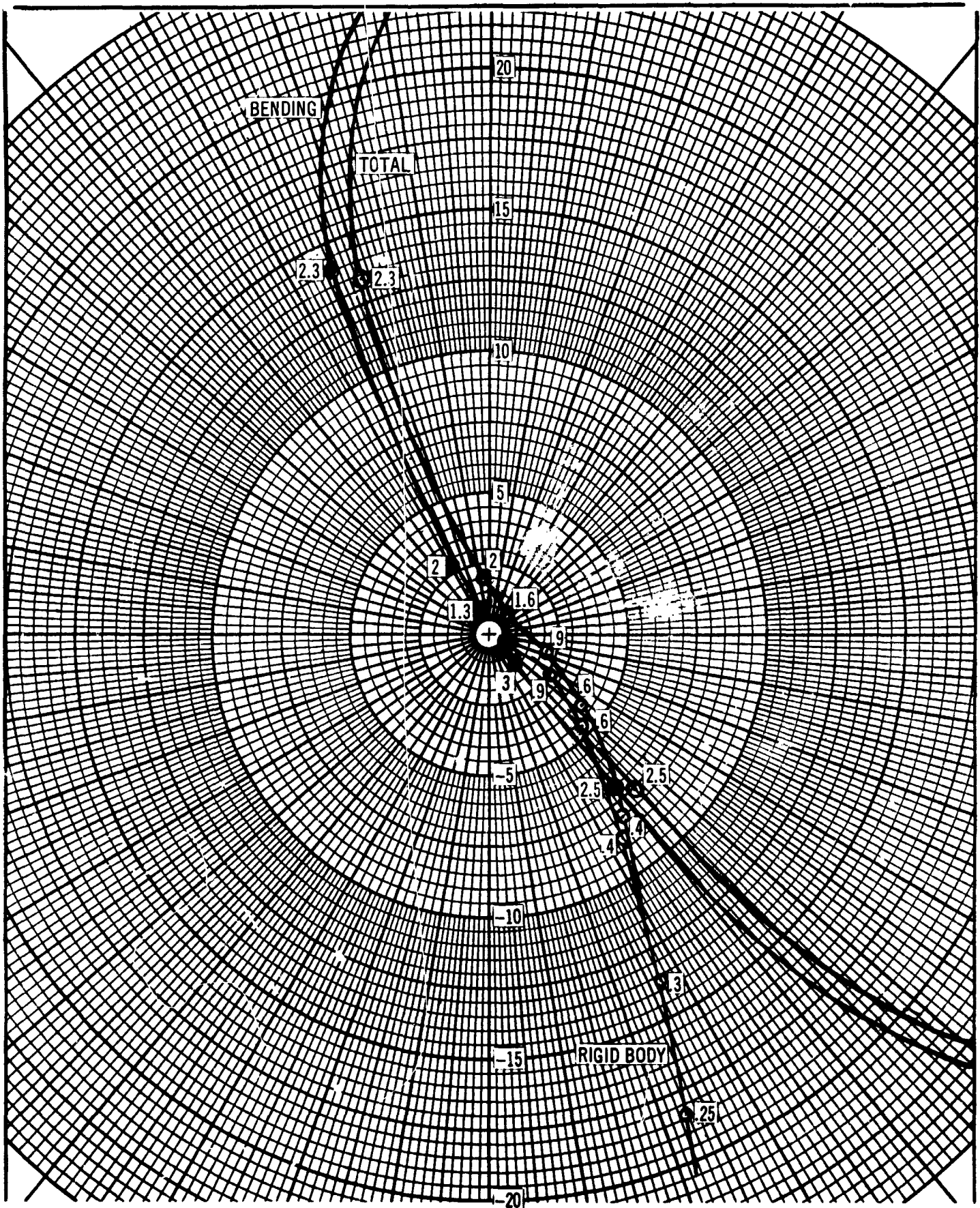


Figure 5-22. Nyquist Diagram – Ideal System

where

$$[\Omega] = [SI - A^* + KH^*]^{-1} [B^* + KH[SI - A]^{-1} B]$$

are plotted for the same system as in Figure 5-23.

5.5.2 Analysis by Root Displays

The roots of the closed-loop system are readily recognized as useful data for the evaluation of system stability and response. However, it is useful to gain insight into the influences which determine the ultimate location of the closed-loop roots. Design optimal control theory locates the roots implicitly, and the theory itself gives the insight. However, suboptimal control presses on the designer the need for hints and guidelines for his choice of the methodology of design.

The roots obtained from the functions described in this section are helpful in producing the required insight. These functions are presented in block diagram form in Figure 5-21.

Numerical references are to the function defined by the diagram with ϕ_c as input and the numbered variable as output. Functions (1), (2), (7), and (9) refer exclusively to the suboptimal control system with plant states assumed to be explicitly available. Functions (3), (4), (5), (6), (8), and (10) are similar to the others, but are for the combined suboptimal control and suboptimal state estimation. The effect of the filler can be seen implicitly in the comparison of these functions.

Functions (1) and (2) define poles and zeros of the plant and control. These are comparable to Functions (5) and (6) and are in fact the same functions described in the previous discussion of Nyquist analysis. Functions (7) and (8) provide for a comparison of the effect of closing the bending feedback loop and are also open-loop functions for closed-loop Functions (9) and (10).

In these studies, most use was made of Function (10) which, of course, provides the closed-loop roots of the closed-loop suboptimal system.

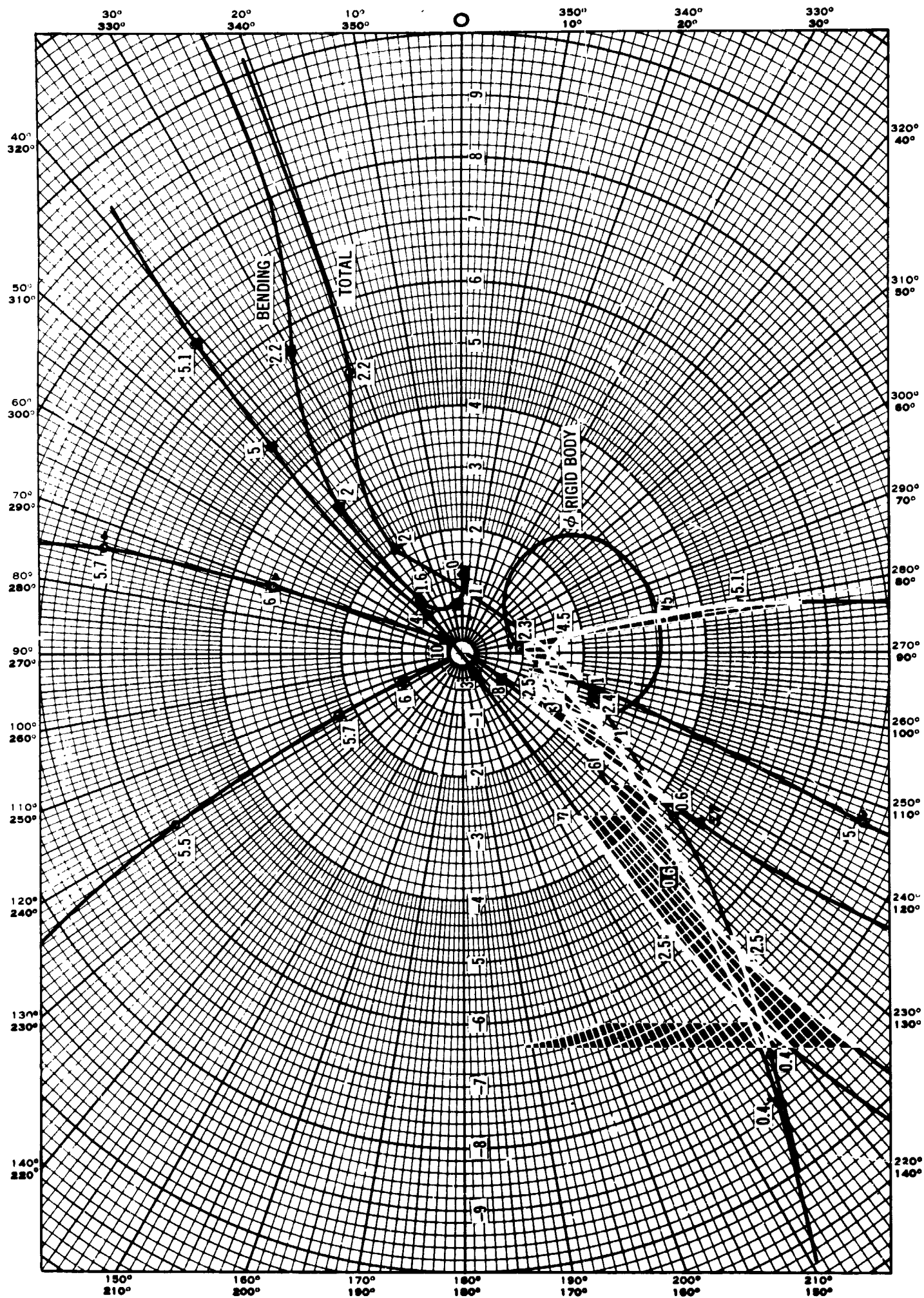


Figure 5-23. Nyquist Diagram Suboptimal System

5.5.3 A Method of System Reduction for Analysis

Attempts to apply conventional system design techniques, such as Nyquist and root locus methods, have been largely frustrated by the presence of large number of parallel paths at most points in the closed-loop system. This method was worked out to alleviate this problem and it is an aid to evaluation of the stability of the system because of the extraneous, 2-system states.

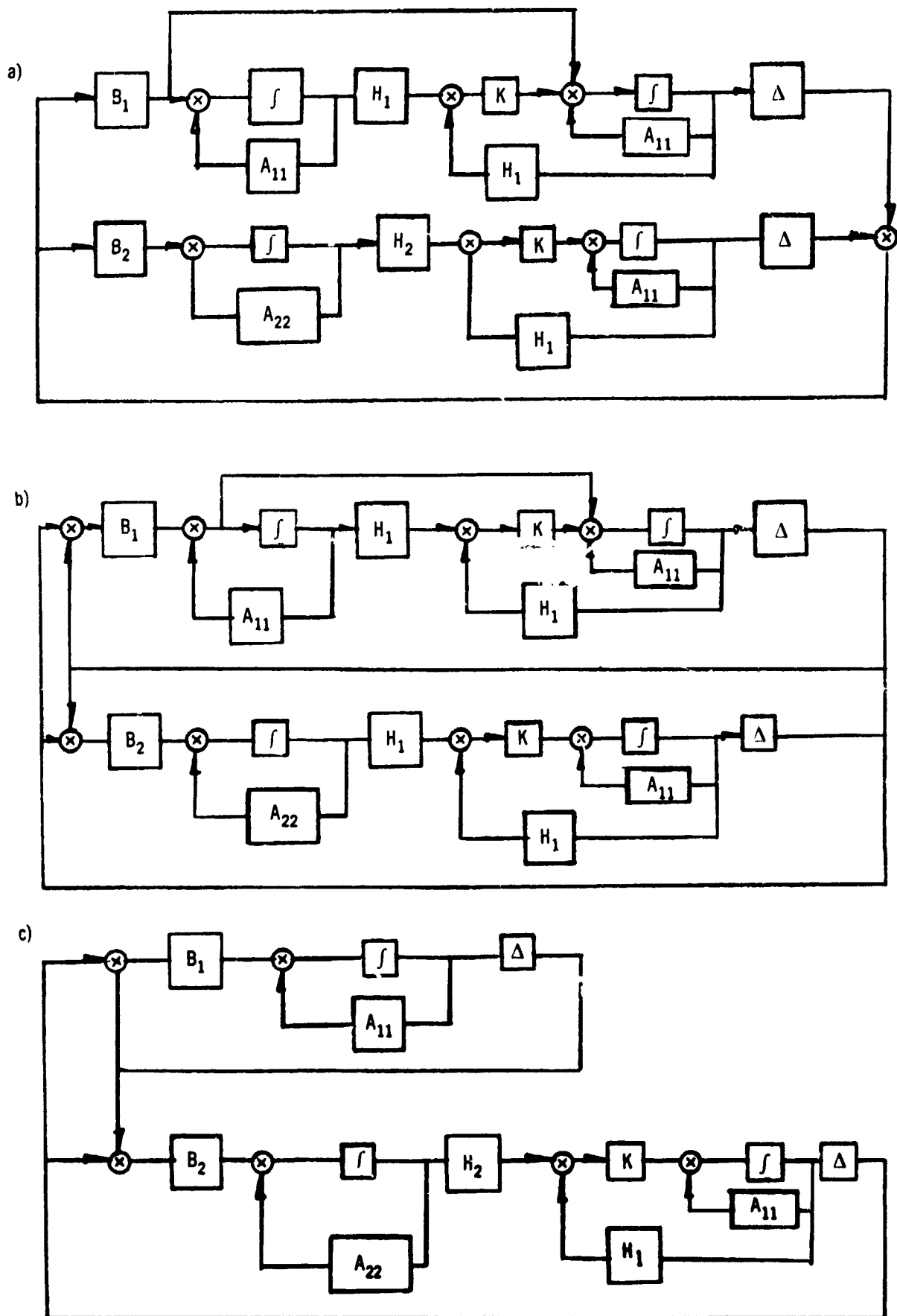
The method is based on the assumption that the closed-loop system can be represented by the block diagram of Figure 5-14. Removing the input and coupling terms A_{12} , A_{21} from this block diagram and using superposition, Figure 5-16 can be arranged as shown in Figure 5-24a. Rearranging the feedback command channel leads to Figure 5-24b. Theorem 1 (subsection 5.1) allows the reduction from Figure 5-24b to 5-24c. This block diagram can be rearranged to the form of Figure 5-24d. It is significant that, for the launch vehicle application, the two parallel feedback paths are scalar.

Rewriting Figure 5-24d in descriptive form yields 5-24e. The system is now in a relatively convenient form for the coupling analysis. Once the optimal control gains have been defined, the feedback loop is defined and can be easily estimated by hand with root locus plots. The 2-system in the forward loop is also independent of the filtering. With three sensors, there are three parallel forward loops to analyze to determine which sensor placement is causing instability. Figure 5-24d shows the potential of trading H_1 against H_2 by sensor placement to achieve satisfactory stability.

5.6 FILTER DEVELOPMENT EXPERIMENTS PERFORMED

5.6.1 White, Uncorrelated Noise Approach

Initially, this series of experiments involved the use of the 20-dimensional system as the plant. It was first decided to attempt to stabilize rigid body rotation and suppress first bending mode deflection. A damping ratio of 0.7 is considered to yield about optimal transient characteristics for rigid



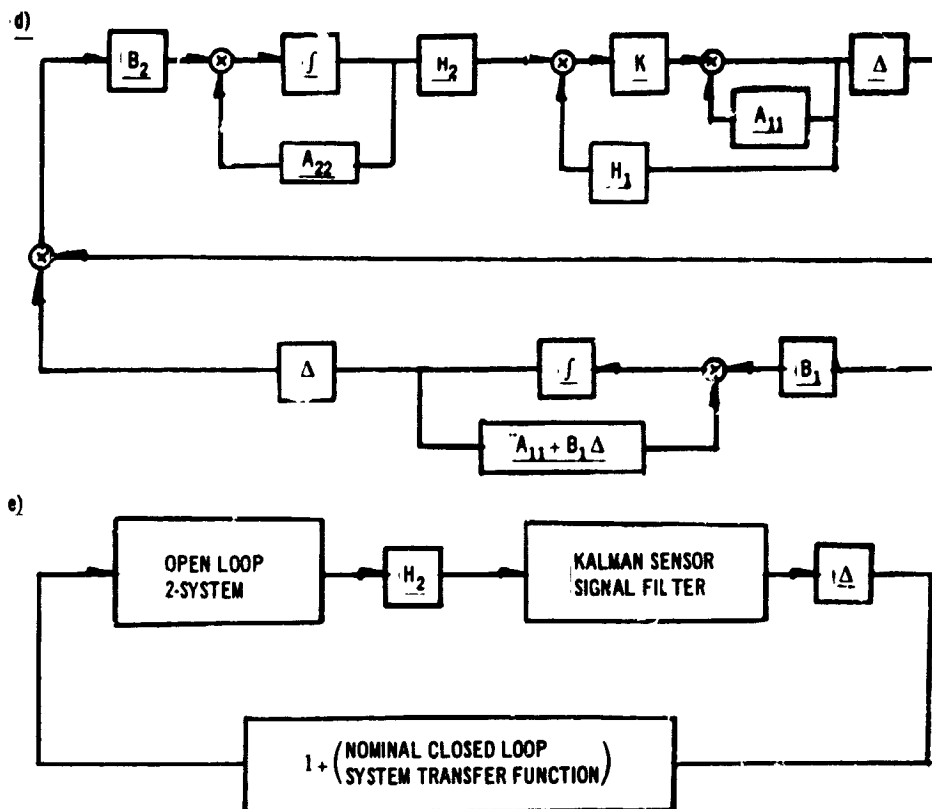


Figure 5-24. Analysis Method – Block Diagram (Sheet 2 of 2)

body rotation and control gains were therefore picked to yield this damping ratio and a damped natural frequency of approximately half the first bending mode frequency (as requested in the Work Statement). Control gains were picked to yield a damping ratio on the first bending mode of 0.3, which seemed ample to meet the objective of suppressing the bending mode deflection. Kalman filters were prepared using System 4-3 as the plant model.

The first series of runs made assumed that the extraneous signals were entering through ξ , as shown as the upper input in Figure 5-17. The coupling and aerodynamic terms between rigid body rotation and the bending terms were dropped and y_i/x_j spectral density asymptotes were plotted. These asymptotes were plotted (e.g., Figures 5-25 and 5-26) along with the chosen white noise spectral density levels. These levels were picked to be approximately equal to the combined power levels from the second, third, and

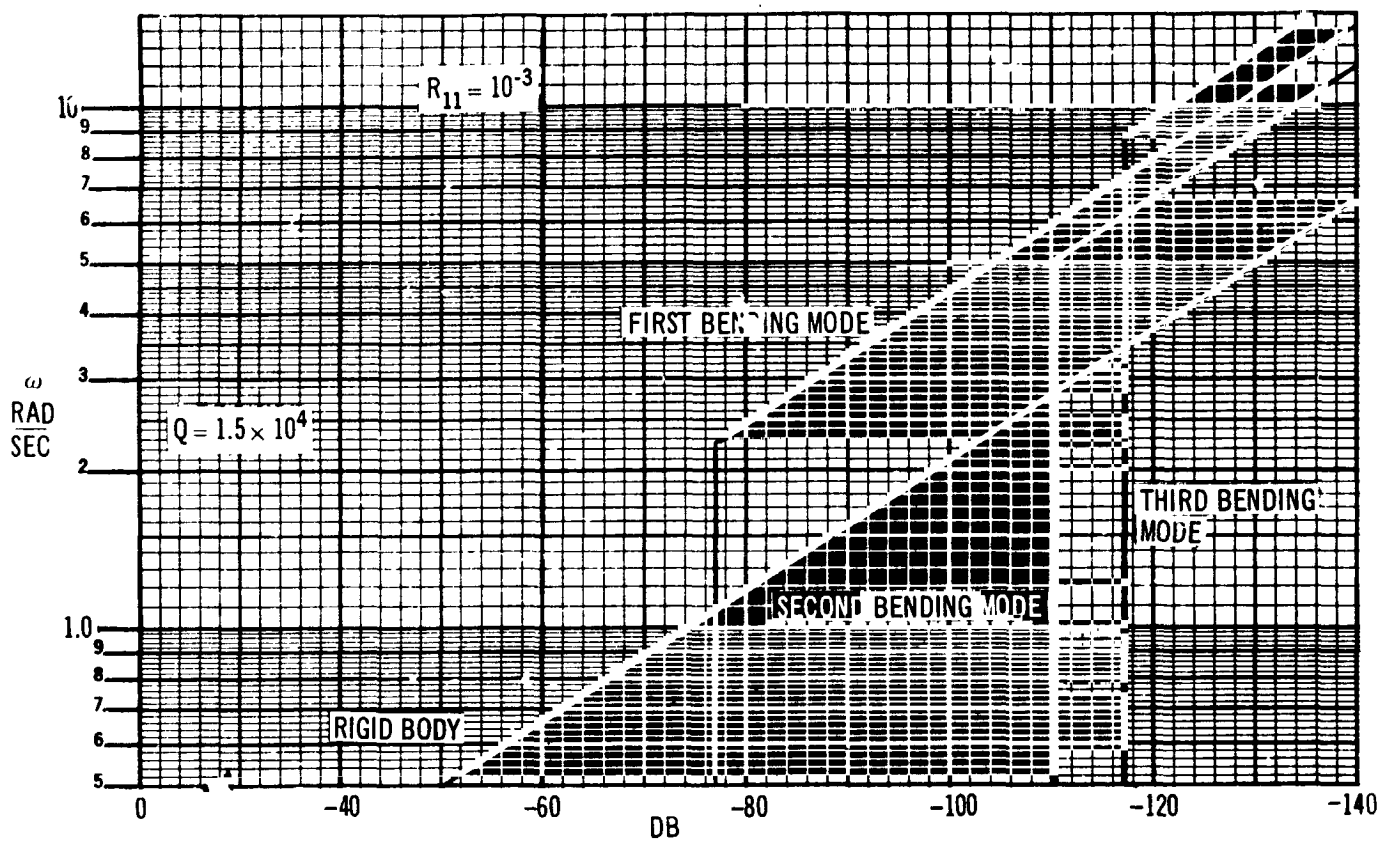


Figure 5-25. Attitude Gyro

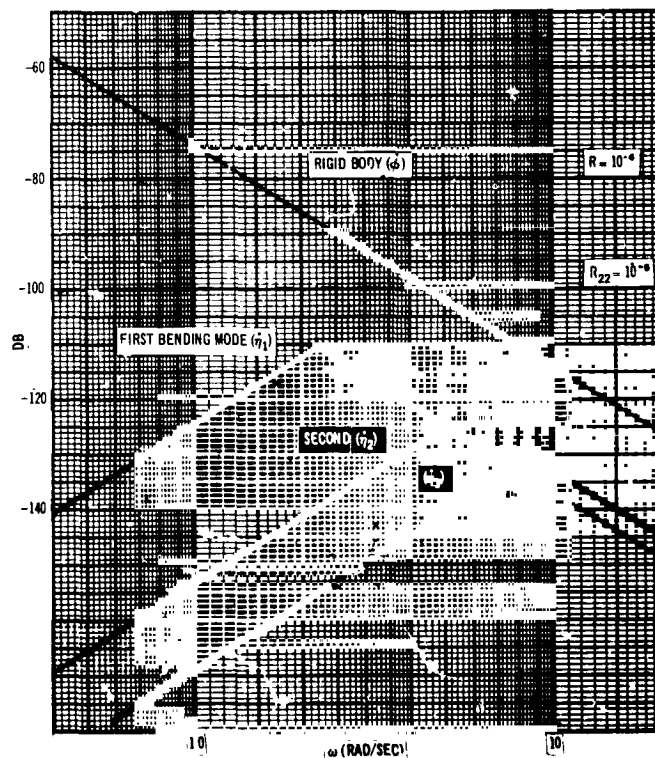


Figure 5-26. Rate Gyro Response to 1.5×10^4 Wind

fourth bending modes at low frequency. The net result was a white noise covariance matrix

$$R = \begin{bmatrix} 10^{-3} & 0 & 0 \\ 0 & 10^{-5} & 0 \\ 0 & 0 & 5 \end{bmatrix}$$

Steady-state Kalman gains were prepared for a range of c values and are presented in Table 5-1. The system closed-loop poles and zeros for the transfer function ϕ/V_w are presented in Table 5-2. Inspection of Table 5-2 shows for the lowest noise filtering ($C = 10^{-1}$) only the second bending mode is unstable; as the white noise level is raised, second bending becomes less unstable, but third and fourth bending go unstable. It is also interesting to note that no stability problems have been encountered with sloshing.

A review of these results led to the observation that the response of the 2-system to U-commands has a greater bearing on stability than external disturbance and the spectral levels used to define the R matrix should therefore be the response to a white U-input signal. Plots were made of the asymptotes of the spectral densities of the bending mode state signals at the three sensors. Again, it was assumed that the modes do not couple with one another. From the three sets of spectral plots the covariance matrix

$$R = C \begin{bmatrix} 10^{-1} & 0 & 0 \\ 0 & 10^0 & 0 \\ 0 & 0 & 10^5 \end{bmatrix}$$

was chosen. A series of steady-state Kalman gains for various values of c was prepared and is shown in Table 5-3.

The system poles and zeros for the transfer function ϕ/V_w are shown in Table 5-4. Inspection of the roots in this table shows that only the second bending mode is unstable in this series, something of an improvement from the previous set.

Table 5-1
WIND RESPONSE KALMAN GAIN VALUES

$$R = C \begin{bmatrix} 10^{-3} & 0 & 0 \\ 0 & 10^{-5} & 0 \\ 0 & 0 & 5.0 \end{bmatrix} \quad \begin{array}{l} \text{Filter Model} = 4-3 \\ Q = 1.5 \times 10^4 \end{array}$$

C	Kalman Gain Matrix, Transposed (K')			
10^{-2}	$\begin{bmatrix} 0.0778 & 0.0201 & 1.214 & 0.002 \\ 0.661 & 43.1 & 20.3 & 1501 \\ 1.43 \times 10^{-4} & -1.735 \times 10^{-4} & -0.026 & -0.00484 \end{bmatrix}$			
10^{-1}	$\begin{bmatrix} 0.0791 & 0.01824 & 1.135 & 0.494 \\ 0.716 & 13.63 & 16.65 & 470 \\ 1.147 \times 10^{-4} & -2.21 \times 10^{-4} & -0.0244 & -0.00594 \end{bmatrix}$			
10^0	$\begin{bmatrix} 0.0831 & 0.01342 & 0.894 & 0.279 \\ 0.848 & 4.31 & 8.26 & 142.8 \\ -2.71 \times 10^{-5} & -1.357 \times 10^{-4} & -0.01925 & -0.00301 \end{bmatrix}$			
10^1	$\begin{bmatrix} 0.0910 & 0.01014 & 0.411 & 0.0818 \\ 0.955 & 1.364 & 1.673 & 42.6 \\ -1.472 \times 10^{-4} & -5.13 \times 10^{-5} & -0.00880 & -4.42 \times 10^{-4} \end{bmatrix}$			
10^2	$\begin{bmatrix} 0.0955 & 0.00958 & 0.1351 & 0.0202 \\ 0.961 & 0.438 & 0.264 & 12.60 \\ -0.250 \times 10^{-4} & -0.320 \times 10^{-5} & -0.00282 & -8.68 \times 10^{-6} \end{bmatrix}$			
10^3	$\begin{bmatrix} 0.0969 & 0.00927 & 0.040 & 0.00520 \\ 0.927 & 0.1592 & 0.0729 & 3.32 \\ -2.83 \times 10^{-4} & -2.84 \times 10^{-5} & -7.62 \times 10^{-4} & -8.33 \times 10^{-6} \end{bmatrix}$			
10^5	$\begin{bmatrix} 0.0972 & 0.00901 & 0.00594 & 5.80 \times 10^{-4} \\ 0.896 & 0.0841 & 0.0472 & 8.24 \times 10^{-2} \\ -2.94 \times 10^{-4} & -2.72 \times 10^{-5} & -3.21 \times 10^{-5} & -1.007 \times 10^{-6} \end{bmatrix}$			

Table 5-2
SYSTEM ROOTS, FILTER DESIGNED ON DISTURBANCE

Transfer Function = ϕ/V_w

$$R = C \begin{bmatrix} 10^{-3} & 0 & 0 \\ 0 & 10^{-5} & 0 \\ 0 & 0 & 5.0 \end{bmatrix}$$

Filter Model = 4-3

Plant = 20-1

$Q = 1.5 \times 10^4$

$t = 24 \text{ sec}$

$C = 10^{-1}$			$C = 10^0$			$C = 10^2$			$C = 10^3$		
Poles	Zeros		Poles	Zeros		Poles	Zeros		Poles	Zeros	
-0.01334	-0.80 ± j2.53	0.040*	0.1080 ± j1.757	-0.0309	-0.0246 ± j0.0216	-0.0546 ± j0.0214	-14.71				
-0.1064	-0.0853 ± j1.742	-0.1001	-0.01191 ± j2.31	-0.0965	-0.1494 ± j2.01	-0.674 ± j0.716	-1.82				
-0.694 ± j0.624	-0.01177 ± j2.31	-0.701 ± j0.626	-0.0575 ± j2.38	-0.668 ± j0.769	-0.0319 ± j2.43	-0.0322 ± j2.09	-0.0720 ± j2.06				
-0.1248 ± j1.745	-0.0537 ± j2.38	-0.229 ± j1.746	-0.0829 ± j2.53	-0.0596 ± j2.08	-0.01193 ± j2.31	-0.01159 ± j2.31	-0.1157 ± j2.31				
-0.0492 ± j2.43	-0.1508	-0.290 ± j2.20	-0.402 ± j3.03	-0.01179 ± j2.31	-0.1585 ± j2.32	-0.0150 ± j2.43	-0.1723 ± j2.43				
-0.275 ± j2.28	-13.93	-0.01316 ± j2.31	0.681 ± j5.12	-0.0211 ± j2.43	0.0469 ± j2.67	-1.211 ± j2.48	-0.797 ± j2.26				
-0.01356 ± j2.31	-0.396 ± j3.06	-0.0453 ± j2.43	-0.142	-1.328 ± j2.32	0.258 ± j4.90	-0.0854 ± j2.65	-0.00521 ± j2.65				
-0.1948 ± j2.69		-0.175 ± j2.67	-25.9	-0.0334 ± j2.66	-0.363	-0.1535	0.1611 ± j4.93				
0.634 ± j5.46*	0.823 ± j5.32	0.554 ± j5.25*	-0.273 ± j9.84	-0.418	-10.17	-10.70	-2.73				
-0.322 ± j9.53	-0.647 ± j9.98	-0.1586 ± j9.47	-10.3 ± j3.04	-10.74	0.0412 ± j9.47	0.1248 ± j5.01*	-10.27				
-0.304 ± j13.15	-0.1309 ± j12.72	-7.64	-0.0505 ± j12.7	0.213 ± j4.99*	-0.0463 ± j12.63	0.0787 ± j9.29*	0.0592 ± j9.42				
-10.49	9.09	-11.47	-6.49 ± j53.6	-0.00140 ± j9.32	-6.5 ± j53.6	0.01549 ± j12.70	-0.0495 ± j12.62				
-22.8	-20.9	0.00539 ± j12.96*		0.01566 ± j12.72*		-6.52 ± j53.6	-6.57 ± j53.6				
-6.52 ± j53.6	-6.45 ± j53.6	-6.51 ± j53.6		-6.52 ± j53.5							

*Unstable poles

Table 5-3
KALMAN GAINS, COMMAND RESPONSE

$$R = C \begin{bmatrix} 10^{-1} & 0 & 0 \\ 0 & 10^0 & 0 \\ 0 & 0 & 10^5 \end{bmatrix} \quad \begin{array}{l} \text{Filter Model 4-3} \\ Q = 1.0 \end{array}$$

C	Kalman Gain Matrix, Transposed (K')			
10^{-5}	$\begin{bmatrix} 1.696 & 7.91 & 53.3 & 266 \\ 0.285 & 3.51 & 8.17 & 115.6 \\ 8.95 \times 10^{-5} & -5.51 \times 10^{-4} & -5.88 \times 10^{-3} & -0.01840 \end{bmatrix}$			
10^{-3}	$\begin{bmatrix} 1.181 & 1.222 & 14.90 & 27.2 \\ 0.0977 & 0.1940 & 0.601 & 4.11 \\ 1.07 \times 10^{-5} & -5.47 \times 10^{-5} & -1.638 \times 10^{-3} & -1.363 \times 10^{-3} \end{bmatrix}$			
10^{-1}	$\begin{bmatrix} 0.511 & 0.1424 & 1.756 & 0.985 \\ 0.01448 & 0.00736 & 0.01202 & 0.1722 \\ -0.719 \times 10^{-6} & -2.94 \times 10^{-6} & -1.682 \times 10^{-4} & -2.26 \times 10^{-5} \end{bmatrix}$			
10^1	$\begin{bmatrix} 0.220 & 0.0245 & 0.0926 & 0.01855 \\ 0.00245 & 3.56 \times 10^{-4} & 2.43 \times 10^{-4} & 6.81 \times 10^{-3} \\ -3.32 \times 10^{-6} & -3.80 \times 10^{-7} & -7.88 \times 10^{-6} & -3.12 \times 10^{-8} \end{bmatrix}$			

Further insight into the nature of the second mode instability can be gained by studying the Nyquist diagrams of Figures 5-22 and 5-23, and the roots in Figure 5-27. Figure 5-27 shows the typical location of the closed-loop system poles of the suboptimal control, suboptimal filter system. The basic rigid body and first bending poles, a and b, are located approximately where they were intended. The filter poles, c, d, and e, are located as a result of the assumed signal-to-noise ratio. Note that root c has minimal damping. Root f is the unstable second bending mode root.

The Nyquist diagram of Figure 5-22 indicates the stability of the rigid body root and the phase stabilization or control of the first bending mode. The second bending mode does not appear since in this system the desired states

Table 5-4

SYSTEM ROOTS, FILTER DESIGN BASED ON COMMAND RESPONSE

Transfer Function = ϕ/V_w

$$R = C \begin{bmatrix} 10^{-1} & 0 & 0 \\ 0 & 10^0 & 0 \\ 0 & 0 & 10^5 \end{bmatrix}$$

Filter Model = 4-3

 $Q_{(u)} = 1$

Plant = 20-1

 $t = 24 \text{ sec}$

$C = 10^{-5}$			$C = 10^{-3}$			$C = 10^{-1}$			$C = 10$		
Poles	Zeros		Poles	Zeros		Poles	Zeros		Poles	Zeros	
-0.1426 ± j2.31	-0.1838 ± j1.087	-0.0566 ± j2.44	-0.207 ± j1.175	-0.242 ± j0.291	-0.582 ± j1.13	-0.01184 ± j0.1084	-0.663 ± j0.881				
-0.0471 ± j2.46	-0.00967 ± j2.31	-0.322 ± j2.27	-0.0626 ± j2.35	-0.0329 ± j2.63	-0.1682 ± j2.17	-0.696 ± j0.615	-0.432 ± j2.12				
-0.00957 ± j2.31	-0.0551 ± j2.33	-0.302 ± j2.48	-0.01029 ± j2.31	-0.0218 ± j2.43	-0.01097 ± j2.31	-0.0236 ± j2.11	-0.01131 ± j2.31				
-0.804 ± j2.51	-0.0410 ± j2.50	-0.01008 ± j2.31	-0.0541 ± j2.51	0.747 ± j4.33	-0.0322 ± j2.43	-0.01129 ± j2.31	-0.01272 ± j2.43				
-1.068 ± j0.864	-0.880 ± j3.49	-1.321 ± j0.0555	-0.461 ± j3.00	-0.0750 ± j2.11	-0.0386 ± j2.63	-0.01296 ± j2.43	-1.065 ± j2.56				
-0.1594 ± j0.853	-0.0673 ± j12.66	-0.1860 ± j0.723	-2.54 ± j2.55	-0.0110 ± j2.31	1.894	-0.943 ± j2.57	-0.00822 ± j2.62				
-0.00944	3.46	-0.1163	0.1523 ± j5.36	-0.0325	-10.73	-0.00952 ± j2.63	0.0180 ± j5.36				
-10.94	-10.70	-10.72	-0.0937 ± j9.27	-10.69	-1.244 ± j2.48	-0.205	-0.599				
0.1804 ± j5.18*	0.236 ± j5.08	-1.169 ± j2.65	24.6	-0.945 ± j2.58	0.735 ± j5.37	-10.69	-10.71				
-6.06 ± j3.67	-7.19 ± j4.66	0.1115 ± j5.36*	-10.79	0.0481 ± j5.37*	-0.0619 ± j9.71	0.00631 ± j5.36*	-0.0459 ± j9.19				
-0.1439 ± j9.32	-0.277 ± j9.49	-0.0607 ± j9.23	-0.0601 ± j12.6	-0.0462 ± j9.20	-0.0635 ± j12.60	-0.0390 ± j9.19	-0.638 ± j12.6				
-6.0690 ± j12.85	-0.650 ± j53.6	-0.0462 ± j12.63	-6.52 ± j53.6	-0.063 ± j12.60	-6.52 ± j53.6	-0.0637 ± j12.60	-6.52 ± j53.6				
-6.52 ± j53.6		-6.52 ± j53.6		-0.652 ± j53.6		-6.52 ± j5.36					

*Unstable poles

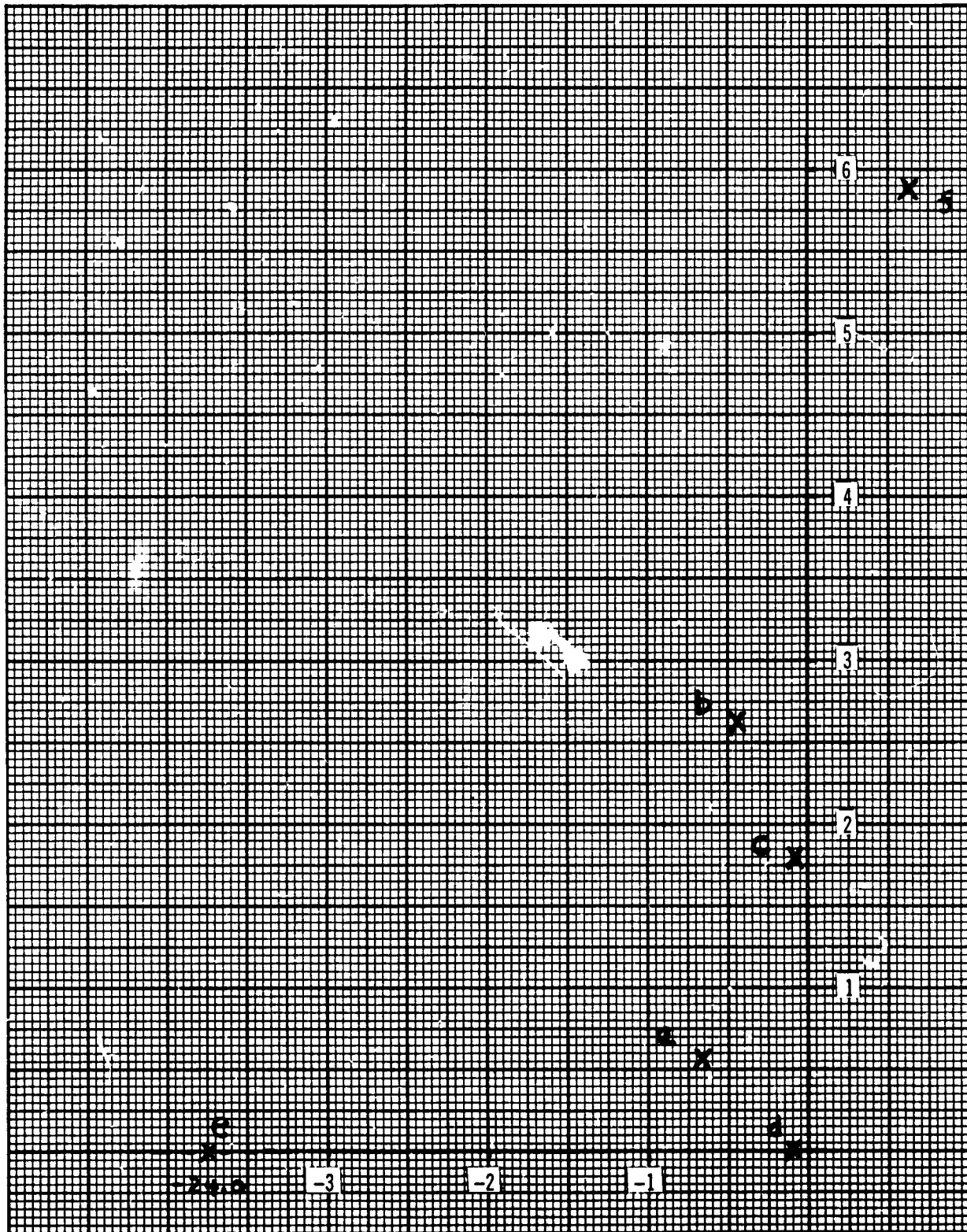


Figure 5-27. Roots, Plant 6-4 with Fourth-Order Filter 4-3

Table 5-5
KALMAN GAINS, 6-D FILTER

$$R = C \begin{bmatrix} 10^{-1} & 0 & 0 \\ 0 & 10^0 & 0 \\ 0 & 0 & 10^5 \end{bmatrix} \quad \begin{array}{l} \text{Filter Model 6-4} \\ Q_{(u)} = 1.0 \end{array}$$

C	Kalman Gain Matrix, Transposed (K')					
10^{-5}	1.711	4.61	52.9	119.1	5.38	-51.3
	0.251	4.04	6.22	137.4	4.58	84.4
	4.02×10^{-6}	-9.15×10^{-4}	-0.0305	-0.0307	-0.00374	5.95×10^{-4}
10^{-3}	1.284	1.232	15.89	19.98	-2.68	-18.3
	0.0785	0.1863	0.001712	4.28	0.306	5.75
	-1.073×10^{-5}	-9.05×10^{-5}	-0.001806	-0.00349	-4.75×10^{-4}	0.001088
10^{-1}	0.514	0.1427	1.705	0.860	-0.316	-0.319
	0.01349	0.00710	0.00409	0.1590	0.00265	0.357
	-7.40×10^{-6}	-3.14×10^{-6}	-1.512×10^{-4}	-3.05×10^{-5}	-2.17×10^{-5}	5.73×10^{-6}
10^1	0.220	0.0245	0.0907	0.01729	-0.00591	-0.00230
	0.00245	3.55×10^{-4}	1.945×10^{-3}	5.75×10^{-3}	3.24×10^{-5}	5.45×10^{-3}
	-3.34×10^{-6}	-3.84×10^{-7}	-0.710×10^{-6}	-1.110×10^{-7}	-1.787×10^{-7}	-5.26×10^{-8}

are assumed to be explicitly observable. Figure 5-23 indicates similar rigid body and first bending mode stability but also indicates the feedback of second bending as a result of the suboptimal estimation of first mode and rigid body states. The second bending states riding through on the suboptimally estimated first bending states are phase-stabilizing. The second bending states on the optimally estimated rigid body states are destabilizing. The net result is an unstable second mode because the filter is unable to adequately reject the second bending states.

Because of the consistent inability to achieve stability in the second bending mode, the next series of filters was prepared with the second bending mode included. The R matrix was again sized from the asymptotes of the spectral densities. The same R matrix as in the last series was adopted. Table 5-5 shows the set of Kalman gains generated. Table 5-6 shows the resulting system poles and zeros. As can be seen, this entire series of sixth-order

Table 5-6

SYSTEM ROOTS, 6-D FILTER

Transfer Function = ϕ/V_w

$$R = C \begin{bmatrix} 10^{-1} & 0 & 0 \\ 0 & 10^0 & 0 \\ 0 & 0 & 10^5 \end{bmatrix}$$

 $Q_{(u)} = 1$

Filter Model 6-4

 $t = 24 \text{ sec}$

Plant = 20-1

Poles	$C = 10^{-5}$			$C = 10^{-3}$			$C = 10^{-1}$			$C = 10^1$		
	Zeros	Poles	Zeros	Poles	Zeros	Poles	Zeros	Poles	Zeros	Poles	Zeros	Poles
-6.52 ± j53.5	-6.51 ± j53.5	-6.52 ± j53.5	-6.52 ± j53.5	-6.52 ± j53.5	-6.52 ± j53.5	-6.52 ± j53.5	-6.52 ± j53.5	-0.01072 ± j0.1086	-0.554 ± j0.835			
-0.1525 ± j12.62	-0.0827 ± j12.60	-0.0625 ± j12.60	-0.0636 ± j12.60	-0.0636 ± j12.60	-0.0636 ± j12.60	-0.0636 ± j12.60	-0.0638 ± j12.60	-0.556 ± j6.41	-0.0425 ± 2.12			
-11.37	-0.001137 ± j3.02	-10.72	-10.89	-10.69	-10.74	-10.69	-10.74	-0.0232 ± j2.11	-0.01490 ± j2.31			
-9.32	-0.579 ± j8.96	-0.1315 ± j9.18	-0.240 ± j9.18	-0.0659 ± j9.19	-0.0879 ± j9.19	-0.0659 ± j9.19	-0.0879 ± j9.19	-0.0328 ± j2.29	-0.01235 ± j2.43			
-0.251 ± j9.09	-5.81	-0.238 ± j5.60	-0.292 ± j5.76	-0.0494 ± j5.37	-0.0584 ± j5.38	-0.0494 ± j5.37	-0.0584 ± j5.38	-0.01255 ± j2.43	-0.00746 ± j2.62			
-6.501	-0.794 ± j6.32	-1.360 ± j5.34	-1.208 ± j5.18	-1.14 ± j5.51	-1.111 ± j5.49	-1.14 ± j5.51	-1.111 ± j5.49	-0.00884 ± j2.62	-0.700 ± j2.78			
-0.504 ± j5.80	-1.23 ± j5.55	-1.461 ± j2.77	-2.14 ± j3.099	-0.641 ± j2.81	-0.828 ± j2.82	-0.641 ± j2.81	-0.828 ± j2.82	-1.117 ± j5.54	1.497			
-1.823 ± j5.43	-0.217 ± j3.03	-0.243 ± j2.74	-0.270 ± j2.93	-0.0341 ± j2.63	-0.0392 ± j2.62	-0.0341 ± j2.63	-0.0392 ± j2.62	-0.517 ± j2.77	-10.71			
-0.235 ± j2.83	-0.0452 ± j2.49	-0.0425 ± j2.45	-0.0505 ± j2.49	-0.0219 ± j2.43	-0.01104 ± j2.31	-0.0219 ± j2.43	-0.01104 ± j2.31	-0.204	-0.0280 ± j5.36			
-0.0377 ± j2.45	-0.00974 ± j2.31	-0.0100 ± j2.31	-0.01004 ± j2.31	-0.01107 ± j2.31	-0.0326 ± j2.43	-0.01107 ± j2.31	-0.0326 ± j2.43	10.59	-1.110 ± j5.54			
-0.01001 ± j2.31	-0.0673 ± j2.32	-0.1574 ± j2.24	-0.0694 ± j2.33	-0.0727 ± j2.11	-0.156 ± j2.17	-0.0727 ± j2.11	-0.156 ± j2.17	-0.0278 ± j5.36	-0.0474 ± j9.19			
-0.124 ± j2.24	-0.0858 ± j0.991	-0.1741 ± j0.906	-0.128 ± j1.09	-0.508 ± j0.613	-0.466 ± j1.041	-0.508 ± j0.613	-0.466 ± j1.041	-0.0397 ± j9.19	-0.0638 ± j12.6			
-0.0295 ± 1.014	-0.00315	-0.668 ± j0.538	-0.000303	-0.264 ± j0.260	-0.000221	-0.264 ± j0.260	-0.000221	-0.0637 ± j12.60	-6.52 ± j53.6			
-0.621 ± j0.607												
-0.00910		-0.01138		-0.0327		-0.0327		-6.52 ± j53.6				

filters achieves complete system stability. This allowed carrying the analysis work of these filters to parameter sensitivity and transient response studies.

For the transient and parameter sensitivity studies the plant model was reduced from 20th to 11th order by discarding the actuator and sloshing mode dynamics. These effects had not proven to be destabilizing in any of the cases previously made. The filtering does not include these states, so there is no danger of parameter mismatch. This order reduction of the plant made available space on the computer for the computation of a series of transfer functions of interest. The poles and zeros of the transfer function ϕ/ϕ_c are shown in Figure 5-28. Vehicle rigid body rotation and engine deflections in response to a stepwind input of 1 msec are shown in Figures 5-29 and 5-30 for the four filters. System pole positions with parameter perturbations are shown in Figures 5-31 through 5-34. Figure 5-29 tends to indicate that the $C = 10$ and $C = 1.0$ autopilots are too slow for satisfactory disturbance suppression. Figure 5-31 indicates instability from parameter mismatch for $C = 10^{-5}$. This leaves the $C = 10^{-3}$ case as the best filter of the set. From this study, it apparently is an acceptable filter.

A very limited effort was made toward developing filtering for the $t = 80$ (Max-Q) and $t = 155$ (burnout) conditions. Noise covariance matrixes were developed in the same manner as before and Kalman matrixes were prepared. These Kalman gains are presented in Table 5-7. The ASP program overflowed in the low c value runs and so only K gains for large c values were developed and appear in Table 5-7. Figures 5-35 and 5-36 show the system closed-loop poles and the zeros for the transfer function ϕ/ϕ_c for the Max-Q and burnout conditions, respectively. All of the Max-Q runs made are unstable in the lateral velocity state (Z). The burnout runs are unstable in the third bending mode.

5.6.2 White, Correlated Noise Approach

This approach, explained in subsection 5.3.3, forms the white noise covariance matrix from the variance of the 2-system subjected to a white noise u -input. The 4-dimensional filter was first investigated. The 2-system was formed by striking out the rigid body, first bending, actuator, and wind

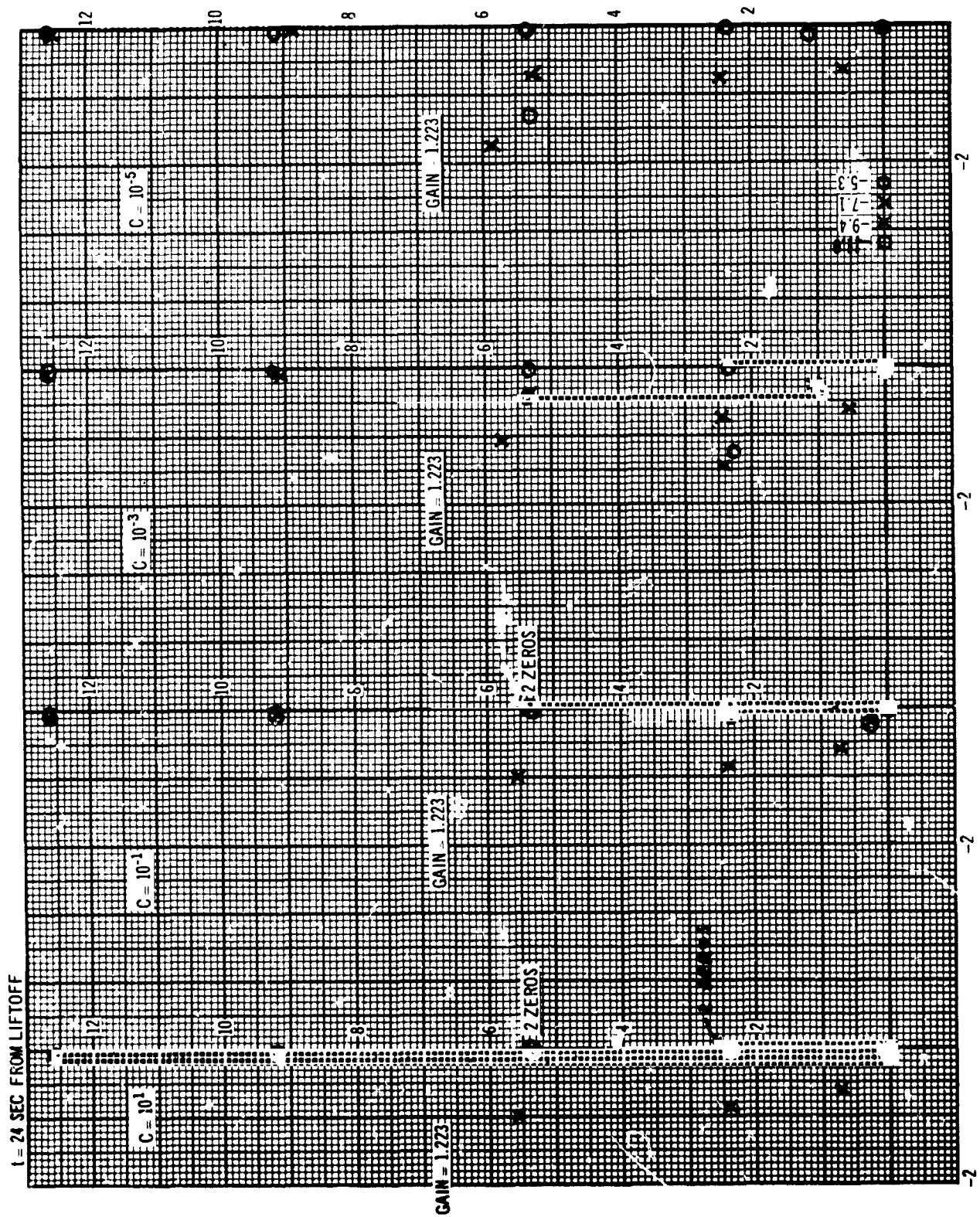


Figure 5-28. System Roots for Varying Noise Level

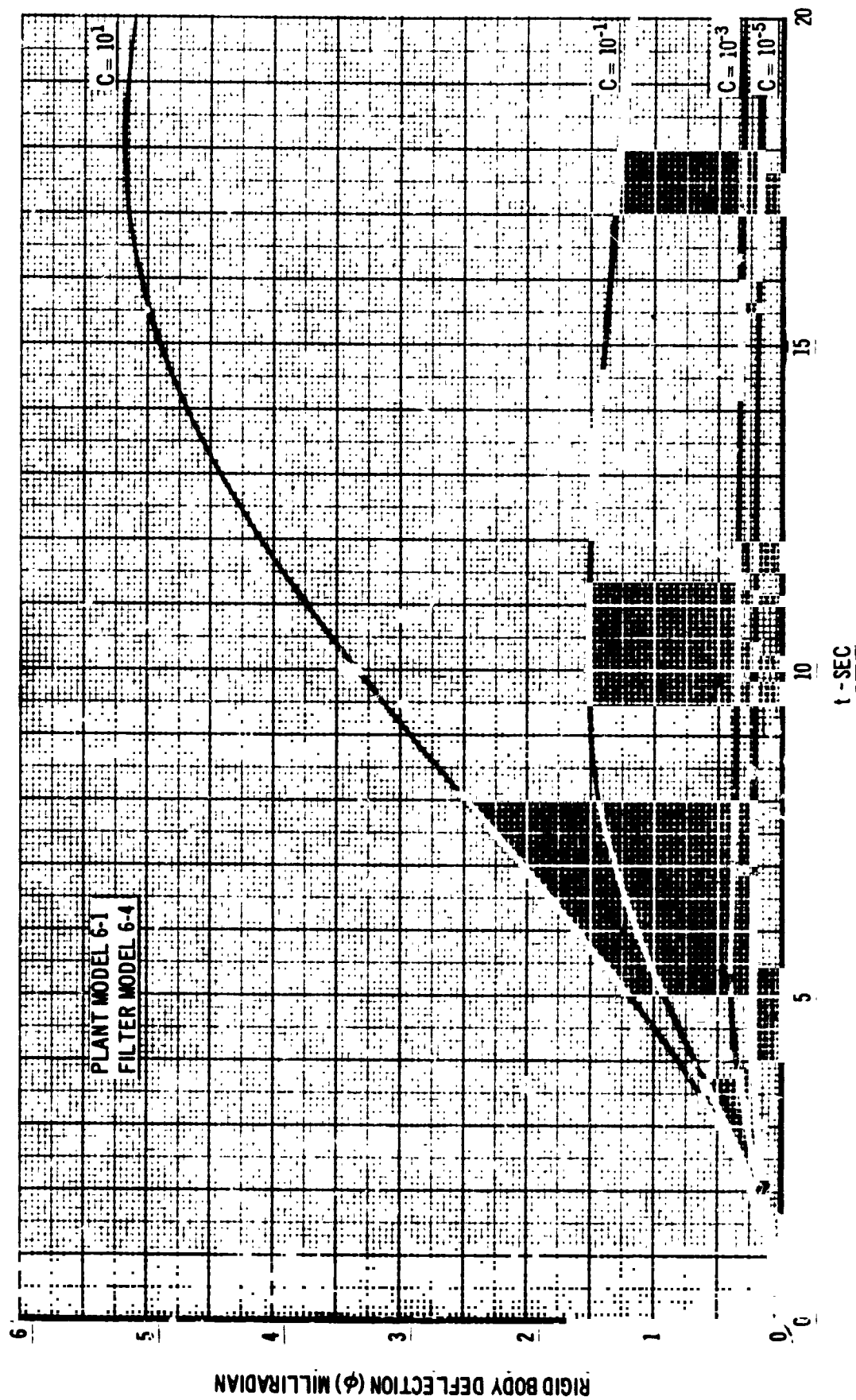


Figure 5-29. Attitude Response to a Step Wind Input

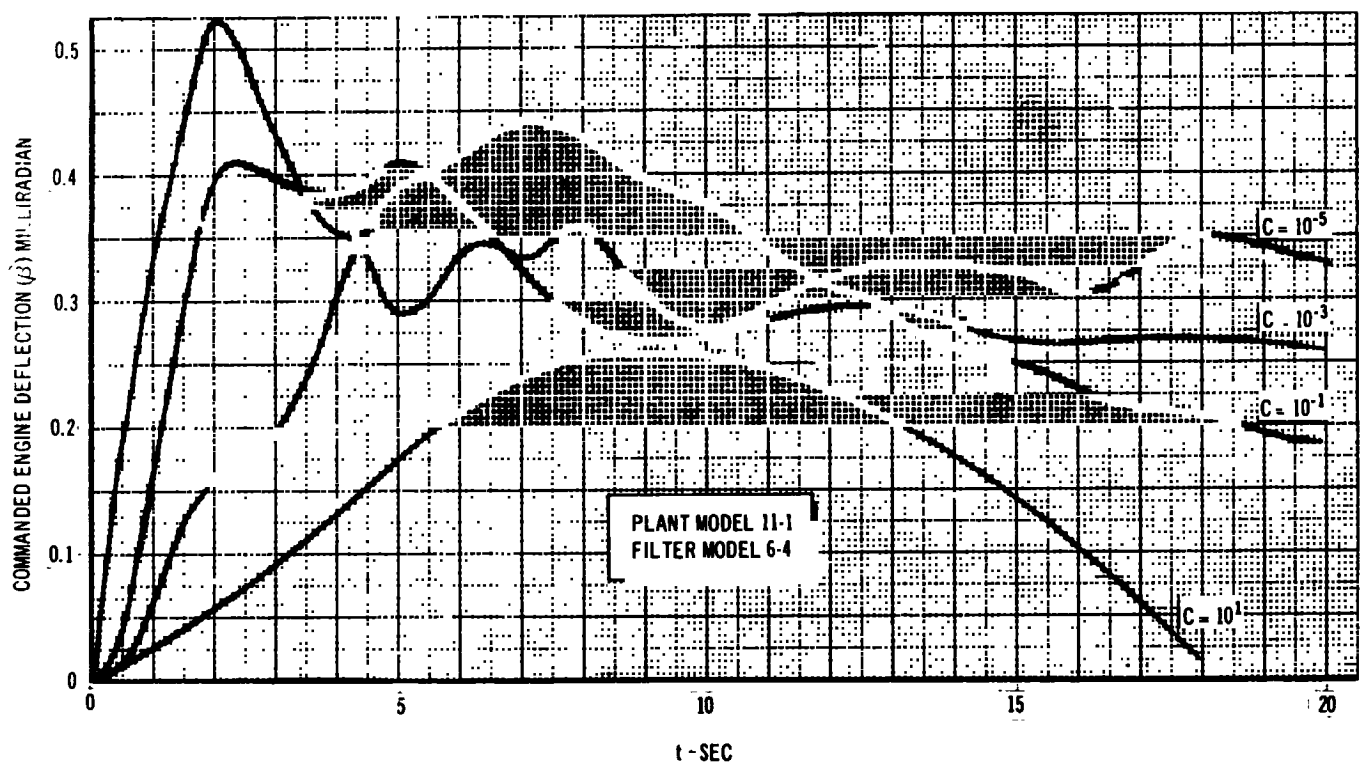


Figure 5-30. Engine Deflection Response to a Step Wind Input

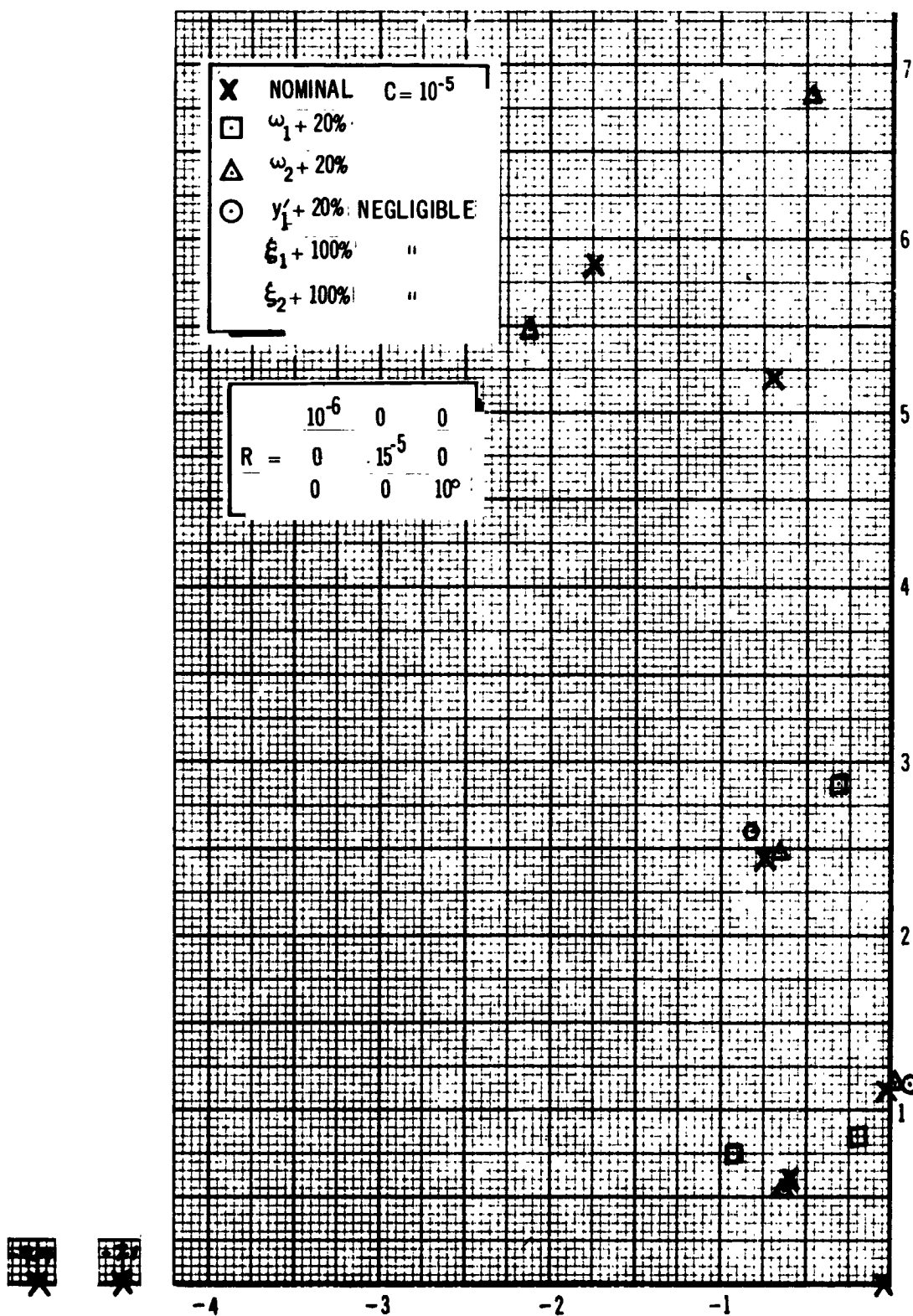


Figure 5-31. Parameter Mismatch Stability

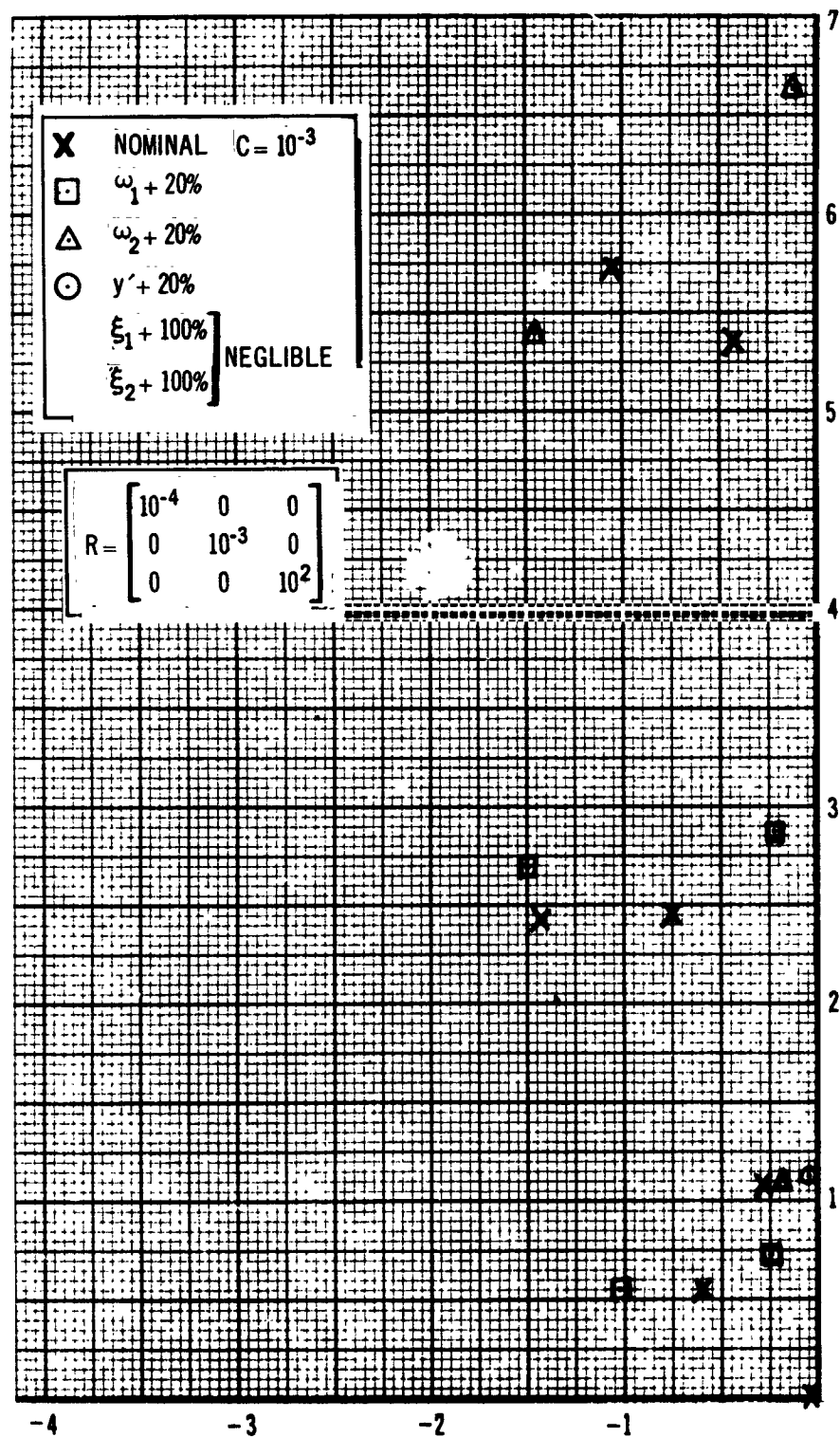


Figure 5-32. Parameter Mismatch Stability

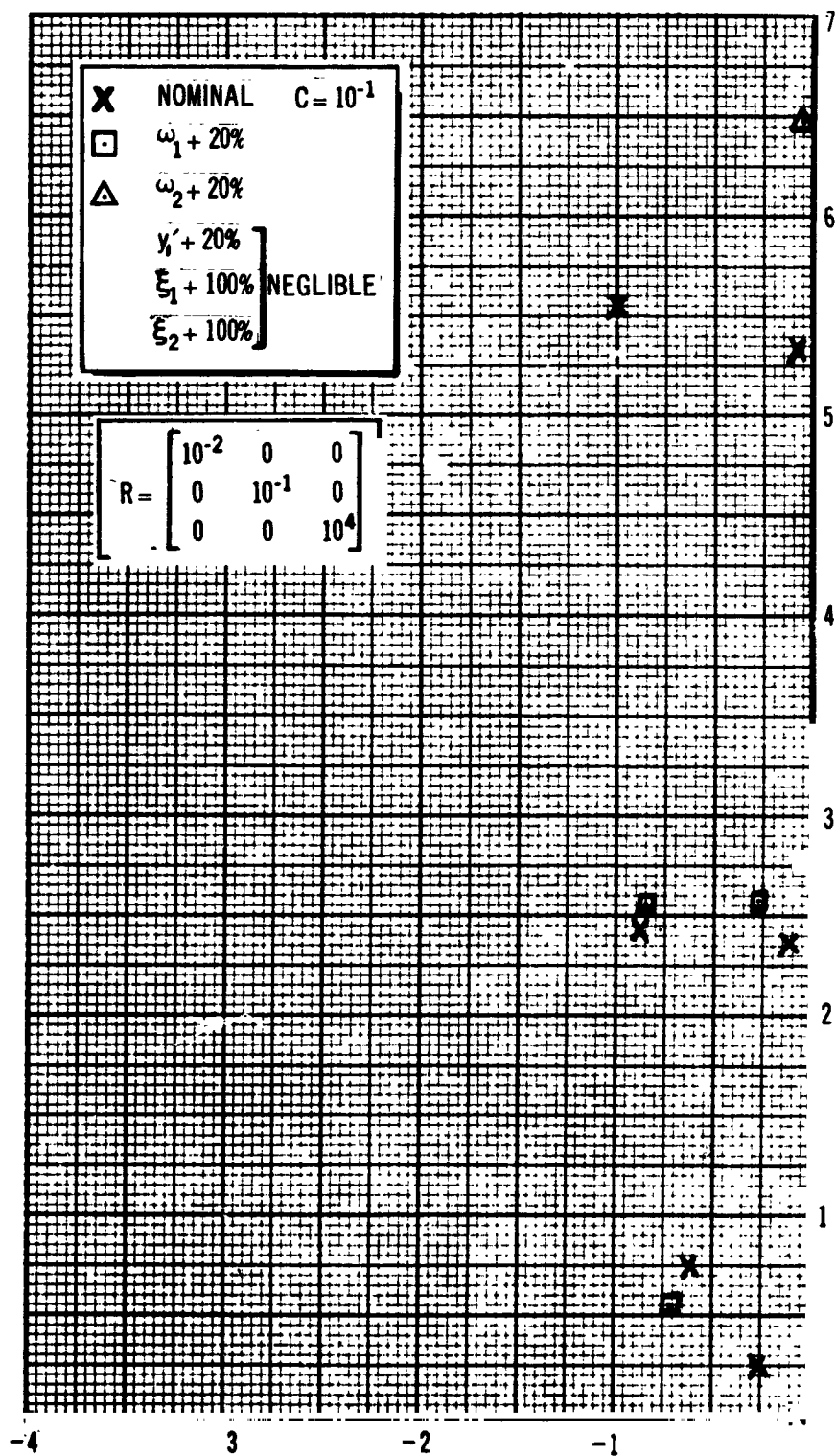


Figure 5-33. Parameter Mismatch Stability

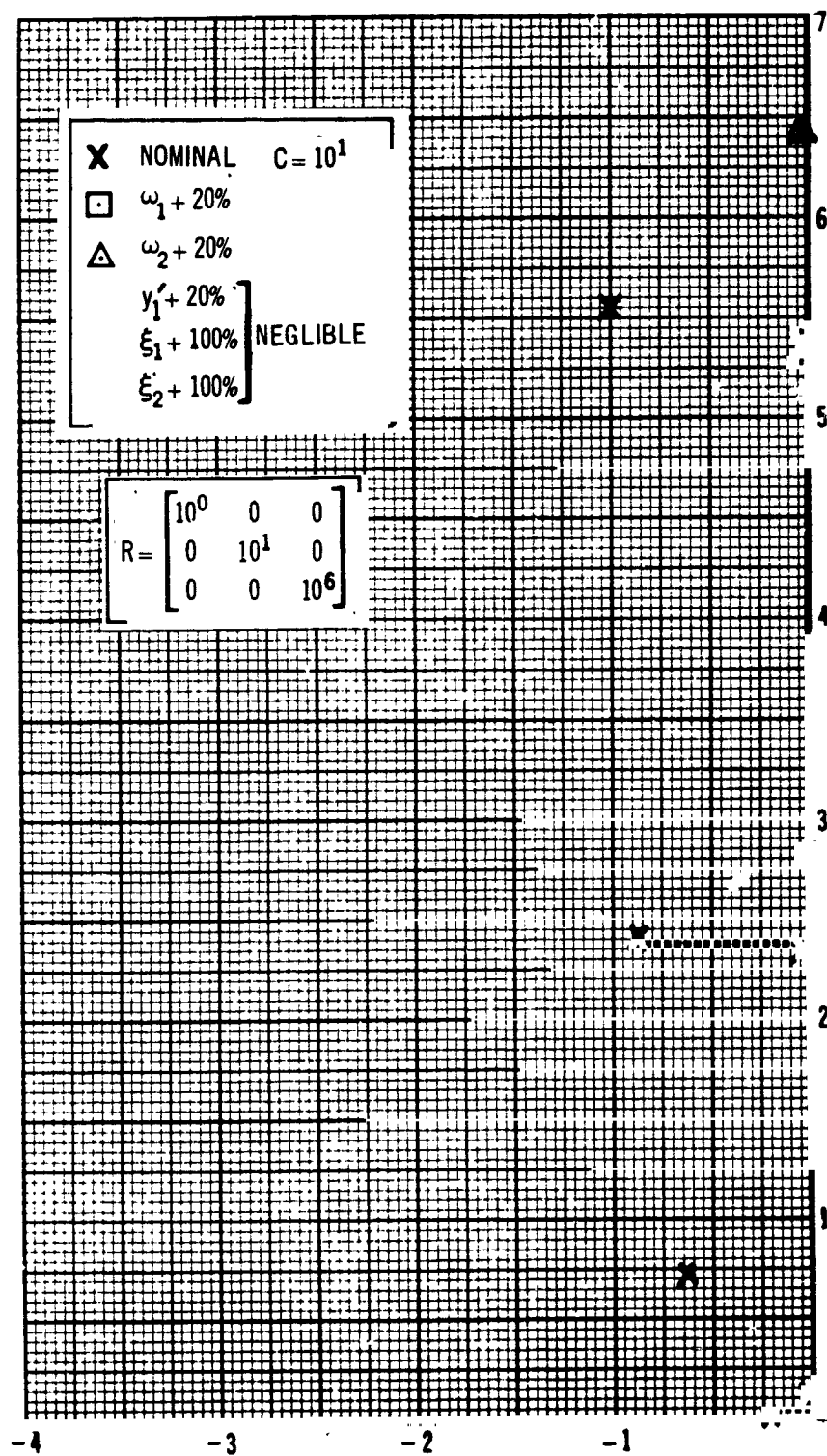


Figure 5-34. Parameter Mismatch Stability

Table 5-7
MAX-Q AND BURNOUT, 6-D KALMAN GAINS

Max Q

$$R = C \begin{bmatrix} 4 \times 10^{-4} & 0 & 0 \\ 0 & 1.4 \times 10^{-6} & 0 \\ 0 & 0 & 1.7 \times 10^3 \end{bmatrix} \begin{matrix} Q_{(u)} = 1 \\ t = 80 \text{ sec} \end{matrix} \quad \text{Filter Model} = 6-5$$

Kalman Gain Matrix, Transposed (K')

$C = 10^2$	$\begin{bmatrix} 0.13 & 0.256 & -0.39 & -4.22 & -1.04 & -2.66 \\ 26.9 & 40.3 & -490 & 40.5 & -277 & 1,375 \\ (0.45 \times 10^{-4}) & (0.135 \times 10^{-3}) & (-0.852 \times 10^{-3}) & (-0.0025) & (-0.49 \times 10^{-3}) & -0.00134 \end{bmatrix}$
$C = 10^4$	$\begin{bmatrix} 0.05 & 0.0046 & 0.854 & 0.0342 & -0.0738 & -0.039 \\ 3.32 & 4.18 & -45 & 47.8 & -20.6 & 175.7 \\ (0.39 \times 10^{-6}) & (0.162 \times 10^{-5}) & (-0.238 \times 10^{-4}) & (-0.2 \times 10^{-4}) & (-0.55 \times 10^{-5}) & (-0.8 \times 10^{-5}) \end{bmatrix}$
$C = 10^6$	$\begin{bmatrix} 0.029 & 0.009 & 0.203 & 0.033 & -0.012 & -0.004 \\ 1.82 & 0.774 & 6.02 & 16.7 & -0.59 & 20.6 \\ (-0.129 \times 10^{-6}) & (-0.24 \times 10^{-7}) & (-0.22 \times 10^{-5}) & (-0.75 \times 10^{-7}) & (-0.87 \times 10^{-7}) & (-0.117 \times 10^{-7}) \end{bmatrix}$

Burnout

$$R = C \begin{bmatrix} 1.1 \times 10^{-4} & 0 & 0 \\ 0 & 1.3 \times 10^{-4} & 0 \\ 0 & 0 & 2.1 \times 10^3 \end{bmatrix} \begin{matrix} Q_{(u)} = 1 \\ t = 155 \text{ sec} \end{matrix} \quad \text{Filter Model} = 6-6$$

$C = 10^2$	$\begin{bmatrix} 1.35 & 0.986 & 29 & 10.1 & -3.56 & -44.6 \\ 4.52 & 18.7 & -306 & -897 & -124 & 49.65 \\ (0.105 \times 10^{-3}) & (0.775 \times 10^{-3}) & (-0.008) & -0.0509 & -0.0036 & -0.0178 \end{bmatrix}$
$C = 10^4$	$\begin{bmatrix} 1.24 & 0.694 & 22.3 & 24.5 & -3.09 & -17.9 \\ 0.782 & 1.78 & -29.8 & -29.3 & -6.31 & 82.5 \\ (0.37 \times 10^{-6}) & (0.128 \times 10^{-4}) & -0.00028 & -0.00086 & -0.00012 & 0.000039 \end{bmatrix}$
$C = 10^6$	$\begin{bmatrix} 0.588 & 0.177 & 3.23 & 1.93 & -0.54 & -0.614 \\ 0.14 & 0.096 & -0.48 & -2.78 & -0.057 & 8.6 \\ (-0.103 \times 10^{-5}) & (-0.195 \times 10^{-6}) & (-0.15 \times 10^{-4}) & (-0.12 \times 10^{-4}) & (-0.654 \times 10^{-5}) & (0.109 \times 10^{-5}) \end{bmatrix}$

states out of the 21-d system and forming state and observation equations with the remaining systems. Equations 5-43 and 5-44 were solved with the ASP program to yield the R matrixes. Table 5-8 shows the developed covariance matrixes and the Kalman gains developed from them for the 4-d filter. Only the 24-sec case was tested for stability. This system is unstable in the second bending mode, as was the case with the uncorrelated noise 4-dimensional filters.

The above process was repeated for a six-dimensional filter. For these cases, the second bending states were also removed from the 2-system before insertion into Equations 5-43 and 5-44.

Table 5-9 presents the resulting 2-system variance matrix and the Kalman gains developed from them. The stability studies of the system using these Kalman gains and the corresponding optimal control gains developed in Section 3 are shown in Figures 5-37, 5-38, and 5-39. The stability problems encountered with the uncorrelated filters are similar in these runs. For low-noise cases, system instability in lateral velocity is encountered at Max-Q and third bending at burnout. However, stability is achieved at all flight conditions as the noise level is raised. At each flight condition, transient studies were made for the state systems, and parameter perturbation studies were made for the lowest noise stable systems. Figures 5-40 through 5-44 apply to the near liftoff case. Figures 5-45 through 5-48 apply to the Max-Q case (80 sec) and Figures 5-49 through 5-51 apply to the near burnout case (155 sec). The transients in each case consist of the observable transient, made assuming optimal gains operating on the states, assuming they are available, and the filtered transient, where the suboptimal filter is used to estimate the states.

The 24-second runs, Figures 5-40, 5-41, and 5-42, are a little slow in filtering. The stable Max-Q runs of Figures 5-45 and 5-46 are unsatisfactory because of ripple at 1 rps. Figure 5-47 indicates the system can easily go unstable on this pole with mis-estimation of the first bending mode influence coefficients. This is a filter pole and may necessitate the addition of the Z-state to the filter model. It is significant that the observable system is not satisfactory in this case, either. The near-burnout run of Figure 5-49

Table 5-8
KALMAN GAINS, CORRELATED NOISE 4-D FILTER, $t = 24$ SEC PLANT
 $Q_{(u)} = 1$

System Variance			Kalman Matrixes								
(R)			$C = 10^{+2}$			$C = 10^0$			$C = 10^{-2}$		
$t = 24 \text{ sec}$ Filter Model 4-3											
2.59	0.001145	552	0.262	0.00358	-0.000202	0.794	0.0347	-0.00061	2.89	0.748	-0.00086
0.00114	24.9	55.7	0.0314	0.000673	-0.000026	0.248	0.019	-0.000175	0.661	0.66	0.00095
552	55.7	7.61×10^5	0.29	0.000411	-0.00028	3.63	-0.0375	-0.00366	14.2	-4.59	-0.025
			0.0852	0.0196	-0.000065	4.37	0.382	-0.00352	85	3.43	-0.0715

$t = 80 \text{ sec}$ Filter Model 4-4		
2.33	0.0221	741
0.0221	30.4	91.8
941	91.8	1.107×10^6

$t = 155 \text{ sec}$		
6.51	0.215	2930
0.215	124.7	42.5
2930	42.5	2.56×10^6

Table 5-9
KALMAN GAINS, CORRELATED NOISE, 6-D FILTER

t = 24 sec			t = 80 sec			t = 155 sec			
2-System Variance	0.197	0.0291	284.5	0.1748	0.0369	332	0.1250	0.01934	36.7
	0.0291	10.04	72.7	0.0369	9.19	101.6	0.01934	11.5	31.3
	284.5	72.7	705,000	332	101.8	970,000	36.7	31.3	1.179×10^6
Kalman Gain Matrixes (K)									
Scale Factor	Filter Model 6-4			Filter Model 6-5			Filter Model 6-6		
$C = 10^{-2}$	6.97	1.13	-0.00193	3.33	1.21	-0.0004	7.43	1.63	0.00186
	1.82	0.98	0.00136	-0.484	1.40	0.0025	2.303	4.33	0.0144
	89.5	-12.2	-0.0569	149	-12.95	-0.0691	234	-81.7	-0.182
	154	16.9	-0.104	149	23.4	-0.0962	561	-95	-0.038
	37.8	-0.92	-0.0258	62.6	-2	-0.0328	80.1	-24	-0.0827
	-448	42.2	0.181	-756	59.9	0.252	-918	115	-0.196
$C = 10^0$	2.62	0.027	-0.00106	3.1	0.0325	-0.00107	6.08	0.176	-0.00025
	1.26	0.0252	-0.00049	2.16	0.04	-0.000726	4.91	0.371	-0.0000138
	13.7	-0.321	-0.0058	24.4	-0.404	-0.0086	46.9	-6.48	-0.00517
	31	0.451	-0.0132	70.3	73.5	-0.025	278	1.19	-0.0285
	-6.21	0.0457	0.0023	-5.05	0.063	0.00144	-2.53	-0.313	-0.00284
	-59.3	1.86	0.0241	-94.8	3.03	0.0325	-273	19	0.0108
$C = 10^2$	0.544	0.00109	-0.00022	0.66	0.00117	-0.000227	1.22	0.00335	-0.000042
	1136	0.00053	-0.000055	0.306	0.00083	-0.000105	0.61	0.00575	-0.0000196
	1.81	-0.0027	-0.00075	5.54	-0.00014	-0.00191	10.2	-0.0912	-0.00045
	1.04	0.018	-0.00043	4.37	0.0288	-0.00151	14.4	0.0393	-0.000673
	-1.01	0.00044	0.0004	-1.37	0.00106	0.00045	-3.85	0.006	-0.000044
	-1.05	0.116	0.00041	-2.33	0.186	0.00078	-9.27	1.22	0.000276

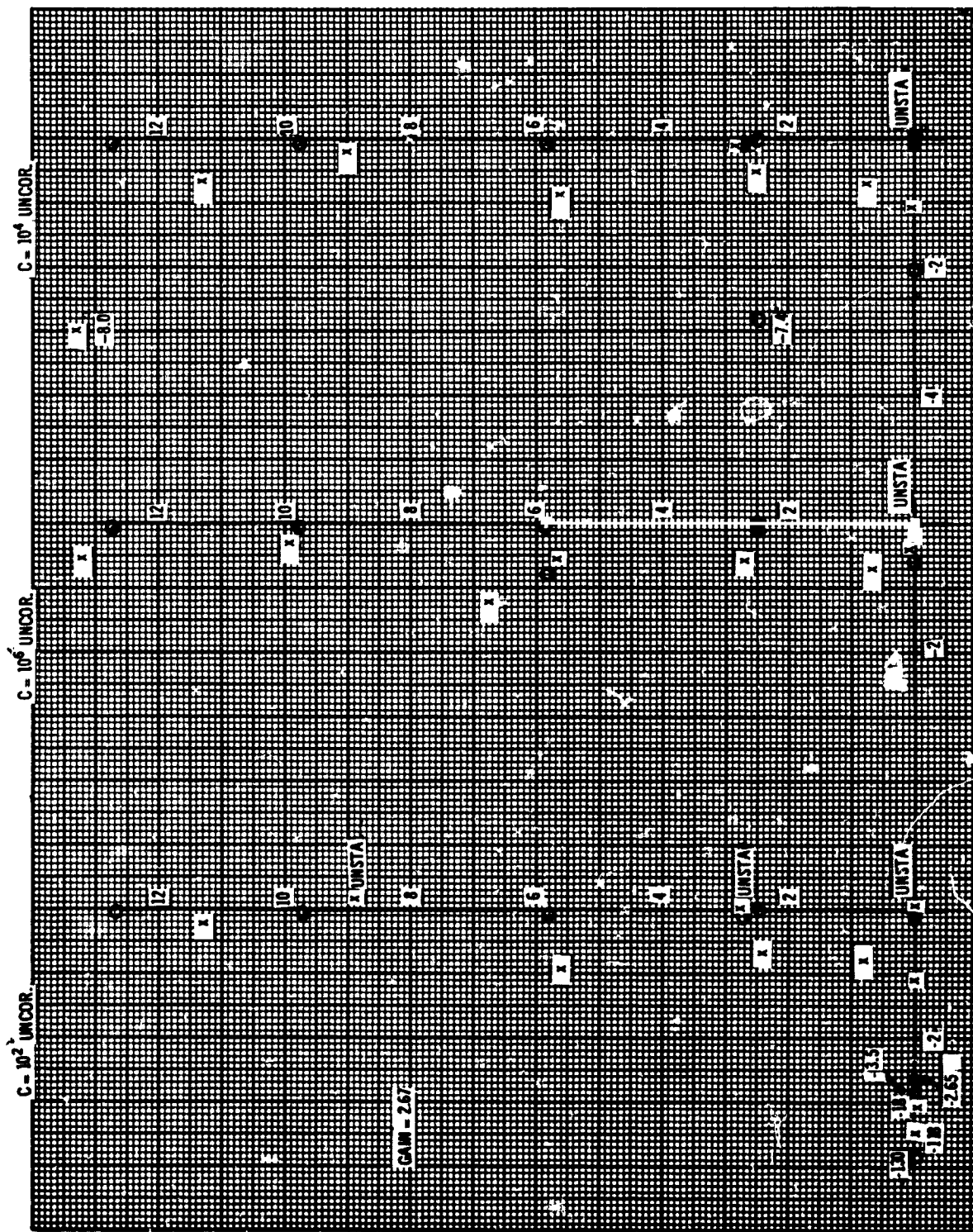


Figure 5-35. System Roots (88 sec.)

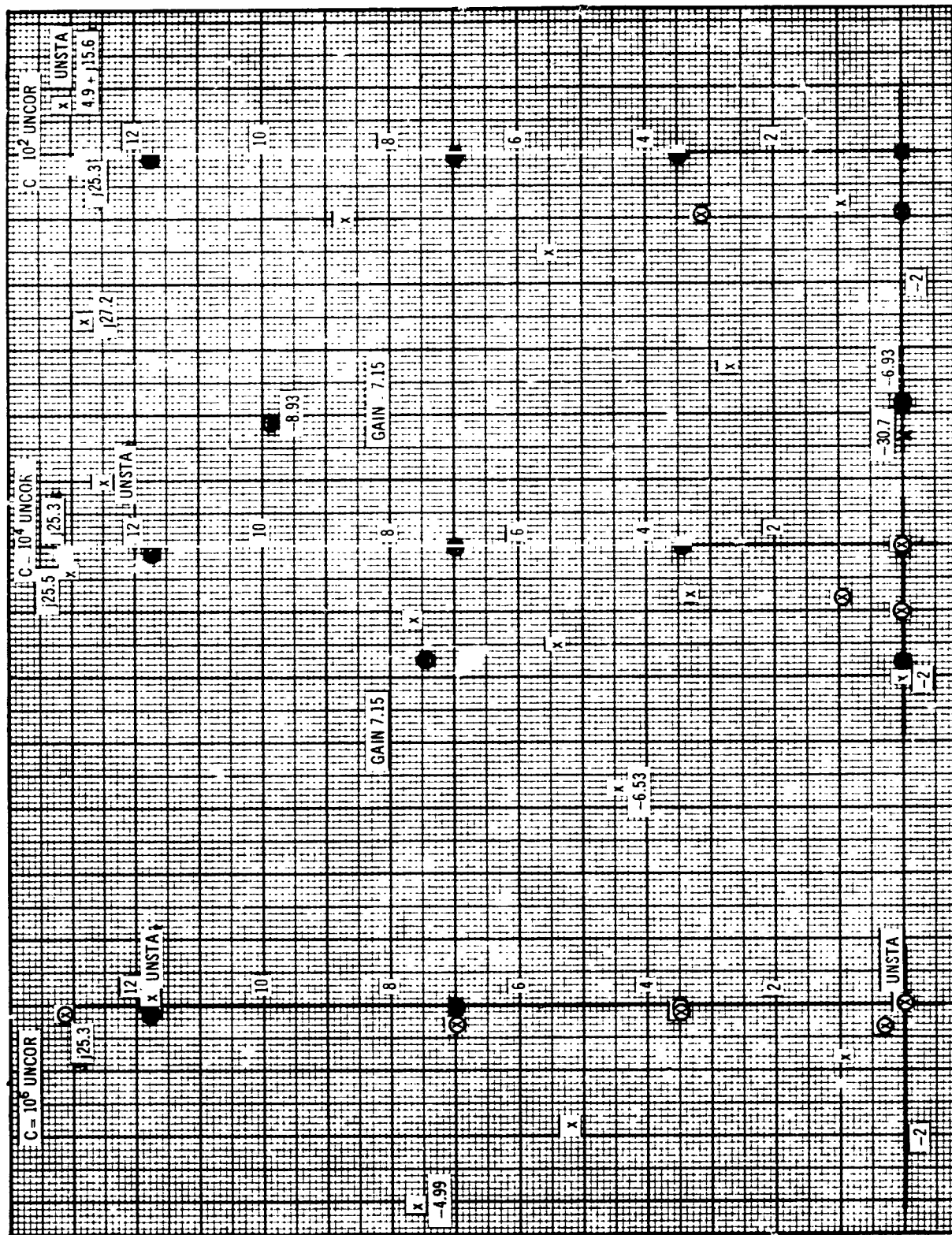


Figure 5-36. System Roots (155 sec)

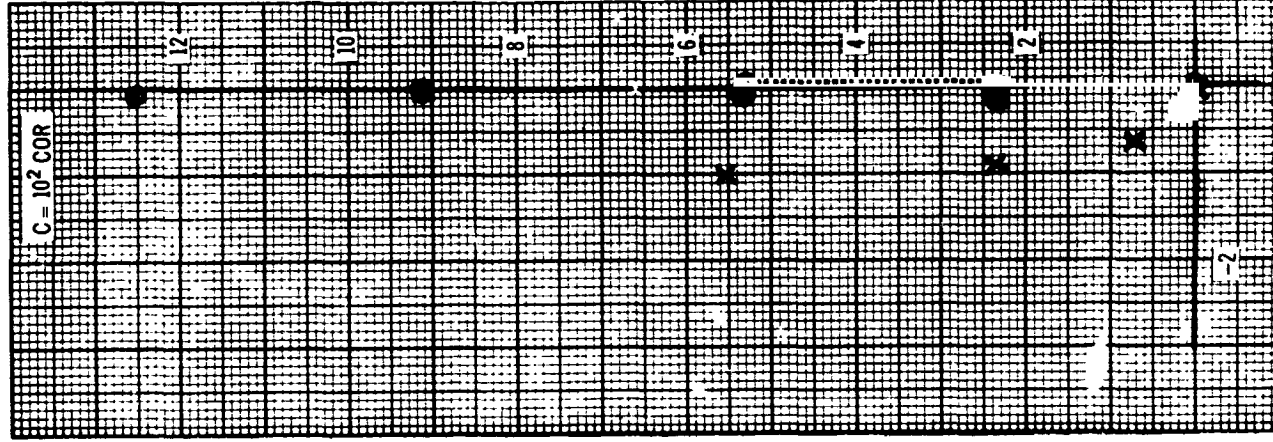
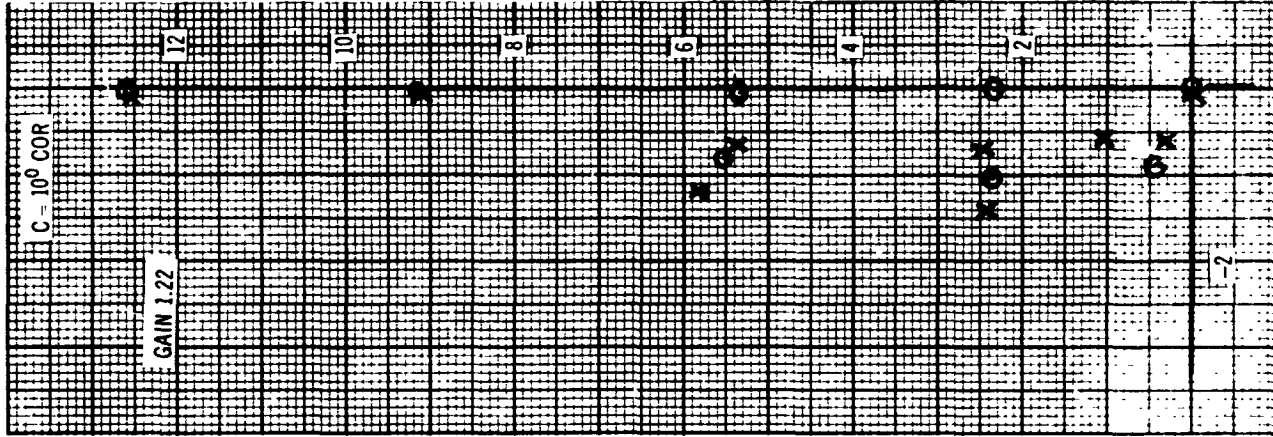
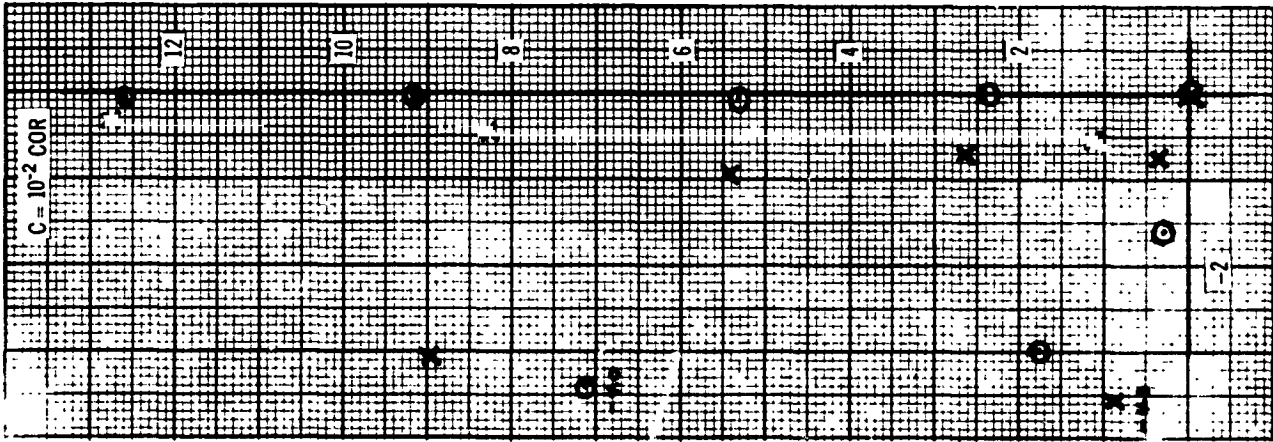


Figure 5-37. System Roots (24 sec)

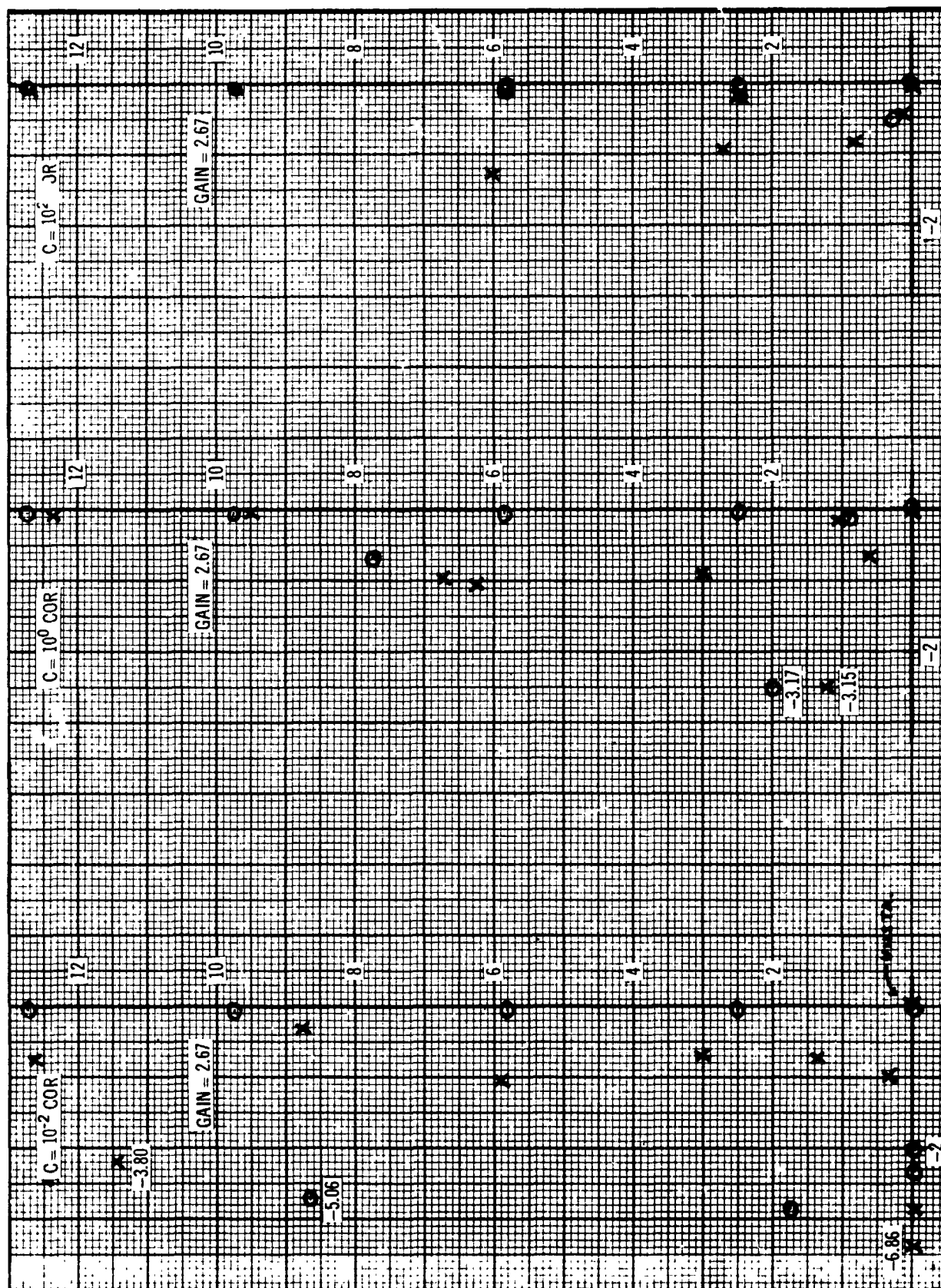


Figure 5-38. System Roots (80 sec)

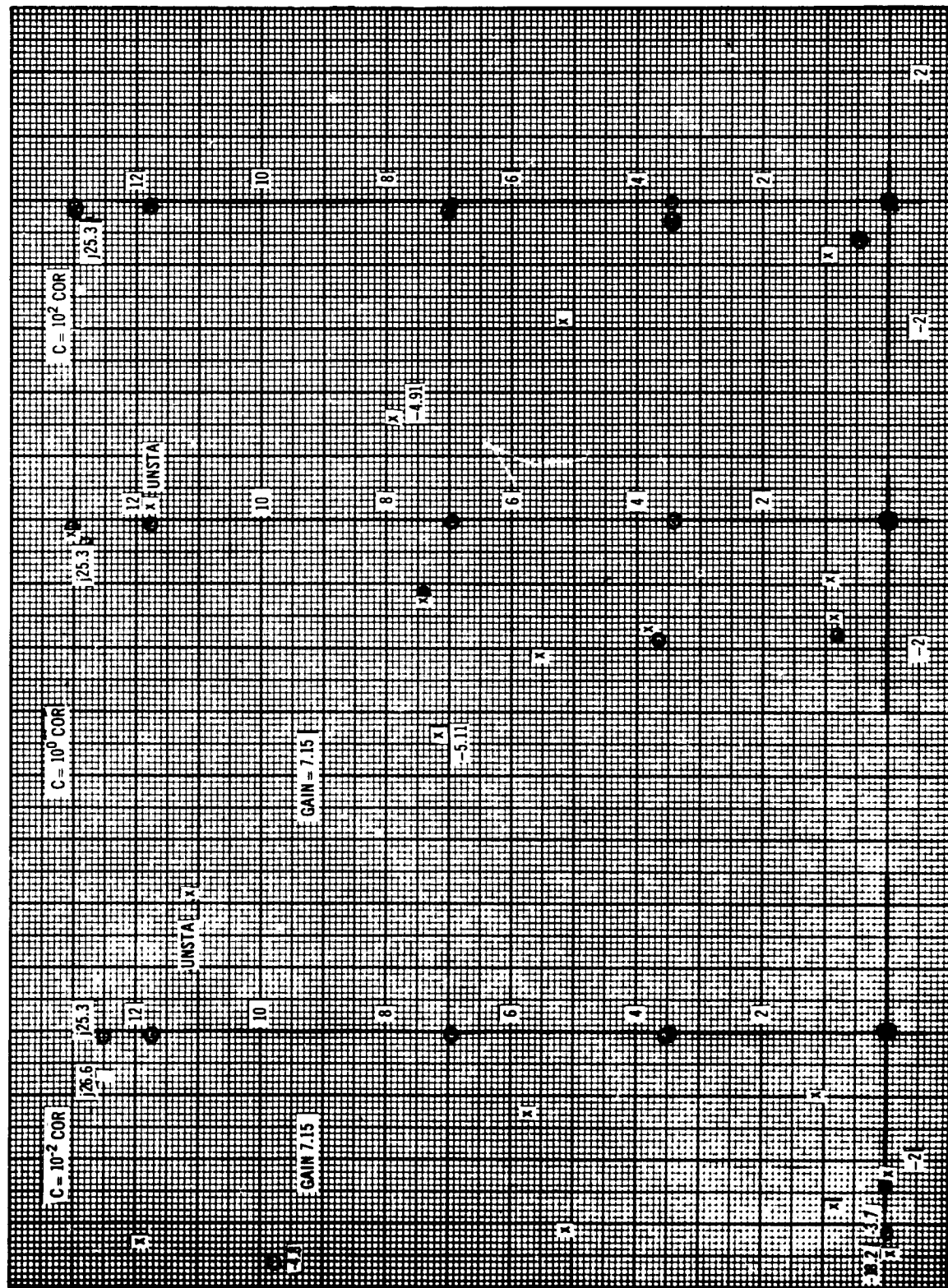


Figure 5-39. System Roots (155 sec)

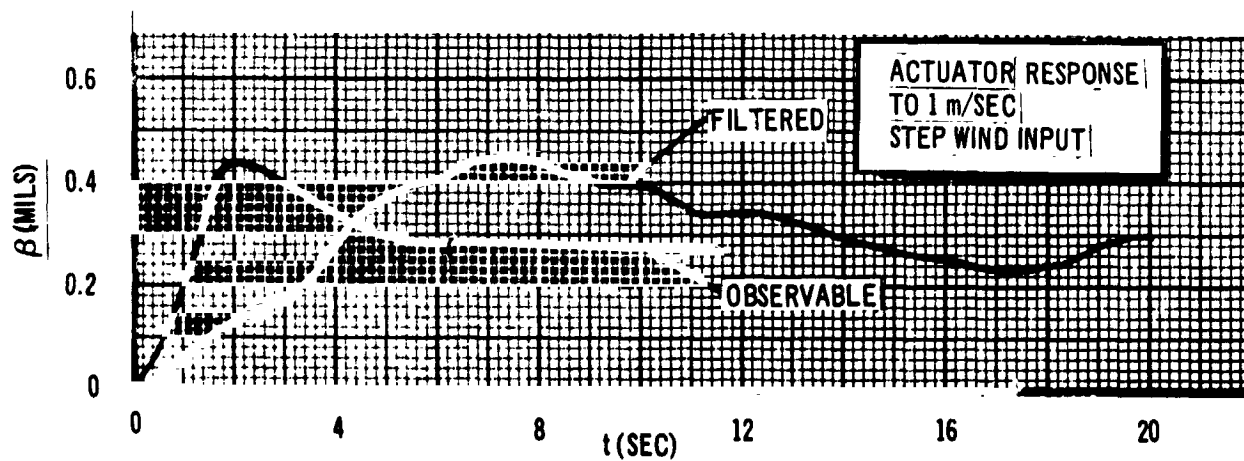
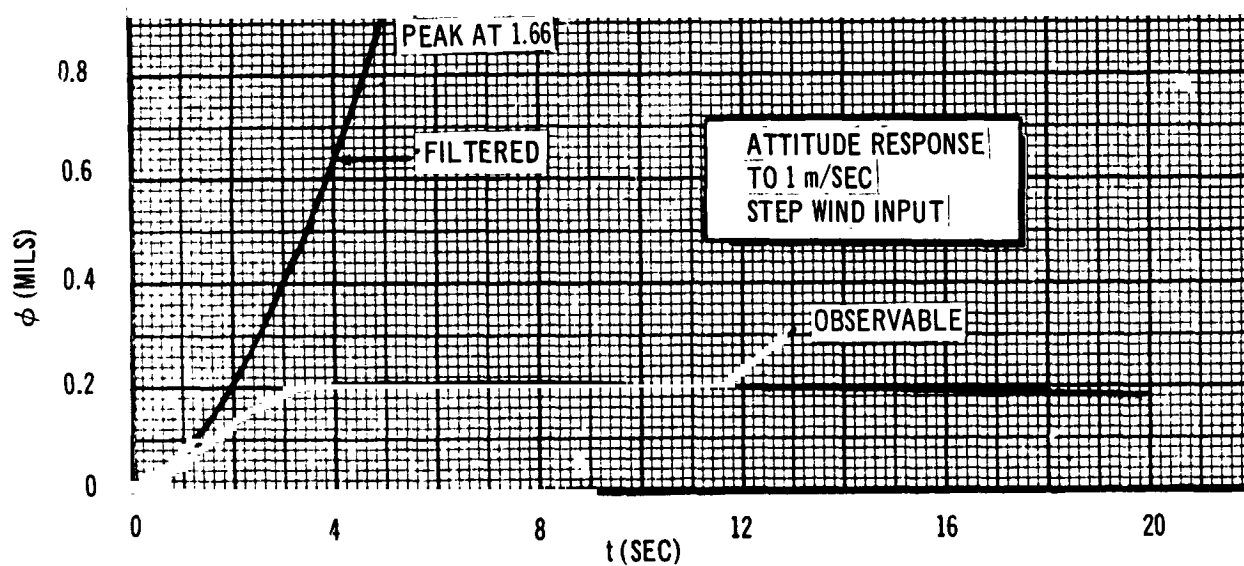
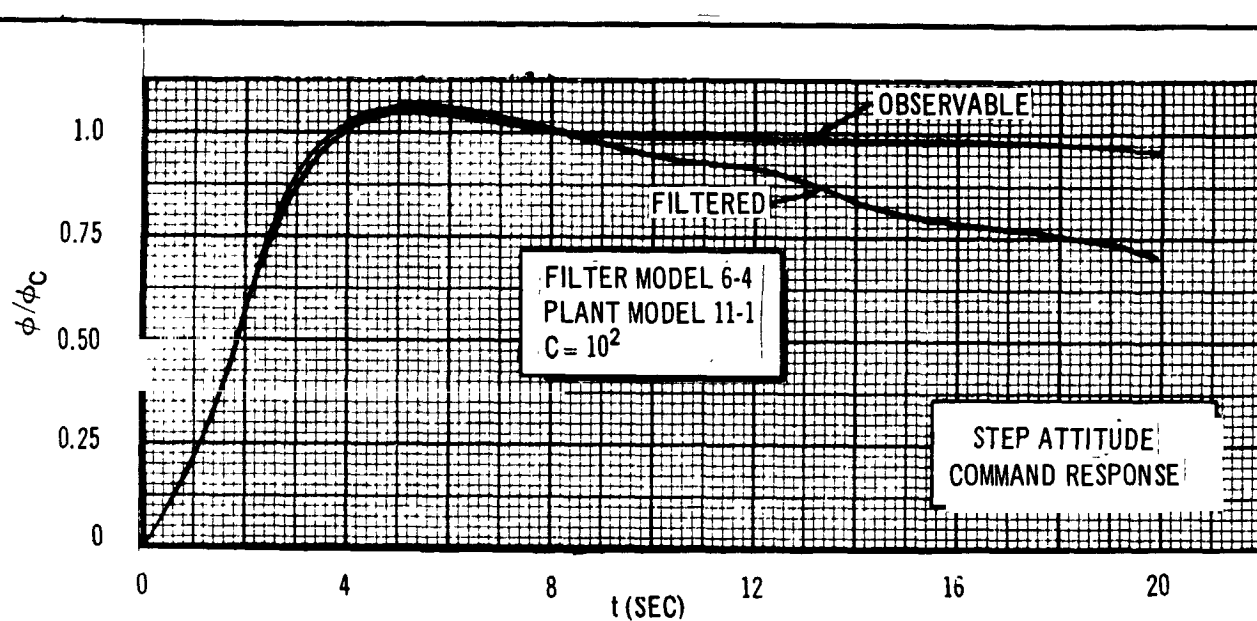


Figure 5-40. Transient Responses

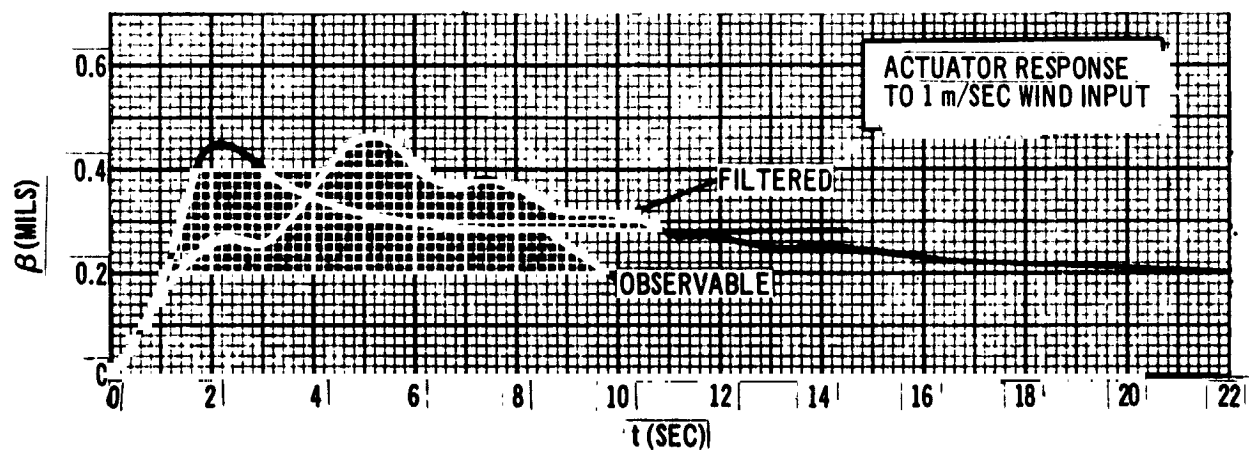
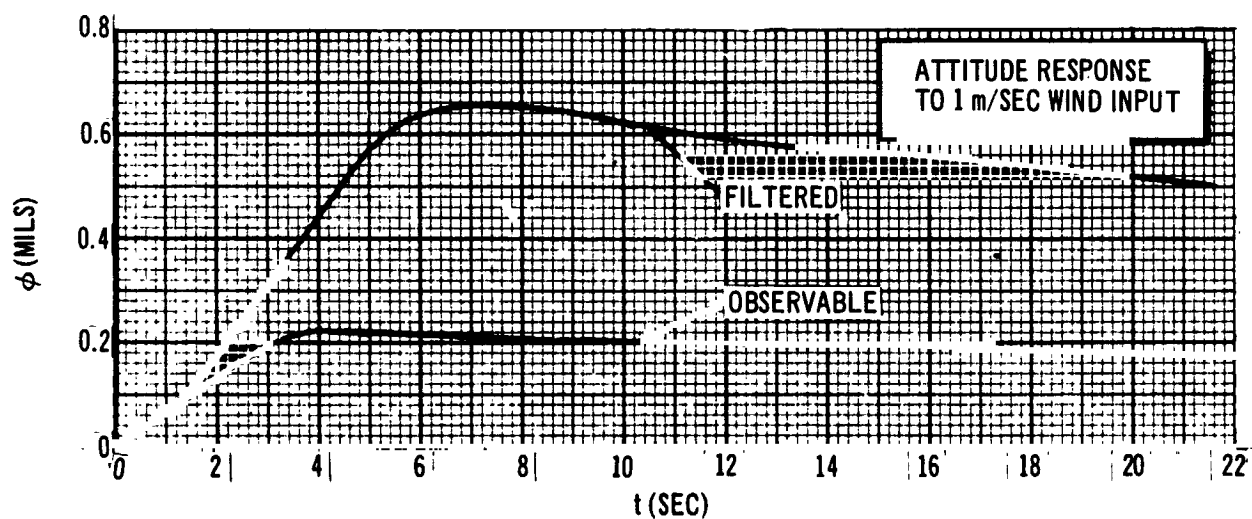
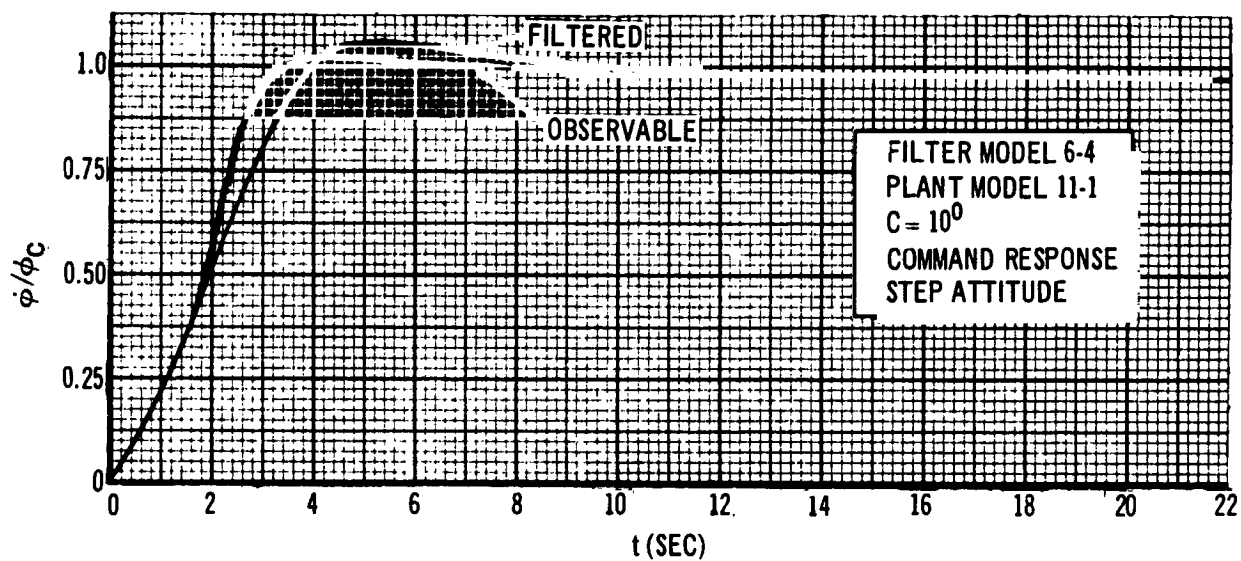


Figure 5-41 Transient Responses

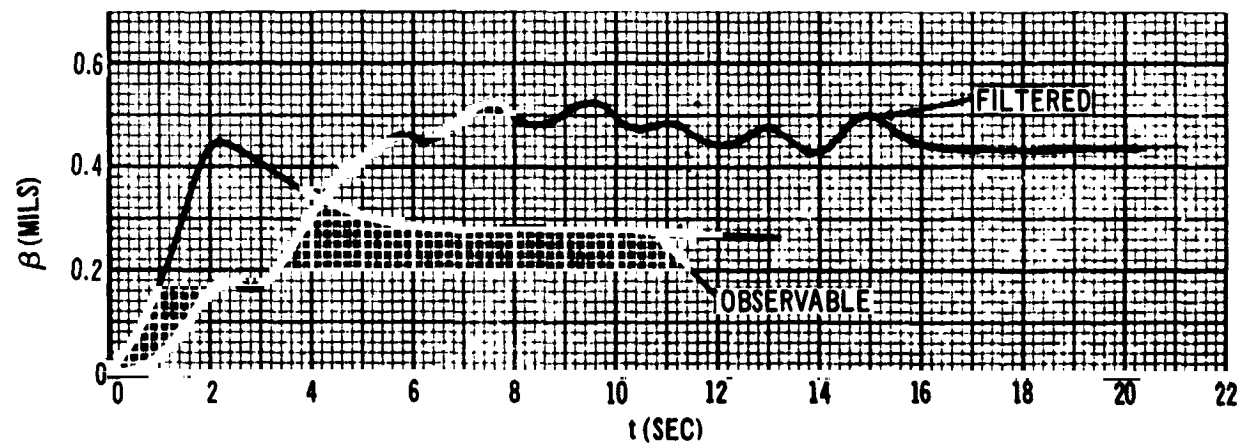
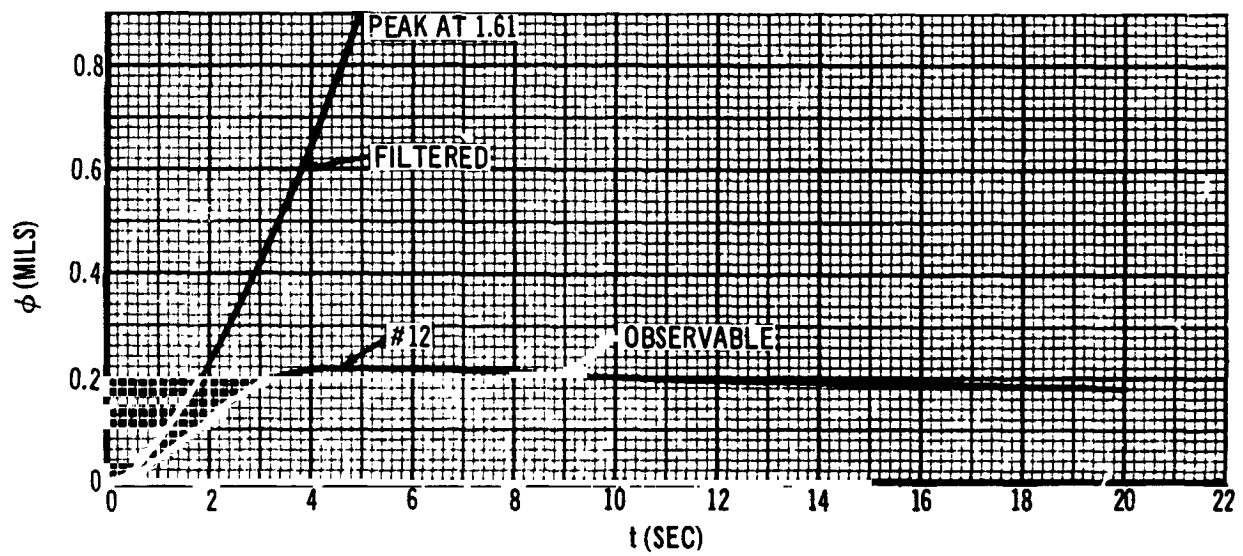
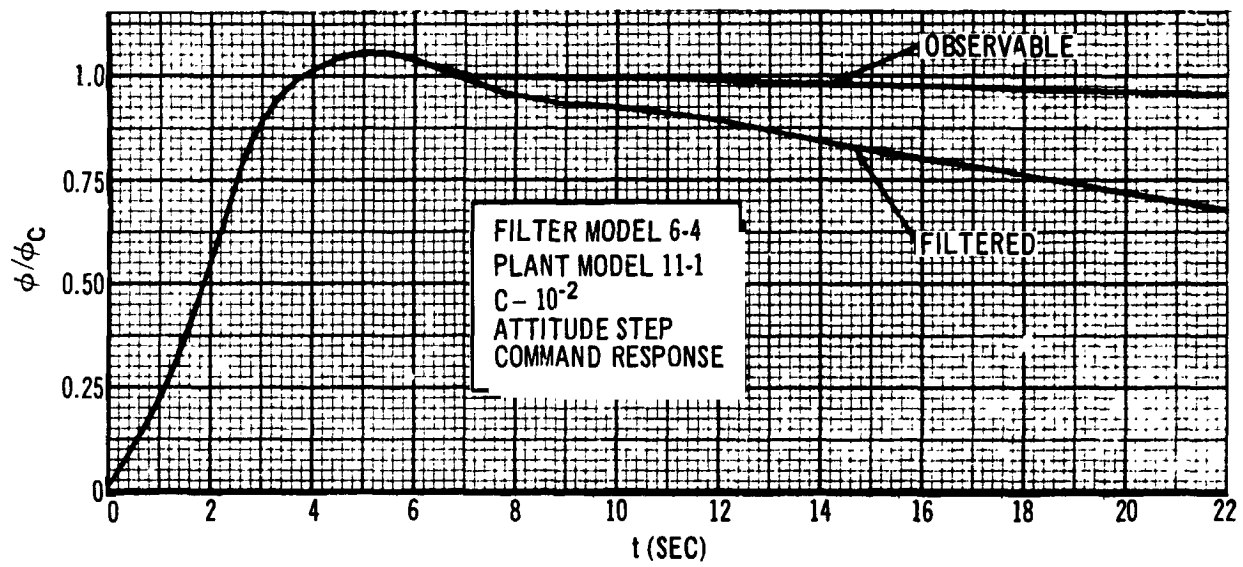


Figure 5-42. Transient Responses

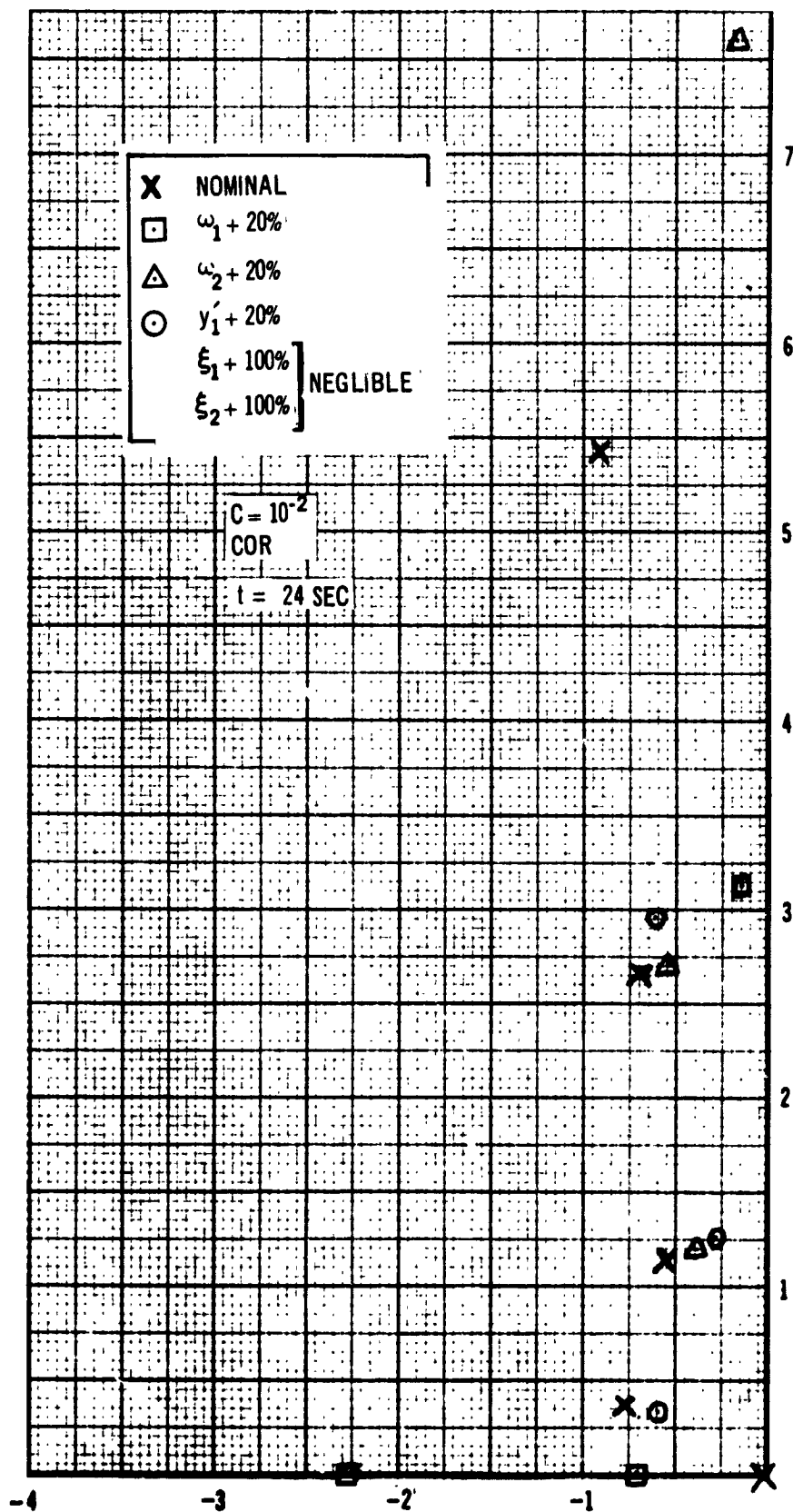


Figure 5-43. Parameter Mismatch Stability

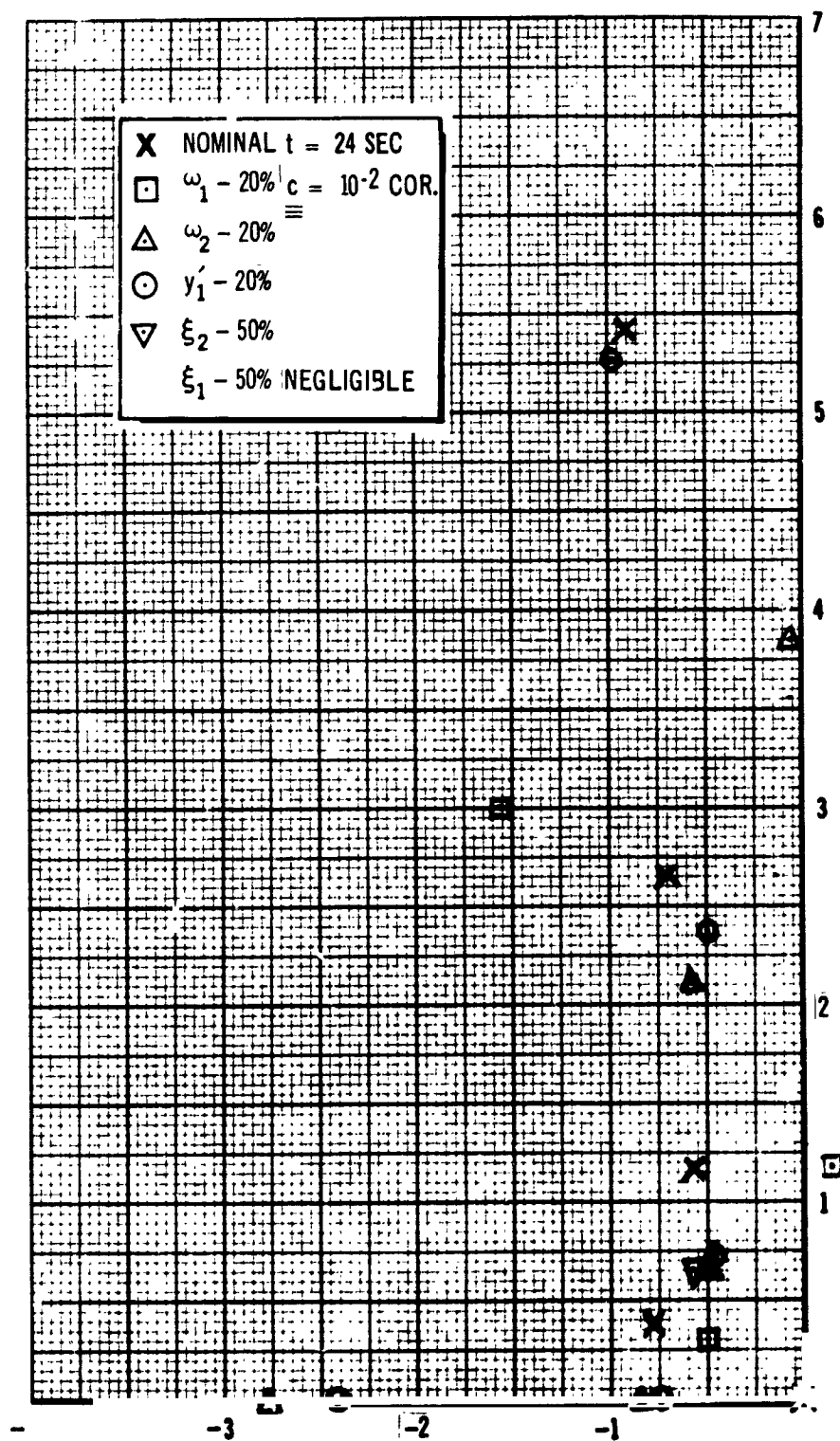


Figure 5-44. Parameter Mismatch Stability

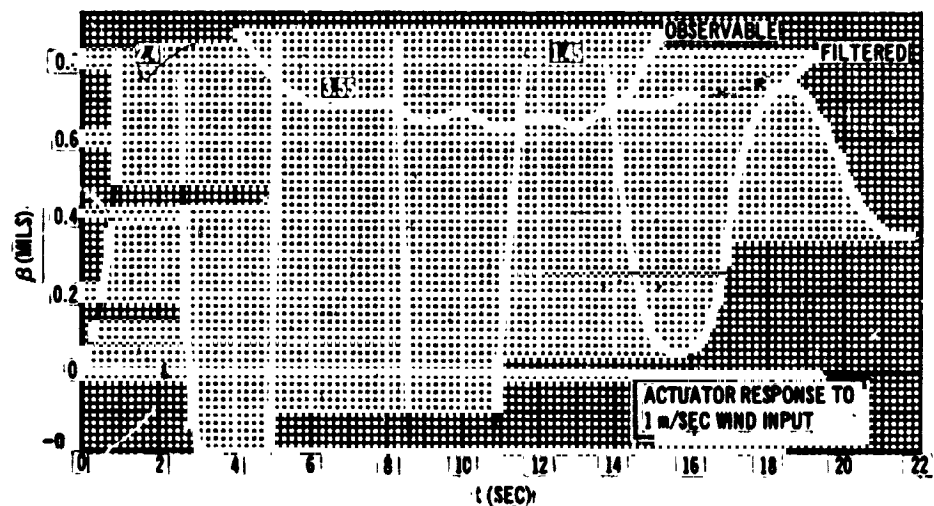
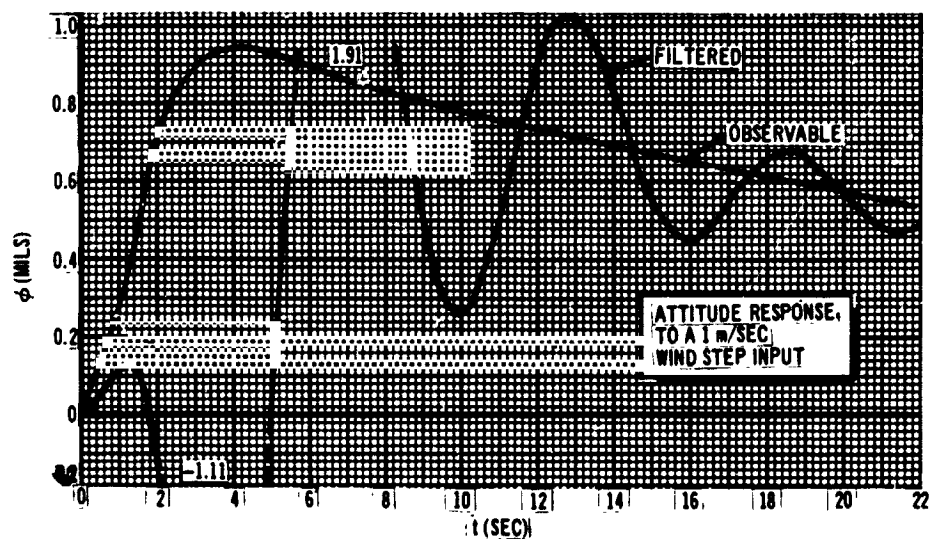
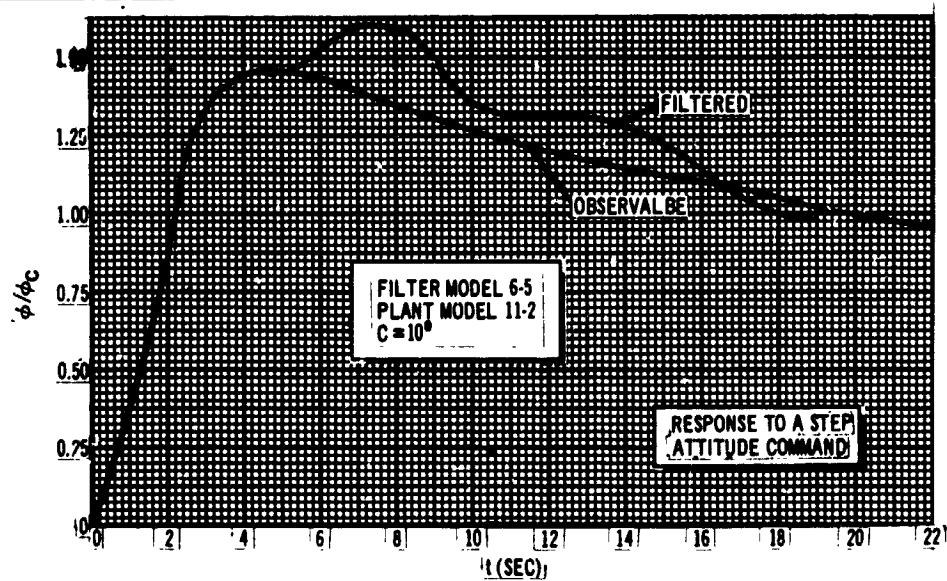


Figure 5-45. Transient Responses

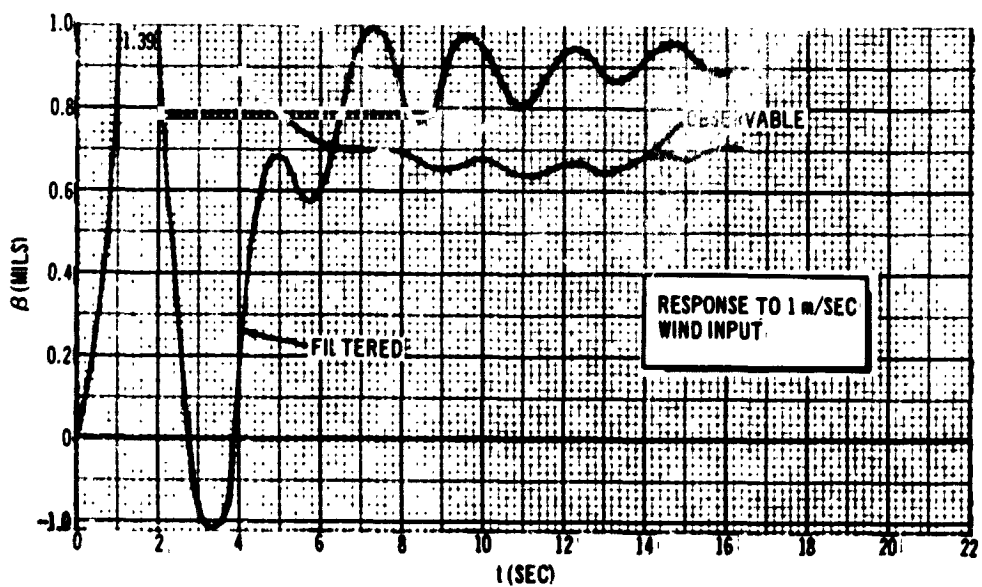
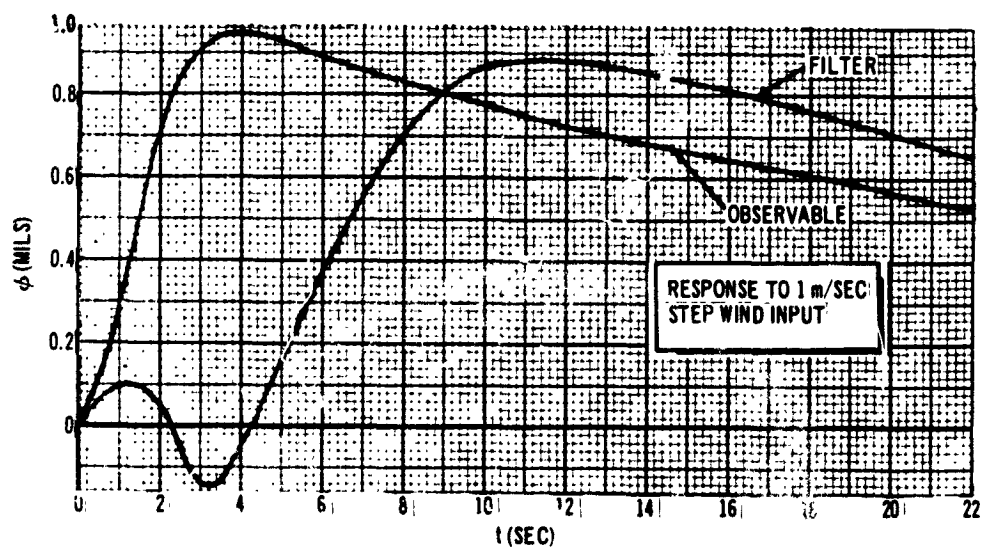
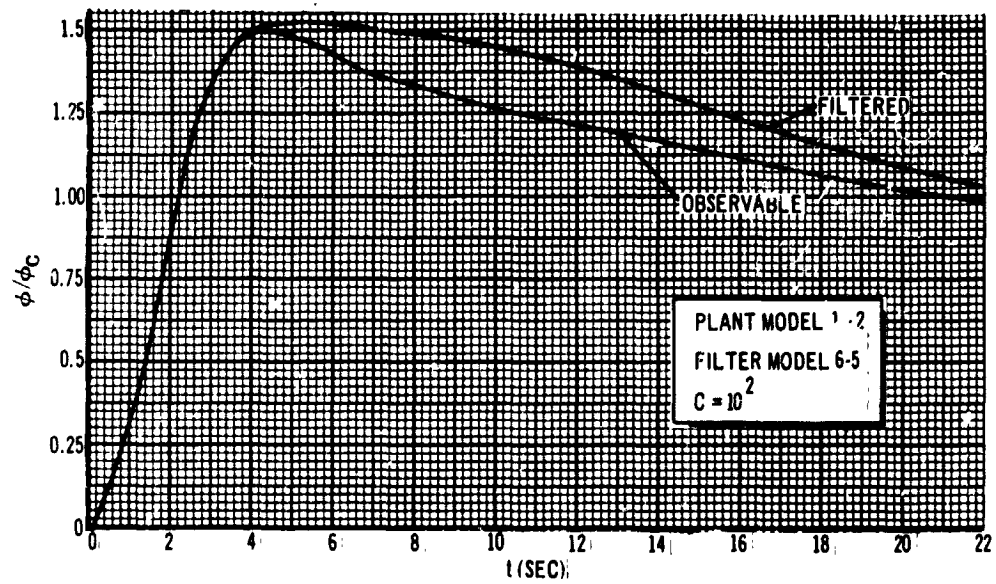


Figure 5-46. Transient Responses

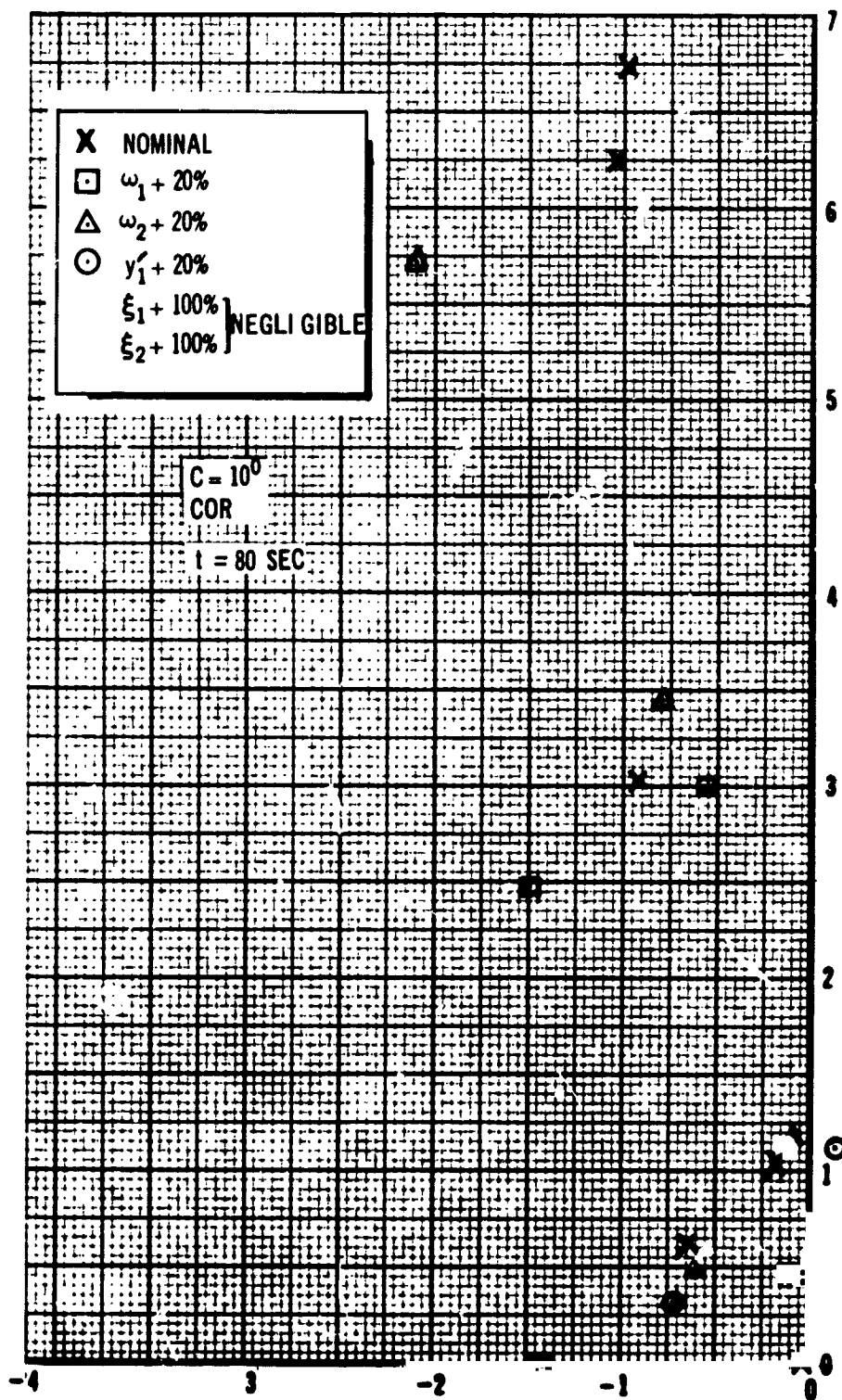


Figure 5-47. Parameter Mismatch Stability

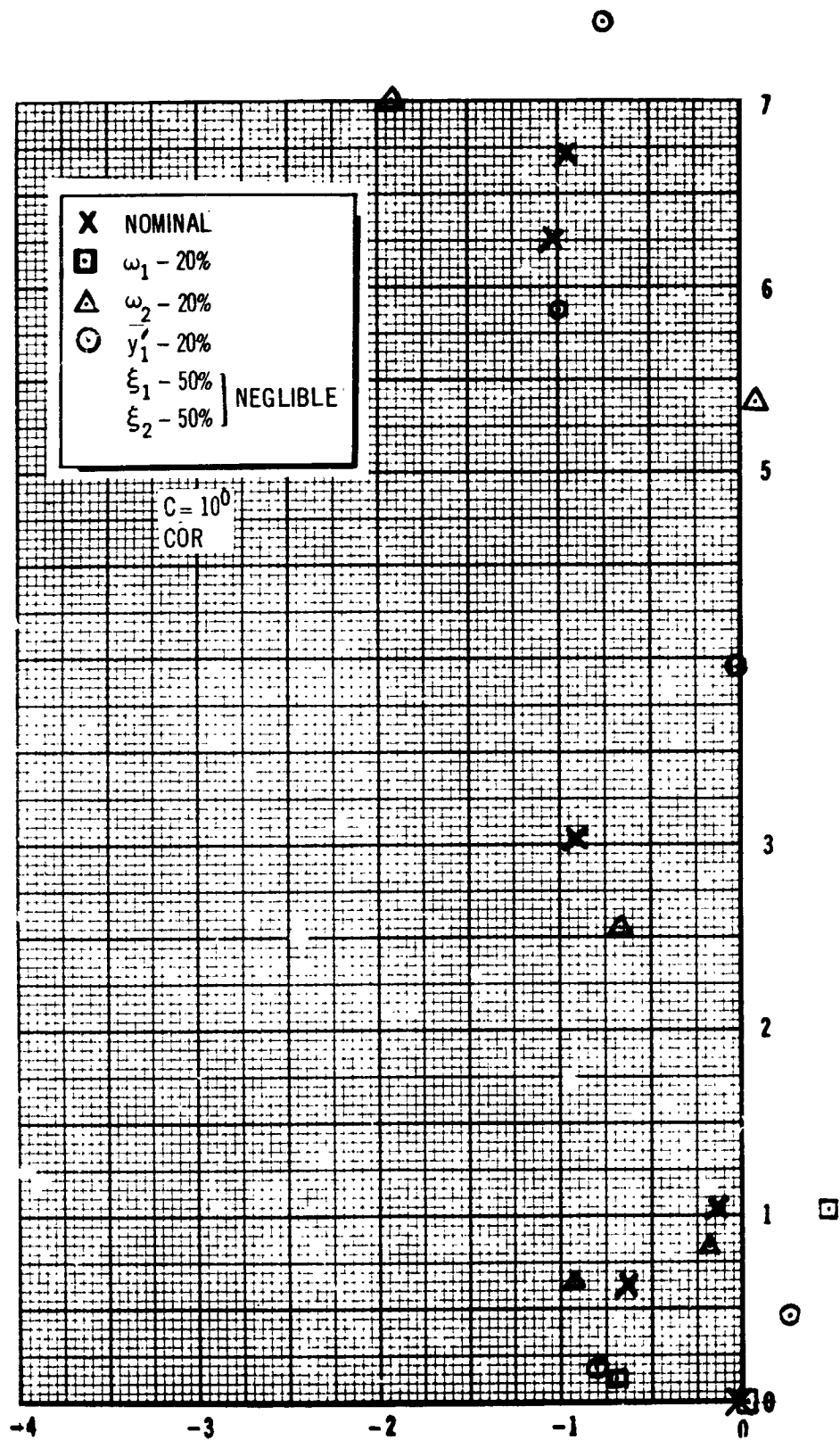


Figure 5-48. Parameter Mismatch Stability (80 sec)

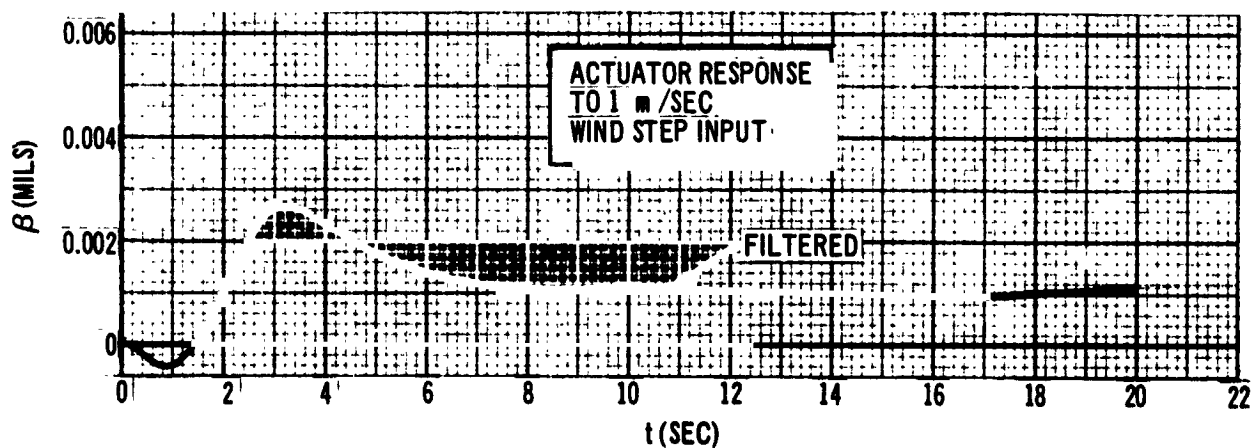
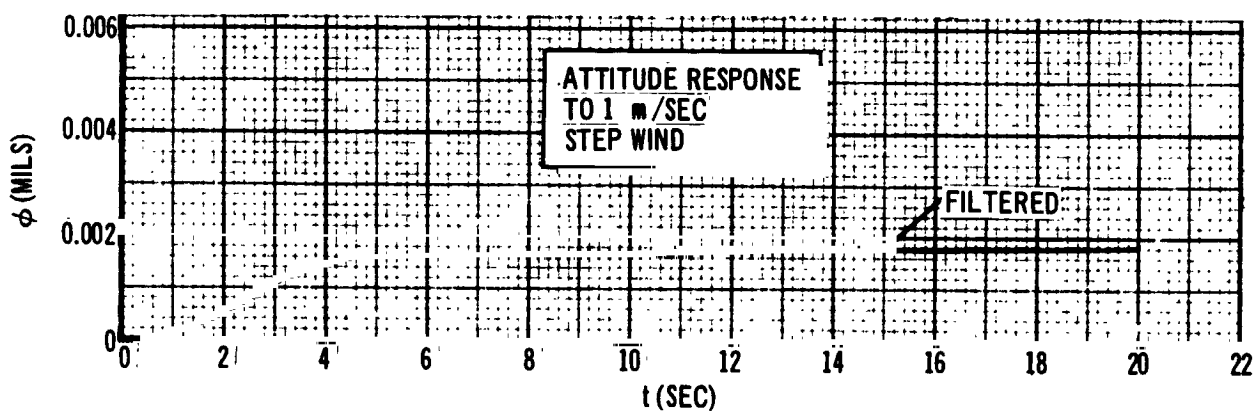
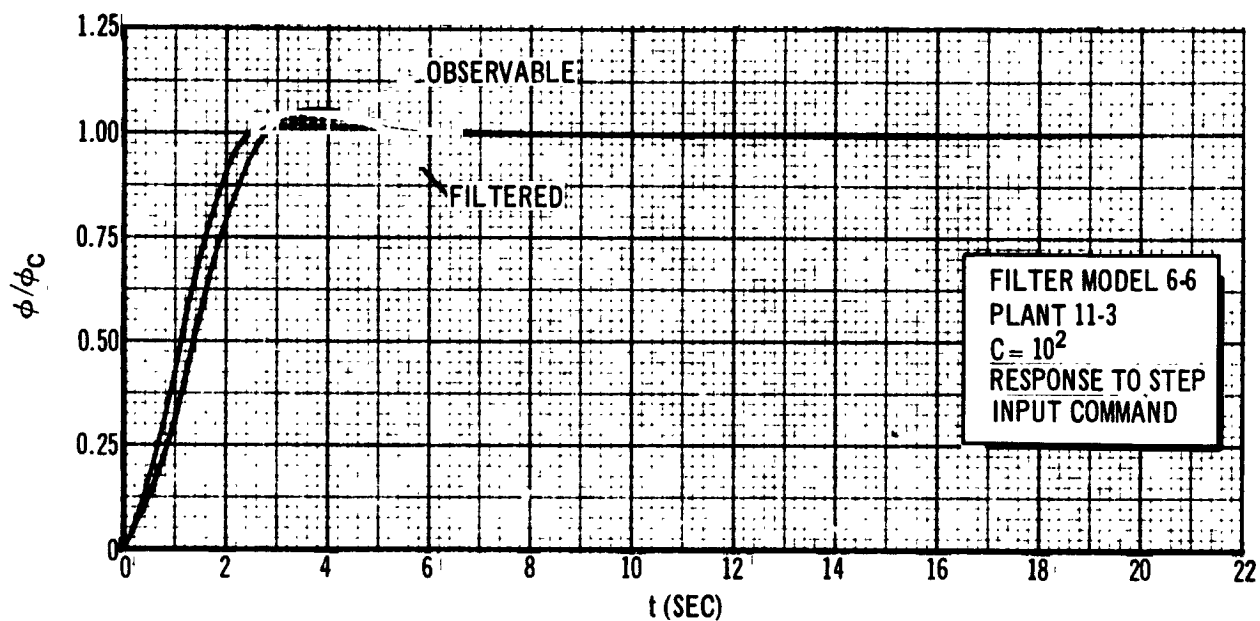


Figure 5-49. Transient Responses

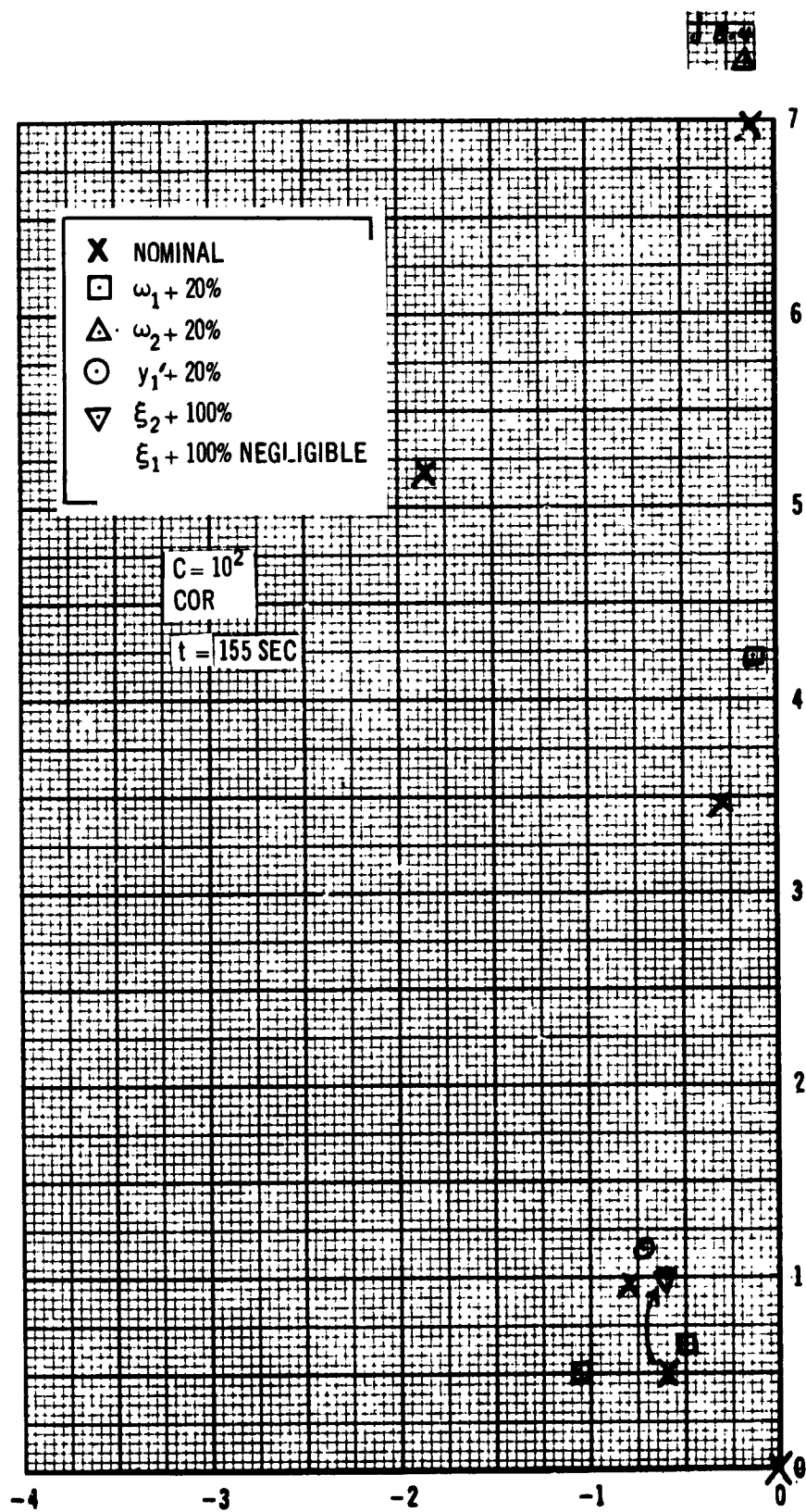


Figure 5-50. Parameter Mismatch Stability

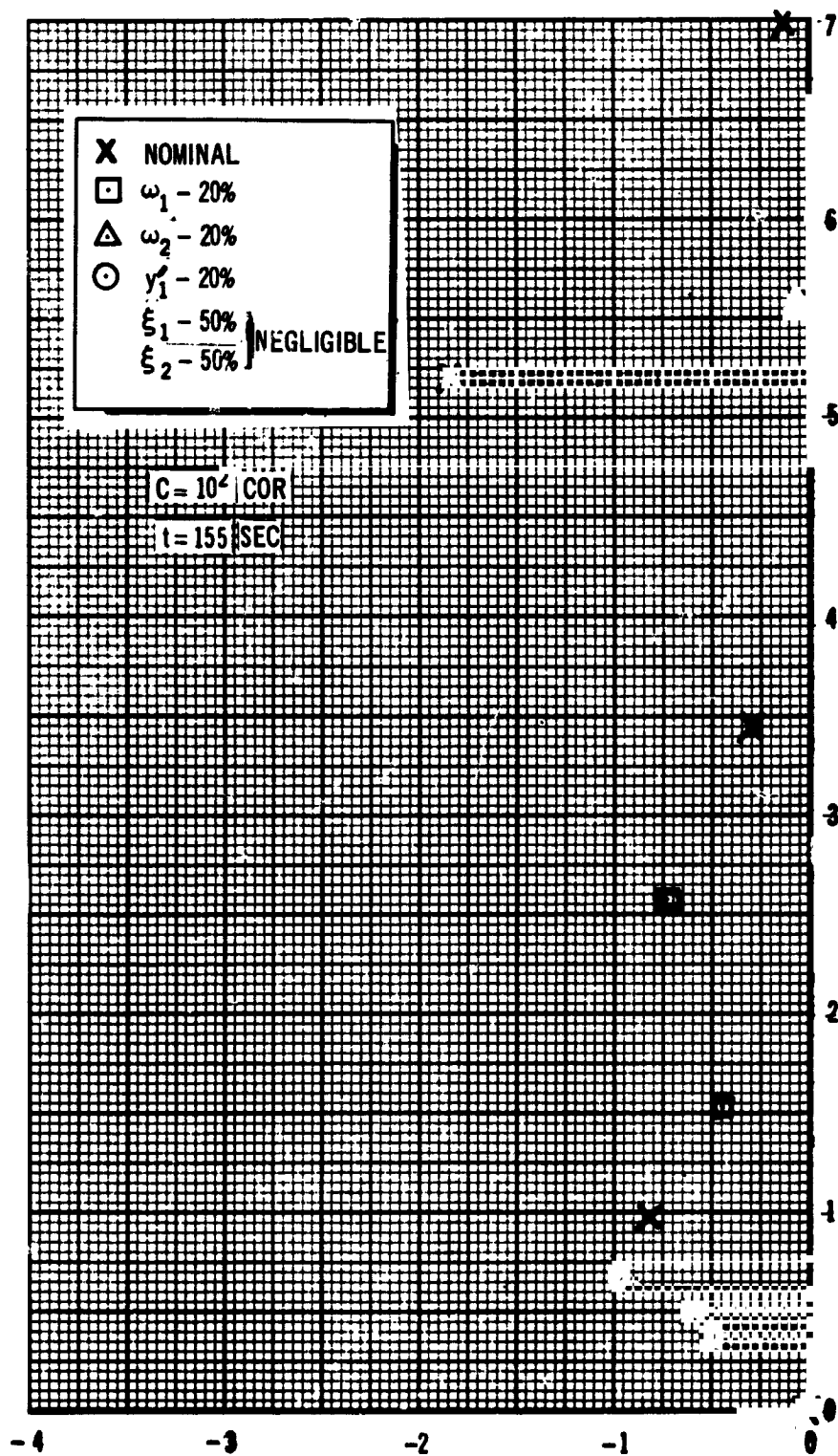


Figure 5-51. Parameter Mismatch Stability

indicates good performance, except β , the actuator response, could benefit from modification. Conditions are favorable at this time because of the low aerodynamic pressure.

5.6.3 Colored Noise

A brief set of experiments was undertaken to determine the advantages of colored noise rather than white noise in the filter. Since attempts to stabilize the system at $t = 24$ sec had failed with a 4-d filter, this situation was returned to. The spectral density asymptote plots described in subsection 5.6.1 were used to develop a second-order Markov process

$$\begin{Bmatrix} \dot{\lambda} \\ \ddot{\lambda} \end{Bmatrix} = \begin{bmatrix} 0 & 1 \\ -25.0 & -1.0 \end{bmatrix} \begin{Bmatrix} \lambda \\ \dot{\lambda} \end{Bmatrix} + \begin{bmatrix} 0 \\ 25.0 \end{bmatrix} \xi \quad (5-68)$$

$$y = \begin{bmatrix} 0.224 & 0 \\ 0 & 1 \\ 224 & 0 \end{bmatrix} \begin{Bmatrix} \lambda \\ \dot{\lambda} \end{Bmatrix} \quad (5-69)$$

The 4-dimensional system (4-3) was augmented with these state values to form System 6-7. The Kalman gains developed for this filter model are shown in Table 5-10. The system stability studies made are shown in Figure 5-52. The figure shows the system is again unstable in the second bending mode. Comparing Figure 5-52 with Table 5-4, using the 4-dimensional filter, indicates no apparent advantage of using the colored noise.

Table 5-10
COLORED NOISE KALMAN GAINS

Filter Model = 6-7

$$Q = \begin{bmatrix} 10^4 & 0 \\ 0 & Q_{22} \end{bmatrix} \quad R = \begin{bmatrix} 10^{-4} & 0 & 0 \\ 0 & 10^{-4} & 0 \\ 0 & 0 & 10^{-4} \end{bmatrix}$$

Scale Factor	Kalman Gain Matrix (K)		
$Q_{22} = 1.5$	0.650	0.427	-0.033
	0.642	1.18	-0.183
	10.50	4.31	-1.67
	16.04	31.9	-4.89
	0.551	0.281	0.955
	0.800	14.06	120.5
$Q_{22} = 1.5 \times 10^{-4}$	0.268	0.0612	-0.1701
	0.1091	0.412	-1.296
	0.959	0.767	-5.51
	2.69	13.26	-43.6
	0.0598	0.0286	-0.1092
	0.0334	0.327	0.541

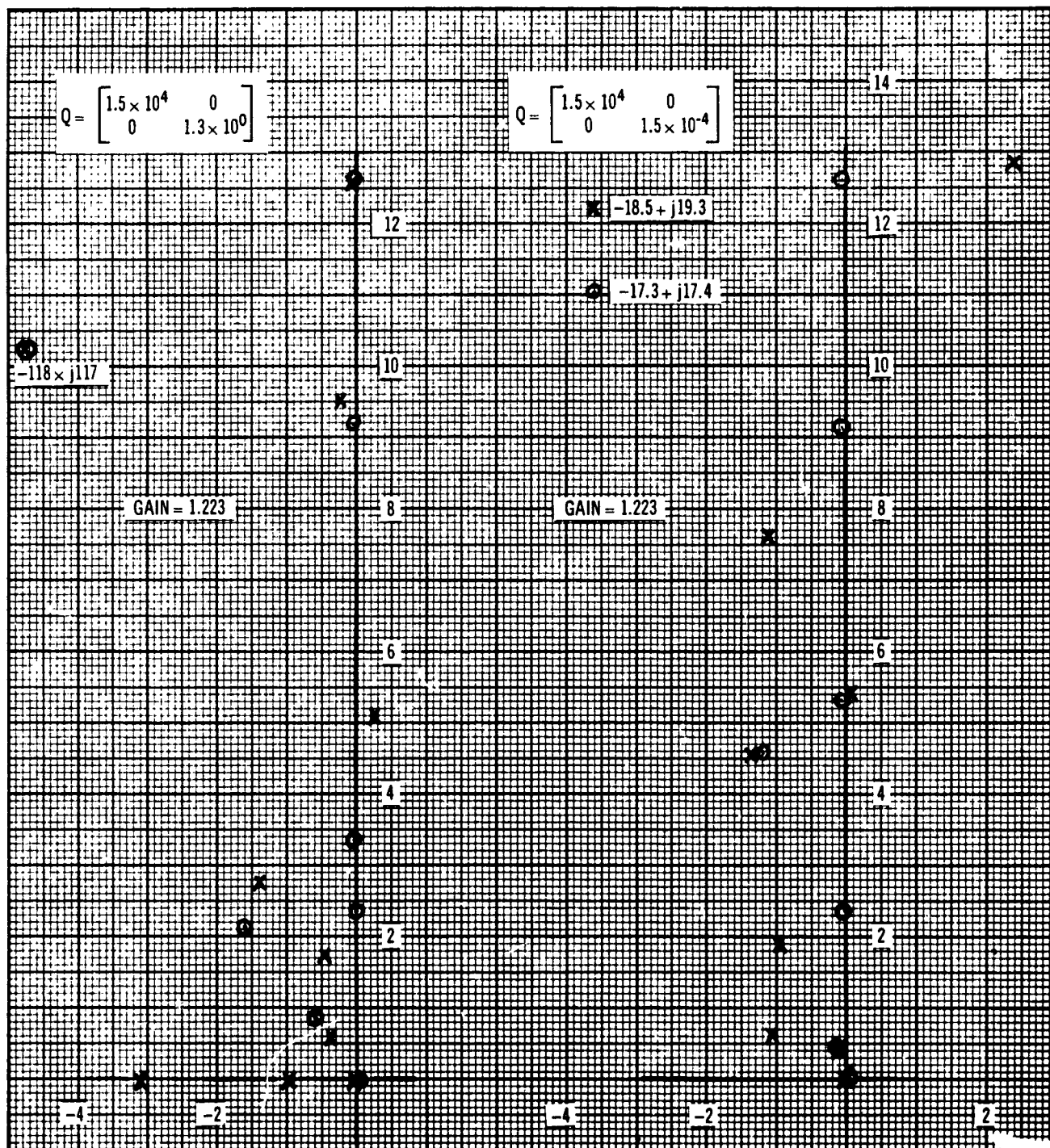


Figure 5-52. Colored Noise Stability

Section 6

COMBINED ESTIMATION

6.1 INTRODUCTION

This section is concerned with the problem of estimating the states and some of the parameters (e. g. , natural frequency of a bending mode) of a linear system. The problem will be termed Combined Estimation.

The method chosen for study was Kalman filtering on an augmented state. The results of simulations with a sixth-order plant were to show the ability of the chosen method to estimate two parameters. It is of particular interest that this estimation was made by an augmented Kalman filter which represented the plant by a fourth- rather than a sixth-order model. This suboptimality increased the error in state and parameter estimation by only a few percent. Further, the plant could be stabilized by feeding back linear combinations of the estimated states.

Some other methods which were found in a literature search on parameter estimation are quasi-linearization (Reference 14) and pseudo-inverse (References 1, 2, 15, and 16). Since the Kalman filtering was already being used for the state estimation part of this study, it was decided to use the same approach on the augmented state. These methods are capable of combined estimation, as opposed to separate state estimation and parameter estimation (or identification, as it is frequently called). (In fact, pseudo-inverse and Kalman filtering are intimately related.) That is, an alternative approach to the problem is to perform the state estimation and parameter estimation separately, but this has not yet been pursued for the current problem. This latter procedure is inherently slower than combined estimation because all errors in measurements are interpreted by the state estimator to be caused by system disturbances changing the states, whereas the parameter identifier interprets these measurement errors as being

caused by parameter mismatches. The discrete identification problem was heuristically solved via a Kalman-type filter by Lee (Reference 15), and the continuous analog has been pursued by Douglas in another application.

Simulations were conducted to simultaneously estimate four states and two parameters of a sixth-order plant. The estimator was designed on the basis of white noise on the measurements of a fourth-order plant. The additional part of the actual measurement was to be rejected by the filter as measurement noise because the plant was of higher order than was assumed for the filter design. It was demonstrated that a feedback gain matrix (previously shown to stabilize the plant when operating on the actual values of the states that are now being estimated) operating on the estimated states would stabilize the plant. In addition, when there was a 50% mismatch in the initial estimate of a parameter, a good estimate was obtained just as well as in the case of a 10% initial mismatch. Further, a sinusoidally varying parameter with a 30-sec period can be tracked with a small lag.

The values of the assumed covariances on the parameter rates of change were studied. Values too large result in undesirable initial transients in parameter estimates; values too small result in insensitivity to estimate errors. The values could be made small in the first few seconds to reduce the transient and subsequently increased to improve the parameter estimation sensitivity.

6.2 COMBINED ESTIMATION VIA CONTINUOUS KALMAN FILTERING

The following text discusses the method of combined estimation of states and parameters for linear systems as essentially derived by Kopp and Orford (Reference 17) and later by Kumar (Reference 9). However, the approach is modified in such a way as to estimate only those parameters which are deemed required, whereas the previous results were for estimating all of the entries of the system dynamical matrix and control distribution matrix, even zeros and ones.

The modification reduces the order of the filter model for this particular case from 24th to 6th order and adds a term to the equations. As a further result of the modification, the computation of the covariance matrix of the estimation error is reduced from the solution of 300 simultaneous first-order differential equations to just 21.

The simulated plant is the sixth-order linear system, denoted as 6-3, which includes the attitude and two bending modes of a flexible booster (coupling of bending modes into attitude being neglected). The model used in the Kalman filter is for a fourth-order linear plant consisting of attitude rate and the first bending mode, plus two unknown parameters (from the first bending mode) which are to be estimated.

6.2.1 Sources of Equations

The general form of a linear dynamical system (Reference 8) is written as

$$\dot{x} = Ax + Bu + G\xi$$

for the plant dynamics, and

$$z = Hx + v$$

for the observation of the plant (these equations are discussed in Section 3, and only a few words of terminology that will be used herein are stated); x is called the state vector, A the dynamical matrix, B the control distribution matrix, u the control input, and the ξ (plant) disturbance (which is a white gaussian random process). Further, H is the measurement matrix, Hx is the measurement, v is the (measurement) noise (which is a random process), and z is the (noisy) observation (of the plant).

This example is for a single-input, single-output system. This means that the control input, u , and the observation, z , are both scalars. Further, the disturbance, ξ , has a covariance matrix, Q , and the noise has a covariance matrix, R , the latter being a scalar (i. e., the variance of v) because the observation is a scalar.

In addition to the foregoing plant equations for the estimation problem, there are equations for the plant model which in theory are nearly the same as the plant. However, since a plant has an infinite number of bending modes, an ordinary differential equation model must be of lower order than the plant. That is, the filter contains an assumed model of the plant dynamics. Here we approximate the plant by using a model without the third bending mode, η_3 .

In the combined estimation problem, the model used in the estimation filter is for an adjoined state vector, which is the state vector of the assumed plant adjoined by the unknown parameters in the A and B matrixes of the assumed plant dynamical equation. The resulting equations have the same form as the state estimation problem. Specifically, for x_a the adjoined state, the filter equations of Kumar have the form of (Reference 9, Page 29)

$$\dot{\hat{x}}_a = \hat{A}_a^+ \hat{x}_a + K_a \bar{z} \quad (6-1)$$

where \hat{x}_a is the estimate of x_a . A discussion of the equation will follow, but first we will note a modification of this equation that was actually used for the specific problem. Namely, for a lower-dimension augmented state

$$\dot{\hat{x}}_a = \hat{A}_a \hat{x}_a + \hat{B}_a u + K_a \bar{z} \quad (6-2)$$

where \hat{B}_a is the estimate of B_a , with B_a defined as $\begin{bmatrix} B \\ 0 \end{bmatrix}$ where the 0 is a matrix with as many rows as there are unknown parameters (in the case of a component being known exactly the estimate is the value itself). Also, \hat{A} is the estimate of A, and \hat{A}_a is an $n \times n$ matrix, for \hat{x}_a an n vector which has \hat{A} as its upper left partition and zeros elsewhere. A_a^+ in the first equation is such that the two equations would be the same when all entries in A and B were unknown. This constitutes part of a modification of the equations of Kumar which allows the parameter part of x_a to be only those parameters which are to be included in the combined estimation problem.

The K_a in either equation is called the Kalman gain; but it is not the same Kalman gain in both equations, and obtaining it will constitute the final modification of Kumar's equation.

6.2.2 Specific Equations for a Sixth-Order Example

The following subsection shows the equations to be solved for the simulation.

6.2.2.1 Plant Equations

The plant equations for the specific problem considered here are for a state vector

$$\mathbf{x} = \begin{pmatrix} \phi \\ \dot{\phi} \\ \delta_1 \\ \dot{\delta}_1 \\ \eta_2 \\ \dot{\eta}_2 \end{pmatrix} \quad (6-3)$$

a dynamical matrix

$$\mathbf{A} = \begin{bmatrix} 0 & 1 & 0 & 0 & 0 & 0 \\ A_{21} & 0 & 0 & 0 & 0 & 0 \\ 0 & 0 & 0 & 1 & 0 & 0 \\ A_{41} & 0 & -\omega_1^2 & -2\xi_1\omega_1 & 0 & 0 \\ 0 & 0 & 0 & 0 & 0 & 1 \\ A_{61} & 0 & 0 & 0 & -\omega_2^2 & -2\xi_2\omega_2 \end{bmatrix}$$

and a control distribution matrix

$$B = \begin{pmatrix} 0 \\ -C2 \\ 0 \\ \frac{R'Y_1(x_\beta)}{m_1} \\ 0 \\ \frac{R'Y_2(x_\beta)}{m_2} \end{pmatrix}$$

This plant is unstable and a feedback gain which stabilized it was included in the simulations.

6.2.2.2 Estimation Equations

For the estimation equation

$$\dot{\hat{x}}_a = \hat{A}_a x_a + \hat{B}_a u + K_a \tilde{z} \quad (6-4)$$

in the special problem being considered, we have

$$A_a = \begin{bmatrix} 0 & 0 & 0 & 0 & 0 \\ 0 & 0 & 1 & 0 & 0 \\ 0 & ES1 & -2\xi_1\omega_1 & 0 & 0 \\ 0 & 0 & 0 & 0 & 0 \\ 0 & 0 & 0 & 0 & 0 \end{bmatrix} = \begin{bmatrix} \hat{A} & 0 \\ 0 & 0 \end{bmatrix} \quad (6-5)$$

$$\hat{x}_a = \begin{pmatrix} \hat{\phi} \\ \hat{\delta}_1 \\ \hat{\delta}_1 \\ ES1 \\ ES2 \end{pmatrix} \quad (6-6)$$

$$B_a = \begin{pmatrix} -C2 \\ 0 \\ ES2 \\ 0 \\ 0 \end{pmatrix} \quad (6-7)$$

where

$$S2 = \frac{R'Y_1(AG) \cdot Y_1(x_\beta)}{m_1} \quad (6-7)$$

and ES2 and ES1 are the estimates of S2 and S1 respectively, and

$$K_a = \frac{1}{R} \begin{pmatrix} p_1 \\ p_2 \\ p_3 \\ p_4 \\ p_5 \\ p_6 \end{pmatrix} \quad (6-8)$$

where

$$p_j \triangleq p_{2j} + p_{4j}$$

The p_{ij} 's are the solutions of the matrix Riccati equation and only the required combinations are shown here in the Kalman gain, K_a , in the form of p_j 's.

The equation for \hat{x}_a is determined by modifying the result of Reference 10 (Page 29) which is

$$\dot{\hat{x}}_a = A_a^+ \hat{x}_a + P_a H_a' R^{-1} \bar{z}$$

or, (6-9)

$$\dot{\hat{x}}_a = A_a^+ \hat{x}_a + K_a \bar{z}$$

This \hat{x}_a is obtained by adjoining all the entries of A and B to x. A_a^+ includes components of u that are placed so as to multiply the estimated components of B. This was obtained via the Reference 9 equation (Page 22), (with notation corrected from \hat{x} to \hat{x})

$$\hat{\dot{x}} = \hat{A}\hat{x} + \hat{B}u$$
(6-10)

Kumar then adjoins all the parameters from A and B to get an augmented state vector. We adjoin only the unknown parameters and get

$$\hat{\dot{x}}_a = \hat{A}_a \hat{x}_a + \hat{B}_a u$$
(6-11)

which corresponds to Kumar's equation (Reference 10, Page 22, notation corrected and modified)

$$\hat{\dot{x}}_a = A_a^+ \hat{x}_a$$
(6-12)

because he includes u in A_a^+ and considers all of the entries of B as unknowns, i.e., as part of x_a .

The rest of the modification of Kumar's equation to get our equation is essentially the recognition that

$$\dot{\hat{x}}_a = \hat{\dot{x}}_a + \text{correction signal} \quad (6-13)$$

and the correction signal is of the form $K_a \tilde{z}$. The computation of K_a requires values of the covariance matrix, P_a , which are obtained as described in subsection 6.2.2.3.

Also

$$\tilde{z} = \phi + \delta_1 - Y_3(AG)\eta_3 - (\hat{\phi} + \hat{\delta}_1) \quad (6-14)$$

i. e. , the observation minus its estimate.

6.2.2.3 Matrix Riccati Equation

A specific 6 x 6 case of a matrix Riccati equation is to be solved in order to provide the terms for the Kalman gain. The general form is

$$\dot{P}_a = \hat{A}_a^* P_a + P_a \hat{A}_a^{*T} - P H_a^T R_a^{-1} H_a P_a + Q_a \quad (6-15)$$

for the problem considered, we write P_a as

$$P_a = \begin{bmatrix} P11 & P12 & P13 & P14 & P15 & P16 \\ & P22 & P23 & P24 & P25 & P26 \\ & & P33 & P34 & P35 & P36 \\ & & & P44 & P45 & P46 \\ & & & & P55 & P56 \\ & & & & & P66 \end{bmatrix} \quad (6-16)$$

where the lower triangle of the matrix is not written because P_a is symmetric

$$\hat{A}_a^* = \left[\begin{array}{cccc|cc} & & & & 0 & 0 \\ & & & & 0 & 0 \\ & & \hat{A} & & 0 & 0 \\ & & & & \delta_1 & \beta \\ \hline 0 & 0 & 0 & 0 & 0 & 0 \\ 0 & 0 & 0 & 0 & 0 & 0 \end{array} \right] \quad (6-17)$$

$$H_a = \left[\begin{array}{cccc|cc} 1 & 0 & 1 & 0 & 0 & 0 \end{array} \right]$$

The way these equations were obtained is as follows. The equation for the error in x , from Reference 10 (Page 24), is

$$\dot{\tilde{x}} = \hat{A}\tilde{x} + \tilde{A}\hat{x} + \tilde{B}u + G\xi \quad (6-18)$$

where $(\tilde{\cdot}) = (\cdot)$ minus its estimate $\equiv (\cdot) - (\hat{\cdot})$. Now, we say that the only part of A that is unknown is $S1$, so that

$$\tilde{A} = A - \hat{A} = \left[\begin{array}{cccc} 0 & 0 & 0 & 0 \\ 0 & 0 & 0 & 0 \\ 0 & 0 & 0 & 0 \\ 0 & 0 & \tilde{S}1 & 0 \end{array} \right] \quad (6-19)$$

and similarly for B , so that

$$\tilde{B} = \left[\begin{array}{c} 0 \\ 0 \\ 0 \\ \tilde{S}2 \end{array} \right] \quad (6-20)$$

so that

$$\begin{aligned}
 \dot{\tilde{x}} &= \begin{bmatrix} \vdots & 0 & 0 \\ \hat{A} & 0 & 0 \\ \vdots & 0 & 0 \end{bmatrix} \begin{bmatrix} \tilde{x} \\ \tilde{S}1 \\ \tilde{S}2 \end{bmatrix} + \begin{bmatrix} 0 & 0 & 0 & 0 \\ 0 & 0 & 0 & 0 \\ 0 & 0 & 0 & 0 \\ 0 & 0 & \tilde{S}1 & 0 \end{bmatrix} \begin{bmatrix} \phi \\ \dot{\phi} \\ \delta_1 \\ \hat{\delta}_1 \end{bmatrix} + \begin{bmatrix} 0 \\ 0 \\ 0 \\ \tilde{S}2 \end{bmatrix} \beta + G\xi \\
 &= \begin{bmatrix} \vdots & 0 & 0 \\ \hat{A} & 0 & 0 \\ \vdots & 0 & 0 \end{bmatrix} \begin{bmatrix} \tilde{x} \\ \tilde{S}1 \\ \tilde{S}2 \end{bmatrix} + \begin{bmatrix} 0 \\ 0 \\ 0 \\ \hat{\delta}_1 \cdot \tilde{S}1 \end{bmatrix} + \begin{bmatrix} 0 \\ 0 \\ 0 \\ \beta \cdot \tilde{S}2 \end{bmatrix} + G\xi
 \end{aligned} \tag{6-21}$$

and noting that $\hat{\eta} \cdot \tilde{S}1$ can be obtained from $\hat{\eta}_1$ put into the first matrix in the proper place to multiply $\tilde{S}1$, and similarly for $\beta \cdot \tilde{S}2$

$$\dot{\tilde{x}} = \begin{bmatrix} \vdots & 0 & 0 \\ \hat{A} & 0 & 0 \\ \vdots & \hat{\eta}_1 & \beta \end{bmatrix} \begin{bmatrix} \tilde{x} \\ \tilde{S}1 \\ \tilde{S}2 \end{bmatrix} + G\xi \tag{6-22}$$

Adjoining the assumed equations for $\tilde{S}1$ and $\tilde{S}2$, i. e., $\dot{\tilde{S}}1 = \theta_1$ and $\dot{\tilde{S}}2 = \theta_2$, θ_1 and θ_2 being mutually independent white random processes, we have

$$\begin{aligned}
 x_a &= \begin{bmatrix} \vdots & 0 & 0 \\ \hat{A} & 0 & 0 \\ \vdots & \eta_1 & \beta \\ 0 & 0 & 0 \\ 0 & 0 & 0 \end{bmatrix} \begin{bmatrix} \tilde{x} \\ \tilde{S}1 \\ \tilde{S}2 \end{bmatrix} + \xi_a \\
 &= \hat{A}_a^* x_a + \xi_a
 \end{aligned} \tag{6-23}$$

where

$$\xi_a \triangleq \begin{pmatrix} G\xi \\ \theta_1 \\ \theta_2 \end{pmatrix}$$

This corresponds to Kumar's equation except that the order of the equation has been reduced to include only the unknown parameters in A and B. The general procedure for this should be clear from this result. \hat{A}_a^* is constructed by putting \hat{A} in the upper left corner and the estimated variables and control inputs are put in the required places in the upper right-hand corner. It then follows from the general theory that the covariance equation for the estimation error is to be solved using R as a scalar, and

$$\begin{aligned} Q_a \delta(t-\tau) &= \begin{bmatrix} \text{cov}(\xi(t), \xi(\tau)) & 0 & 0 \\ 0 & \text{cov}(\theta(t), \theta(\tau)) & 0 \\ 0 & 0 & \text{cov}(\psi(t), \psi(\tau)) \end{bmatrix} \\ &= \text{cov}[\xi_a(t), \xi_a(\tau)] \end{aligned} \quad (6-24)$$

more specifically, Q_a is

$$Q_a = \begin{bmatrix} Q22 & 0 & Q24 & 0 & 0 \\ 0 & 0 & 0 & 0 & 0 \\ Q24 & 0 & Q44 & 0 & 0 \\ 0 & 0 & 0 & Q55 & 0 \\ 0 & 0 & 0 & 0 & Q66 \end{bmatrix} \quad (6-25)$$

6.2.2.4 Combined Estimation Equations: Summary and Block Diagrams

The general form of those equations shown in subsections 6.2.2.1, 6.2.2.2, and 6.2.2.3 is shown here together with additional equations that are required.

The plant equation is

$$\dot{\mathbf{x}} = \mathbf{A}\mathbf{x} + \mathbf{B}\mathbf{u} + \mathbf{G}\xi \quad (6-26)$$

From this is generated (among other things) ϕ and η_1 .

Then

$$\begin{aligned} \delta_1 &\triangleq -Y_1(AG)\eta_1 \\ z &= \phi + \delta_1 + Y_3(AG)\eta_3 \end{aligned} \quad (6-27)$$

and

$$\tilde{z} = \phi + \delta_1 - Y_3(AG)\eta_3 - (\hat{\phi} + \hat{\delta}_1) \quad (6-28)$$

The estimation equations are then

$$\dot{\hat{\mathbf{x}}}_a = \mathbf{A}_a \hat{\mathbf{x}}_a + \hat{\mathbf{B}}_a \mathbf{u} + \mathbf{K}_a \tilde{z} \quad (6-29)$$

where

$$\mathbf{K}_a \triangleq \mathbf{P}_a \mathbf{H}_a^T \mathbf{R}^{-1}$$

and \mathbf{P}_a is determined by

$$\dot{\mathbf{P}}_a = \hat{\mathbf{A}}_a^* \mathbf{P}_a + \mathbf{P}_a \hat{\mathbf{A}}_a^{*T} - \mathbf{P}_a \mathbf{H}_a^T \mathbf{R}^{-1} \mathbf{H}_a \mathbf{P}_a + \mathbf{Q}_a \quad (6-30)$$

Figures 6-1 to 6-3 show the block diagrams for the above-mentioned equations. A notation was adopted at a matrix multiplication block to show which matrix was to be the operator (premultiply) and which was to be

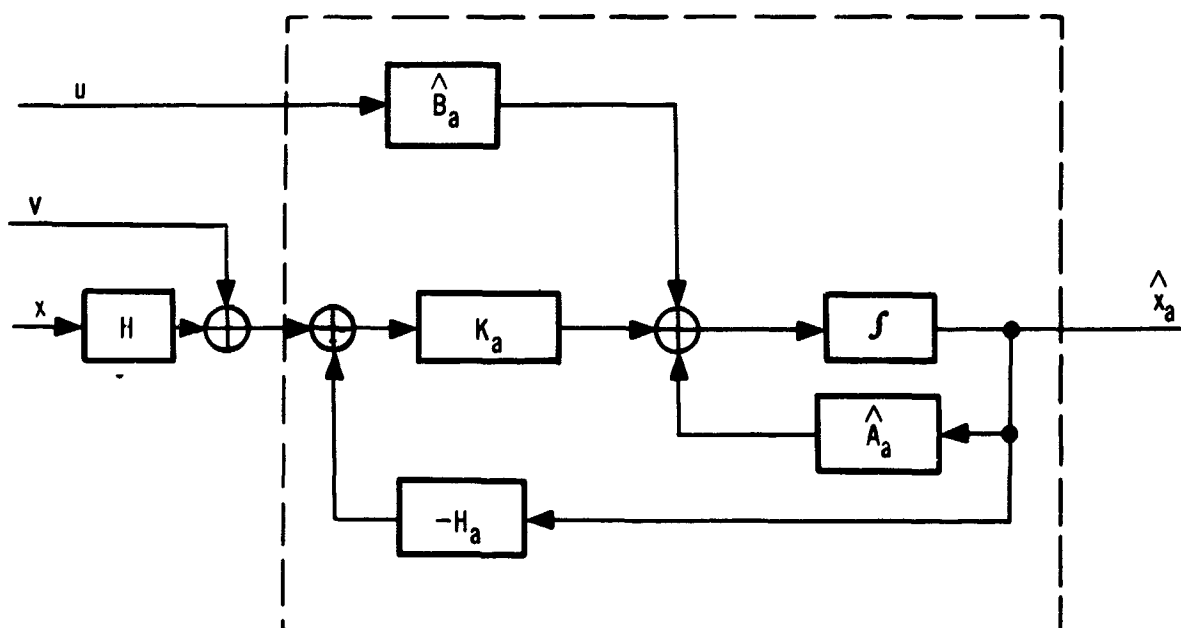


Figure 6-1. Block Diagram for Kalman Filter for Adjoined State

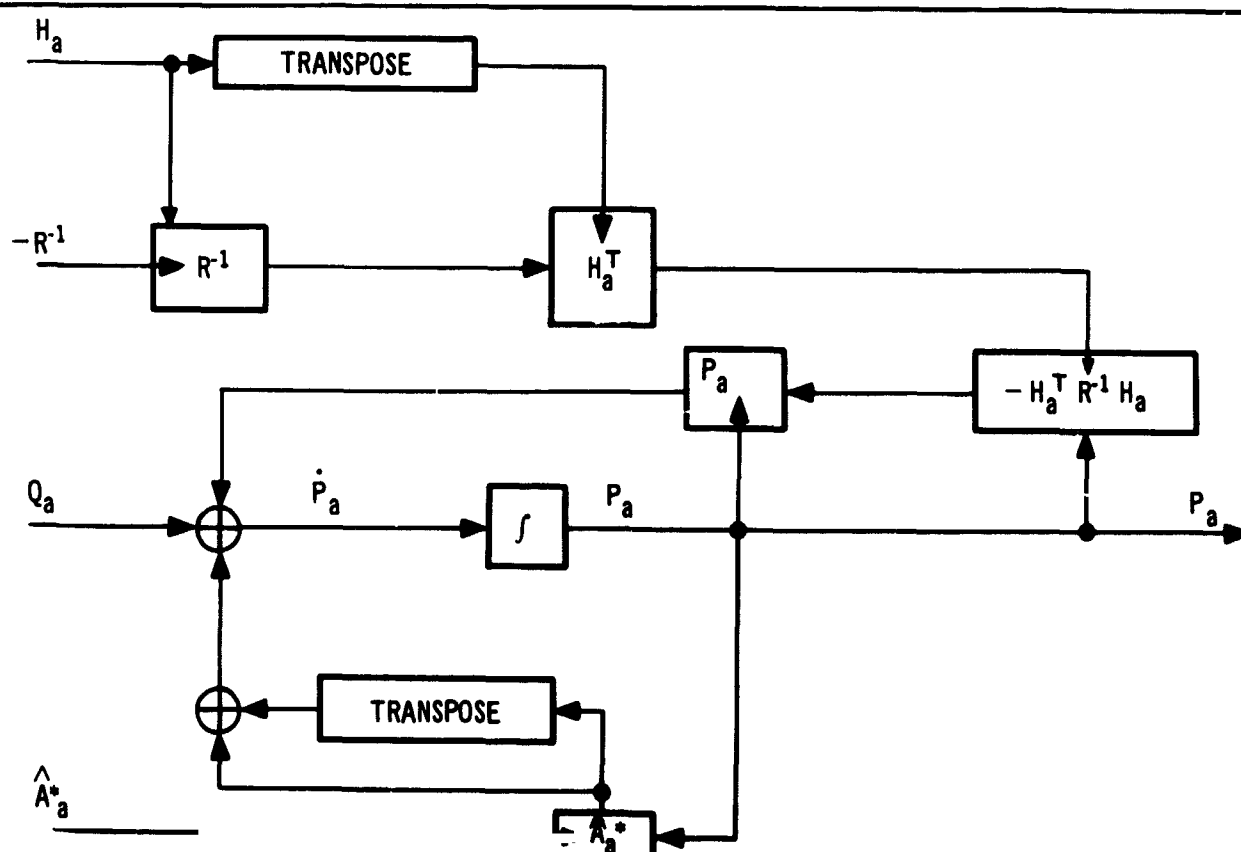


Figure 6-2. Block Diagram for Solving Matrix Riccati Equation for Covariance of Estimation Error

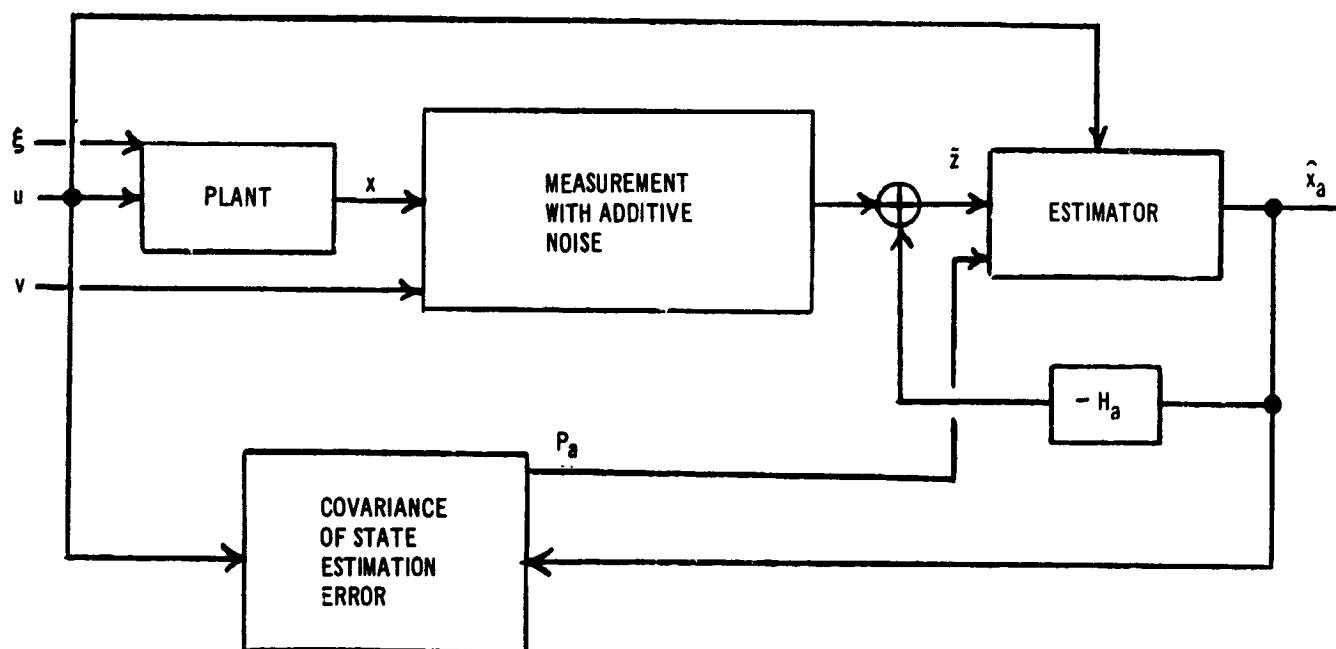


Figure 6-3. Block Diagram for Simulation of Combined Estimation Equations

operated on. The arrowhead inside of the box indicates the operator. For example, in Figure 6-2, R^{-1} is an input which becomes an operator on H_a to yield $R^{-1}H_a$.

6.3 SIMULATION OF COMBINED ESTIMATION; SIXTH-ORDER PLANT WITH TWO UNKNOWN PARAMETERS

Several simulation experiments were made with the sixth-order plant which has just been discussed. The two unknown parameters to be estimated are the influence coefficient and the natural frequency of the first bending mode. The purpose of these experiments was to establish the behavior of the combined estimator when the states of the third bending were allowed to influence the attitude measurement but were not included in the filter model.

The major variables studied in the experiments were: the noise-to-signal covariance ratio, the effects of parameter mismatch, and parameter tracking ability. For convenience, plant activity was created through the introduction of two sinusoids of differing frequencies. A more realistic but less convenient input would have been a noise spectrum which induced plant activity that is representative of that created by wind and command disturbances expected in a mission.

Some type of excitation must be included in simulations; otherwise, the state estimates would remain zero and no parameter estimation could be conducted. Further, the excitation must be of a type which excites states in a frequency range affected by the parameters which are to be estimated. For example, consider the case of estimating the natural frequency and gain of a second-order system. With a Bode plot in mind, it is seen that a sinusoidal excitation at one frequency gives only enough information to either estimate the gain or natural frequency, but not both. Even two sinusoidal inputs at a low frequency (with respect to the natural frequency) cannot give information to estimate the natural frequency. There must be excitation at a frequency in the range of the natural frequency and also in at least at one other frequency. Also, if a real system were such that wind and normal autopilot excitations did not excite the required frequencies for parameter estimation, then an artificial excitation would have to be included in the system. That is, parameter estimation requires inputs at certain frequencies and in that way is more difficult than state estimation. The frequency requirement of the input is not just a characteristic of using Kalman filtering but is a basic requirement of any parameter estimation technique.

6.3.1 Numerical Data

In order that the measurement coefficient on the first bending mode could be estimated, the assumed model used in the Kalman filter was taken to have the state modified from $(\phi, \dot{\phi}, \eta_1, \dot{\eta}_1)^T$ to $(\phi, \dot{\phi}, \delta_1, \dot{\delta}_1)^T$, where δ_1 is

defined as the product of the coefficient of η_1 in the measurement matrix with η_1 itself. The state portion of the dynamical matrix is then

$$\text{state portion of } A_a = \begin{bmatrix} 0 & 1 & 0 & 0 \\ A21 & 0 & 0 & 0 \\ 0 & 0 & 0 & 0 \\ A41 & 0 & A43 & A44 \end{bmatrix}$$

where

$$A21 = 0.00858$$

$$A41 = (0.299) \cdot 0.1155 \text{ (nominal)}$$

$$A43 = -5.66 \text{ (nominal)} \equiv S1$$

$$A44 = -0.234$$

and the state portion of the control distribution matrix is

$$\text{state portion of } B_a = \begin{pmatrix} 0 \\ B2 \\ 0 \\ B4 \end{pmatrix}$$

where

$$B2 = 0.363$$

$$B4 = 15.19 \cdot 0.1155 \text{ (nominal)} \equiv S2$$

and then the state portion of the augmented measurement matrix is

$$\text{state portion of } H_a = [1 \ 0 \ 1 \ 0]$$

The combined estimation problem for this sixth-order plant with two unknown parameters and an assumed plant model of fourth order was simulated for

various combinations of Q_a and R . The simulations were begun with the following Q_a :

$$Q_{22} = 1.865 \times 10^{-4}$$

$$Q_{24} = Q_{42} = 6.99 \times 10^{-3}$$

$$Q_{44} = 2.5 \times 10^{-1}$$

$$Q_{55} = 2.5 \times 10^{-1}$$

$$Q_{66} = 2.85 \times 10^{-2}$$

and all other entries zero. These will be termed nominal values and were computed from

$$Q_a^s = GQ_v G^T \quad (6-31)$$

where

$$G^T = [0, 1.113 \times 10^{-4}, 0, 3.88 \times 10^{-3}]$$

and

$$Q_v = 1.5 \times 10^4$$

and

$$Q_{55} = [10\% \text{ of nominal } S_1]^2$$

$$Q_{66} = [10\% \text{ of nominal } S_2]^2$$

and

$$Q_a = \begin{bmatrix} Q_a^s & 0 & 0 \\ 0 & Q55 & 0 \\ 0 & 0 & Q66 \end{bmatrix}$$

It was subsequently realized that Q55 and Q66 should have been divided by the computing interval used in the digital simulation. The value of R in the estimation equations was first selected to be 10^{-4} . This value was selected because it was approximately the level of the spectral density of the third bending mode.

The system had a feedback gain matrix of

$$[3.22, 5.68, -0.264, -0.737, 0, 0]$$

operating on \hat{x}_a .

All reported simulations were for no actual input disturbances of measurement noise but for a sinusoidal dither signals of 1.1 and 3.3 rad/sec and 0.02 degree of β amplitude. A disturbance on this system would help the estimation. A noise on the measurements will slow the parameter estimation process because there will not be as much information in the measurement and, consequently, the gains corresponding to the parameters must be reduced.

6.3.2 Simulation Results

The results for nominal Q_a showed the parameter estimate to be insensitive to parameter errors. When runs were made for no mismatch of parameters, the state estimates were within 0.1%, for ϕ and 2% for η_1 .

The values of Q55 and Q66 were subsequently changed by 8 and 10 orders of magnitude in order to obtain sensitivity of the parameter estimates. In order to observe the amount of sensitivity, S1 was varied sinusoidally (with a

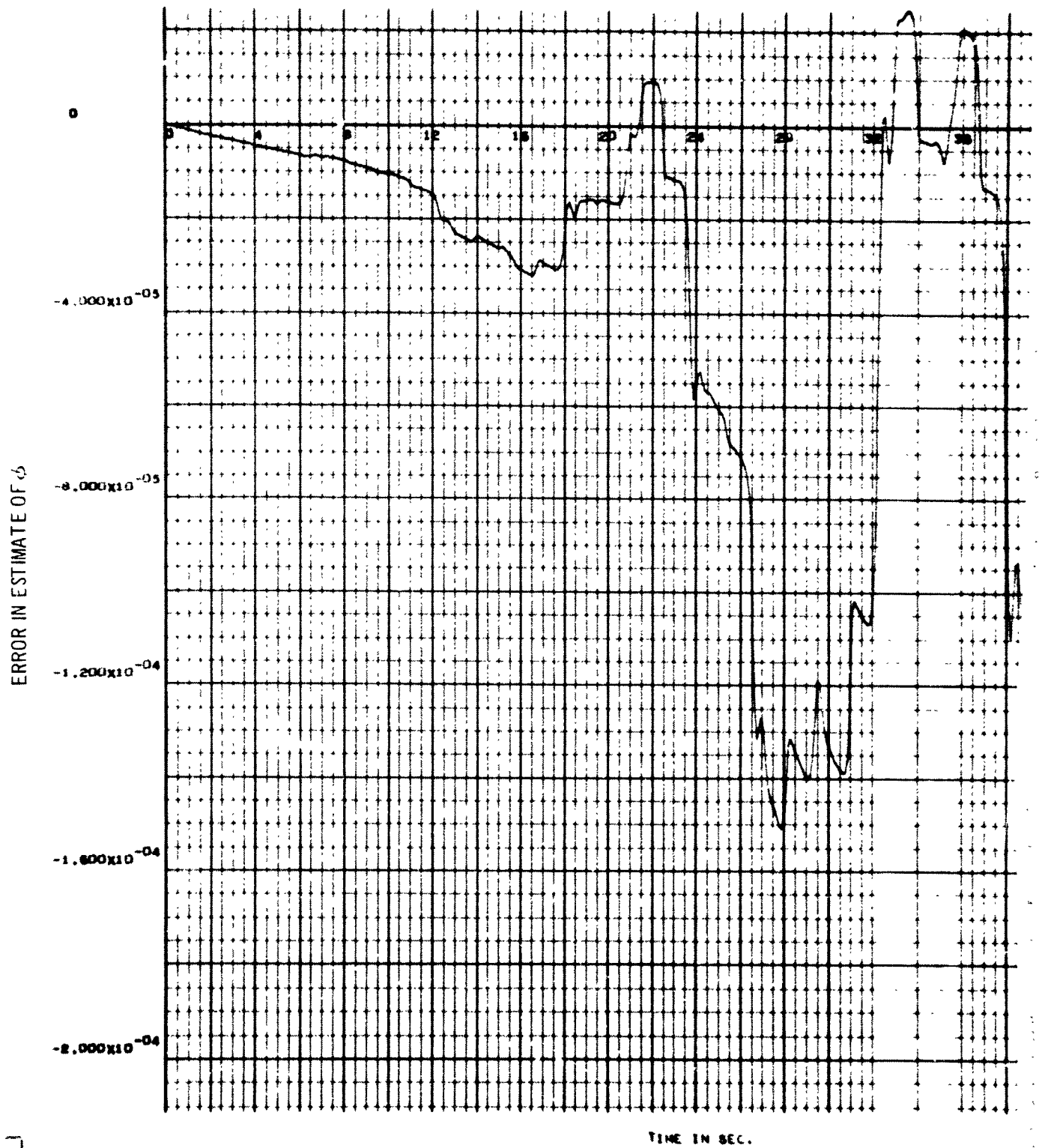
period of 10 sec and 10% of nominal amplitude). The results of simulations for this Q_a and for R increased by two and three orders of magnitude are shown in Figures 6-4 and 6-5. These illustrations show that the results were essentially the same for the two values of R . Secondly, they show that the state estimates were not as good as when the parameter estimates were insensitive to parameter errors. Figures 6-4 and 6-5 also show that the parameter estimates have oscillations of approximately 25% around their nominal values.

When the values of Q_{55} and Q_{66} were subsequently set to 0, which is the case of state estimation only, the resulting errors in ϕ and η_1 were approximately 2% of their maximum values, as shown in Figure 6-6, and it was then concluded that the effect of parameter estimation is to increase the state estimation error. However, it is pointed out that the time history of the error in ϕ is quite different for this combined estimation simulation than for state estimation, which is seen by comparison of Figure 6-5 to Figure 6-6. This large difference in the type of time history was found to be caused by the sinusoidal excitation of parameter S_1 , by making this same simulation except without the third bending mode and with and without the sinusoidal excitation of parameter S_1 , as shown in Figures 6-7 and 6-8. Increasing the values of Q_{55} and Q_{66} two more orders of magnitude resulted in smaller errors in the estimates of the states but larger transients in the estimates of the parameters.

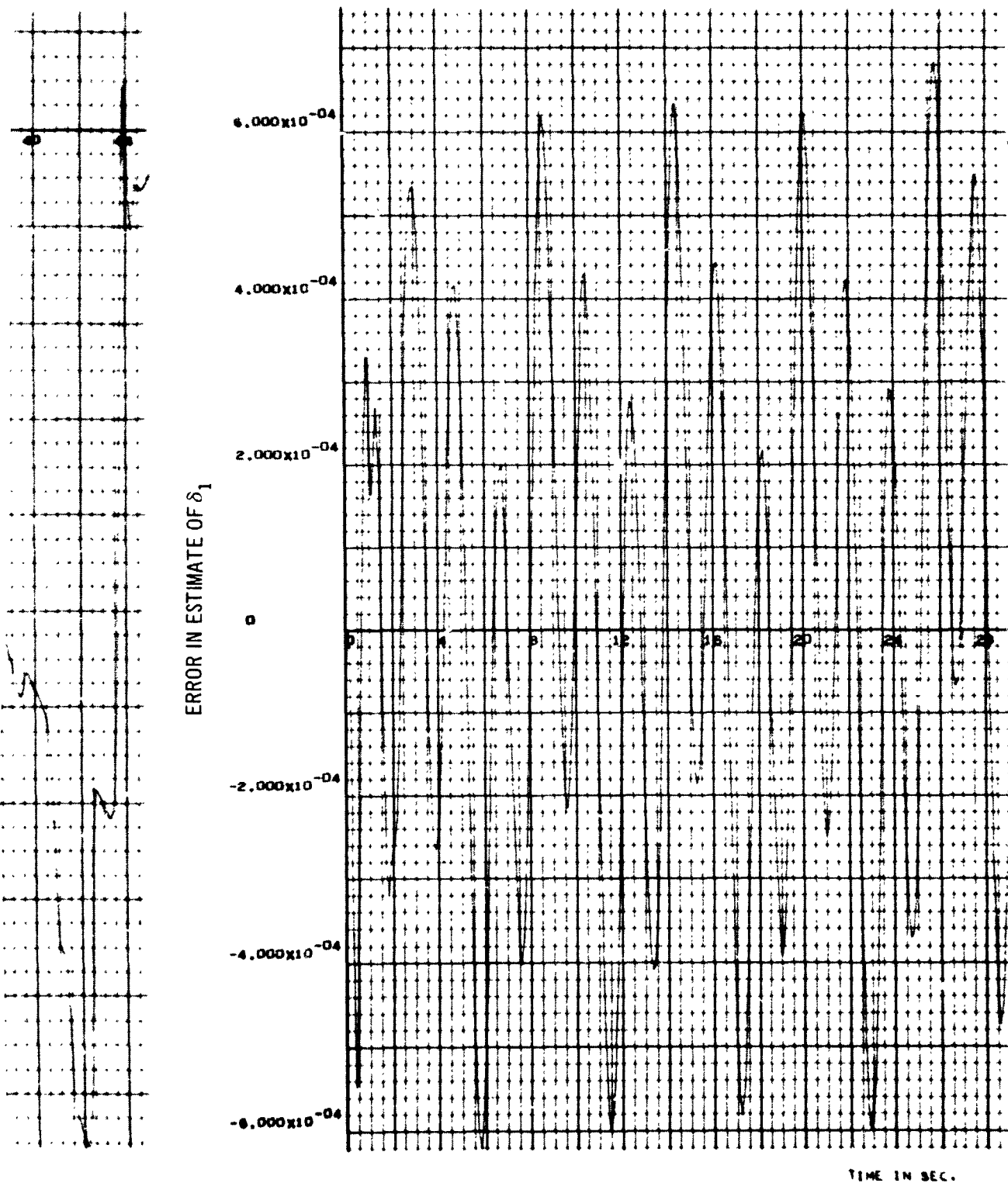
The effect of the third bending is to increase the error in the estimate of ϕ and η_1 and also to add an oscillation on the estimate of η_1 . However, these latter oscillations were usually less than 4% of the maximum value. The effect of the third bending on parameter S_1 was to increase the error in its estimate, but this error was reduced to less than 5% after 10 sec, following transients to about 40% during the first few seconds. This large transient can be reduced by lowering the value of Q_{55} .

COMBINED ESTIMATION FOR 6-TH ORDER PLANT (4)

CASE



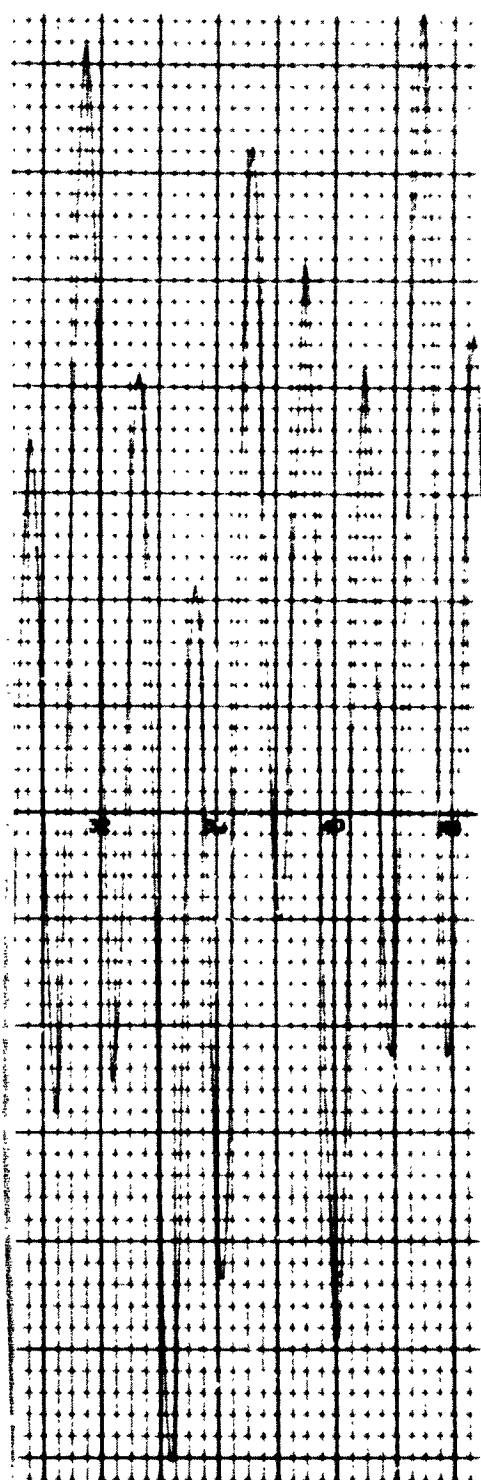
COMBINED ESTIMATION FOR 6-TH ORDER PLANT (4)



159-2

CASE 1

SMALL ESTIMATION FOR 10 TO 1000



ERROR IN ESTIMATE OF SI

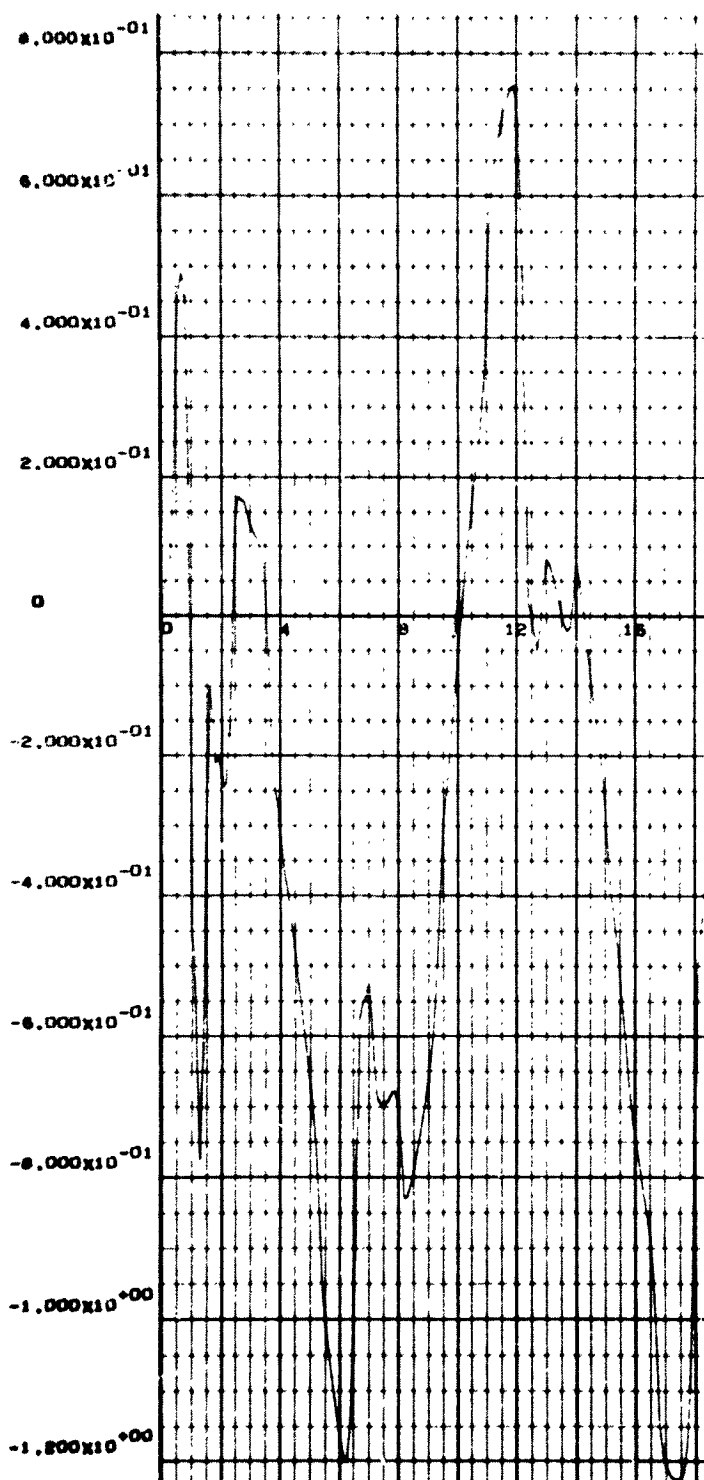


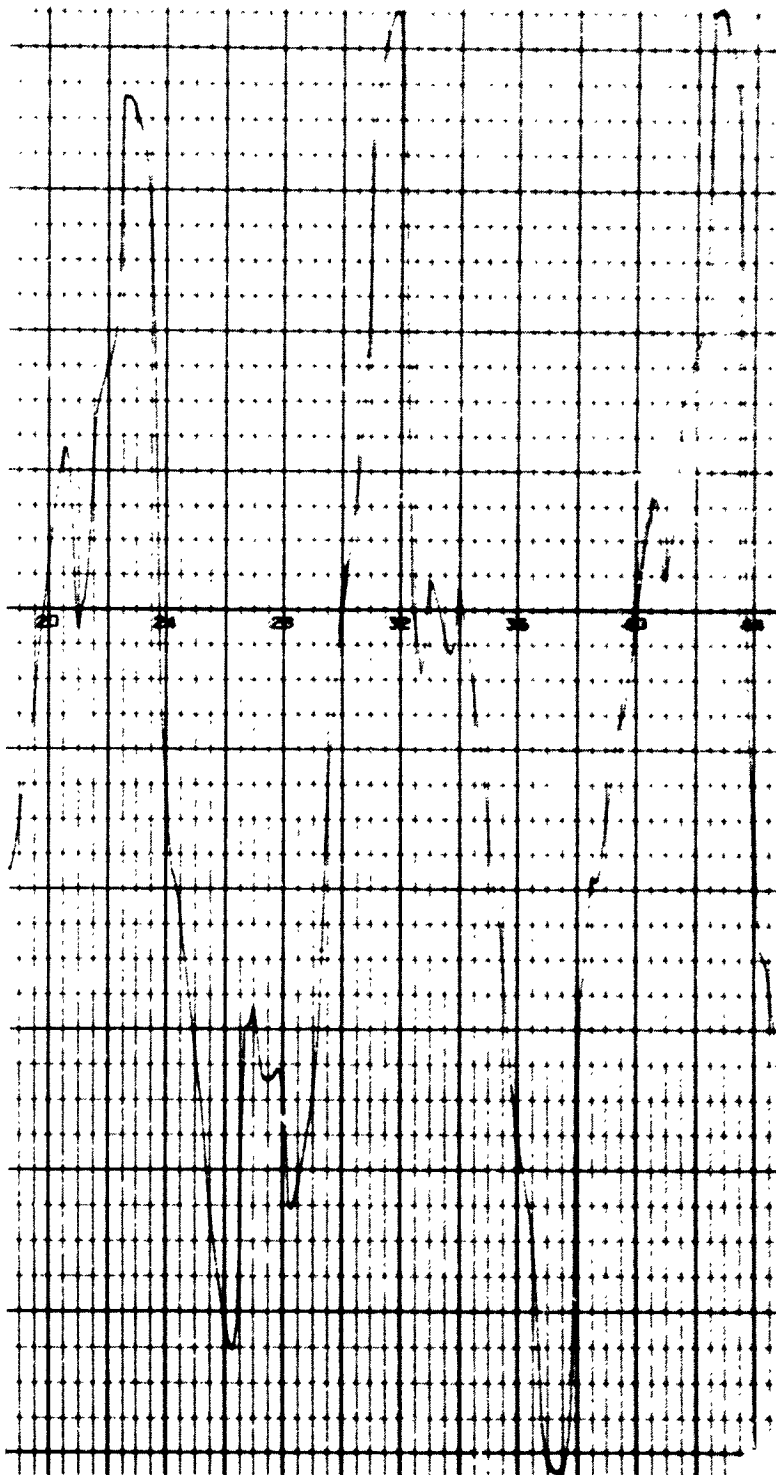
Figure 6-4. Nominal Q_0 , Except $Q_{55} = 2.5 \times 10^7$ and $Q_{66} = 2.85 \times 10^8$, $R = 10^{-2}$ SI Sinusoid:

159.3

ANT (4)

CASE

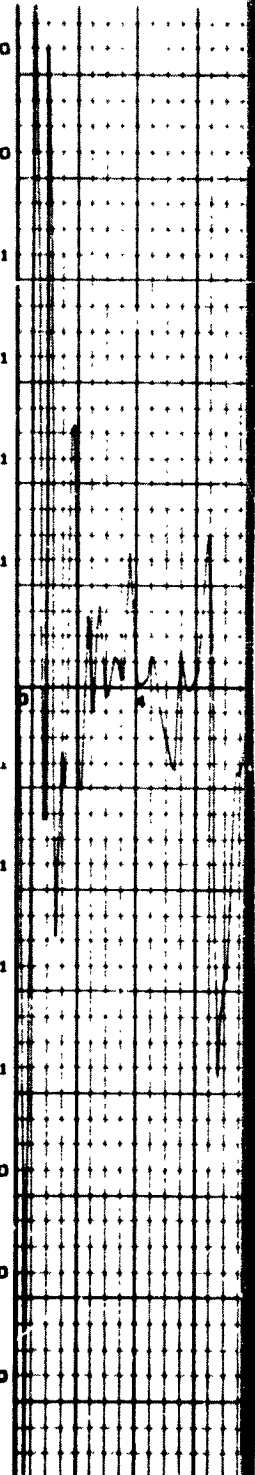
COMBINED



TIME IN SEC.

ERROR IN ESTIMATE OF S2

$1.200 \times 10^{+00}$
 $1.000 \times 10^{+00}$
 8.000×10^{-01}
 6.000×10^{-01}
 4.000×10^{-01}
 2.000×10^{-01}
0
 -2.000×10^{-01}
 -4.000×10^{-01}
 -6.000×10^{-01}
 -8.000×10^{-01}
 $-1.000 \times 10^{+00}$
 $-1.200 \times 10^{+00}$
 $-1.400 \times 10^{+00}$

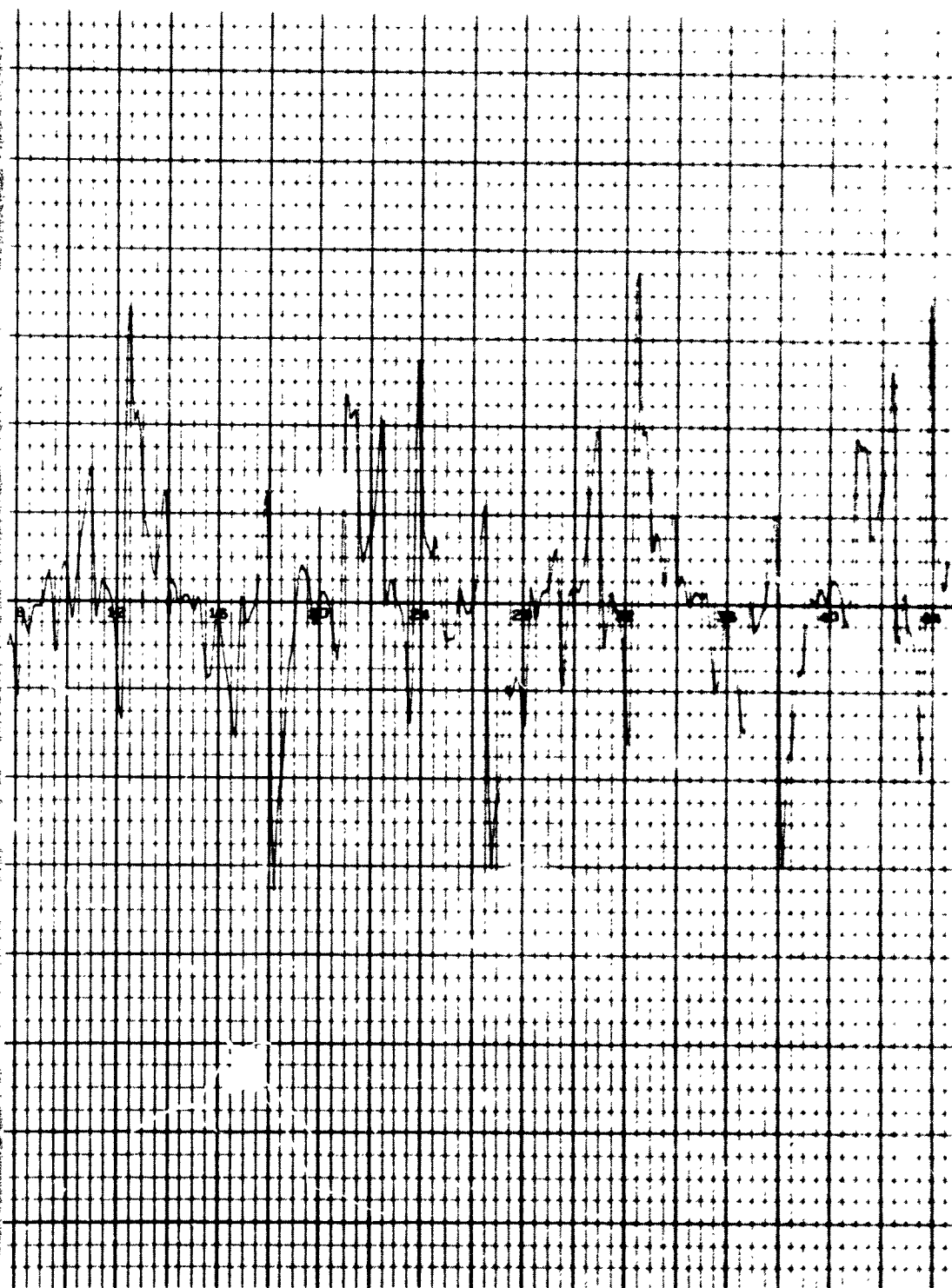


al with 10 - Sec Period and 10% of Nominal Amplitude

159-4

ESTIMATION FOR 6-TH ORDER PLANT (4)

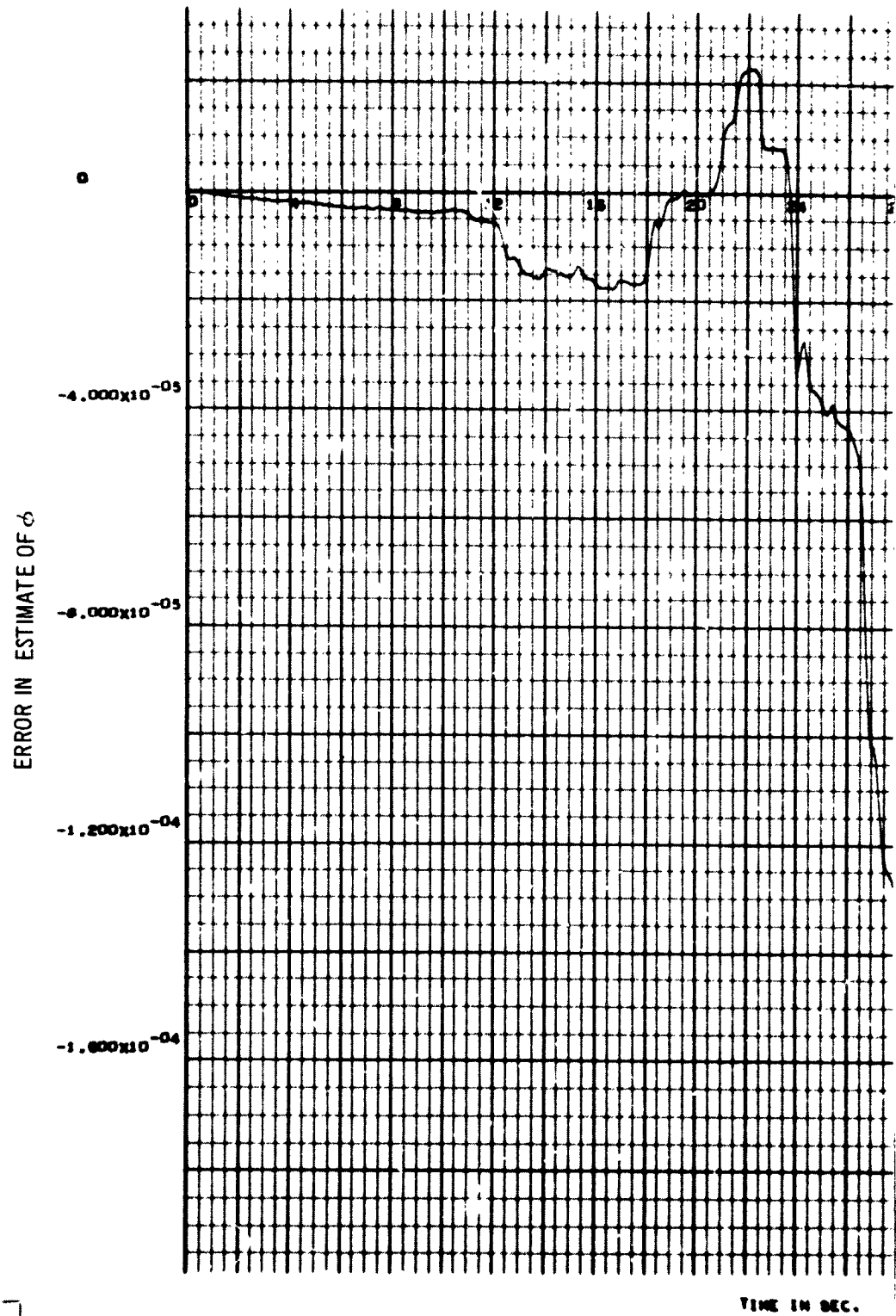
CASE



TIME IN SEC.

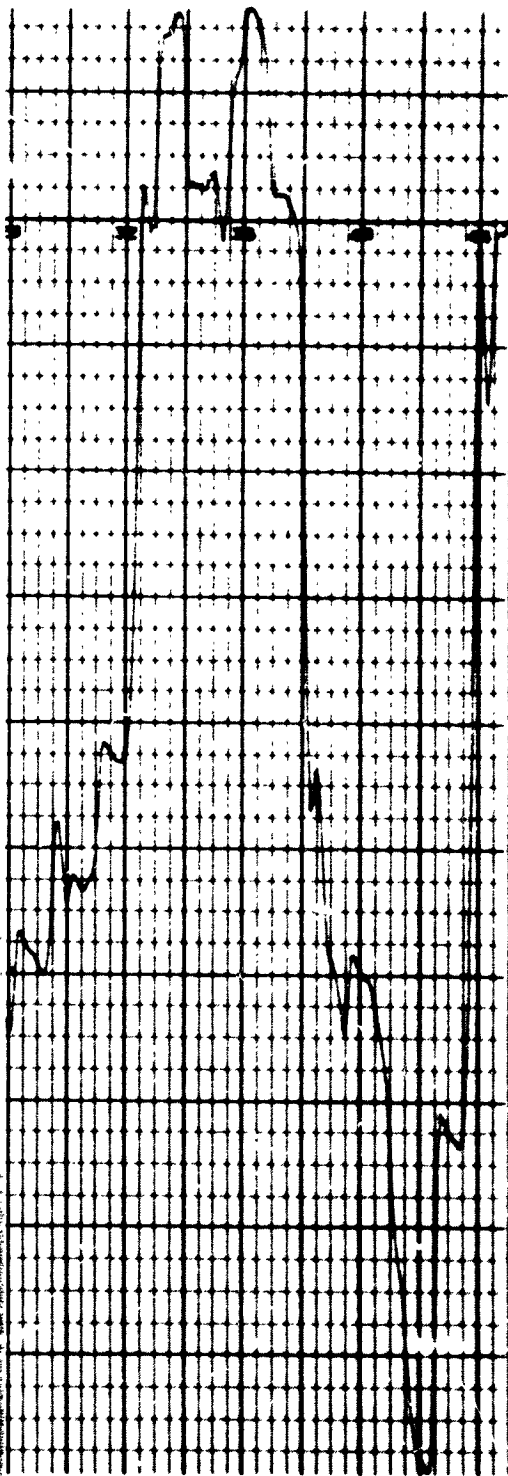
159-5

COMBINED ESTIMATION FOR 6-TH ORDER PLANT (4)



CASE 2

COMBINED ESTIMATION FOR 6-TH ORDER



ERROR IN ESTIMATE OF δ_1

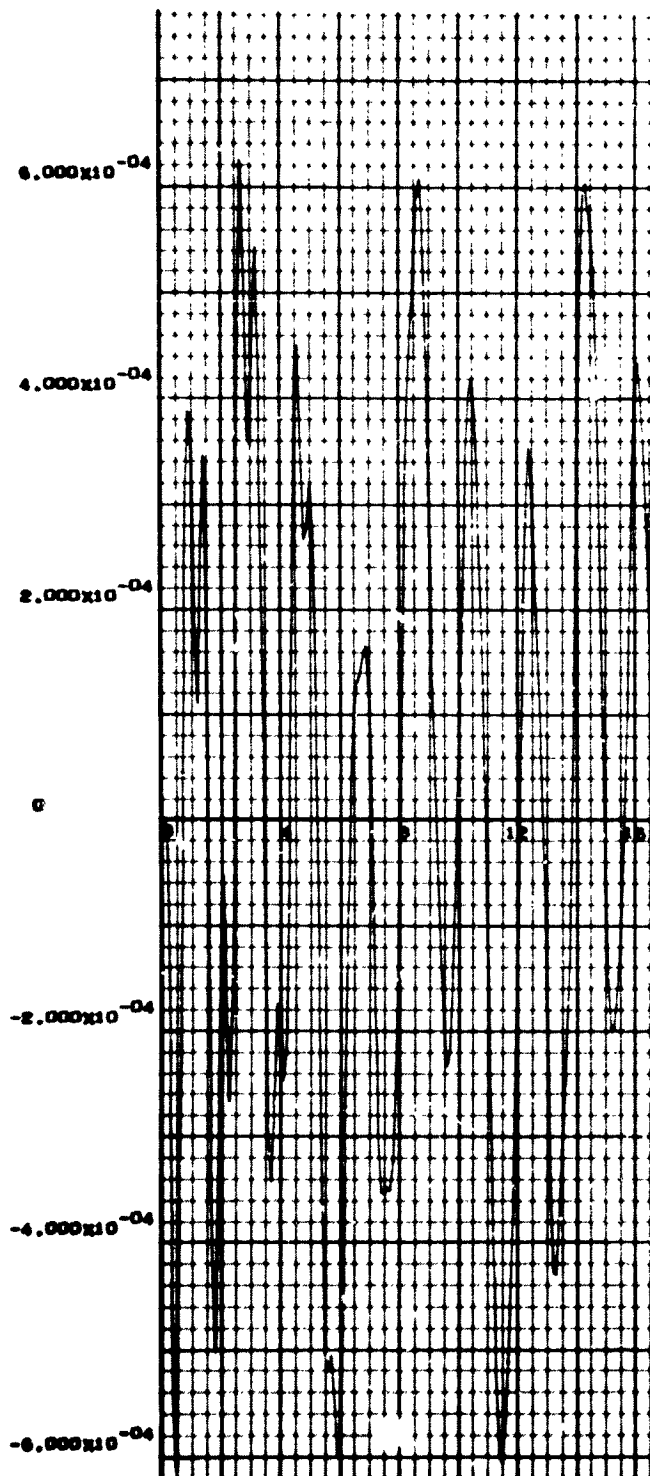


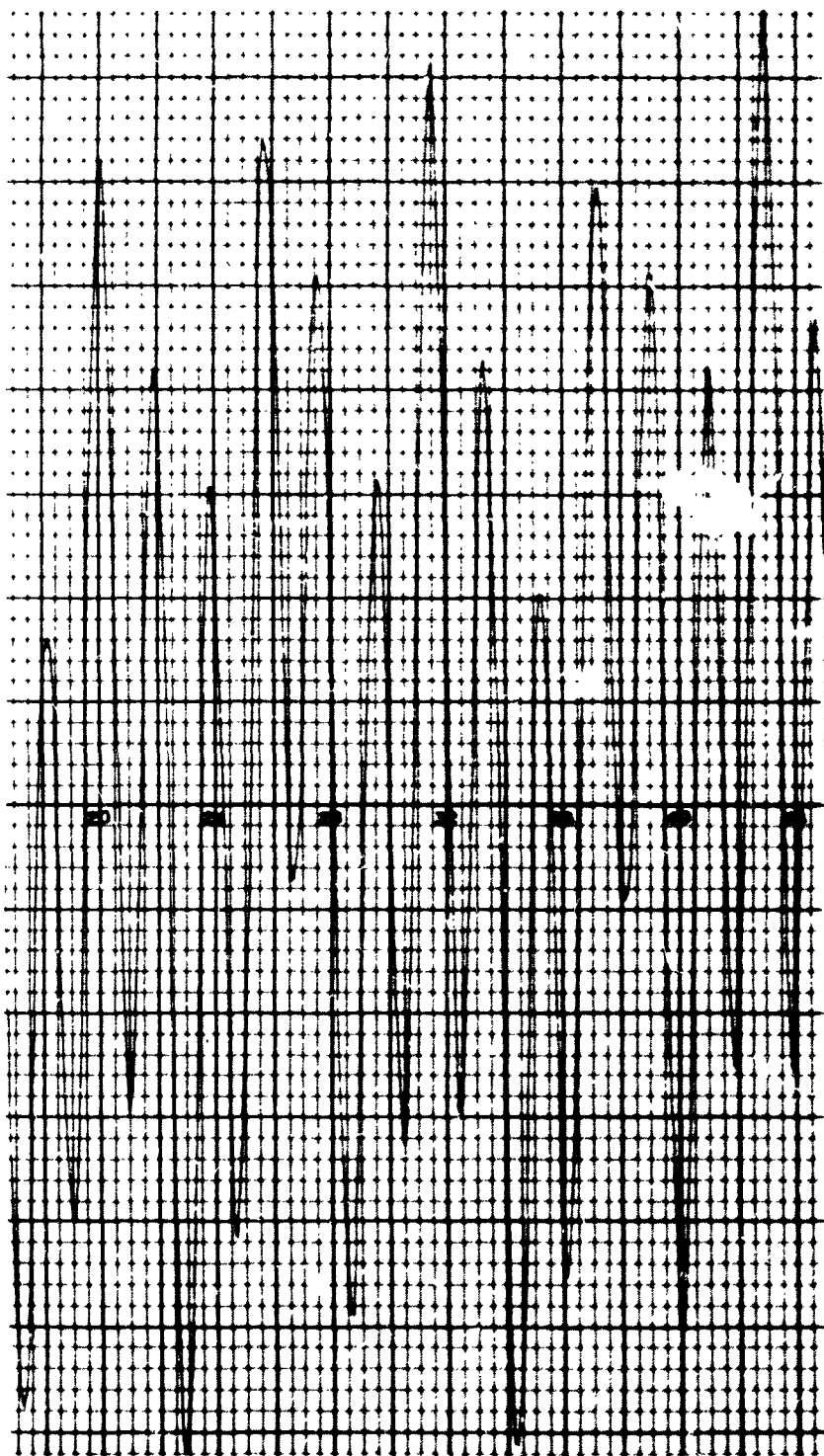
Figure 6

160-2

R PLANT (4)

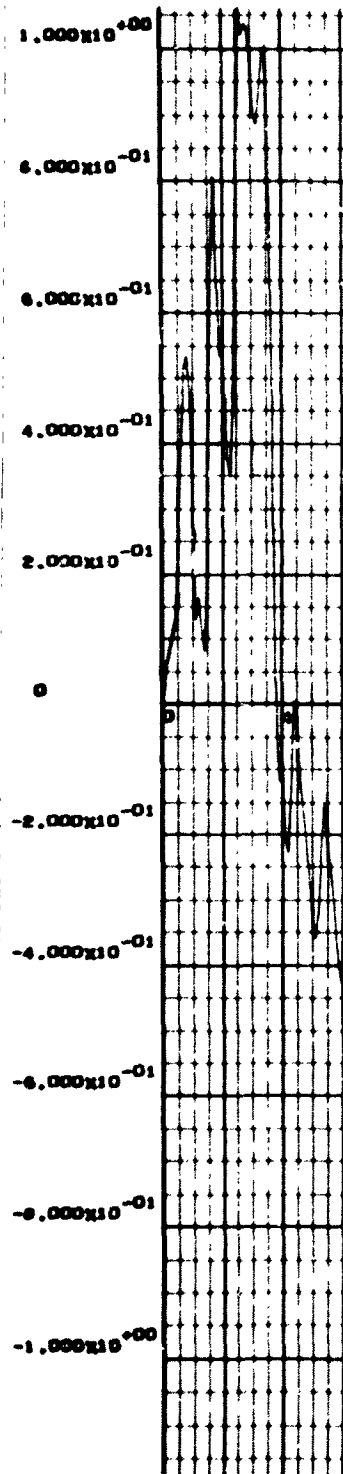
CASE 2

COMBINE



TIME IN SEC.

ERROR IN ESTIMATE OF S1

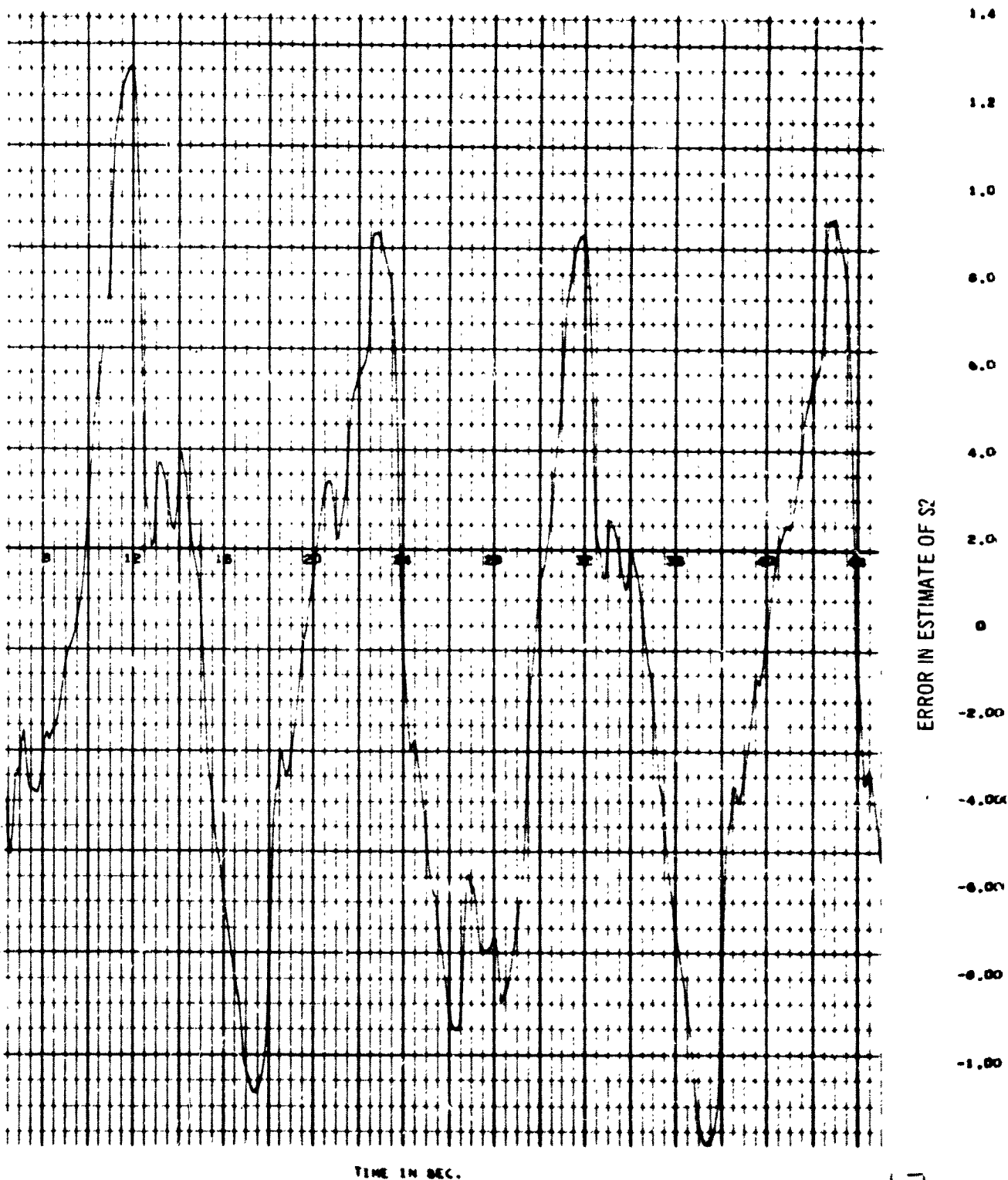


-5. Nominal Q_a , Except $Q_{55} = 2.5 \times 10^7$ and $Q_{66} = 2.85 \times 10^8$, $R = 10^{-1}$ S1 Sinusoidal with 10

160-3

ESTIMATION FOR 6-TH ORDER PLANT (4)

CASE 2

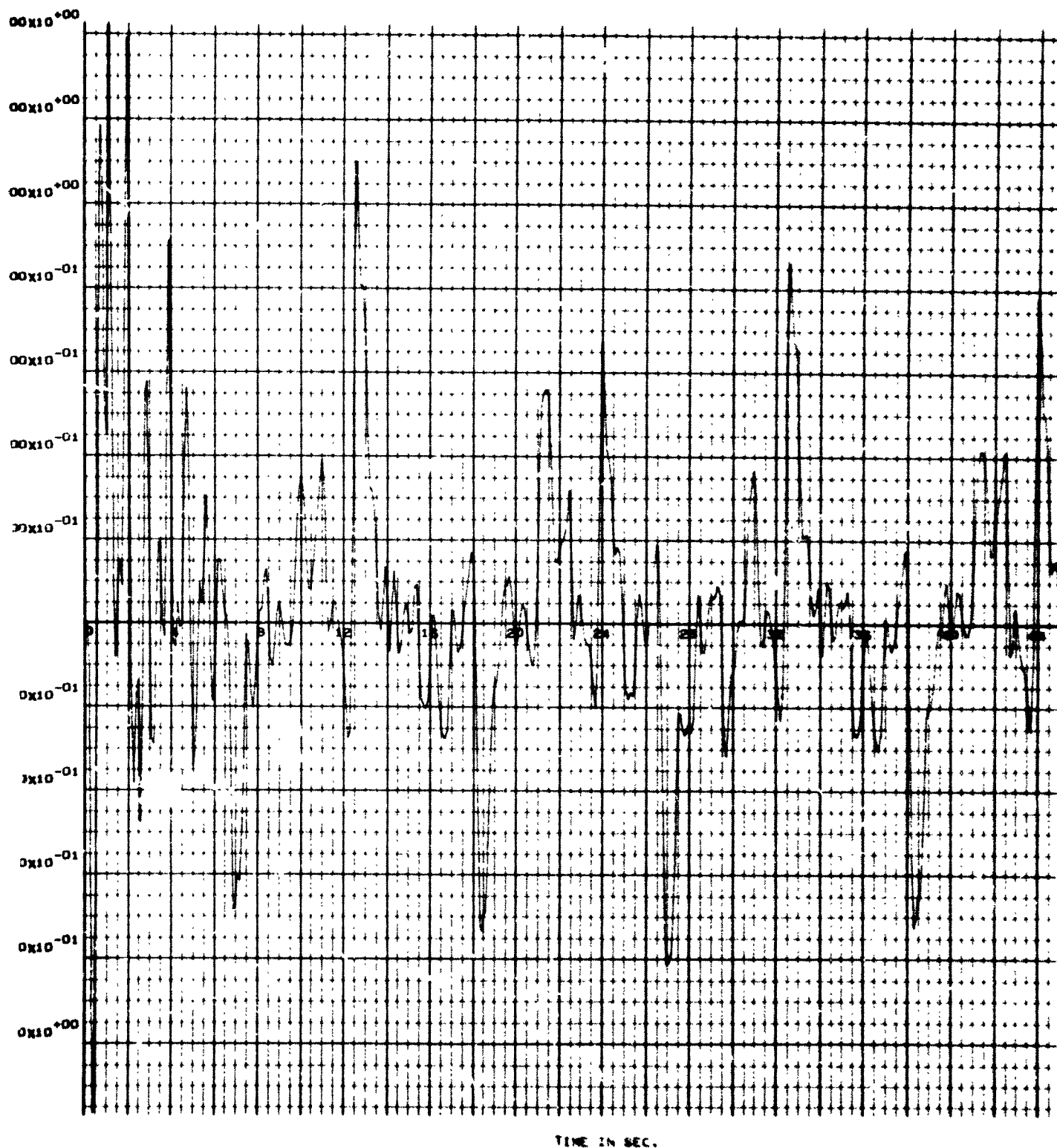


1-Sec Period and 10% of Nominal Amplitude

160-4

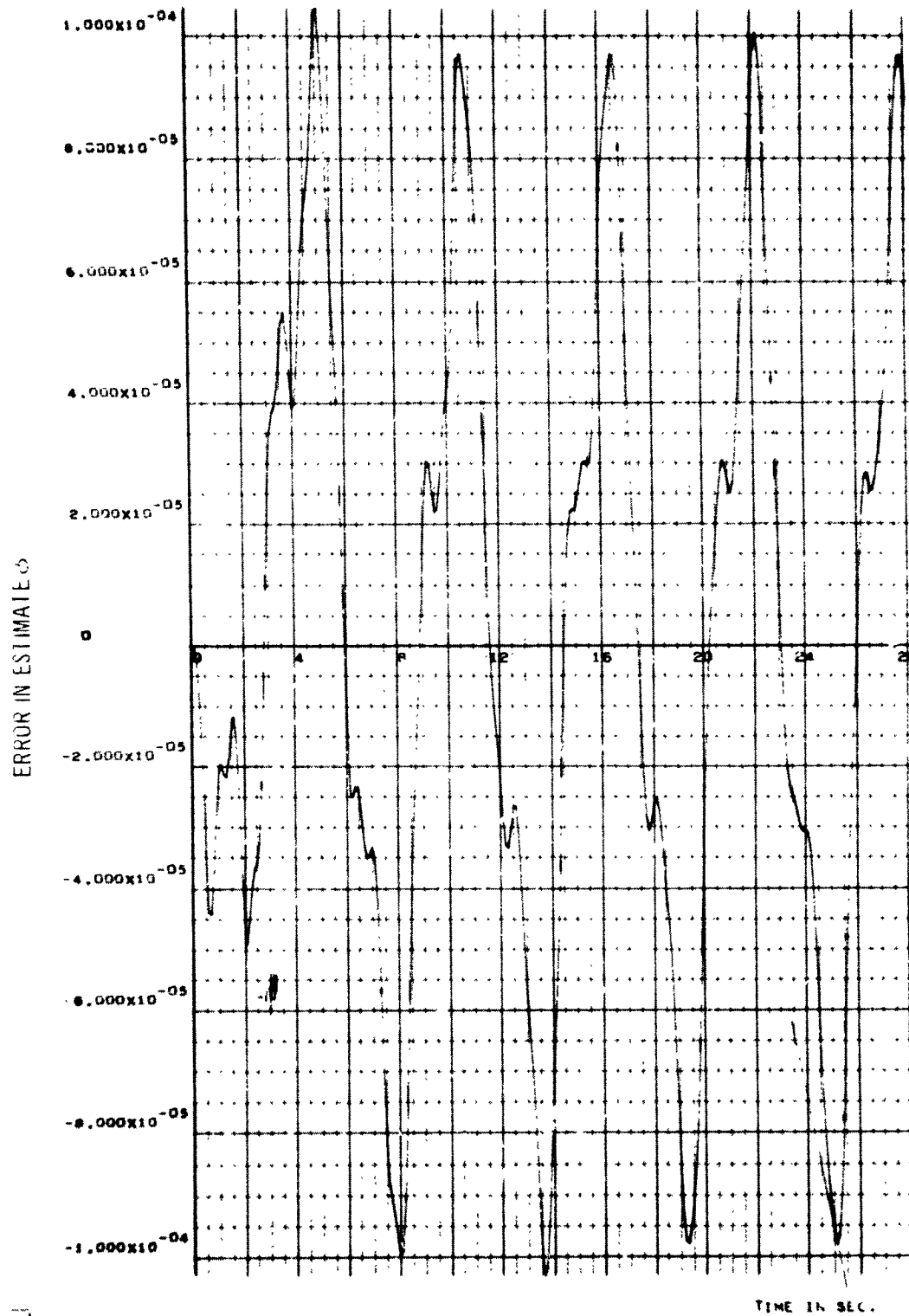
COMBINED ESTIMATION FOR 5-TH ORDER PLANT (4)

CASE 2



160-5

COMBINED ESTIMATION FOR 6-TH ORDER PLANT (5)



161-1

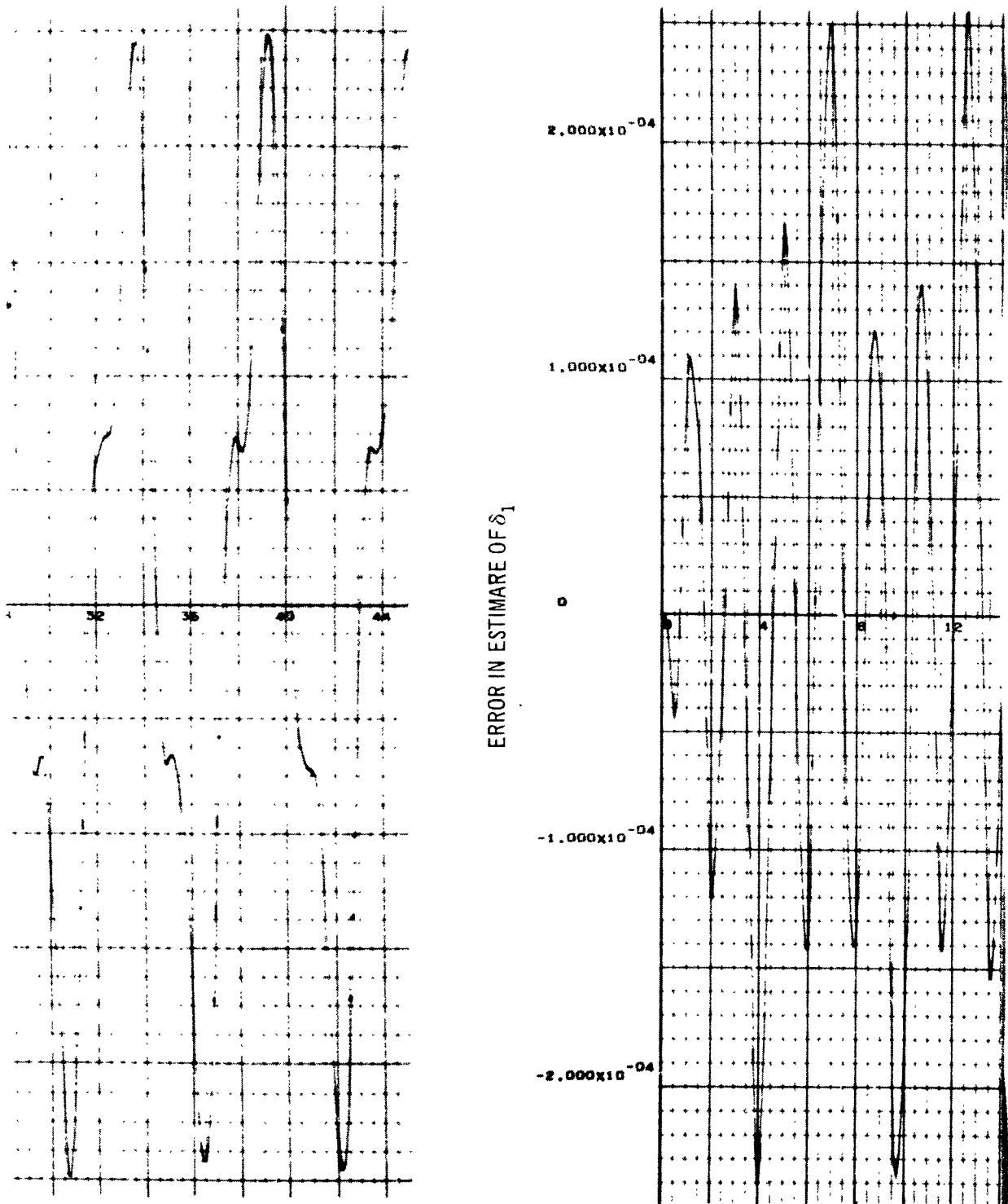
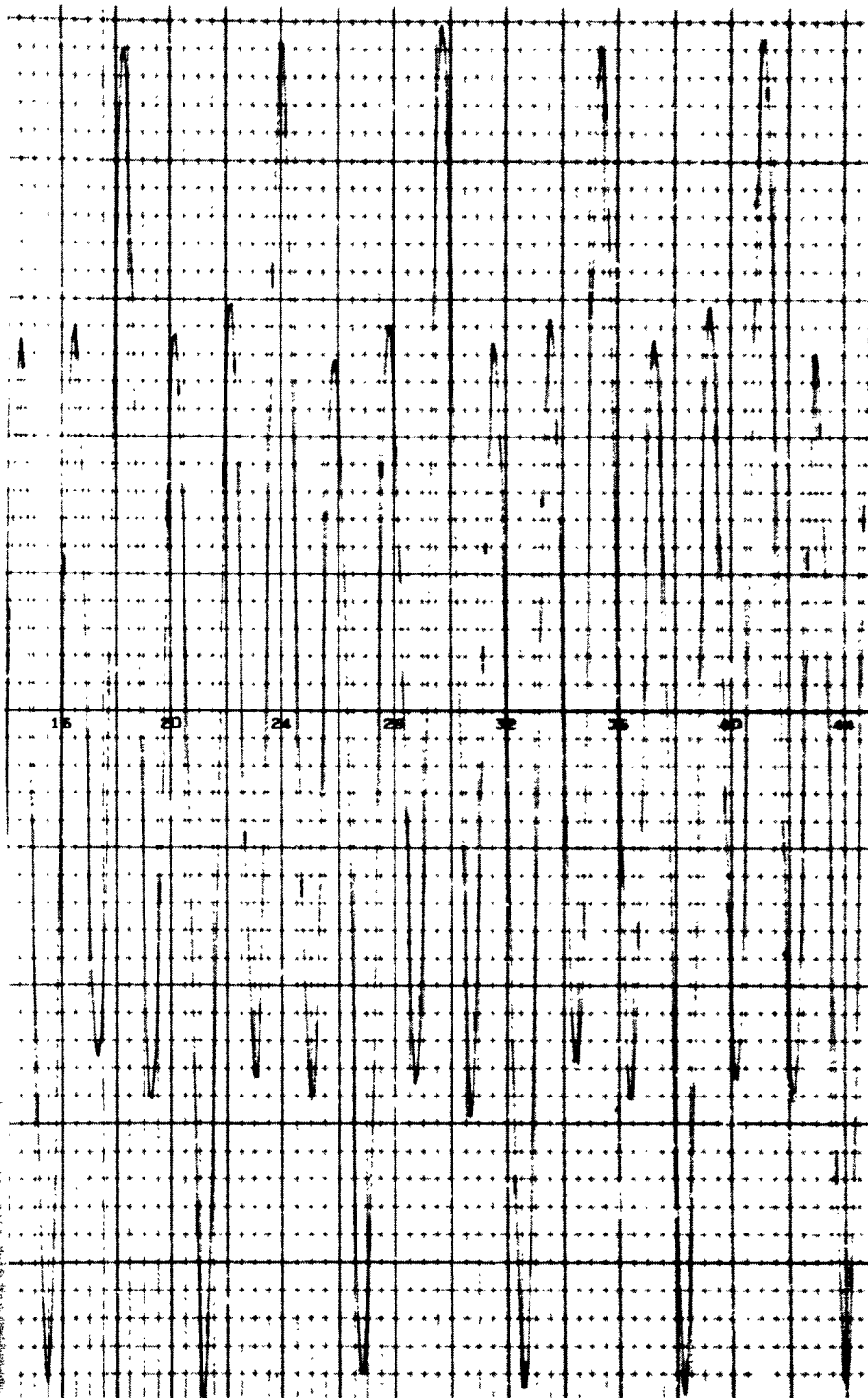


Figure 6-6. Nominal Q_a , Except $Q_{55} = Q_{66} = 0$, $R = 10^{-1}$, S_1 Constant

161-2

TH ORDER PLANT (5)

CASE 3



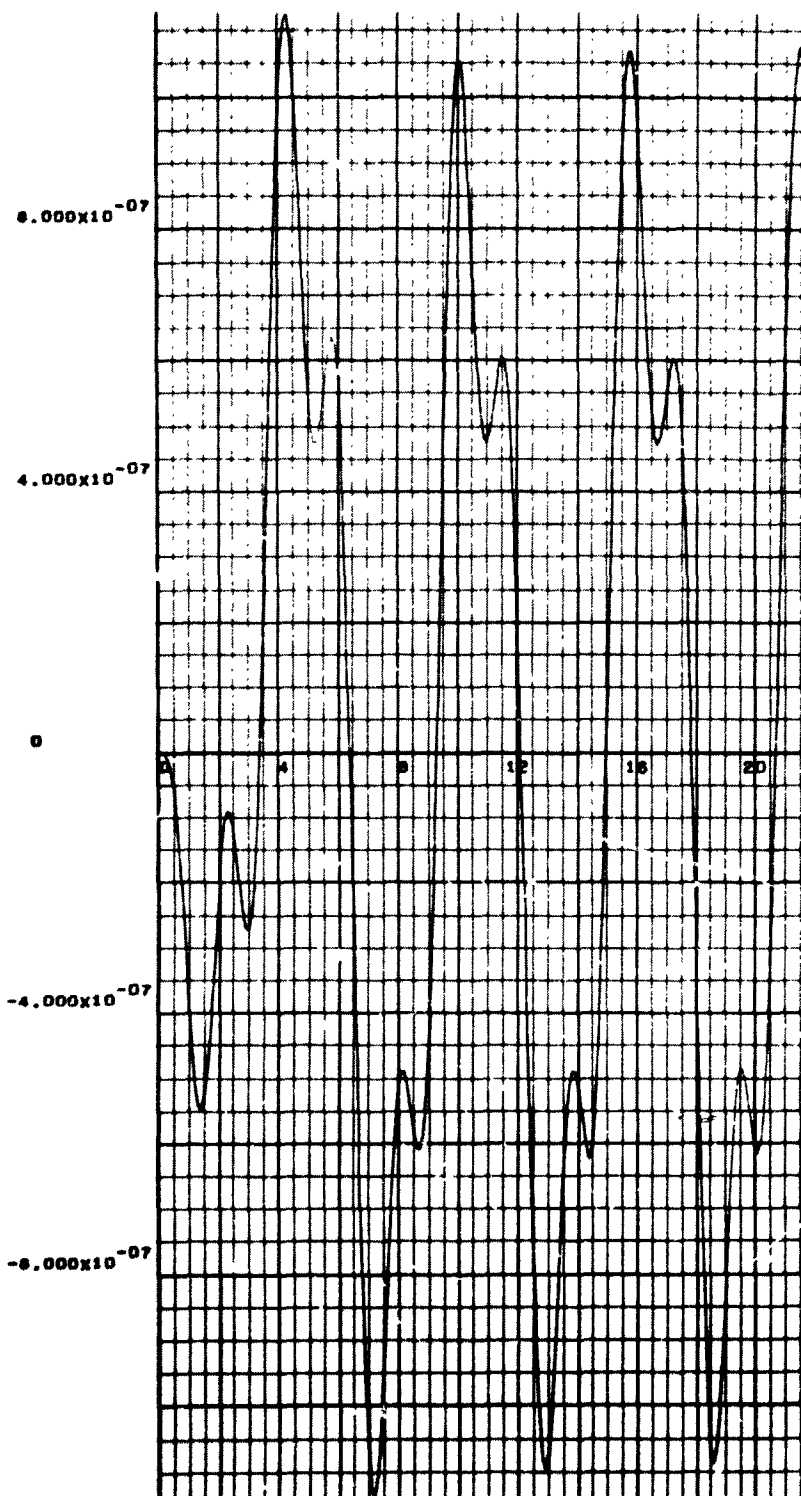
TIME IN SEC.

3

161

COMBINED ESTIMATION FOR 6-TH ORDER PLANT (8)

ERROR IN ESTIMATE OF ϕ



CASE 1

MEINER FST:

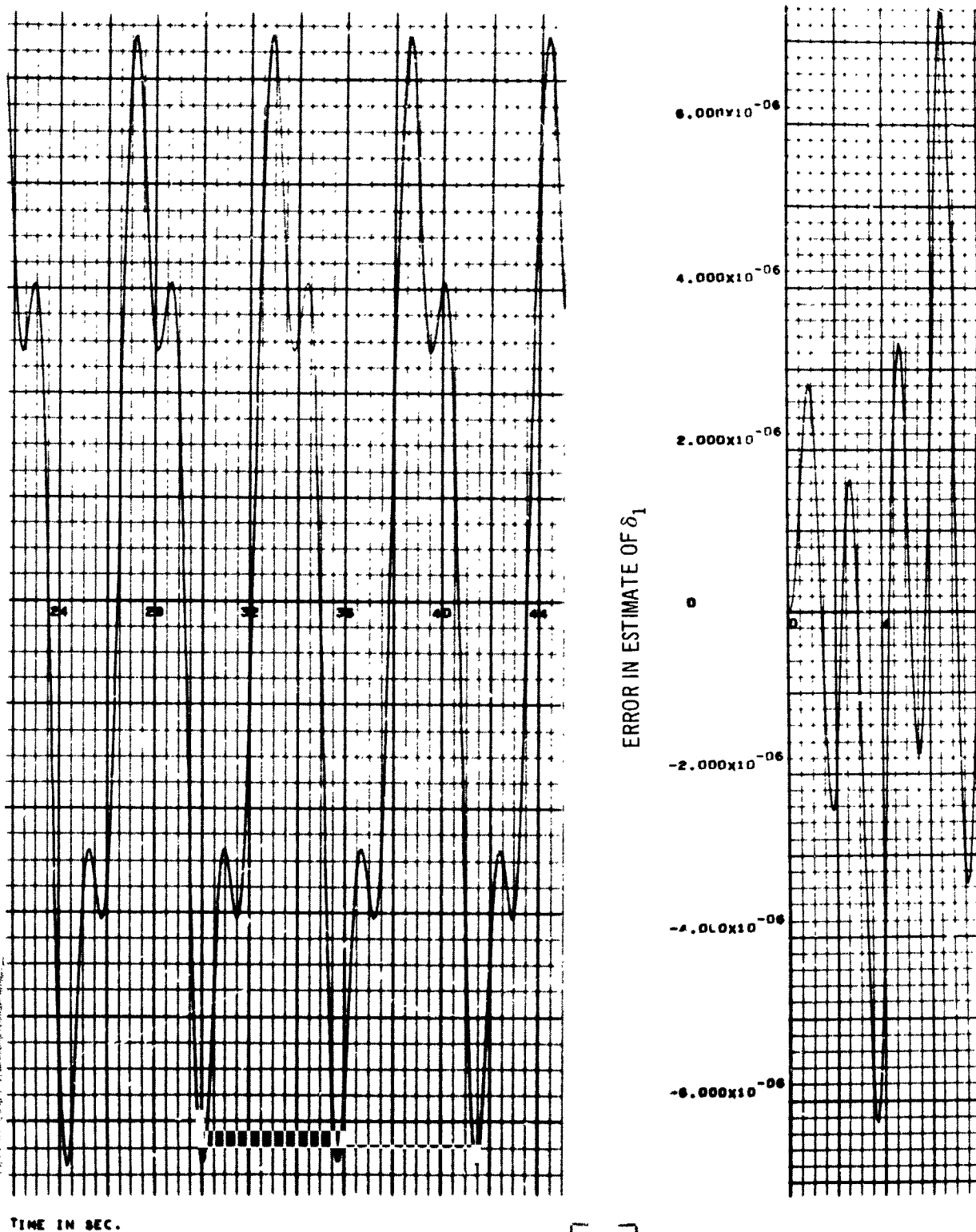
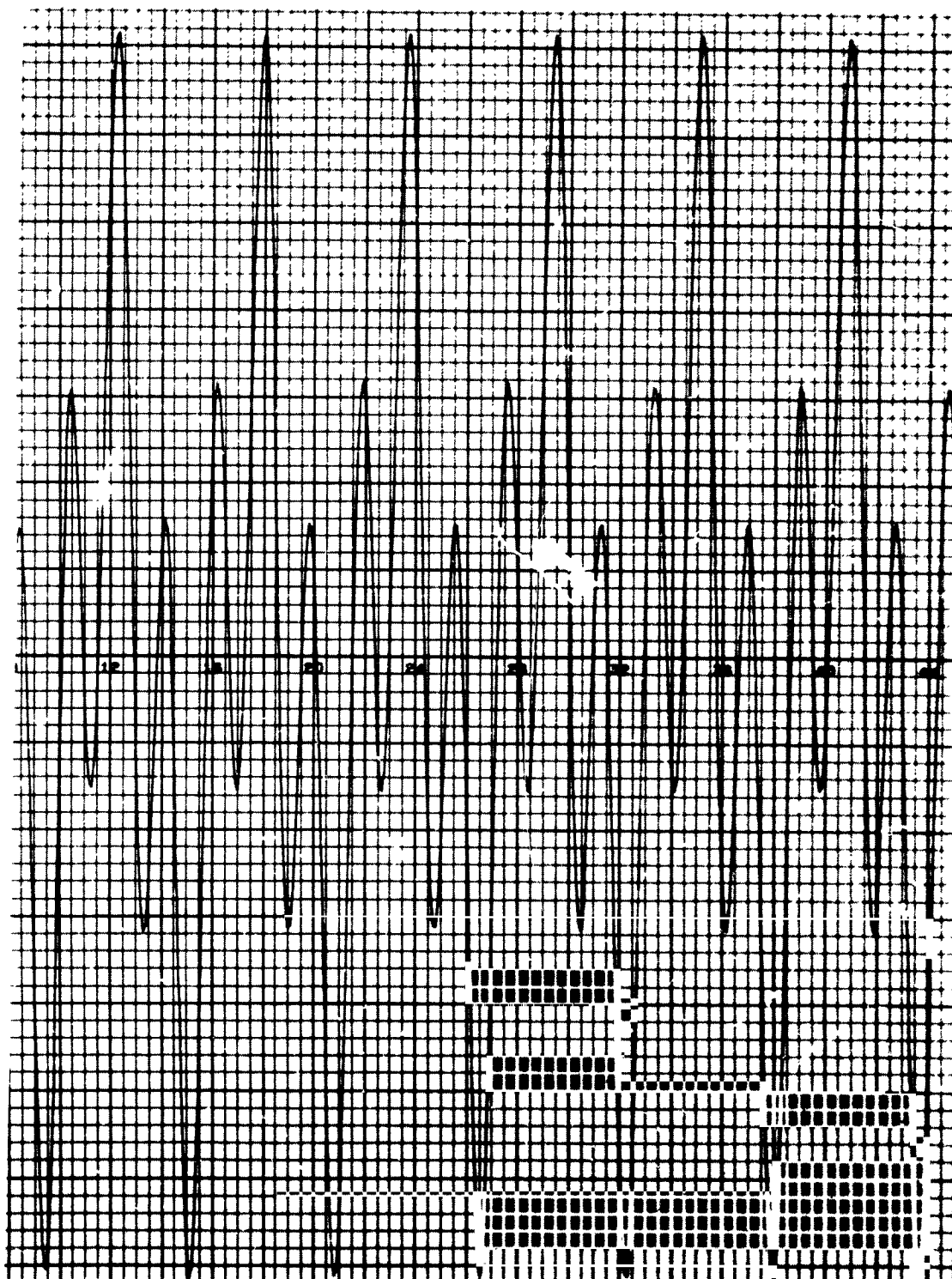


Figure 6-7. Nominal Q_a Except $Q_{55} = Q_{66} = 0, R = 10^{-1}$ S1 Constant and no 3rd Bending

162-2

IMATION FOR 6-TH ORDER PLANT (8)

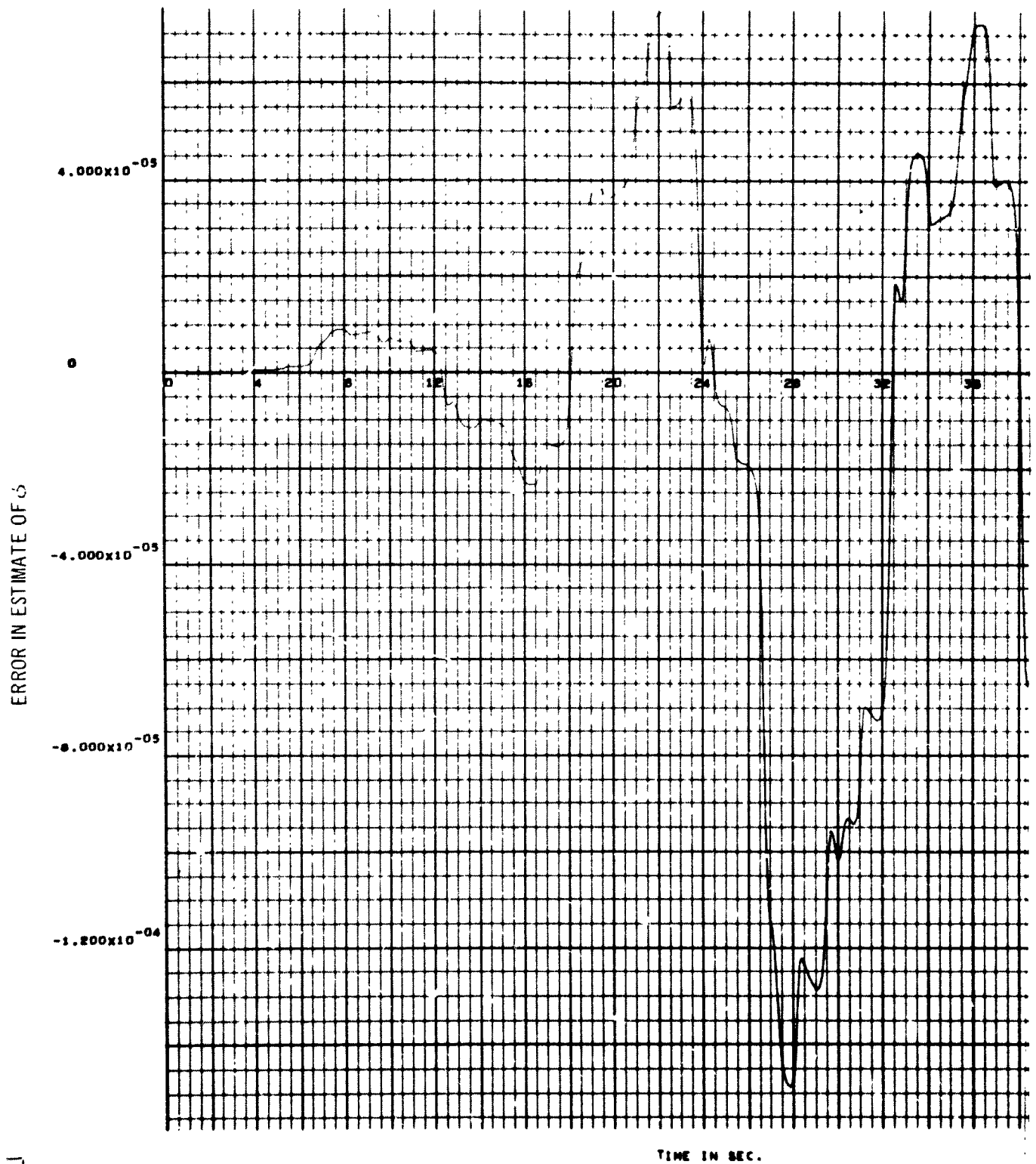
CASE 1



TIME IN SEC.

Mode in Plant

162-3



103-1

E 2

COMBINED ESTIMATION FOR 6-TH ORDER PLANT (8)

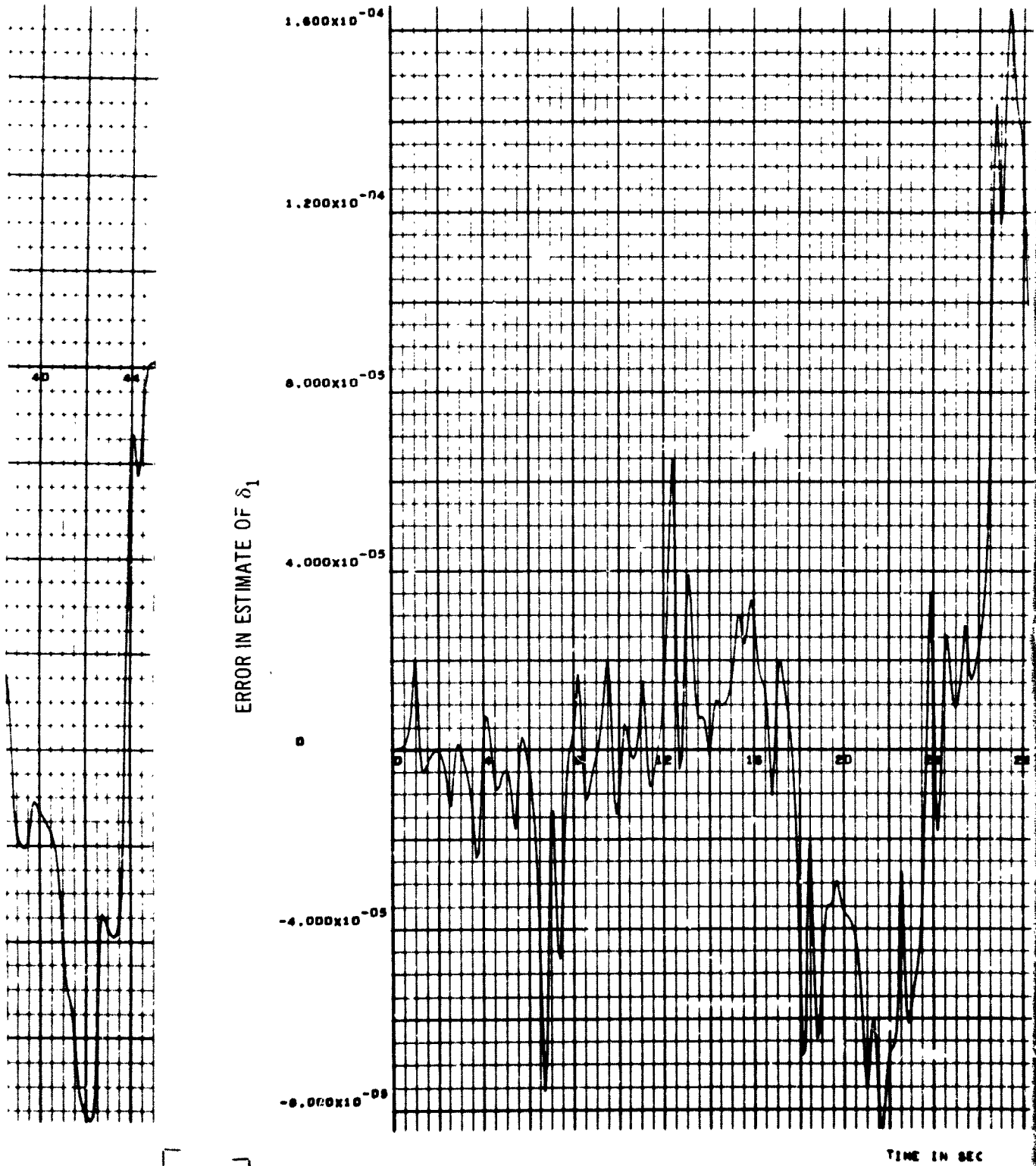
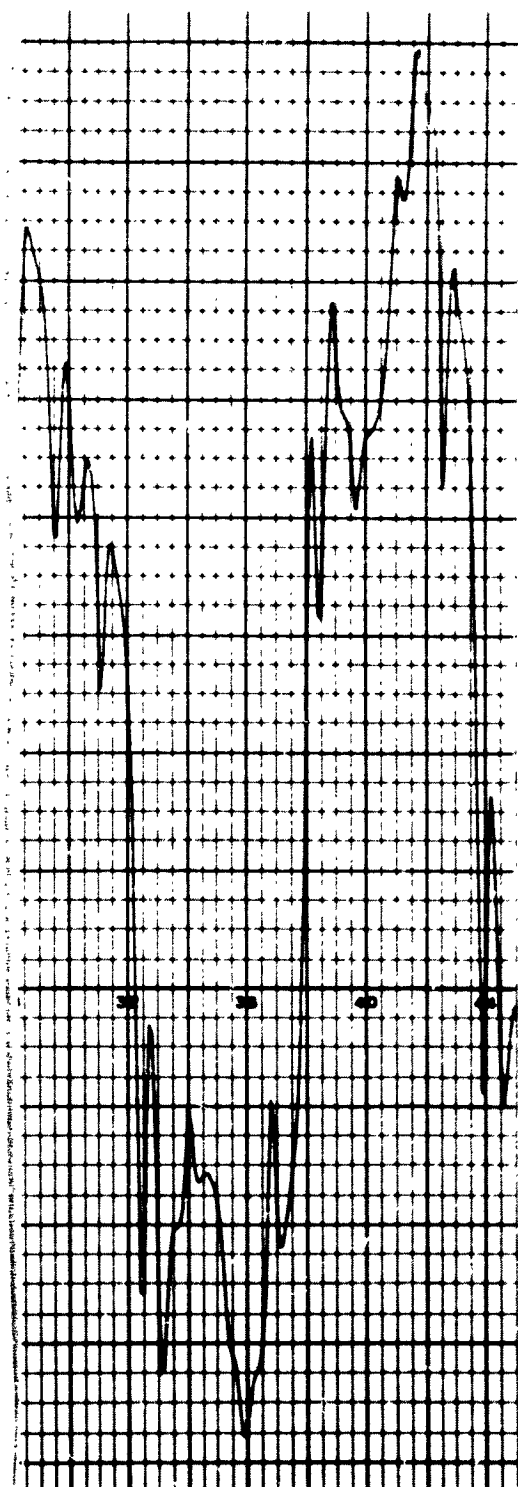


Figure 6-8. Nominal Q_a , Except $Q_{55} = 2$.

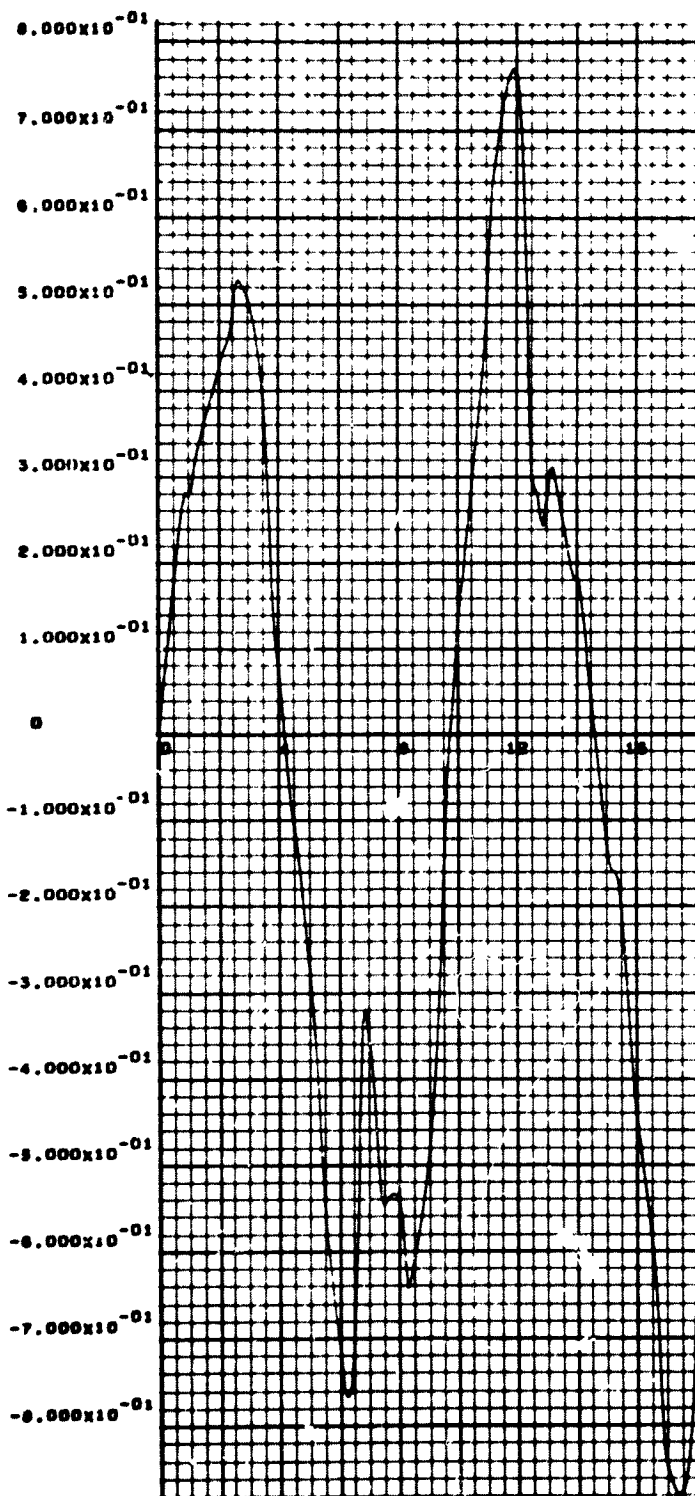
163-2

CASE 2

COMBINED ESTIMATION FOR 6-TH ORDER P



ERROR IN ESTIMATE OF S1



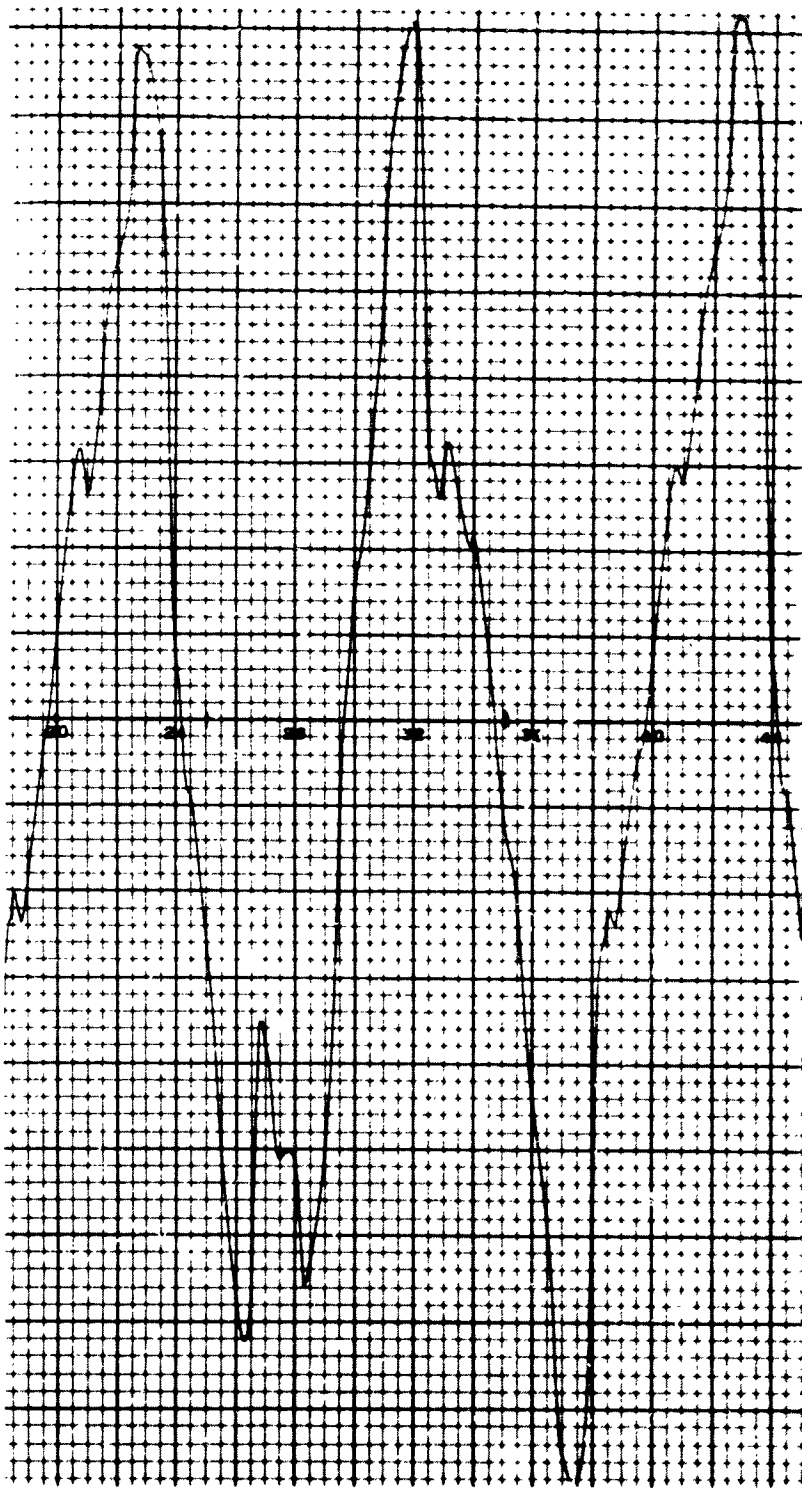
5×10^7 and $Q66 = 2.85 \times 10^8$, $R = 10^{-1}$, S1 Sinusoidal with 10- Sec Period and 10% of Nominal Amplit

163-3

LANT (0)

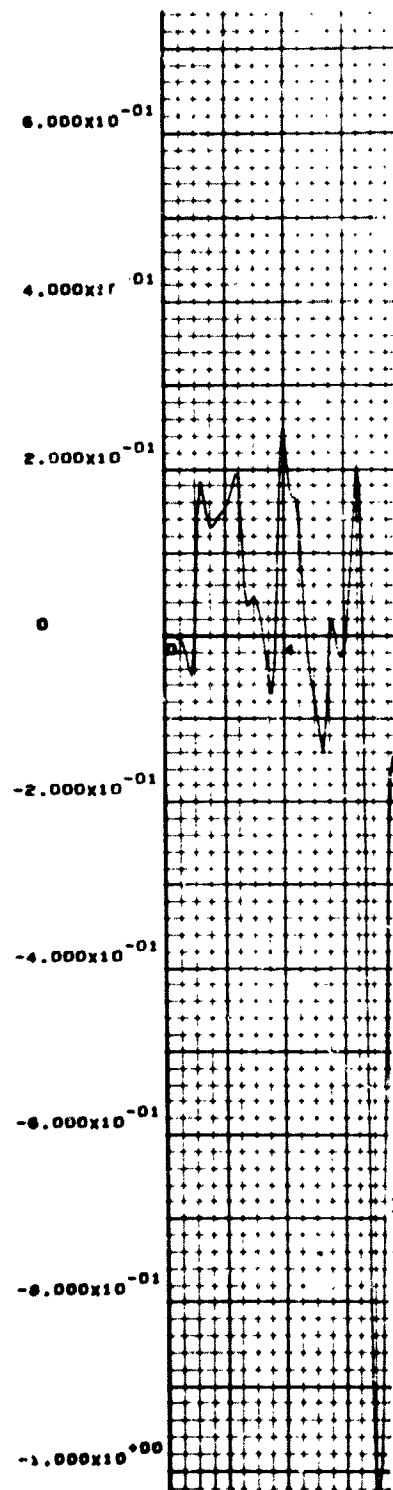
CASE 2

COMBINED ES



TIME IN SEC.

ERROR IN ESTIMATE OF S2

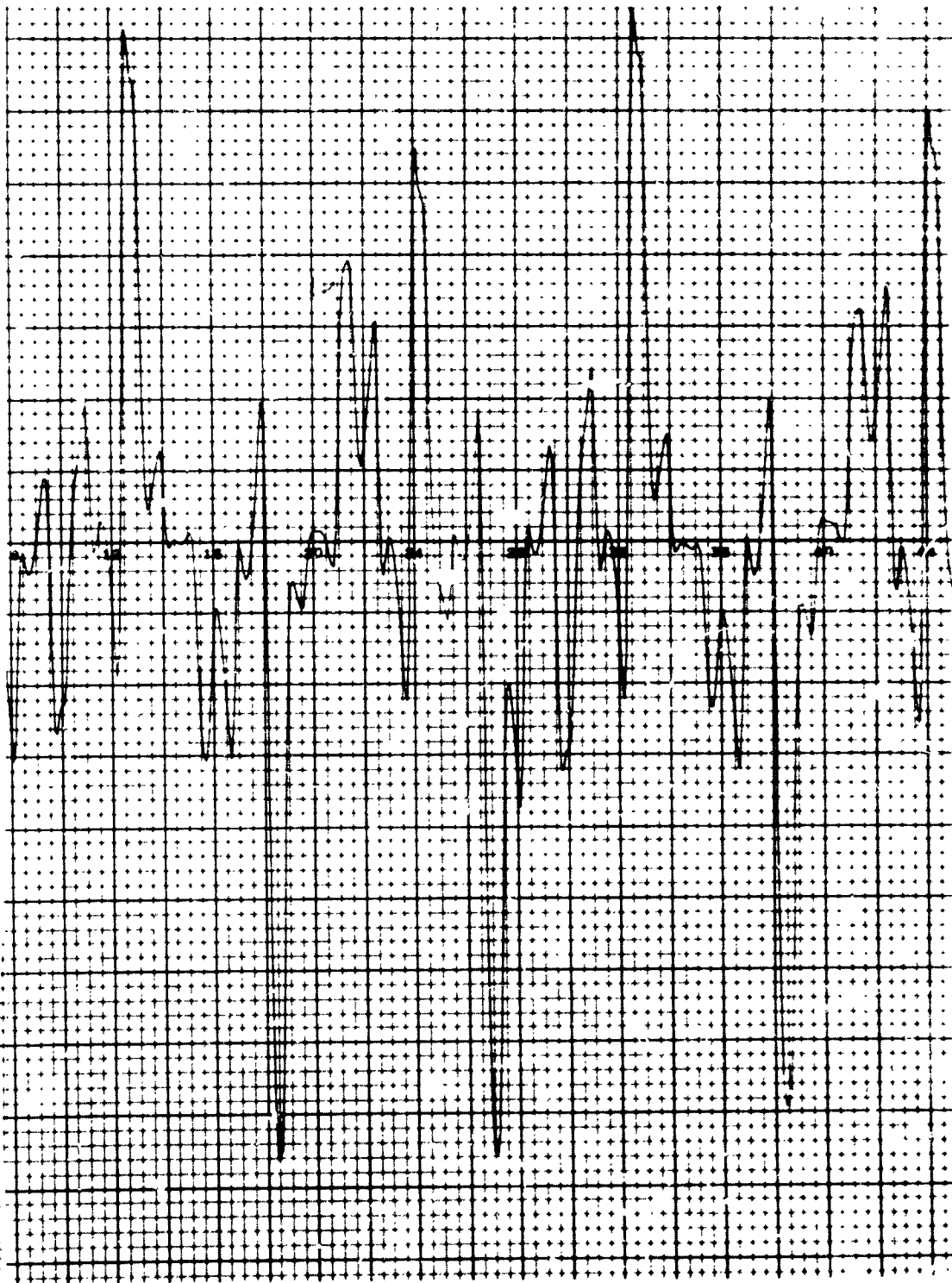


ude, and No 3rd Bending Mode in Plant

169-4

TIMING FOR 6-TH ORDER PLANT (8)

CASE 2



TIME IN SEC.

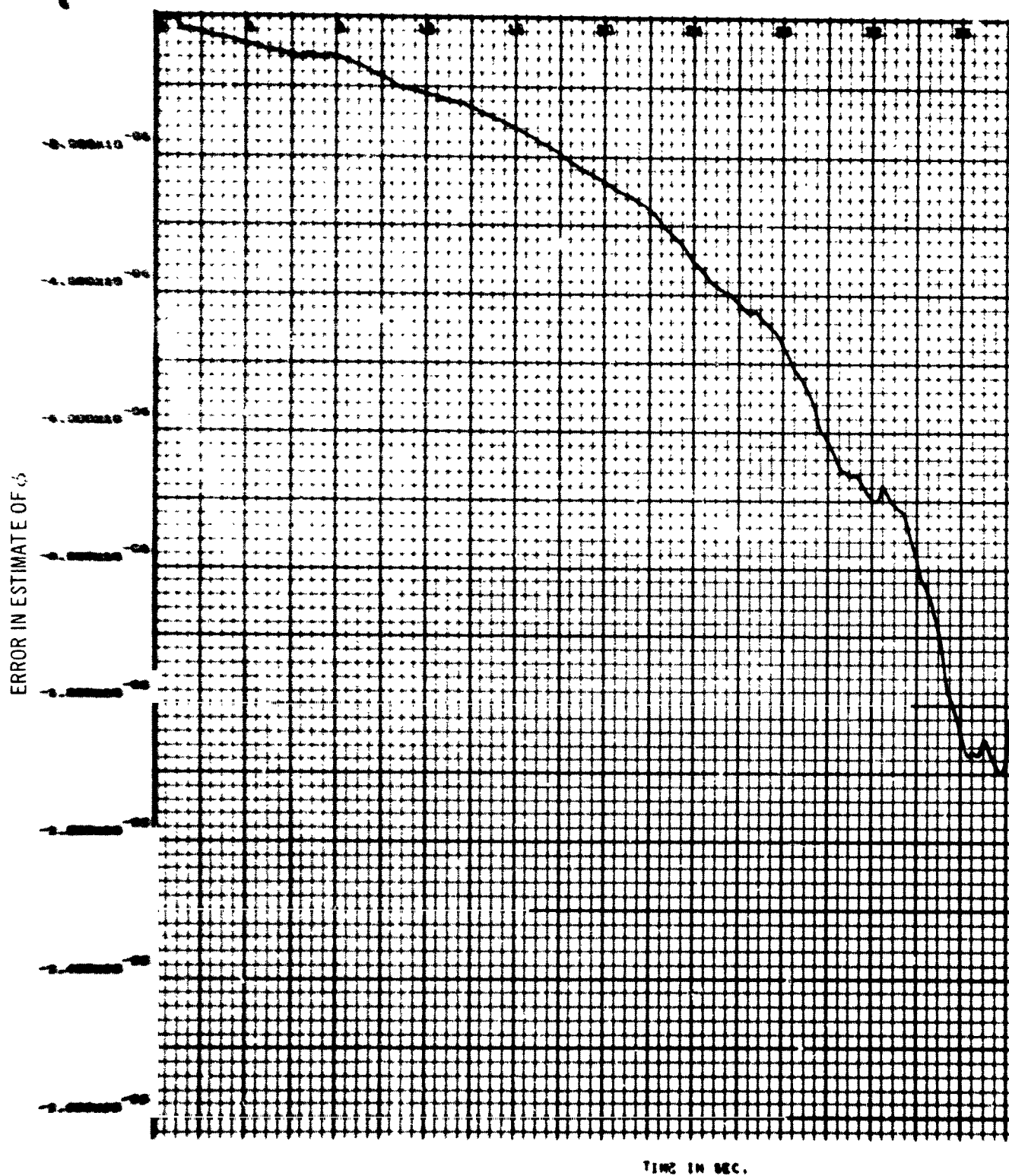
Subsequent runs were made with all entries of Q_a except Q55 and Q66 set equal to zero. This corresponds to the case of measurement error being attributed entirely to the parameter errors. Simulations were made for the following cases:

1. With and without the third bending mode.
2. Mismatched initial value for S1 estimate, S1 varying sinusoidally with an amplitude of 10% of its nominal value and a 30-sec period, and S1 remaining constant with its estimate set initially to that value.

When there was no third bending, the errors in the estimates of states were negligible, as shown in Figure 6-9. When the initial value of S1 was mismatched by 10% (Figure 6-10), the error in ϕ and η_1 remained small and the error in S1 decreased to 1% in 3.5 sec. The error in S2 remained negligible. The addition of the sinusoidally varying S1 resulted in its estimate varying sinusoidally with a small time lag (corresponding to 35 to 45 degrees). It was interesting to note that, in this latter case, the estimate of S1 had a carrier-type frequency superimposed on it which was at 2.2 rad/sec. It was concluded that the 2.2 rad/sec is caused by the beat frequency between the two input dither signals, which are 3.3 and 1.1 rad/sec.

The addition of third bending resulted in large initial transients in the estimate of S1. The transients were reduced to less than 3% after 13 sec. The error in the estimate of S2 was similar. However, the state estimates were kept to within a 2% error. Mismatching the initial condition on the estimate of S1 by 10% and 50% gave essentially the same results. It is concluded that initial parameter mismatches are no problem. Also, it is expected that these initial transients can be reduced by decreasing the values of Q55 and Q66. They can subsequently be increased to improve the parameter estimation sensitivity.

A simulation was made without the computer card which generated η_1 , and the result, shown in Figure 6-11, was that the estimate of S2 was approximately zero. This is exactly what one would expect in such a case, because S2 is proportional to the gain in the first bending mode, and if there is no bending mode, that gain is zero.



105-1

1

NOISE ESTIMATION FOR 4TH ORDER PLANT (14)

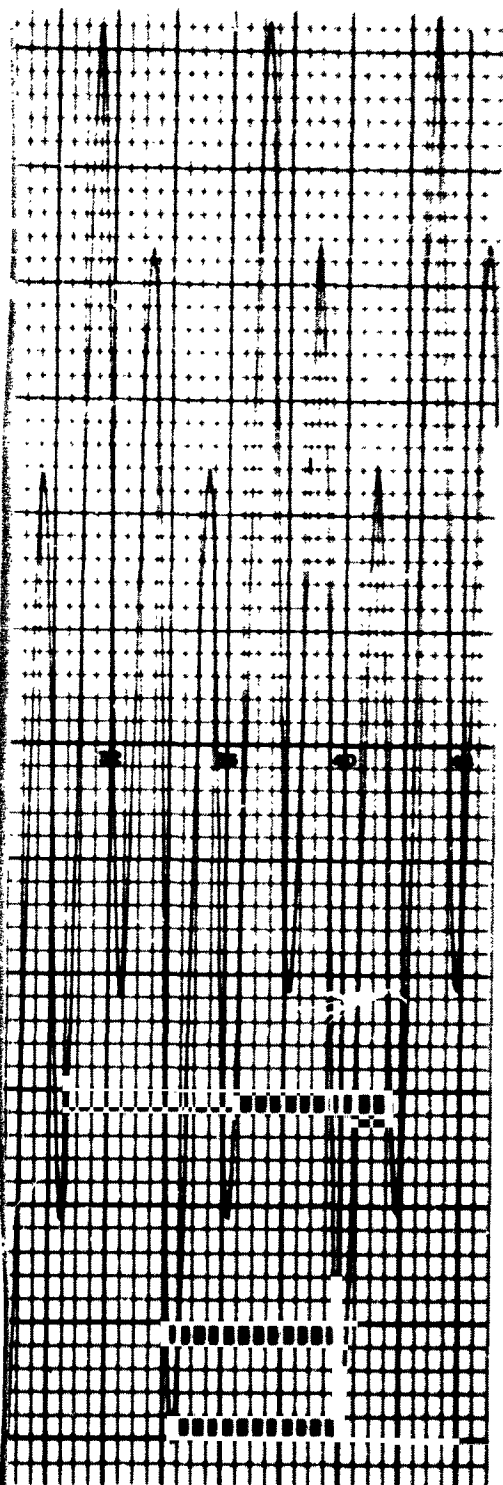


Figure 6-9. $Q55 = 5 \times 10^7$

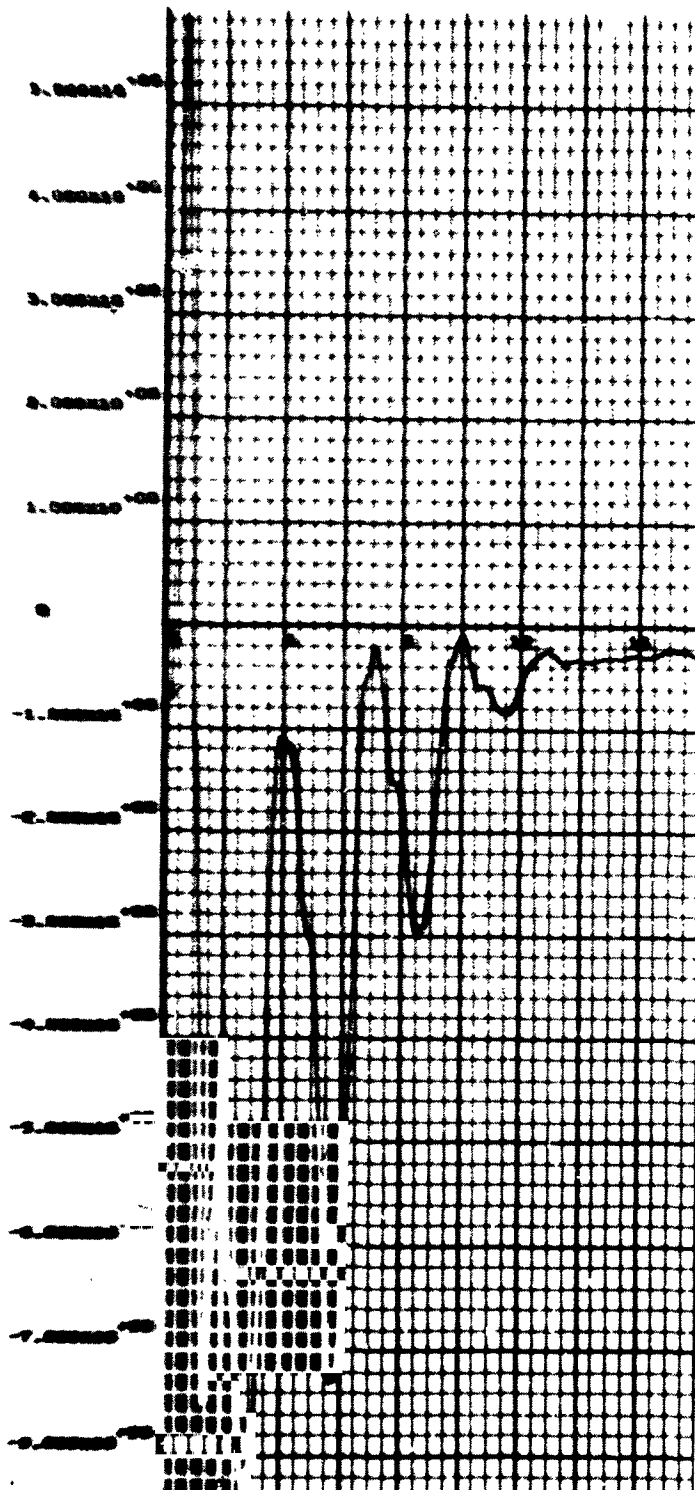
165-2

CASE 1

COMBINED ESTIMATION FOR 6-TH ORDER



ERROR IN ESTIMATE OF S1



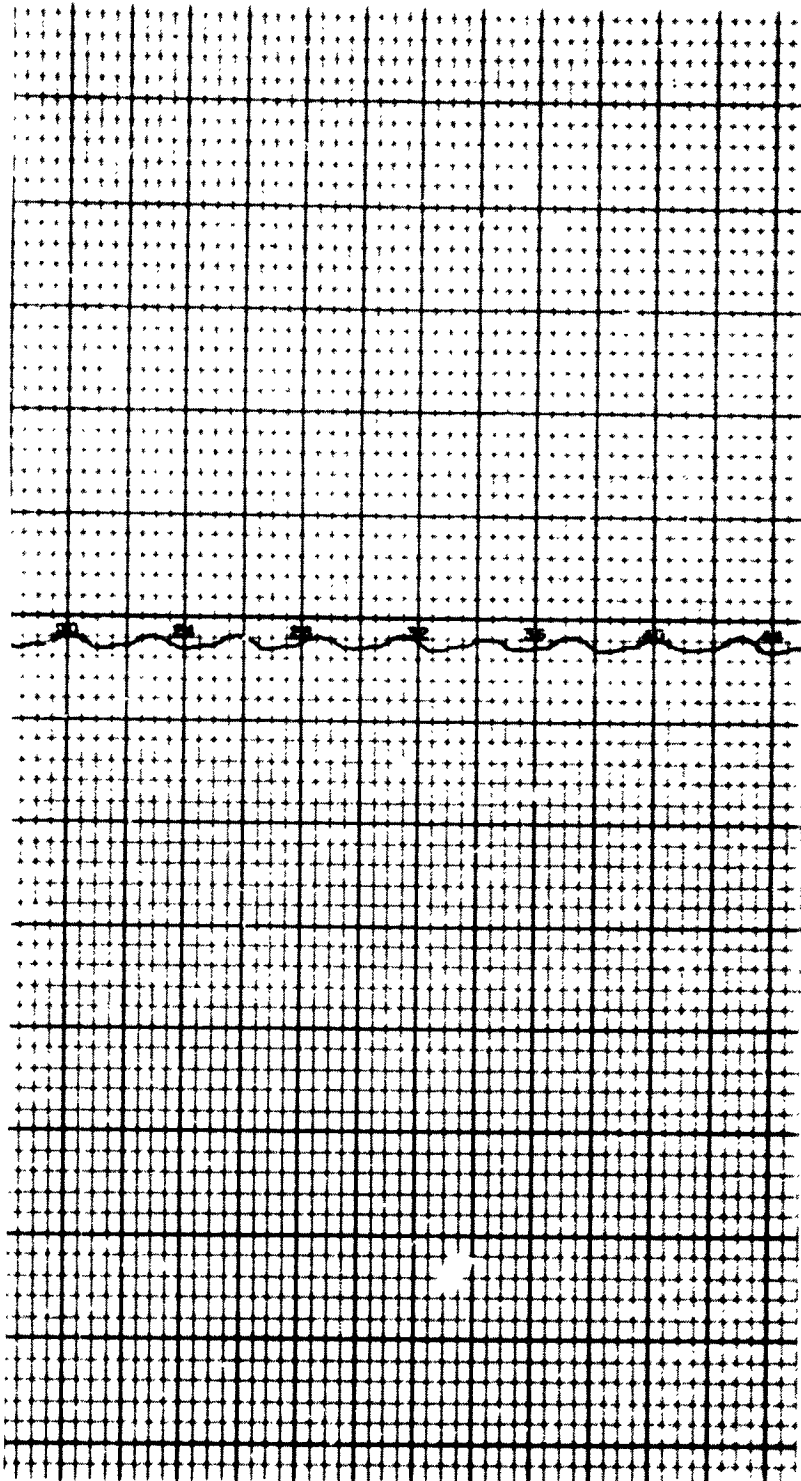
$Q_{66} = 4 \times 10^6$, all other Entries of Q_a are Zero, $R = 10^{-3}$ S1 Constant, no. 3rd Bending Mode

165-3

PLANT (4)

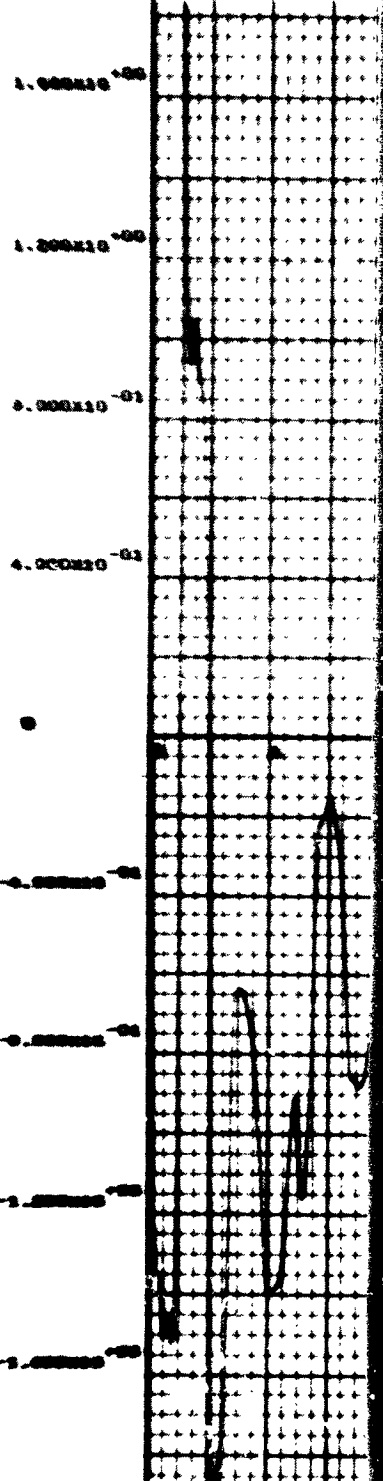
CASE 1

COMBINED



TIME IN SEC.

ERROR IN ESTIMATE OF S2



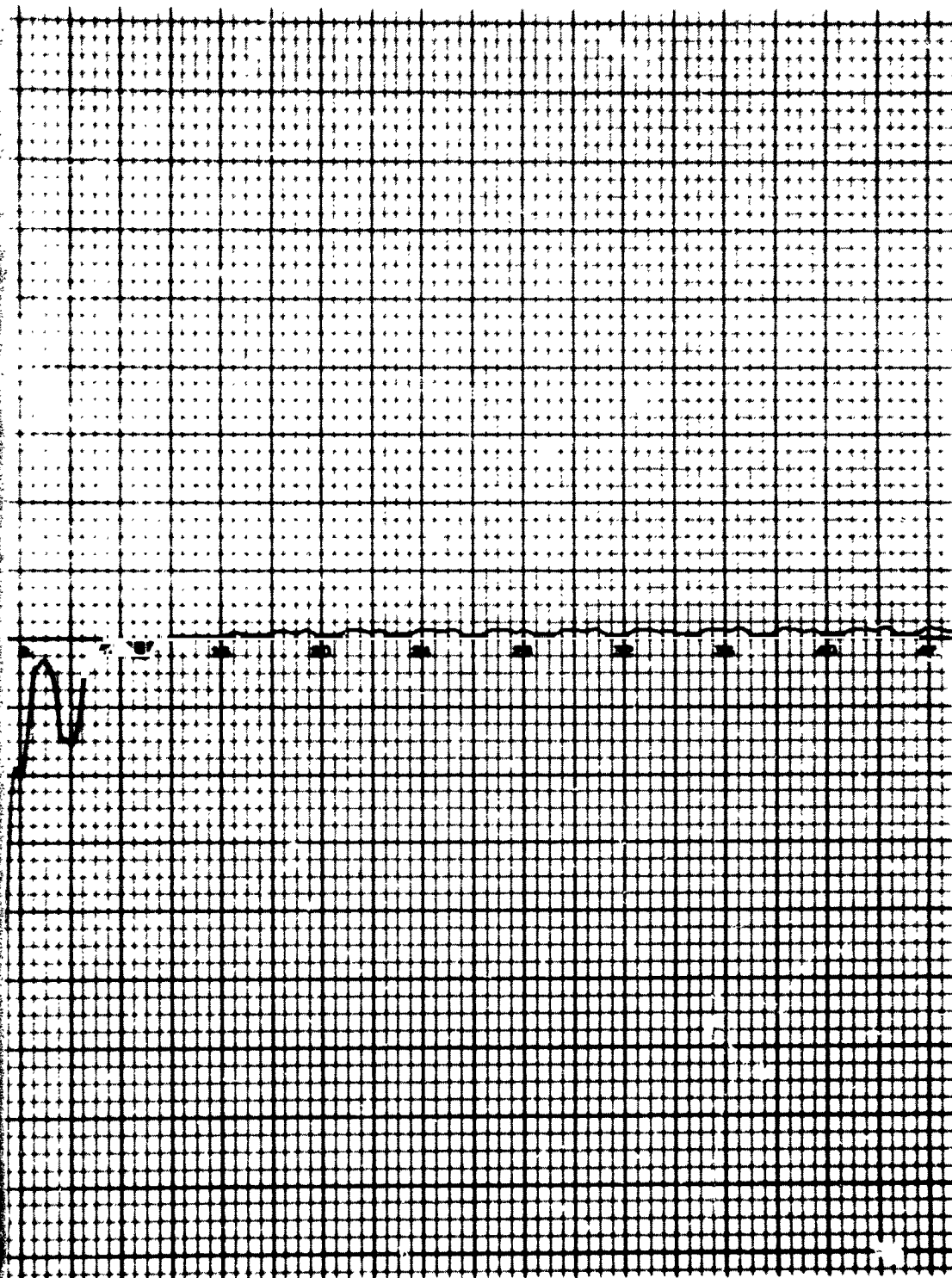
in Plant

165-4

STINA CON FOR 5 TH ORDER PLANT (12)

CASE 1

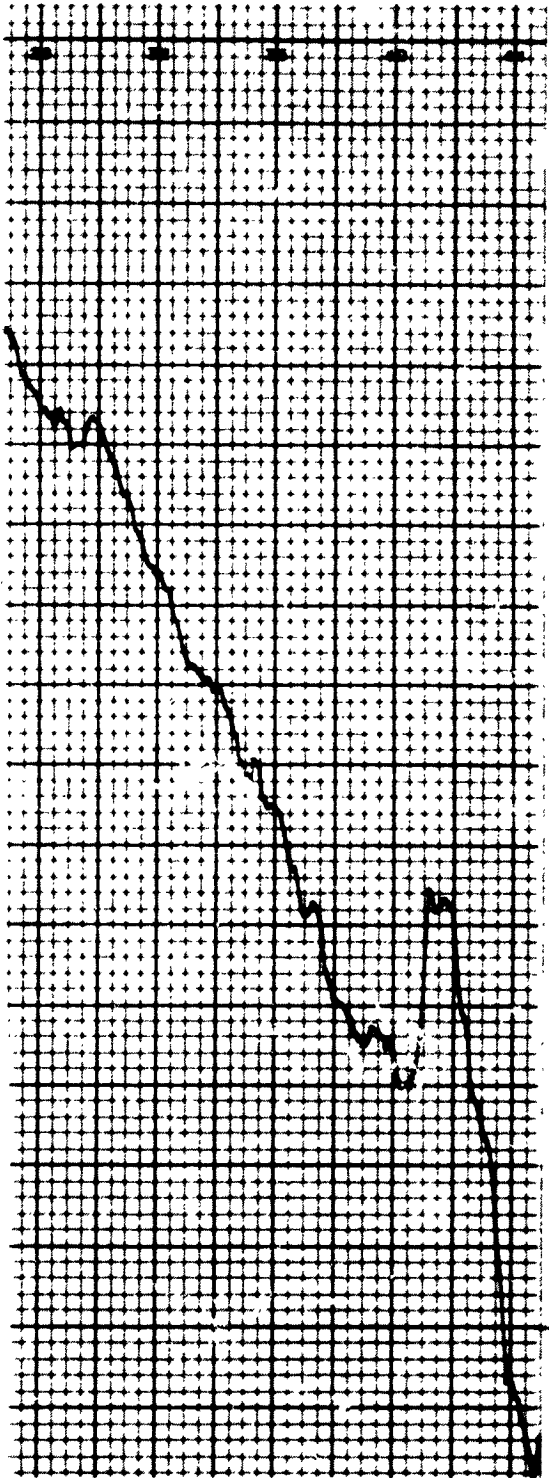
U



TIME IN SEC.

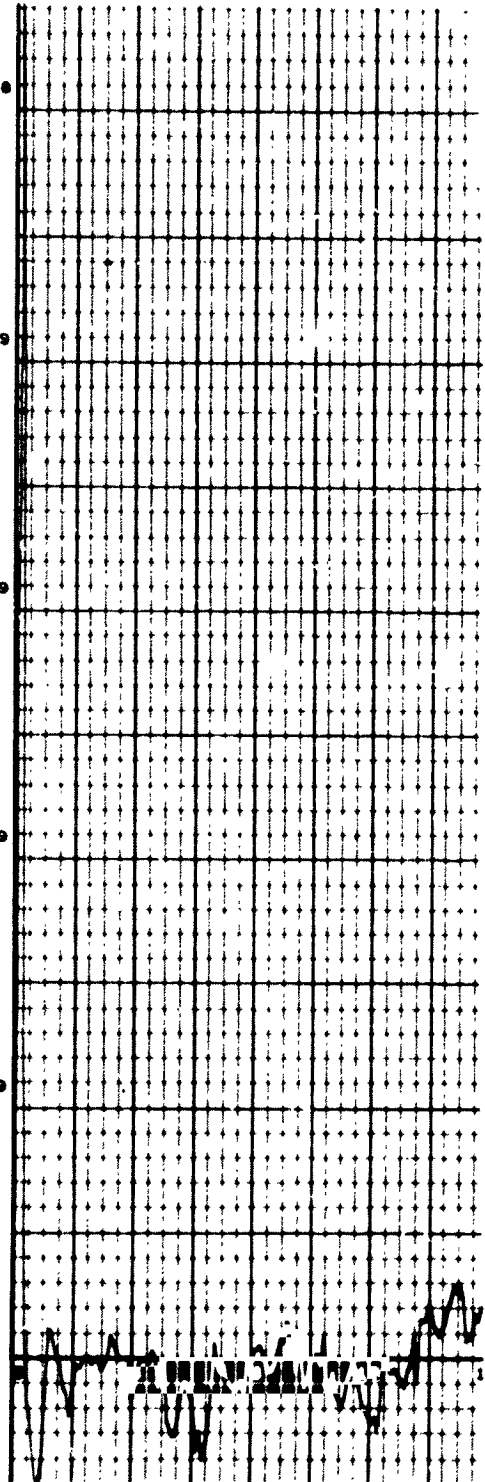
456 1

THE NO. 1 ST. NAT. W. F. 1 - 1

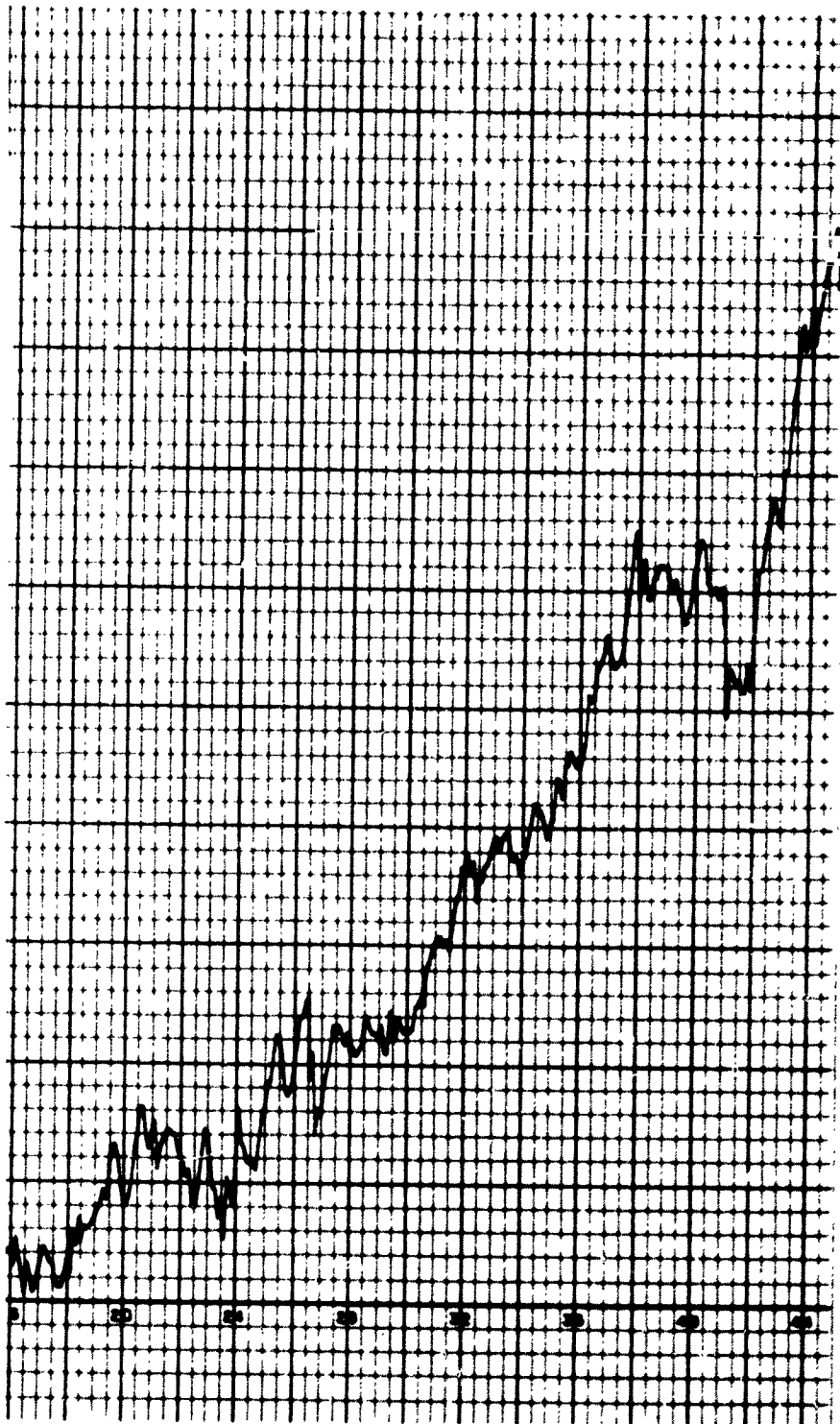


ERROR IN ESTIMATE OF δ_1

1.000x10⁻⁰⁸
8.000x10⁻⁰⁹
6.000x10⁻⁰⁹
4.000x10⁻⁰⁹
2.000x10⁻⁰⁹



166-2



ERROR IN ESTIMATE OF S1

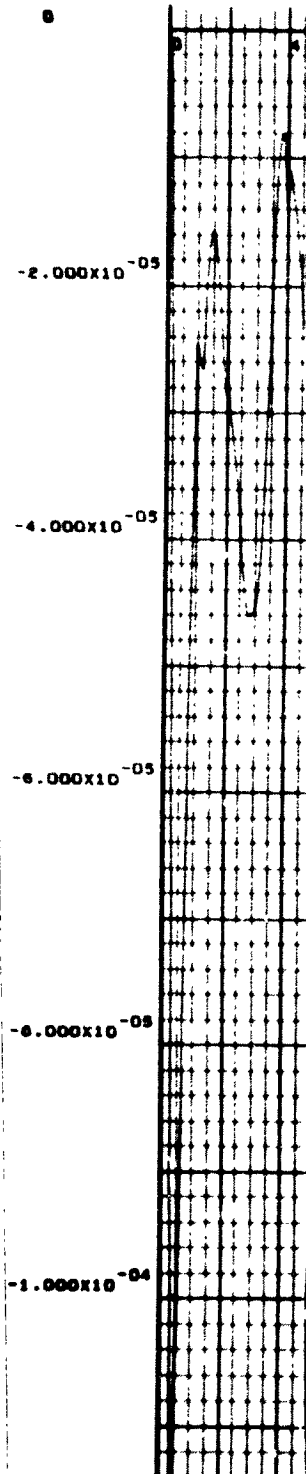
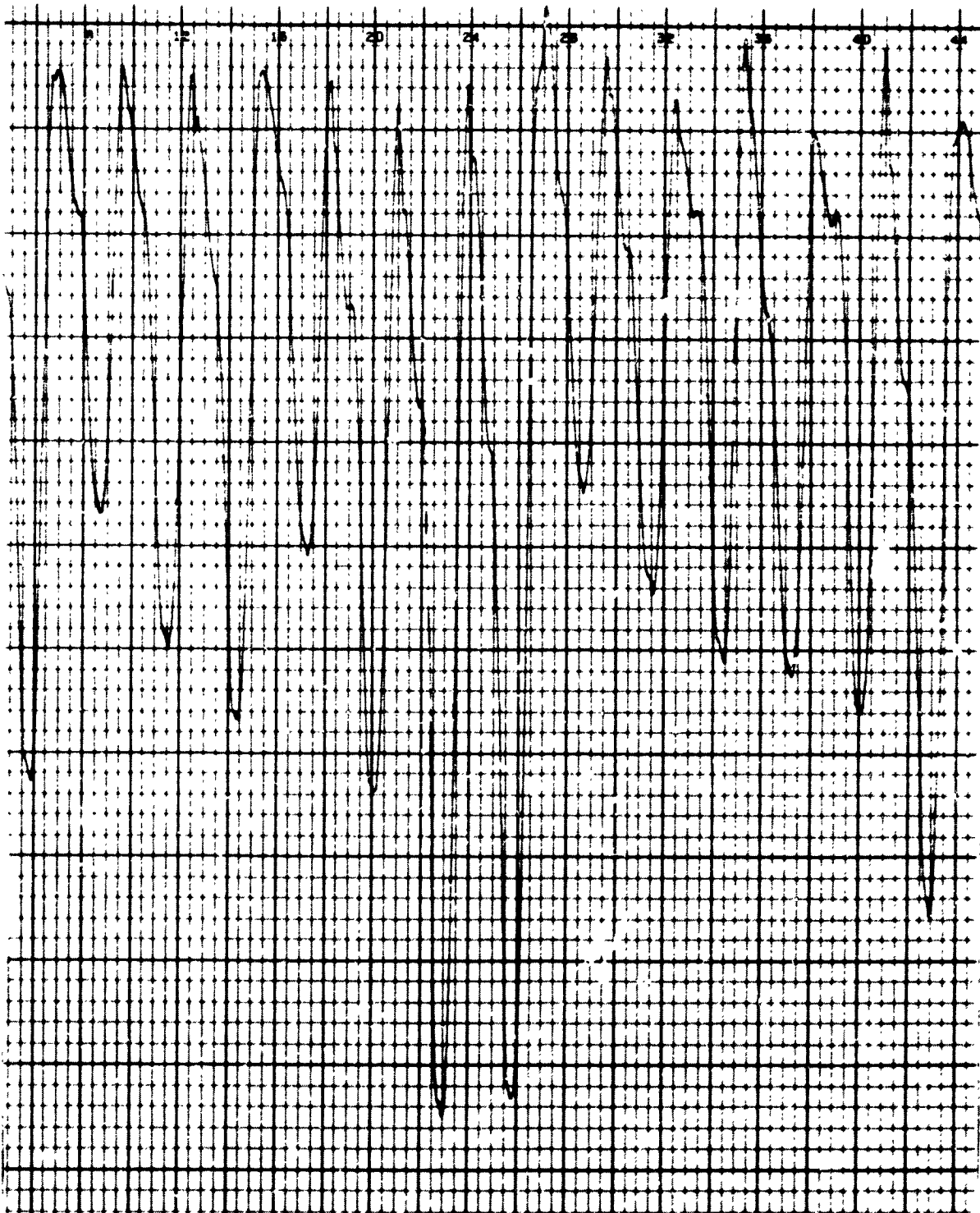


Figure 6-10. $Q_{55} = 5 \times 10^7$ $Q_{66} = 4 \times 10^6$ All Other Entries of Q_a are Zero, $R = 10^{-3}$, Estimate of S1 is 90% \hat{S}_1 and no 3rd Bending Mode in Plant

STATE ESTIMATION OF A 10 ORDER PLANT (11)

Fig.



TIME IN SEC.

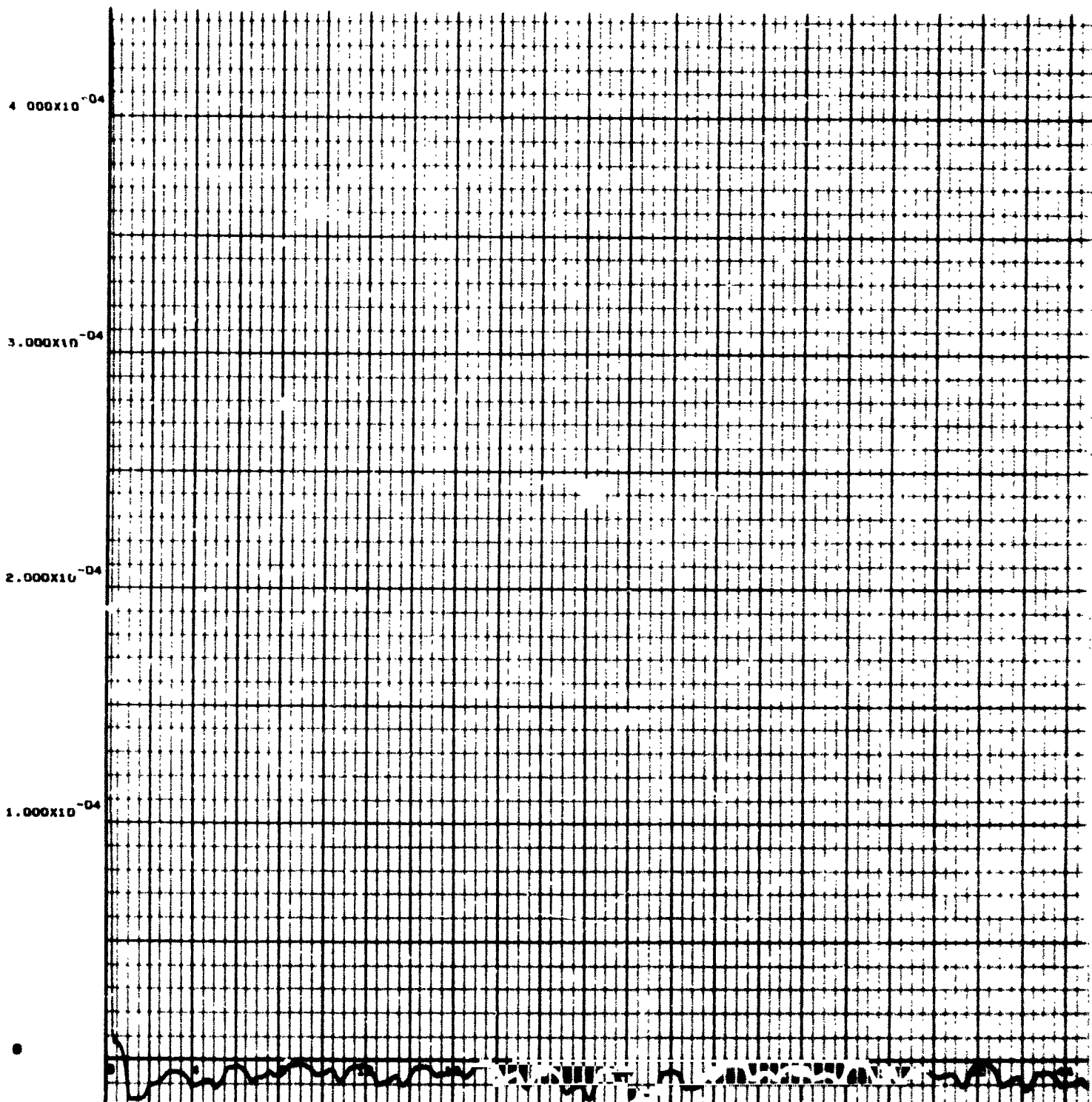
S1 Constant Initial Condition on

166-4

COMBINED ESTIMATE IN FLUX - IN LOWER PLANT

1.53

L



TIME IN SEC.

r

166-5

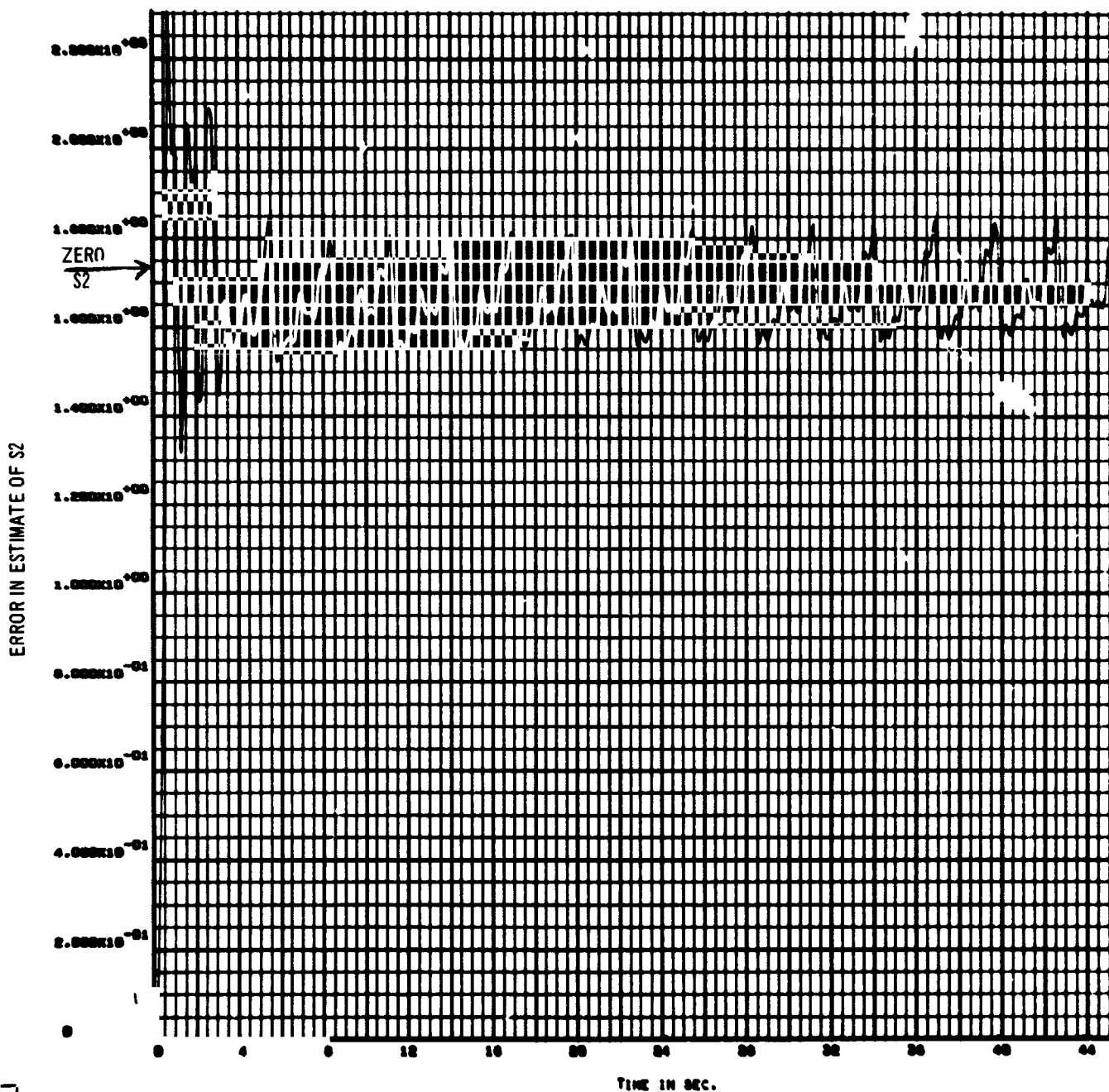


Figure 6-11. $Q_{55} = 5 \times 10^7$, $Q_{66} = 4 \times 10^6$, All Other Entries of Q_a Are Zero, $R = 10^{-3}$, S_1 is 90% S_1 , and No 1st Bending Mode in Plant

BLANK PAGE

Section 7

COMPUTATIONAL PROBLEMS

The major difficulties encountered in performance of this study have been involved with computer operations. This chapter describes these difficulties and the methods developed to avoid them.

7.1 SOLUTION OF THE RICCATI EQUATION

This equation expressed in the general form

$$\dot{P} + PA + A^T P + PBP = C \quad (7-1)$$

appears in the solutions of quadratic optimal control gains, the Kalman filter gain matrix, and system covariance matrixes. P , A , G , and Q are $n \times n$ matrixes. The matrix P is positive-definite and symmetric. It can be seen by inspection that this equation is nonlinear.

The question can be raised as to how long a time must the transient solution be run before the equilibrium condition for P is reached. Potter (Reference 5) has shown that the Ricatti equation will be at least as well-damped as the original system with transfer matrix A .

7.1.1 Solution by Direct Integration

The most direct method of solution involves simple integration of Equation 7-1. This can be costly from a computing standpoint unless an integration scheme using a variable integration time is utilized. Another potential pitfall can occur if the transient solution of Equation 7-1 carries P to a nonpositive-definite condition. If this occurs, the equation may act in an unstable mode and diverge. This problem can be avoided by carefully picking $P_{(0)}$ or by utilizing a method suggested by Reference 17. The discrete version of Equation 7-1 is used. The recursion equations are set up to solve for \sqrt{P} and then this term is squared and positive definiteness is ensured for P , which ensures stable transient behavior.

7.1.2 Solution by Linear Substitution (ASP Program)

If two vectors, \underline{Y} and \underline{Z} , are defined such that

$$\begin{Bmatrix} \dot{\underline{Y}} \\ \dot{\underline{Z}} \end{Bmatrix} = \begin{bmatrix} A & B \\ C & -A' \end{bmatrix} \begin{Bmatrix} \underline{Y} \\ \underline{Z} \end{Bmatrix} \quad (7-2)$$

it can be shown by direct substitution into Equation 7-1 that

$$P = Z Y^{-1} \quad (7-3)$$

Equation 7-2 is linear and has a solution

$$\begin{aligned} \begin{Bmatrix} \underline{Y}(t+\tau) \\ \underline{Z}(t+\tau) \end{Bmatrix} &= e^{\begin{bmatrix} A & B \\ C & -A' \end{bmatrix} \tau} \begin{Bmatrix} \underline{Y}(t) \\ \underline{Z}(t) \end{Bmatrix} \\ &= \begin{bmatrix} \theta_{11} & \theta_{12} \\ \theta_{21} & \theta_{22} \end{bmatrix} \begin{Bmatrix} \underline{Y}(t) \\ \underline{Z}(t) \end{Bmatrix} \end{aligned} \quad (7-4)$$

Then, by substitution

$$P(t+\tau) = [\theta_{21} + \theta_{22} P(t)] [\theta_{11} + \theta_{12} P(t)]^{-1} \quad (7-5)$$

This is the method used by the ASP program for solving Riccati equations.
The matrix

$$e^{\begin{bmatrix} A & B \\ C & -A' \end{bmatrix} \tau} \triangleq e^{S\tau} \quad (7-6)$$

is solved by Taylor series expansion

$$e^{S\tau} = I + (S\tau) + \frac{(S\tau)^2}{2} + \dots \quad (7-7)$$

The ASP program uses the first 36 terms of this series. In order to calculate e^{ST} to n -digit accuracy, the criterion¹⁰⁰

$$\frac{(\|S\| \tau)^{36}}{(36)!} < 10^{-n} \quad (7-8)$$

should be satisfied, where $\|S\|$ is the largest term in the S matrix. Typically, one needs four-place accuracy. In this case, Equation 7-8 yields the criterion

$$\tau < \frac{10}{\|S\|} \quad (7-8a)$$

for the computing interval.

The setting of τ may satisfy Equation 7-8a for proper series convergence but may encounter computer overflow problems ($|S_{ij} \tau| > 10^{38}$) which might make a usable τ prohibitively short. This problem can be alleviated by proper balancing of the terms in the S matrix. The terms can be adjusted by using the facts that the optimal control is only dependent on the ratios between the costs and that the Kalman filtering is only dependent on the ratio between the disturbance and noise covariance matrixes. The absolute values of the cost matrixes or covariance matrixes can therefore be scaled larger or smaller to minimize the larger terms in S .

Once a satisfactorily small τ is chosen and Equation 7-6 is computed, the solution for larger values of τ can be computed using the identity

$$e^{S(N\tau)} = (e^{S\tau})^N \quad (7-9)$$

which can be costly from a computing standpoint and is subject to round-off error. Both these problems can be reduced by using the recursion routine

$$Q_{(K+1)} = Q_{(K)} Q_{(K)} \quad (7-10)$$

where

$$Q_{(1)} = e^{S\tau}$$

until 2^K is in the neighborhood of N .

The ASP program has several drawbacks that reduce its effectiveness. These are

1. Poor program documentation.
2. No reference-case setup.
3. Machine language coding.

To eliminate these drawbacks, the method of solution was coded as a FORTRAN IV subroutine. (This subroutine is presented in Appendix A.)

7.1.3 Solution by the Newton-Raphson Method

For most of the studies made, only the steady-state solution of Riccati equations are of interest; Equation 7-1 can therefore be reduced to the algebraic equation

$$0 = -PA - A'P + PBP + C \quad (7-11)$$

or

$$0 = f(P) \quad (7-12)$$

equations of this type can often be solved for by the recursion relationship

$$P_{(K)} = P_{(K-1)} - J_{(K-1)}^{-1} f(P_{K-1}) \quad (7-13)$$

where

$$J_{ijmn} = \frac{\partial f_{ij}}{\partial P_{mn}}$$

Bellman and Kalaba (Reference 18) show that this equation will be rapidly (quadratically) convergent to the solution if it is convergent at all.

The Jacobian has a general solution which can be derived in the following manner; the coefficients of $f(P)$ have the general form

$$f_{ij} = -\sum_K P_{iK} A_{Kj} - \sum_K A_{Ki} P_{jK} + \sum_L \sum_K P_{jL} P_{iK} B_{KL} + C_{ij} \quad (7-14)$$

the general partial derivative can be written

$$\begin{aligned} \frac{\partial f_{ij}}{\partial P_{mn}} &= -\frac{\partial}{\partial P_{mn}} \left(\sum_K P_{iK} A_{Kj} \right) - \frac{\partial}{\partial P_{mn}} \left(\sum_K P_{jK} A_{Ki} \right) \\ &+ \sum_L P_{jL} \frac{\partial}{\partial P_{mn}} (P_{iK} B_{KL}) \\ &+ \sum_K P_{iK} \frac{\partial}{\partial P_{mn}} \left(\sum_L P_{jL} B_{KL} \right) \end{aligned} \quad (7-15)$$

which has the following solutions

$$\frac{\partial f_{ij}}{\partial P_{Mn}} = 0$$

$$\frac{\partial f_{ij}}{\partial P_{mn}} = -A_{nj} + \sum_K P_{jK} B_{nK}, \quad i = m, \quad j \neq m$$

$$\frac{\partial f_{ij}}{\partial P_{mn}} = -A_{ni} + \sum_K P_{iK} B_{Kn}, \quad i \neq m, \quad j = m$$

$$\frac{\partial f_{ij}}{\partial P_{mn}} = -A_{ni} - A_{nj} + \sum_K (P_{iK} B_{Kn} + P_{jK} G_{nK}) \quad , \quad i, j = m$$

Since P is symmetric, it is likely that linear dependence would occur in Equation 7-13. To avoid this and to save computer space, P is rearranged from an $[N \times N]$ matrix to an $[n] [N + 1]/2$ - order vector in the computer subroutine developed. All the terms below the major diagonal in the P matrix and the corresponding terms in the Jacobian are discarded in this process. The FORTRAN IV subroutine developed which use the matrixes A , B , C and P_0 to solve Equation 7-11 is presented in Appendix A. The system order (N) is limited to about 15 if used with an IBM (7094) computer with a 32,000-word memory book. This is due to the Jacobian (J) which takes $[N(N+1)/2]^2$ storage spaces.

From a practical standpoint, this routine has not proved to be very useful; it worked successfully with a 2-dimensional test case and converged very rapidly, achieving 5-digit accuracy in 6 iterations of Equation 7-13. The solution of Kalman gains for System 4-2 was then attempted. In this case the method failed because the Jacobian (J) was too empty to have an inverse. When a second sensor, a rate gyro, was included, the Jacobian had an inverse but the method failed to iterate to a steady-state solution in all the attempts made. Apparently the method is convergent only in a very small neighborhood in P space.

7.2 SYSTEM POLE-ZERO SOLUTION

A basic method of system evaluation during this study has been based on system transfer function pole-zero evaluation. Considerable difficulty was encountered in calculating these roots from state equations. This subsection describes the computational methods investigated and the resulting performance achieved with each.

Conventionally, the transfer function of a system is expressed

$$\frac{y}{u} = \frac{K(S + Z_1)(S + Z_2) \dots}{(S + P_1)(S + P_2)(S + P_u) \dots} \quad (7-16)$$

where

- u = scalar input function
- y = scalar output function
- K = transfer function gain
- Z_i = i^{th} transfer function zero
- P_i = i^{th} transfer function pole
- S = Laplace operator

This transfer function can also be expressed in the state-space form

$$\dot{\underline{x}} = A \underline{x} + Bu \quad (7-17)$$

$$y = c \underline{x} \quad (7-18)$$

where

- \underline{x} = the N-dimensional state vector
- A = NXN transfer matrix
- B = an NX1 column-matrix
- C = A 1XN row-matrix
- U = scalar driving function
- y = scalar output function

The system has generally been expressed in the state-space form of Equations 7-17 and 7-18 during the study. Since the transfer function is defined in either way, it follows that the desired roots in Equation 7-16 can be determined from the matrixes A, B, and C.

7.2.1 Recursion Equation Solution

This method, presented by Zadeh and Desoer (Reference 13) is by far the simplest method of root determination. The transfer equation polynomial is found by the following recursion equations

$$Q_1 = I \quad (7-19)$$

$$b_n = \frac{1}{n} \text{tr} [AQ_n] \quad n = 1, 2 \dots K \quad (7-20)$$

$$Q_{n+1} = AQ_n + b_n I \quad n = 1, 2 \dots K-1 \quad (7-21)$$

$$Q_{K+1} = 0, \text{ a check} \quad (7-22)$$

The final transfer function Equation 7-16 is

$$\frac{y}{u} = \frac{CQ_1 B S^{k-1} + CQ_2 B S^{k-2} + \dots + CQ_K B}{S^k + b_1 S^{k-1} + \dots + b_K} \quad (7-23)$$

The polynomials can be factored by Lin's method to obtain the poles and zeros. The subroutine utilizing this method called TRAFN, (Transfer Function) is presented in Appendix A. It is coded in double precision. It was found that three-digit accuracy cannot be achieved in the roots derived for systems above eighth-order and therefore this subroutine was of very little value for this study.

7.2.2 Solution by Eigenvalues

If one takes the Laplace transform of Equation 7-17, one gets

$$\underline{x} S = \underline{A} \underline{x} + \underline{B} u(s) \quad (7-24)$$

collecting terms

$$[I_s - A] \underline{x} = + B u(s) \quad (7-25)$$

and solving for \underline{x}

$$\underline{x} = + [I_s - A]^{-1} B u \quad (7-26)$$

and

$$y = C_{adj} \frac{[I_s - A]^1}{[I_s - A]} B u \quad (7-27)$$

it is clear that the denominator of Equation 7-16 must be the solution to the determinant $|I_s - A|$, but the roots of the polynomial $|I_s - A|$ are the eigenvalues of A. Often there are more eigenvalues in $|I_s - A|$ than there are poles in Equation 7-16. In this event, there will be roots present in $C_{adj}|I_s - A|^1 B$ which will cancel these extraneous eigenvalues.

The solution of the eigenvalues of a matrix is a general problem treated in the literature. The following methods were evaluated for use:

1. Power Method (Reference 19) -- For 26-order problems studied, this method converged to eigenvalues for about 60% of the cases run. It finds the larger roots accurately but gets no significant digit accuracy with small roots around the origin.
2. Danielewsky's Transformation (Reference 20) with Lin Root Finder (Reference 21) -- Three-digit accuracy has been achieved with the 26-order check matrixes evaluated. This approach has proved to be the most accurate approach tried. However, the Lin root finder has failed in approximately 15% of the cases attempted.
3. Hessenburg Transformation with Q-R Transform Root Finder (Reference 22) -- This method has worked on all cases tested but has not been used to any extent because of its late discovery.

Brockett (Reference 23) presents an inverse matrix; the eigenvalues contain the zeros of Equation 7-16. This inverse matrix is

$$\left[A - \frac{1}{k} B C A^\alpha \right] \quad (7-28)$$

where

$$k = C A^{\alpha-1} B \quad (7-29)$$

and

k = transfer function gain in Equation 7-16.

α = difference between the number of transfer function poles and zeros. Thus must be at least plus 1.

Brockett does not suggest a method of determining α , but it can be found by hunting on the value $C A^j B$, which will be zero until

$$j = \alpha - 1 \quad (7-30)$$

The zeros of the transfer function Equation 7-16 are found by determining the eigenvalues of Equation 7-28 in the same ways as described for pole determination. Normally, there will be fewer zeros than poles, and since Equation 7-28 is of the same dimension as A , there will be a surplus of eigenvalues in the zero determination. In theory, this surplus will consist of a multiplicity of eigenvalues at the origin. In practice, because of round-off errors, this multiplicity will consist of small roots clustered around the origin. It is occasionally very difficult to discriminate these roots from valid low-frequency roots. In most cases the errors in these low-frequency roots have led to very inaccurate steady-state solutions when transient response runs have been generated from the computed transfer functions.

The above equations for finding the inverse system matrix have been coded in a subroutine, ZEROS, presented in Appendix A. The addition operations are performed in double precision to reduce round-off error.

Section 8

CONCLUSIONS

This section relates the work accomplished in relation to the design philosophy underlying the study. The observations are based to a large extent on the experiences of the past contract year.

8.1 DESIGN REQUIREMENTS

What are the basic requirements on the control system for a flexible launch vehicle? The control system must control so that the vehicle is suitably responsive to commands, suitably responsive to winds, and stable. It should be as simple in concept and mechanization as is compatible with the performance requirements.

A system was developed which has a control natural frequency that is half of the first bending natural frequency. The first bending mode is controlled to a critical damping ratio of 0.3. The system appears to recover acceptably from the upsetting influence of a sudden wind force. The system is stable and shows tolerance to variation in plant parameters. The entire mission has not been thoroughly analyzed, but it appears that similar statements will hold true throughout the mission.

It appears plausible at this time that a system can be mechanized with a limited number of gain changes as a function of time, and that parameter identification may be unnecessary. This being granted, the system mechanization is little different from traditional designs. Only the linear ordinary differential equations (usually mechanized as passive networks) relating transducer response to control commands are different.

The location of sensors has not been stressed in this study because the method is relatively insensitive to the location chosen.

The added function of parameter identification will probably be needed only to attain either additional responsiveness or adaptivity (i. e. , very tight control of loads and wind response and/or tolerance to exceptionally large parameter uncertainties).

8.2 RESPONSE TO COMMANDS

The control commands on a large vehicle may be programmed or may be dynamic in the sense that the missile is continually guided to a path suitable for the solution of the mission problem. In either event, the control system should minimize the dynamic error from the intended path, as prescribed by the commands, without introducing excessive loads on the vehicle. Because of mission and guidance system requirements, there is some acceptable maximum response time. One of the basic problems in design of a control system for the flexible launch vehicle is to provide for adequate speed of response to commands without designing a system very susceptible to sloshing and bending.

No difficulty has been encountered in specifying the rigid body and first-mode response. Higher modes could be controlled if desired. There is some limitation on root location when several modes are to be controlled, but this has not been a serious problem. Sloshing has not been a problem. Second and higher bending modes have been gain-stabilized (their contribution has been removed from the feedback to the control).

8.3 RESPONSE TO WINDS

The control system must also provide for the vehicle to be suitably unresponsive to winds, particularly the jetstream or windshear through which the missile must move. The response of the missile as it proceeds through windshear is a highly dynamic problem and results in three phenomena which can be quite detrimental. First, the relatively steady components of the wind cause the vehicle to drift away from the desired trajectory unless the control system is specifically designed to prevent the effect. Second, the dynamic changes in wind velocity tend to cause the missile to develop angle of attack. This can produce loads in excess of the structural capability of

the airframe. Third, the engine may be driven against the deflection limit, with ensuing loss of control. Therefore, design of the control system must consider the dynamic response of the vehicle to wind; the design must minimize the structural loading encountered during a traverse of the jetstream.

A minimum of effort was applied explicitly to this problem, because this study related only secondarily to loads. However, attention was given this problem by choosing, from filters which provided acceptable stability, the one which gave the minimum dynamic attitude excursion when driven by a step wind.

The trajectory response to wind, the loads developed in a shear, and the control system sensitivity to parameter variations are very closely related. It appears that improving system design can reduce loads until parameter sensitivity and/or complexity pinch too much. Much work remains in this area, particularly if the contribution of the bending mode deflection to load are to be considered. The theory is available for a more systematic approach and future work should move in this direction.

8.4 STABILITY

It is important that the control system provide for suitable response to commands and to wind disturbances, but it is mandatory that the control system be stable. The control system design needs to be stable for the nominal parameters assigned in the analysis and synthesis process and because of the uncertainty of the parameters encountered in the actual flight environment. It can be extremely expensive (if not impossible) to measure all these parameters before firing the vehicle.

By the theorem of Section 5, the optimal control and optimal filter problem are separable. Thus, if optimal control is specified by performance criteria, the stability is determined by the filter. The stability of roots whose location is specified by the optimal control has not been a problem, since they have been set well into the left half plane. The stability of the remaining roots and their sensitivity to parameter variations are highly dependent on the filter design. The usual modes for their stabilization

appear. They can be phase-stabilized (controlled) by moving them into the group of controlled roots, or they can be gain-stabilized by the methods discussed in subsection 5.4. This effort has been successful in producing stability on all the roots, and considerable tolerance to parameter variation has been shown. However, a systematic way of choosing the best suboptimal filter technique for the least sensitivity is still to be developed.

8.5 SIMPLICITY

The requirement for the control system to be simple, usually thought to be equivalent to reliable, tends to mitigate against what has been called the adaptive control system. While common sense may indicate that adaptivity is undesirable, because of its tendency to increase complexity, it may in fact be necessary to achieve a proper balance among the requirements of response to commands, response to wind, and stability.

As stated earlier, without parameter estimation, the system mechanization is comparable to that of more conventionally designed systems. With parameter identification, necessary only if demanded by wind-induced effects or excessive parameter uncertainty, the present technique appears excessively complex. (The matrix Riccati equation must be solved in real time.) The technique presented here is considerably simplified from the underlying theory and it appears that further simplification (through approximation) is possible (and certainly desirable).

8.6 COMPLEXITY OF PLANT

The control system for a flexible launch vehicle must cope with extraordinary complexity. The concepts of body bending, actuator resonance, control surface or engine inertial coupling flutter, and sloshing are not foreign to the design of other aerospace vehicles. However, the importance of the coupling of these phenomena has never been so pronounced as in the flexible launch vehicle control system. It is this complexity that causes the traditional tools of control engineering, which have been quite adequate for low-order, lightly coupled systems, to be marginal or inadequate for the analysis and synthesis of control systems for the flexible launch vehicle.

Modern control theory has provided systematic technique and method for the synthesis of control systems of virtually unlimited complexity. Using these techniques and emphasizing quadratic optimal control, state estimation via Kalman-Bucy filter methods, and parameter estimation by closely related methods, a highly systematic approach can be developed to the synthesis of the flexible launch vehicle control system.

Considerable progress has been made in the development of tools for handling the required high-order matrix manipulations. It is clear that with these tools control systems can be designed which are well beyond the comprehension of the average designer using conventional techniques. While it is true that the resultant linear controls and filters can be reduced to scalar networks (one input, one output), it is virtually inconceivable that the same filter would be developed by an individual with even the keenest of intuitive insights.

8.7 INTEGRATION

The design process for integrating suboptimal control and state and parameter estimation is approximately as follows:

1. Prepare the system equations in state-space form.
2. Examine the open-loop roots and decide which ones must be altered. For example, the damping on one or several bending modes may be increased.
3. Approximate the high-order system by a low-order system containing only the states to be controlled.
4. Place costs on the states to be stabilized and on commands.
5. Determine roots and/or transient response as a function of the weights, choosing weights that produce a satisfactory system.
6. Prepare a Kalman filter to estimate all the states required for control. Represent the other states of the full dimensional systems as noise (using the methods of Section 5). Use several signal-to-noise ratios and generate several sets of the gains required in the filter.
7. Using the control and filters as developed above, evaluate system stability, transient response, and parameter sensitivity.
8. If the only systems giving satisfactory (usually fast enough) response are unstable in one or two state variables, decide to include these in the filter, and return to Step 6.

9. Repeat Steps 1 through 8 for sufficient flight environments to cover the mission. Determine the states which must be included in the filter to cover the mission.
10. Determine if a compromise set of Kalman gains (one filter) will be satisfactory or if switching or time-variable gains must be used.
11. If parameter sensitivity is not acceptable, determine if parameter estimation is required, what parameters must be identified, and design the parameter identifier.

Section 9

SYMBOLS

A	Reference area, in aerodynamic terms
A	Plant dynamical matrix
A_a	Augmented state dynamical matrix
\hat{A}_a	Estimate of A_a
A_a^+	Augmented state and control distribution matrix
A_{ij}	Submatrixes of A
A_{PR}	Plant dynamical matrix prior to simplifying manipulations
B	Plant control distribution matrix
B_a	Augmented state control distribution matrix
\hat{B}_a	Estimate of B_a
B_{BB}	Input multiplier to a body bending mode
B_i	Submatrixes of B
B_{PR}	Plant control distribution matrix prior to simplifying manipulations
B_{RB}	Input multiplier to a rigid body mode
C	Measurement matrix, eliminated in algebraic simplification
C	Frequently used scalar gain, often subscripted
C_1	Aerodynamic moment coefficient
C_2	Control moment coefficient

D	Sensor observation matrix ($D = H - CA$)
$E \left\{ \right\}$	Expected value of $\left\{ \right\}$, the statistical "expected value of" operator
ES1	Estimate of S1
ES2	Estimate of S2
F	Vehicle thrust force
F	A convenient matrix
G	Plant disturbance distribution matrix
G_i	Submatrixes of G
G_{PR}	Plant disturbance distribution matrix prior to simplifying transformation
H	Measurement matrix
H_a	Augmented measurement matrix
I_E	Moment of inertia of engine
K	Kalman gain matrix
K_a	Kalman gain matrix for augmented state estimate
K_{OPT}	Optimal control gain matrix
K_ϕ	Bending influence coefficient (effect in ϕ)
l	Moment arm
L_2	Cost on θ (rigid body attitude)
L_4	Cost on η_1 (body bending deflection)
L_6	Cost on η_2 (second bending mode deflection)
m	Vehicle mass
M	Observability matrix
N'	Aerodynamic force, normal to missile centerline

P	Riccati equation dependent variable matrix
P	Covariance matrix of error in estimation
P_a	Covariance matrix of error in estimation of augmented state vector
p_{ij}	Element of P_a in i th row and j th column
q	Dynamic pressure
Q	Covariance of disturbance vector
R	Covariance of noise vector
R'	Thrust of deflecting engines
s	Laplace transform variable
S_E	Engine inertia term
	$S_E = I_E m_E$
$S1$	Parameter to be estimated
	$S1 = -\omega_1^2$
$S2$	Parameter to be estimated
	$S2 = \frac{R'Y_1(x\beta)}{m_1} Y_1'(AG)$
t	Real time
T	Terminal time
\underline{u}	(or u) Plant control input vector
v	White noise vector with covariance $V\delta(t - \tau)$
V	Vehicle velocity m/sec
V_w	Velocity of wind
x	Vehicle station
\underline{x}	(or x) state vector

\underline{x}_a	Augmented state vector
\underline{x}_i	Subvector of \underline{x}
x_β	Vehicle station at engine hinge
X	Vehicle drag force
\overline{X}	Variable used to solve the matrix Riccati equation
Y	Noise-free sensor signals, usually subscripted RG, AG, or AC
\overline{Y}	Variable used to solve the matrix Riccati equation
$Y_{K(x)}$	Amplitude of Kth bending mode at station x
$Y'_{K(x)}$	Slope of Kth bending mode at station x
\underline{Z}	Noisy sensor signal, vector (also Z)
Z	Vehicle lateral displacement in reference coordinates
σ_w	Constant related to Markov wind
β	Engine deflection
δ_1	Scalar variable related to η_1 by
$\delta_1 = Y'_1(RG) \cdot \eta_1$	
Δ	Optimal control gain matrix (with subscript, appropriate element of Δ)
η_K	Generalized displacement in Kth bending mode
λ_1	Cost on terminal condition
λ_2	Cost on state deviation
λ_3	Cost on control
ξ	Critical damping ratio
ξ_-	System disturbance vector (white)

ξ_a	Augmented white noise disturbance vector
ξ_{BB}	Closed loop damping ratio for a body bending mode
ρ_j	$\rho_j = P_{2j} + P_{4j}$
τ	Sampling interval
τ	Miscellaneous time augment
ϕ	Vehicle angular displacement
$\phi_{(w)}$	Spectral density
ω	Frequency variable
ω_{BB}	Closed loop body bending mode bandwidth
ω_i	Natural frequency of ith bending mode
ω_{RB}	Closed loop rigid body bandwidth
ω_{sj}	Natural frequency of jth sloshing mode
$()^*$	Conjugate transpose
$()^{-1}$	Inverse of matrix ()
$(\underline{\quad})$	Signifies a vector
$()'$	Transpose of matrix ()
$(\hat{\quad})$	Least square estimate of ()
$(\tilde{\quad})$	An estimation error in ()
$()_{AG}$	Refers to attitude reference, also (AG)
$()_{AC}$	Refers to accelerometer, also (AC)
$()_E$	Relates to gimballed engine
$()_{RG}$	Refers to rate gyro, also (RG)
$()_{sj}$	Refers to jth sloshing mode

()_w Refers to wind inputs

⊙ Terms in a series in which are contained τ^n , $n > 1$

Section 10
REFERENCES

1. E. G. Rynaski et al. Design of Linear Flight Control Systems Using Optimal Control Theory. ASD-TDR-63-376, April 1964.
2. E. G. Rynaski and W. F. Whitbeck. The Theory and Application of Linear Control. AFFDL-TR-65-28, October 1965.
3. E. E. Fisher. An Application of the Quadratic Penalty Function Criterion to the Determination of a Linear Control for a Flexible Vehicle. AIAA Journal, Vol. 3, No. 7, July 1965.
4. P. R. Schultz. An Optimal Control Problem with State Vector Measurement Errors. A Chapter in Advances in Control Systems, edited by C. T. Leondes, Vol. 1, Academic Press, 1964.
5. J. E. Potter. A Guidance-Navigation Separation Theorem. AIAA Paper No. 64-653, August 1964.
6. T. L. Gunkel II and G. F. Franklin. A General Solution for Linear Sampled-Data Control. ASME, J. of Basic Engr., June 1964, pages 197-203.
7. P. D. Joseph and J. T. Tou. On Linear Control Theory. AIEE Paper No. 61-728, September 1961, pages 193-196.
8. R. E. Kalman and R. S. Bucy. New Results in Linear Filtering and Prediction. ASME Basic Engineering, Series D, March 1961.
9. K. S. P. Kumar. On Identification of Control Systems. AIAA, No. 10, October 1963.
10. R. E. Kalman et al. An Automatic Synthesis Program for Optimal Filters and Control Systems. RIAS Report, NASA CR 58829, 1964.
11. D. Garner. Control Theory Handbook. NASA TMX-53036, April 1964.
12. R. L. Bisplinghoff et al. Aerolelasticity, Addison Wesley Publishing Company, Inc., Reading, Massachusetts, 1955.
13. L. A. Zadeh and C. A. Desoer. Linear System Theory. McGraw-Hill Publishing Company, Inc., 1963.
14. R. Bellman, H. Kagiwada, and R. Kalaba. Quasi Linearization, System Identification and Prediction. Int. J. Engr. Sc., Vol. 3 pages 327-334, Pergamon Press, 1965.
15. R. C. K. Lee. Optimal Estimation, Identification, and Control. Research Monograph No. 28, Massachusetts Institute of Technology Press, Cambridge, Massachusetts.

16. F. H. Kishi. Control Systems Theory Applied to the Re-entry of Aerospace Vehicles - III. FDL-TDR-64-48, Part I, August 1964.
17. R. E. Kopp and R. J. Orford Linear Regression Applied to System Identification for Adaptive Control Systems. AIAA Journal, Vol. 1 No. 10, 1963.
18. R. E. Bellman and R. E. Kalaba. Quasilinearization and Nonlinear Two-Point Boundary Value Problems. American Elsevier Publishing Company, Inc., New York, 1965, pages 11-12.
19. J. H. Wilkenson. The Algebraic Eigenvalue Problem. Oxford University Press, London, 1965.
20. V. N. Fadecra. Computational Methods of Linear Algebra. Dover Publications, Inc., New York, 1959.
21. F. B. Hildebrand. Methods of Applied Mathematics. Prentice-Hall Inc., Second Edition, 1965.
22. B. N. Parlett. Eigenvalues of Real Matrices. Share Program NYME1G5.
23. R. W. Brockett. Poles, Zeros, and Feedback: State Space Interpretation. IEEE Trans. on Automatic Control, AC-10, No. 2

Appendix A
COMPUTER ROUTINES

BLANK PAGE

Appendix A COMPUTER ROUTINES

A. 1 SYSTEM REDUCTION TO STATE-SPACE FORM

Purpose

This Program presents launch vehicle dynamical equations in the form

$$\dot{\underline{x}} = \underline{A}\underline{x} + \underline{B}u \quad (A-1)$$

$$y = \underline{H}x \quad (A-2)$$

where A, B, and H are the program outputs. The vehicle model contains the following dynamic components:

1. Vehicle lateral velocity.
2. Rigid body angular displacement.
3. Three sloshing modes.
4. Four bending modes.
5. Third order engine-actuator subsystem.
6. First-order Markov wind generator

System Equations:

The basic system equations were furnished by Marshall Space Flight Center and are as follows

Translation

$$\ddot{Z} = -\frac{N'}{mV} \dot{Z} + \left(\frac{N'}{m} + \frac{F - X}{m} \right) \phi_R - \frac{1}{m} \sum m_{sj} \ddot{Z}_{sj} - \frac{F}{m} \sum_K Y_K (x_\beta)_{nk} \\ + \frac{R'}{m} \beta_R + \frac{N'}{mv} V_w \quad (A-3)$$

Rotation

$$\ddot{\phi}_R = -\frac{C_1}{V} \dot{Z} - C_1 \phi_R - \frac{C_1}{V} V_w - C_2 \beta_R \quad (A-4)$$

j^{th} Sloshing Mode

$$\begin{aligned} \ddot{Z}_{sj} = & \left(\frac{F - X}{m} \right) \phi_R - \omega_{sj}^2 Z_{sj} - \left(\frac{F - X}{m} \right) \sum_K Y'_K(X_{sj}) n_K - \ddot{Z} + l_{sj} \ddot{\phi}_R \\ & - \sum_K Y_K(X_{sj}) \ddot{n}_K \end{aligned} \quad (A-5)$$

i^{th} Bending Mode

$$\begin{aligned} \ddot{\eta}_i = & -\frac{G_i}{V} \dot{Z} + G_i \phi_R - \frac{1}{m_i} \left(\frac{F - X}{m} \right) \sum_j m_{sj} Y'_i(X_{sj}) Z_{sj} - \omega_i^2 \eta_i \\ & - \frac{R'_i}{m_i} Y_i(X_\beta) \sum_K Y'_K(X_\beta) n_K - 2\xi_i \omega_i \dot{\eta}_i + \frac{R'_i}{m_i} Y_i(X_\beta) \beta_R + \frac{G_i}{V} V_w \\ & + \frac{1}{m_i} [S_E Y_i(X_\beta) + I_E Y'_i(X_\beta)] \ddot{\beta}_R - \frac{1}{m_i} \sum_j m_{sj} Y_i(X_{sj}) \ddot{Z}_{sj} \\ & - \frac{1}{m_i} [S_E Y_i(X_\beta) + I_E Y'_i(X_\beta)] \sum_K Y'_K(X_\beta) \ddot{n}_K \end{aligned} \quad (A-6)$$

where

$$G_i = \frac{qA}{m_i C} \int_0^l \frac{\partial C_{Z\alpha}}{\partial X} Y_i(X) dX \quad (A-7)$$

Engine/Actuator

$$\ddot{\beta}_R = C_{\ddot{\beta}} \ddot{\beta}_R + C_{\dot{\beta}} \dot{\beta}_R + C_{\beta} \beta_R + C_{\beta} u \quad (\text{A-8})$$

Markov Wind

$$\dot{V} = -\alpha_w V_w + \zeta \quad (\text{A-9})$$

The following are the combinations of the system states seen by the attitude gyro, rate gyro, and the accelerometer, respectively

$$Y_{AG} = \phi - \sum_i Y_i' (X_{AG}) \eta_i \quad (\text{A-10})$$

$$Y_{RG} = \dot{\phi} - \sum_i Y_i' (X_{RG}) \dot{\eta}_i \quad (\text{A-11})$$

$$Y_{AC} = -J_A \ddot{\phi} + \sum_i Y_i (X_{AC}) \ddot{\eta}_i - \left(\frac{F - X}{m} \right) \phi + \frac{F - X}{m} \sum_i Y_i' (X_A) \dot{\eta}_i \quad (\text{A-12})$$

The definitions of the terms in these equations are presented in Tables A-1 and A-2.

To solve for A, B, and H, Equations A-3 through A-12 are arranged in the form

$$F\dot{X} = A_{PR} \underline{X} + B_{PR} u \quad (\text{A-13})$$

$$\underline{Y} = CX + DX \quad (\text{A-14})$$

where

$$\underline{X} = [\dot{Z} \phi \dot{\phi} Z_{S1} \dot{Z}_{S1} Z_{S2} \dot{Z}_{S2} Z_{S3} \dot{Z}_{S3} \eta_1 \dot{\eta}_1 \eta_2 \dot{\eta}_2 \eta_3 \dot{\eta}_3 \eta_4 \dot{\eta}_4 \beta \dot{\beta} \ddot{\beta} V_w]' \quad (A-15)$$

$$\underline{Y} = [Y_{AG} \ Y_{RG} \ Y_{AC}]' \quad (A-16)$$

Computer locations 1 through 96 contains the program input data, which consists of the launch vehicle, parameters. These parameters, together with their descriptions, units, and storage spaces are listed in Table A.1. Equations A-3 through A-9 appear in the system matrixes of Equations A-13 and A-14 in the same order as presented here. The matrix elements are coded individually or in groups from left to right, and downward. Table A-3 contains the computer terms used for the various matrixes.

Once the elements of the matrixes in Equations A-13 and A-14 are computed, the equations are regrouped to assume the form of Equations A-1 and A-2.

$$\underline{X} = F^{-1} A_{P_R} X + F^{-1} B_{P_R} u \quad (A-17)$$

$$= A\underline{X} + Bu \quad (A-18)$$

Using Equation A-18, Equation A-14 can be written

$$\underline{Y} = C\underline{X} + D(A\underline{X} + Bu) \quad (A-19)$$

for this system $DB = 0$, so Equation A-19 simplifies to

$$Y = (C + DA) \underline{X} \quad (A-20)$$

so the observation matrix is

$$H = C + DA \quad (A-21)$$

Table A-1
DOCUMENTATION OF TERM DEFINITIONS USED
IN PROGRAM H266 (page 1 of 4)

Location	Computer Symbol	System Symbol	Definition or Description
1	C1	$\frac{N'}{I_{XX}} l_{CP}$	Aerodynamic effectiveness parameter (1/sec ²)
2	C2	$\frac{R'}{I_{XX}} l_{CG}$	Control engine effectiveness parameter (1/sec ²)
3	AN	N'	$C_{Z\alpha} qA$, aerodynamic force (kg)/(rad)
4	V	V	Velocity (m/sec)
5	FC	F	Total thrust of booster (kg)
6	EX	X	Drag force (kg) $C_{D_0} qA$
7	ALW	W	Angle of attack due to wind (rad/sec), break freq.
8	RP	R'	$\frac{1}{2} F$, thrust of control engine (kg)
9	SE	S_E	First moment of swivel about gimbal point, (Kg-sec ²)
10	AM	m	Total mass of vehicle (kg-sec ² /m)
11	AMS(1)	m_{s1}	First slosh mass $\left(\frac{Kg - sec^2}{m}\right)$
12	AMS(2)	m_{s2}	Second slosh mass $\left(\frac{Kg - sec^2}{m}\right)$
13	AMS(3)	m_{s3}	Third slosh mass $\left(\frac{Kg - sec^2}{m}\right)$
14			
15	ALS(1)	l_{S1}	Distance from vehicle c. g. to slosh mass c. g., $(X_{cg} - X_{S1})$ (m)
16	ALS(2)	l_{S2}	$(X_{cg} - X_{S2})$ m
17	ALS(3)	l_{S3}	$(X_{cg} - X_{S3})$ m
18			
19	YPB(1)	$Y'_1(X_\beta)$	Normalized slope of i th mode at station X_β engine (1/m)
20	YPB(2)	$Y'_2(X_\beta)$	Normalized slope of i th mode at station X_β engine (1/m) for 2 nd mode
21	YPB(3)	$Y'_3(X_\beta)$	Normalized slope of i th mode at station X_β engine (1/m) for 3 rd mode
22	YPB(4)	$Y'_4(X_\beta)$	Normalized slope of i th mode at station X_β engine (1/m) for 4 th mode
23	YB(1)	$Y_1(X_\beta)$	Normalized displacement of 1 st mode at engine station (ND)
24	YB(2)	$Y_2(X_\beta)$	Normalized displacement of 2 nd mode at engine station (ND)
25	YB(3)	$Y_3(X_\beta)$	Normalized displacement of 3 rd mode at engine station (ND)

Location	Computer Symbol	System Symbol	Definition or Description
26	YB(4)	$Y_4(X_\beta)$	Normalized displacement of <u>4th</u> mode at engine station (ND)
27			
28	Z(1)	ξ_1	<u>1st</u> mode bending damping (ND)
29	Z(2)	ξ_2	<u>2nd</u> mode bending damping (ND)
30	Z(3)	ξ_3	<u>3rd</u> mode bending damping (ND)
31	Z(4)	ξ_4	<u>4th</u> mode bending damping (ND)
32	W(1)	W_1	<u>1st</u> bending mode frequency (rad/sec)
33	W(2)	W_2	<u>2nd</u> bending mode frequency (rad/sec)
34	W(3)	W_3	<u>3rd</u> bending mode frequency (rad/sec)
35	W(4)	W_4	<u>4th</u> bending mode frequency (rad/sec)
36	YXS(1, 1)	$Y_1(X_{S1})$	<u>1st</u> bending mode displacement at <u>1st</u> slosh mass cg (ND)
37	YXS(1, 2)	$Y_2(X_{S1})$	<u>2nd</u> bending mode displacement at <u>1st</u> slosh mass cg (ND)
38	YXS(1, 3)	$Y_3(X_{S1})$	<u>3rd</u> bending mode displacement at <u>1st</u> slosh mass cg (ND)
39	YXS(1, 4)	$Y_4(X_{S1})$	<u>4th</u> bending mode displacement at <u>1st</u> slosh mass cg (ND)
40	YXS(2, 1)	$Y_1(X_{S2})$	<u>1st</u> bending mode displacement at <u>2nd</u> slosh mass cg (ND)
41	YXS(2, 2)	$Y_2(X_{S2})$	<u>2nd</u> bending mode displacement at <u>2nd</u> slosh mass cg (ND)
42	YXS(2, 3)	$Y_3(X_{S3})$	<u>3rd</u> bending mode displacement at <u>2nd</u> slosh mass (ND)
43	YXS(2, 4)	$Y_4(X_{S2})$	<u>4th</u> bending mode displacement at <u>2nd</u> slosh mass (ND)
44	YXS(3, 4)	$Y_1(X_{S3})$	<u>1st</u> bending mode displacement at <u>3rd</u> slosh mass (ND)
45	YXS(3, 2)	$Y_2(X_{S3})$	<u>2nd</u> bending mode displacement at <u>3rd</u> slosh mass (ND)
46	YXS(3, 3)	$Y_3(X_{S3})$	<u>3rd</u> bending mode displacement at <u>3rd</u> slosh mass cg (ND)
47	YXS(3, 4)	$Y_4(X_{S3})$	<u>4th</u> bending mode displacement at <u>3rd</u> slosh mass cg (ND)
48		q	Dynamic pressure (Kg/m ²)
49	AIE	I_E	Engine moment of inertia about gimbal point, (Kg-m-sec ²)
50	AIX	I_{xx}	Pitch plane moment of inertia about vehicle cg, (Kg-m-sec ²)
51	ZS(1)	ξ_{S1}	<u>1st</u> tank slosh damping (ND)

Table A-1 (page 3 of 4)

Location	Computer Symbol	System Symbol	Definition or Description
52	ZS(2)	ξ_{S2}	<u>2nd</u> tank slosh damping (ND)
53	ZS(3)	ξ_{S3}	<u>3rd</u> tank slosh damping (ND)
54	WS(1)	W_{S1}	<u>1st</u> slosh tank frequency (rad/sec)
55	WS(2)	W_{S2}	<u>2nd</u> slosh tank frequency (rad/sec)
56	WS(3)	W_{S3}	<u>3rd</u> slosh tank frequency (rad/sec)
57	YPS(1, 1)	$Y'_1(X_{S1})$	<u>1st</u> bending mode normalized slope at <u>1st</u> slosh mass cg, (1/m)
58	YPS(1, 2)	$Y'_2(X_{S1})$	<u>2nd</u> bending mode normalized slope at <u>1st</u> slosh mass cg, (1/m)
59	YPS(1, 3)	$Y'_3(X_{S1})$	<u>3rd</u> bending mode normalized slope at <u>1st</u> slosh mass cg, (1/m)
60	YPS(1, 4)	$Y'_4(X_{S1})$	<u>4th</u> bending mode normalized slope at <u>1st</u> slosh mass cg, (1/m)
61	YPS(2, 1)	$Y'_1(X_{S2})$	<u>1st</u> bending mode normalized slope at <u>2nd</u> slosh mass cg, (1/m)
62	YPS(2, 2)	$Y'_2(X_{S2})$	<u>2nd</u> bending mode normalized slope at <u>2nd</u> slosh mass cg, (1/m)
63	YPS(2, 3)	$Y'_3(X_{S2})$	<u>3rd</u> bending mode normalized slope at <u>2nd</u> slosh mass cg, (1/m)
64	YPS(2, 4)	$Y'_4(X_{S2})$	<u>4th</u> bending mode normalized slope at <u>2nd</u> slosh mass cg, (1/m)
65	YPS(3, 1)	$Y'_1(X_{S3})$	<u>1st</u> bending mode normalized slope at <u>3rd</u> slosh mass cg, (1/m)
66	YPS(3, 2)	$Y'_2(X_{S3})$	<u>2nd</u> bending mode normalized slope at <u>3rd</u> slosh mass cg, (1/m)
67	YPS(3, 3)	$Y'_3(X_{S3})$	<u>3rd</u> bending mode normalized slope at <u>3rd</u> slosh mass cg, (1/m)
68	YPS(3, 4)	$Y'_4(X_{S3})$	<u>4th</u> bending mode normalized slope at <u>3rd</u> slosh mass cg, (1/m)
69	BM(1)	M_1	<u>1st</u> bending mode generalized mass, (Kg-sec ² /m)
70	BM(2)	M_2	<u>2nd</u> bending mode generalized mass, (Kg-sec ² /m)
71	BM(3)	M_3	<u>3rd</u> bending mode generalized mass, (Kg-sec ² /m)
72	BM(4)	M_4	<u>4th</u> bending mode generalized mass, (Kg-sec ² /m)
73	G(1)	G_1	$\frac{qA}{M_i} \sum \frac{\partial C_{Z\alpha}}{\partial X_n} \Delta X_n Y_i(X_n), i = 1, 2, 3, 4. i = 1$
74	G(2)	G_2	Generalized aerodynamic force function, (Kg) $i = 2$
75	G(3)	G_3	Generalized aerodynamic force function, (Kg) $i = 3$
76	G(4)	G_4	Generalized aerodynamic force function, (Kg) $i = 4$
77	YA(1)	$Y_1(X_A)$	<u>1st</u> bending mode normalized displacement at accelerometer sta. (ND)

Location	Computer Symbol	System Symbol	Definition or Description
78	YA(2)	$Y_2(X_A)$	2nd bending mode normalized displacement at accelerometer sta. (ND)
79	YA(3)	$Y_3(X_A)$	3rd bending mode normalized displacement at accelerometer sta. (ND)
80	YA(4)	$Y_4(X_A)$	4th bending mode normalized displacement at accelerometer sta. (ND)
81	YPRG(1)	$Y'_1(X_{RG})$	1st bending mode normalized slope at rate gyro station, (1/m)
82	YPRG(2)	$Y'_2(X_{RG})$	2nd bending mode normalized slope at rate gyro station, (1/m)
83	YPRG(3)	$Y'_3(X_{RG})$	3rd bending mode normalized slope at rate gyro station (1/m)
84	YPRG(4)	$Y'_4(X_{RG})$	4th bending mode normalized slope at rate gyro station (1/m)
85	YPMG(1)	$Y'_1(H_{IG})$	1st bending mode normalized slope at attitude gyro station, (1/m)
86	YPMG(2)	$Y'_2(H_{IG})$	2nd bending mode normalized slope at attitude gyro station, (1/m)
87	YPMG(3)	$Y'_3(H_{IG})$	3rd bending mode normalized slope at attitude gyro station, (1/m)
88	YPMG(4)	$Y'_4(H_{IG})$	4th bending mode normalized slope at attitude gyro station, (1/m)
89	X(89)	$C_{\dot{\beta}}$	Actuator transfer function relating $(\ddot{\beta}/\dot{\beta})$, (1/sec ³)
90	X(90)	$C_{\ddot{\beta}}$	Actuator transfer function relating $(\ddot{\beta}/\ddot{\beta})$, (1/sec ²)
91	X(91)	$C_{\ddot{\beta}}$	Actuator transfer function relating $(\ddot{\beta}/\ddot{\beta})$, (1/sec)
92	ALA	l_A	Distance from vehicle CG to accelerometer, $(X_{CG} - X_A)$, (m)
93	YPA(1)	$Y'_1(X_A)$	1st bending mode normalized slope at accelerometer sta X_A , (1/m)
94	YPA(2)	$Y'_2(X_A)$	2nd bending mode normalized slope at accelerometer sta. X_A , (1/m)
95	YPA(3)	$Y'_3(X_A)$	3rd bending mode normalized slope at accelerometer sta. X_A , (1/m)
96	YPA(4)	$Y'_4(X_A)$	4th bending mode normalized slope at accelerometer sta. X_A , (1/m)

Table A-2
DEFINITION OF SYMBOLS NOT DEFINED IN PROGRAM H266 LIST

Symbol	Definition	Unit
ϕ	Attitude angle	Rad
α	Angle of attack	Rad
β	Control deflection angle	Rad
V_w	Wind velocity	m/sec
I_{xx}	Pitch plane moment of inertia about the CG	Kg-m-sec ²
a_{LA}	Vehicle longitudinal acceleration	m/sec ²
l_{CP}	Distance from vehicle CG to the CP ($X_{CG} - X_{CP}$)	m
l_{CG}	Distance from engine gimbal to vehicle CG; ($X_{CG} - X_{\beta}$)	m
l_E	Distance from engine gimbal to engine mass CG; ($X_{\beta} - X_E$)	m
Z_{sj}	Slosh mass displacement, normal to reference	m
$(X_{sj} - X_{\beta})$	Distance from engine gimbal to slosh mass CG	m
A	Cross sectional reference area	m ²
η_i	Generalized displacement of the i^{th} mode (normal coordinates)	m
$Y_i(x)\eta_i$	Displacement at Sta. X due to the i^{th} mode	m
$Y_i'(x)\eta_i$	Angular displacement at Sta. X due to the i^{th} mode	Rad
$Y_i''(x)\eta_i$	Angular rate at Sta. X due to the i^{th} mode	Rad/sec
$Y_i'''(x)\eta_i$	Angular acceleration at Sta. X due to the i^{th} mode	Rad/sec ²

Symbol Subscripts	Definition	Unit
CG	Center of gravity	
CP	Center of pressure	
LA	Longitudinal acceleration	
ϕ	Position gryo	
A	Accelerometer	
E	Engine	
α	Angle of attack	
S	Slosh	
R	Rigid body	
B	Bending body	
W	Wind	
j	j^{th} slosh tank	
i	i^{th} bending mode	
X	Vehicle station	
β	Engine gimbal	
R, B	Rigid body plus bending body	

BLANK PAGE

C6/Q2/66

H311 CONKAL - EFN SOURCE STATEMENT - IFN(S) -

```

DIMENSION X(200),RX(200),B(21),C(3,21),D(3,21),FTR(21,21)
1 A(21,21)=APR(21,21),FUP(21,21),H(3,21),FIO(21),FIP(21),FTQ(21)
2 FTS(21),AMS(3),ALS(3),YPB(4),YB(4),Z(4),YXS(4,3),YPS(4,3)
3 BM(4),G(4),YA(4),YPG(4),YPMG(4),ZS(3),WS(3),FMA(21,21)
4 KTEMP(63),ITEMP(63),YPA(4),CB(3),BPL(21),CPL(21)
5 WURK(250),IERR(3),EIGV(22,2)
EQUIVALENCE (CL,X(1)),(C2,X(2)),(AN,X(3)),(V,X(4)),(FC,X(5))
1 (EX,X(6)),(ALW,X(7)),(KP,X(8)),(SE,X(9)),(AM,X(10)),(APS,X(11))
2 (ALS,X(15)),(YPB,X(19)),(YB,X(23)),(Z,X(28)),(W,X(32))
3 (VXS,X(36)),(AIE,X(49)),(AIX,X(50)),(ZS,X(51)),(WS,X(54))
4 (VPS,X(57)),(BM,X(69)),(G,X(73)),(YA,X(77)),(YPRG,X(81))
5 (VPMG,X(85)),(ALA,X(92)),(YPA,X(93)),(CB,X(89))
1 CALL INPUT1 (X,X(200),RX)
DC10I=1,21
DGLCJ=1,21
DGLCJ=1,21
APR(1,J)=C.C
FTR(1,J)=C.C
FMA(1,J)=C.C
10 A(1,J)=C.C
DU15K=1,17,2
I=1+K
J=2+K
15 APR(1,J)=1.0
APR(1,1)=-AN/(AM*V)
APR(1,21)=AN/(AM*V)
APR(1,2)=AN/AM+(FC-EX)/AM
APR(1,18)=KP/AM
D02CK=1,4
J= 8+2*K
20 APR(1,J)=-FC*YPB(K)/AM
APR(3,1)=CL/V
APR(3,2)=-CL
APR(3,18)=-C2
APR(3,21)=-CL/V
D025K=1,3
I=3+2*K
APR(1,2)= (FC-EX)/AM
J1=2+2*K
J2=3+2*K
APR(1,J1)=-WS(K)**2
APR(1,J2)=-2.0*ZS(K)*S(K)
D025L=1,4
J3=8+2*L
25 APR(1,J3)=-YPS(L,K)*(FC-EX)/AM
D03CK=1,4
I=9+2*K
J1=8+2*K
J2=9+2*K
APR(1,1)=-G(K)/V
APR(1,2)=G(K)
APR(1,J1)=-W(K)**2
APR(1,J2)=-2.0*Z(K)*W(K)
APR(1,18)=KP*YB(K)/BM(K)
APR(1,20)= (SE*YB(K)+AIE*YPB(K))/BM(K)
APR(1,21)= G(K)/V

```

8

2

```

H311          CUNNALL      -      EFM      SOURCE STATEMENT - IFN(S) -
DU2HL=1,3
J3=2+2*L
28 APR(I,J3)=-((FC-EX)*AMS(L)*YPS(K,L))/(AP*BM(K))
DU3OL=1,4
J4=8+2*L
30 APR(I,J4)=APR(I,J4)-KP*YB(K)*YPH(L)/BM(K)
APR(19,20)=1.0
APR(20,18)=CH(1)
APR(20,19)=CH(2)
APR(20,20)=CH(3)
APR(21,21)=-ALW
DU35K=1,21
35 FMA(K,K)=1.0
DU4OL=1,2
J=3+2*L
40 FMA(I,J)= AMS(L)/AM
DU45K=1,3
I=3+2*K
FMA(I,I)= 1.0
FMA(I,3)=-ALS(K)
DC45L=1,4
J=9+2*L
45 FMA(I,J)=YXS(L,K)
DU5OK=1,4
I=9+2*K
DU48L=1,3
J1=3+2*L
48 FMA(I,J1)=AMS(L)*YXS(K,L)/BM(K)
DU5OL=1,4
J2=9+2*L
50 FMA(I,J2)=FMA(I,J2)+(SE*YB(K)+AIE*YPB(K))*YPB(L)/BM(K)
DU55I=1,3
DU55J=1,21
C(I,J)=C.C
55 D(I,J)=C.C
C(1,2)=1.C
C(2,3)=1.C
C(3,2)=-((FC-EX)/AM
DU6OL=1,4
J1=8+2*L
J2=9+2*L
C(1,J1)=-YPMG(L)
C(2,J2)=-YPRG(L)
C(3,J2)=-YPA(L)
60 D(3,J2)=YAL(L)
DU12OI=1,21
DU12OJ=1,21
120 FTR(I,J)=FMA(I,J)
CALL SUD (FTR,21,21,21,1,0,1,SIGUIG,IERROR,ITEMP,SCALEB)
DU125I=1,21
DU125J=1,21
A(I,J)=0.C
DU125K=1,21
125 A(I,J)=A(I,J)+FTR(I,K)*APR(K,J)
DU13OI=1,21
130 B(I)=-CB(I)*FTR(I,20)

```

191

57H266
58H266
59H266
60H266
61H266
62H266
63H266
64H266
65H266
66H266
67H266
68H266
69H266
70H266
71H266
72H266
73H266
74H266
75H266
76H266
77H266
78H266
79H266
80H266
81H266
82H266
83H266
84H266
85H266
86H266
87H266
88H266
89H266
90H266
91H266
92H266
93H266
94H266
95H266
96H266
97H266
98H266
99H266
100H266
101H266
102H266
103H266
10J
105H266
106H266
107H266
108H266
109H266
110H266
111H266
112H266

C6/02/66

H311 CONKAL - EFN SOURCE STATEMENT - I+H(S) -

```

00135I=1,3
00135J=1,21
M(I,J)=C(I,J)
00135K=1,21
135 M(I,J)=H(I,J)+D(I,K)*A(K,J)
    WRITE(6,500)
    WRITE(6,500)
    WRITE(6,400)
400 FORMAT (1H0,9X,14H4 PRIME MATRIX)
    CALL PKMAT(APK,21)
    WRITE(6,500)
    WRITE(6,410)
410 FORMAT (1H0,9X,8H5 MATRIX)
    CALL PKMAT(FMA,21)
    WRITE(6,500)
    WRITE(6,420)
420 FORMAT (1H0,9X,16H5 INVERSE MATRIX)
    CALL PKMAT(FTR,21)
    WRITE(6,500)
    WRITE(6,430)
430 FORMAT (1H0,9X,28H4 MATRIX=F INVERSE X A PRIME)
    CALL PKMAT(A,21)
    WRITE(6,500)
    WRITE(6,440)
440 FORMAT (1H0,9X,17H4 MATRIX=(C + DA))
    WRITE(6,500)
    WRITE(6,450)
450 FORMAT (1H0,9X,8H5 MATRIX)
    WRITE(6,500)(b(i),i=1,21)
499 FFORMAT (3110)
500 FFORMAT (1H0,E12.5,6(4X,E12.5))
GO TO 1
END

```

235
236
237
238
239
240
241
242
243
244
245
246
247
248
249
250
251
252
253

113H266
114H266
115H266
116H266
117H266
118H266
119H266
120H266
121H266
122H266
123H266
124H266
125H266
126H266
127H266
128H266
129H266
130H266
131H266
132H266
133H266
134H266
135H266
136H266
137H266
138H266
139H266
140H266
141H266
142H266
143H266
144H266
145H266
146H266

P311

06/02/66

PAGE 4

\$1BFTC PRMAT

10PRMT

06/02/66

F311 PRMAT - EFN SOURCE STATEMENT - IPN(S) -

```

SUBROUTINE PRMAT(ARAY,M)
DIMENSION ARAY (M,21)
WRITE(6,500)
DO450 I=1,M
  450 WRITE (6,500) (ARAY(I,J),J=1,7 )
  WRITE (6,550)
  DO451 J=1,M
    451 WRITE(6,500) (ARAY(I,J),J=8 ,14)
    WRITE (6,550)
    DO452 I=1,M
      452 WRITE (6,500) (ARAY(I,J),J=15,21)
      500 FORMAT(1H0,E12.5,6(4X,E12.5))
      WRITE (6,550)
      550 FORMAT(1H1)
    RETURN
  END

```

20PRMT
30PRMT
40PRMT
50PRMT
60PRMT
70PRMT
80PRMT
90PRMT
100PRMT
110PRMT
120PRMT
130PRMT
140PRMT
150PRMT
160PRMT
170PRMT

1
5
11
15
21
25
31

A. 2 RICCATI DIFFERENTIAL EQUATION SOLUTION

Purpose: To find the solution $P(t)$ to the matrix Riccati equation $\dot{P}(t) + PA + A^T P - PGP + Q = [0]$ at a specified time where A^T is the transpose of A . The above n^{th} order nonlinear differential equation is replaced by a $2n^{\text{th}}$ order linear first order matrix differential equation whose solution is straightforward. See the METHOD and EQUATIONS section below for details.

Use: CALL RICAT (pOmat, amat, gmat, qmat, n, tstart, tlast, itengi, itnorm, pmat, itau, tau, ierror)

where

Input

pOmat is a REAL two dimensional (2l by 2l) array which contains $[P(t_{\text{start}})]$.

amat is a REAL two dimensional (2l by 2l) array which contains $[A]$.

gmat is a REAL two dimensional (2l by 2l) array which contains $[G]$.

qmat is a REAL two dimensional (2l by 2l) array which contains $[Q]$.

n is an INTEGER variable or constant which denotes the number of rows (or columns) in $[P]$, $[A]$, $[G]$, $[Q]$, and $[P]$. Thus n is the order of a matrix. n must be less than or equal to 2l.

tstart is a REAL variable or constant which denotes the starting value for t.

itengi is an INTEGER variable or constant which denotes the number of iterations which are to be performed on the $\dot{P}(t)$ equation using the tau specified by the engineer.

(If itengi is given a non-zero value, $\tau = (t_{\text{last}} - t_{\text{start}})/itengi$ will be used unless it is deemed to be too large.) If itengi = 0, this subprogram will calculate a τ from the norm of $[Z]$ and do itnorm iterations on $P(t)$. (itnorm is defined immediately following.)

itnorm is an INTEGER variable or constant which denotes the number of iterations which are to be done on the P(t) matrix with the value of τ calculated from the norm of [Z]. If itengi $\neq 0$, but the τ calculated by $\tau = (t_{\text{last}} - t_{\text{start}})/\text{itengi}$ is deemed too large by this subprogram, then itnorm iterations will be done on P(t) using a τ calculated from the norm of [Z].

Output

pmat is a REAL two dimensional (21 by 21) array in which the last iteration of P(t) will be stored.

itau is an INTEGER variable which will be set to 1 if the τ used was calculated from the norm of [Z]. Otherwise itau will be set to zero.

tau is a REAL variable which will be set equal to the value of τ used in calculating the P(t) matrixes.

ierror is an INTEGER variable which will be set equal to 1 if any of the $[\theta_{11}] + [\theta_{12}][P(t)]$ matrixes could not be inverted. Otherwise it will be set to zero.

Accuracy:

This subroutine should provide four decimal place accuracy in the elements of $[\theta]$ except that elements with absolute values greater than 10^3 may have only six significant digits.

Method and Equations:

The n^{th} order matrix Riccati equation

$$\dot{P} = -PA - A^T P + PGP - Q$$

is equivalent to the equation

$$P = YX^{-1}$$

where

$$\begin{bmatrix} \dot{X} \\ \dot{Y} \end{bmatrix} = \begin{bmatrix} -A & G \\ Q & A^T \end{bmatrix} \begin{bmatrix} X \\ Y \end{bmatrix} = Z \begin{bmatrix} X \\ Y \end{bmatrix}$$

The $2n^{\text{th}}$ order linear first order matrix differential equation has the solution

$$\begin{bmatrix} X(t+\tau) \\ Y(t+\tau) \end{bmatrix} = \begin{bmatrix} e^{\tau Z} \end{bmatrix} \begin{bmatrix} X(t) \\ Y(t) \end{bmatrix} = \begin{bmatrix} \theta \end{bmatrix} \begin{bmatrix} X(t) \\ Y(t) \end{bmatrix}$$

where

$$[e^{Z\tau}] = [\theta] = [I] + [\tau Z] + \frac{[\tau Z]^2}{2!} + \frac{[\tau Z]^3}{3!} + \dots + \frac{[\tau Z]^n}{n!}$$

Partitioning the above transition matrix, $[\theta]$, we have

$$\begin{bmatrix} X(t+\tau) \\ Y(t+\tau) \end{bmatrix} = \begin{bmatrix} \theta_{11} & \theta_{12} \\ \theta_{21} & \theta_{22} \end{bmatrix} \begin{bmatrix} X(t) \\ Y(t) \end{bmatrix}$$

Since

$$P = YX^{-1}$$

then

$$\begin{aligned} P(t+\tau) &= [Y(t+\tau)][X(t+\tau)]^{-1} \\ &= [\theta_{21}X(t) + \theta_{22}Y(t)][\theta_{11}X(t) + \theta_{12}Y(t)]^{-1} \end{aligned}$$

Using the fact that $Y(t) = P(t)X(t)$, we have the following iterative procedure for calculating the solution for the matrix Riccati equation as a function of time

$$P(t+\tau) = [\theta_{21} + \theta_{22}P(t)][\theta_{11} + \theta_{12}P(t)]^{-1}$$

If τ is calculated from the norm of $[Z]$ to provide the accuracy mentioned above, the following formula is used:

$$\tau = \frac{(t_{\text{last}} - t_{\text{start}})}{\|Z\|}$$

where $\|Z\|$ is the norm of $[Z]$ defined by

$$\|Z\| = \text{Min} \left\{ \max_i \left(\sum_j |z_{ij}| \right), \max_j \left(\sum_i |z_{ij}| \right) \right\}$$

where

$$[Z] \equiv [z_{ij}]$$

Storage Requirements: This subprogram requires about 8018 words of core storage. Of this 8018 words, 5292 words are used for storage of three 42 by 42 matrixes which are used when calculating $[\theta]$, 567 words are used for storage of two 21 by 21 temporary arrays and two 21 by 3 temporary arrays[roughly 300 words of coding are used in determining when the matrix Taylor series for $[\theta]$ has converged; and roughly 120 words of coding are used in computing τ from the norm of $[Z]$.

The 8018 words of storage mentioned above do not include the 2205 words which are required for storage of $[A]$, $[G]$, $[Q]$, $[P]$, and $[PO]$ which are all 21 by 21 arrays.

H311

01/29/66

PAGE 3

\$IBFIC RICAL DECK

RICAO010

C1/29/66

```

H311 RICAT - EFN SOURCE STATEMENT - IFN(S) -
SUBROUTINE RICAT ( PU, A, G, Q, N, ISTART, TFINAL, ITER, ITER2,
. P, ITAU, TAU, IERROR)
.
. RICATTI METHOD FOR SOLVING A CONTROL OPTIMIZATION DIFFERENTIAL
. EQUATION
. ( THIS VERSION OF RICAT PRINTS COMMENTS ON THE TAYLOR
. SERIES USED TO COMPUTE THE THETA (TRANSITION) MATRIX )
.
DOUBLE PRECISION DPSUM, DPSUN
. THET22, P, TEMP1, TEMP2
. DIMENSION PO(21,21), A(21,21), G(21,21), Q(21,21), P(21,21),
. THETA(42,42), TAUZ(42,42), TERM(42,42), THET11(21,21),
. THET12(21,21), THET21(21,21), THET22(21,21),
. TEMP1(21,21), TEMP2(21,21), RTEMP(3,21),
. ITEMP( 3,21)
. EQUIVALENCE (TERM(1, 1), THET11), (TERM(22,11), THET12),
. (TERM(1,22), THET21), (TERM(22,32), THET22)
.
ND = 21
ZERO = 0.
ONE = 1.
TWO = 2.
LTHMAX = 37
THEEPS = 1.E-6/FLOAT(N)
.
IERROR = C
ITAU = -1
NN = 2*N
.
FORM Z MATRIX
.
40 CONTINUE
DO 60 J = 1,N
DO 60 I = 1,N
JPN = J+N
IPN = I+N
TAUZ(I ,J ) = -A(I,J)
TAUZ(IPN,J ) = Q(I,J)
TAUZ(I ,JPN) = G(I,J)
60 TAUZ(IPN,JPN) = A(J,I)
.
IF (ITAU .EQ. 1) GO TO 78
.
COMPUTE A NORM OF (Z)
.
ROWMAX = 0.
COLMAX = 0.
DO 72 J = 1,N
ROWSUM = 0.
COLSUM = 0.
DO 68 I = 1,N
ROWSUM = ROWSUM + ABS(TAUZ(J,I))
68 COLSUM = COLSUM + ABS(TAUZ(I,J))
IF (ROWSUM .GT. ROWMAX) ROWMAX = ROWSUM

```

RICA0020
 RICA0030
 RICA0080
 RICA0120
 RICA0160
 RIC 0170
 RIC 0180
 RICA0200
 RICA0220
 RICA0360
 RICA0400
 RICA0440
 RICA0480
 RICA0520
 RICA0560
 RICA0600
 RICA0640
 RICA0655
 RICA0660
 RICA0667
 RICA0720
 RICA0760
 RICA0800
 RICA0920
 RICA1080
 RICA1120
 RICA1160
 RICA1320
 RICA1360
 RICA1460
 RICA1462
 RICA1464
 RICA1480
 RICA1520
 RICA1560
 RICA1600
 RICA1640
 RICA1680
 RICA1720
 RICA1760
 RICA1800
 RICA1801
 RICA1802
 RICA1803
 RICA1806
 RICA1809
 RICA1812
 RICA1815
 RICA1818
 RICA1821
 RICA1824
 RICA1827
 RICA1830
 RICA1833
 RICA1836

```

1311 R1CAT - EFN SOURCE STATEMENT - IFN(S) - C1/29/66
      SIGTHE = ALOGIC(THHAX/FBOUND)
      WRITE (6,643) SIGTHE
643  FORMAT (1/ 50H A LARGE ELEMENT OF THE THETA (TRANSITION) MATRIX
      . 14HHAD ONLY ABOUT .F4.1. 35H SIGNIFICANT DIGITS WHICH IS LESS T
      . 21HHAN THE MINIMUM CF 6. )
      GO TO 616
C 700 WRITE (6,703) L
703  FORMAT ( 50H1 R1CAT ERROR - THE ( (THETA(1,1)) + (THETA(1,2))
      . 46H* (P(T)) ) MATRIX COULD NOT BE INVERTED IN THE , 14, 5TH IT
      . 27HERRATION FOR THE P(T) MATRIX )
      IERROR = 1
      GO TO 380
C
      END
      R1CA6800
      R1CA6820
      R1CA6860
      R1CA6862
      R1CA6864
      R1CA6900
      R1CA6960
      R1CA7040
      R1CA7080
      R1CA7120
      R1CA7160
      R1CA7180
      R1CA7200
      R1CA7240
      R1CA7280
      280
      281
      283

```

```

H311 NICAL - 2FN SOURCE STATEMENT - IFN(S) - 01/29/66
DU 190 I=1,NV
190 THETA(I,J) = THETA(I,J) + TERM(I,J)
C
IF (ITAU.EQ. 1 .AND. L.GE. LTHMAX) GO TO 210
IF (ICGNV.EQ. 0) GO TO 110
C
210 CONTINUE
IF (L.GT. 50) WRITE (6,193) L, TAU, ZNORM
193 FORMAT(///16H RICAL COMMENT - , 14.23H TERMS WERE REQUIRED TO
. 23H OBTAIN THETA. TAU WAS , E12.4 , 16H NORM OF Z WAS ,
. E12.4 )
C
C
WRITE (6,211) L, TRPMX, EROUND
211 FORMAT (// 18H RICAL COMMENTS . /
. 14. 45H TERMS OF MATRIX TAYLOR SERIES FOR THE THETA
. 34H(TRANSITION) MATRIX WERE COMPUTED. / 20H THE LARGEST ELEMENT
. 19H IN THESE TERMS WAS , E16.8 /
. 57H THE ERROR BOUND ON THE ERROR IN THE THETA MATRIX WAS ,
. E16.8 )
C
THMAX = 0.
DO 214 J=1,NV
DO 214 I=1,NV
214 IF (ABS(THETA(I,J)) .GT. THMAX) THMAX = ABS(THETA(I,J))
C
IF (EBOUND/THMAX .GT. 1.E-6 .AND. ITAU .EQ. 0) GO TO 640
C
IF (ITAU .EQ. 0) WRITE (6,217) TAUCAL, TAU
217 FORMAT (// 25H RICAL COMMENT TAU = , E15.8 , 10H WOULD HAV
. 38HE BEEN USED IF THE TAU YOU SPECIFIED ( , E15.8,11H ) HAD NOT
. 7HWORKED. )
C
IF (ITAU .EQ. 0) LP = ITER
IF (ITAU .EQ. 1) LP = ITER2
C
C STURE THETA PARTITIONS
C
220 DO 240 J=1,N
DO 240 I=1,N
JPN = J+N
IPN = I+N
THET11(I,J) = THETA(I ,J )
THET21(I,J) = THETA(IPN,J )
THET12(I,J) = THETA(I ,JPN)
240 THET22(I,J) = THETA(IPN,JPN)
C
C PRESET FOR P CALCULATION LOOP
C
DO 260 J=1,N
DO 260 I=1,N
260 P(I,J) = PO(I,J)
L=0
C
270 L =L+1
C
RICA3080
RICA3120
RICA3130
RICA3140
RICA3160
RICA3170
RICA3175
RICA3180
RICA3182
RICA3184
RICA3186
RICA3192
RICA3196
RICA3198
RICA3199
RICA3200
RICA3202
RICA3203
RICA3204
RICA3205
RICA3224
RICA3250
RICA3253
RICA3256
RICA3259
RICA3266
RICA3269
RICA3272
RICA3280
RICA3282
RICA3283
RICA3284
RICA3287
RICA3290
RICA3293
RICA3320
RICA3322
RICA3340
RICA3360
RICA3400
RICA3440
RICA3480
RICA3520
RICA3560
RICA3600
RICA3640
RICA3680
RICA3720
RICA3760
RICA3800
RICA3840
RICA3880
RICA3920
RICA3940
RICA3980
RICA4000

```



```

H311 RICAT - EFN SOURCE STATEMENT - IFN(S) -
C1/29/66
DO 300 J=1,N
DO 300 I=1,N
DPSUM = 0.00
DPSUN = 0.00
DO 280 K=1,N
DPSUM = DPSUM + THET22(I,K) * P(K,J)
DPSUN = DPSUN + THET12(I,K) * P(K,J)
280 TEMPI(I,J) = DPSUM + THET21(I,J)
300 TEMP2(I,J) = DPSUN + THET11(I,J)
C
CALL SID(TEMP2, N, ND, 0, 0, 0, SIGDIG, IERR, RTEMP, ITEM,
SCALEB)
C
WRITE (6,305) SIGDIG
305 FORMAT (// 9H SIGDIG = , F10.2 )
IF (IERR .EQ. -1) GO TO 700
C
DO 340 J=1,N
DO 340 I=1,N
DPSUM = 0.00
DO 320 K=1,N
320 DPSUM = DPSUM + TEMPI(I,K) * TEMP2(K,J)
340 P(I,J) = DPSUM
C
DO 360 I=2,N
IM1 = I-1
DO 360 J=1,IM1
P(I,J) = ( P(I,J) + P(J,I) ) / TWO
360 P(J,I) = P(I,J)
370 IF (I .LT. LP) GO TO 270
C
380 CONTINUE
RETURN
C
600 WRITE (6,610) TAUCAL, TAU
C
610 FORMAT (///16H RICAT COMMENT - / 6H TAU = ,E16.8, 5H WAS,
. 25HUSED INSTEAD OF THE TAU = ,E16.8, 21H WHICH YOU SPECIFIED,
. 40H THE LATTER VALUF OF TAU WAS DEEMED TOO /14H LARGE BECAUSE )
C
WRITE (6,613) L
613 FORMAT ( 28H AT LEAST ONE ELEMENT IN THE , I4, 10H1H TERM OF
. 60H THE TAYLOR SERIES FOR THE THETA (TRANSITION) MATRIX EXCEDE
. 8H0 2557. )
616 ITAU = 1
TAU = TAUCAL
GO TO 40
C
620 WRITE (6,610) TAUCAL, TAU
C
623 FURNAT (// 50H THE MAGNITUDE OF THE ERROR IN THE THETA MATRIX EX,
. 35HCEDEED THE MAXIMUM OF .006 WHEN THE , I4, 15H15TH TERM WAS ADD
. 2HED )
GO TO 616
C
640 WRITE (6,610) TAUCAL, TAU

```

RICA4040
RICA4080
RICA4120
RICA4140
RICA4160
RICA4200
RICA4220
RICA4240
RICA4260
RICA4440
RICA4480
RICA4520
RIC 4530
RIC 4540
RIC 4542
RICA4560
RICA4600
RICA4640
RICA4680
RICA4720
RICA4760
RICA4800
RICA4840
RICA4880
RICA5040
RICA5080
RICA5120
RICA5160
RICA5320
RICA5340
RICA5360
RICA5480
RICA5520
RICA6040
RICA6060
RICA6080
RICA6120
RICA6200
RICA6220
RICA6240
RICA6280
RICA6320
RICA6360
RICA6400
RICA6440
RICA6480
RICA6520
RICA6560
RICA6600
RICA6640
RICA6660
RICA6680
RICA6720
RICA6760
RICA6780

231
232

271

272

276
277

279

1

01/29/66

```

H311 RICAT -- EFN SOURCE STATEMENT - IFN(S) -
72 IF (COLSUM .GT. COLMAX) COLMAX = COLSUM
C
ZNORM = AMINI( ROWMAX, COLMAX )
C
TAUCAL = 10./ZNORM
C
IF (ITER .GT. 0) GO TO 76
74 ITAU = 1
TAU = TAUCAL
GO TO 78
76 ITAU = 0
TAU = (TFINAL - TSTART) /FLOAT(ITER)
C
DO 80 J=1,NN
DO 80 I=1,NN
TAUZ(I,J) = TAU * TAUZ(I,J)
TERM(I,J) = TAUZ(I,J)
80 THETA(I,J)= TAUZ(I,J)
C
DO 100 K=1,NN
100 THETA(K,K) = THETA(K,K) + ONE
C
ICGVN = 0
TRMXSM = 0.
TRMXM = 0.
FL = 1.00
L = 1
C
110 L = L+1
FL = FL + 1.00
DO 140 J=1,NN
DO 140 I=1,NN
DPSUM = 0.00
DO 120 K=1,NN
120 DPSUM = DPSUM + TAUZ(I,K) * TERM(K,J)
140 TEMPI(I,J) = DPSUM / FL
C
TERMAX = 0.
DO 160 J=1,NN
DO 160 I=1,NN
IF (ABS(TEMPI(I,J)) .GT. TERMAX ) TERMAX = ABS(TEMPI(I,J))
160 TERM(I,J) = TEMPI(I,J)
C
IF (TERMAX .GT. TRMXM ) TRMXM = TERMAX
IF (TERMAX .GT. 2557. .AND. ITAU .EQ. 0) GO TO 600
TRMXSM = TRMXSM + TERMAX
ENOUND = 1.E-7 * TRMXSM
IF (ENOUND .GT. .6CE-2 .AND. ITAU .EQ. 0) GO TO 620
C
DO 170 J=1,NN
DO 170 I=1,NN
170 IF (ABS(TERM(I,J)).GT. THEEPS) GO TO 180
C
ICGVN = 1
C
180 DO 190 J=1,NN

```

RICA1840
 RICA1842
 RICA1844
 RICA1845
 RICA1846
 RICA1847
 RICA1848
 RICA1852
 RICA1856
 RICA1860
 RICA1864
 RICA1868
 RICA1870
 RICA1872
 RICA1880
 RICA1900
 RICA1920
 RICA1960
 RICA2000
 RICA2040
 RICA2080
 RICA2100
 RICA2120
 RICA2160
 RICA2180
 RICA2200
 RICA2240
 RICA2245
 RICA2250
 RICA2260
 RICA2280
 RICA2320
 RICA2360
 RICA2400
 RICA2440
 RICA2520
 RICA2530
 RICA2540
 RICA2560
 RICA2600
 RICA2620
 RICA2640
 RICA2641
 RICA2645
 RICA2650
 RICA2660
 RICA2663
 RICA2665
 RICA2672
 RICA2680
 RICA2720
 RICA2760
 RICA2780
 RICA2800
 RICA2900
 RICA3040

A-3 Riccati Equation Steady-State Solution by Quasilinearization "QUASI"

This FORTRAN-IV subroutine solves the matrix equation

$$0 = -PA - A^T P + PGP^T - Q$$

The method of solution is described in subsection 7.1.3 The call-instruction is:

CALL RICSS (A, G, Q, PO, E, NS, NAR, NCY, PT2, DT, NC)

Input

- A = An N x N matrix.
- G = An N x N matrix.
- Q = An N x N matrix.
- PO = An N x N positive-definite, symmetric matrix, an initial estimate of the matrix -P.
- E = A small positive scalar used to terminate the iteration process when $\|\dot{P}\| < E$.
- NS = N, the dimension of the (A). This is presently limited to 12.
- NAR = The dimension of the square arrays in which A, G, Q, and PO are stored.
- NCY = The maximum number of iterations which the subroutine will be allowed to cycle through. This is needed in case the iterative process is not convergent.

Output

- PT2 = $\|P\| = \sum P_{KK}$
- DT = $PT2_{(K)} - PT2_{(K-1)}$
- NC = The number of cycles iterated through before DTLE
- PO = The P_0 -matrix is replaced by P-steady state

This subroutine calls on matrix inversion subroutine "SID" with cards 122 and 123. This or a comparable subroutine must be made available.

Subroutine listing follows.

M311

A-3

SIRFTC RICSS DECK

02/10/66

PAGE 3

1010H266

```

H311  RICSS      -  FFN  SOURCE STATEMENT -  IFN(S)  -
C
SURROUTINE RICSS (A,G,O,PO,E,NS,NAR      ,NCY,PT2,DT,NC)
DIMENSION A(NAR,NAR),G(NAR,NAR),Q(NAR,NAR),PO(NAR,NAR),POV(144)
1      ,PV(144),AJ(78,78)
2      ,RTMP(50),ITEMP(50),SCALER(15)
C
EQUIVALENCE (P(1,1),PV(1)),(PO(1,1),POV(1))
C
PT1=0.0
NSR=NS*(NS+1)/2
C
-----
BEGIN P-MATRIX CYCLING
C
DO120L=1,NCY
C
CALCULATE JACOBIAN
C
I2=0
DO50J=1,NS
DO50I=1,J
I2=I2+1
J2=0
DO50N=1,NS
DO50M=1,N
J2=J2+1
AJ(I2,J2)=0.0
C
IF(I.NE.M) GO TO 30
AJ(I2,J2)=-A(N,J)
DO20K=1,NS
20  AJ(I2,J2)=AJ(I2,J2)+PO(J,K)*G(N,K)
C
30  IF(J.NE.M) GO TO 50
AJ(I2,J2)=AJ(I2,J2)-A(N,I)
DO40K=1,NS
40  AJ(I2,J2)=AJ(I2,J2)+PO(I,K)*G(K,N)
50  CONTINUE
C
INVERT JACOBIAN
C
CALL SIN (AJ,NSR,78,78,1.0,1      ,SIGDIG,IEPROR,RTMP)
1
C
COMPUTE F
C
I2=0
DO60I=1,NS
DO60J=1,NS
P(I,J)=0.0
DO60K=1,NS
60  P(I,J)=P(I,J)+G(I,K)*PO(J,K)

```

02/10/66

M311 9ICSS - CFA SOURCE STATEMENT - I=CN(S) -

```

C
  I2=0
  D070J=1,NS
  D070I=1,J
  '2=I2+1
  FV(I2)=O(I,J)
  D070K=1,NS
70 FV(I2)=FV(I2)-P0(I,K)+A(K,J)-A(K,I)+P0(J,K)+P0(I,K)*P(K,J)
C
C
C
  CONTRACT P0
  I2=0
  D080J=1,NS
  D080I=1,J
  I2=I2+1
80 P0V(I2)=P0(I,J)
C
C
C
  COMPUTE P(K+1)
  D090I=1,NSR
  P(V,I)=P0V(I)
  D090K=1,NSR
90 P(V,I)=P(V,I)-A(J,I,K)+FV(K)
C
C
C
  EXPAND P0* INTO P0
  I2=0
  D100J=1,NS
  D100I=1,J
  I2=I2+1
  P0(I,J)=P(V,I2)
100 P0(J,I)=P(V,I2)
C
C
C
  COMPUTE TRACE OF P0 AND COMPARE WITH THE PREVIOUS TRACE
  PT2=0.0
  D110K=1,NS
110 PT2=PT2+ P0(K,K)
  WRITE(6,500) PT2
  WRITE(6,500)
  NT=ARS(PT2-PT1)
  PT1=PT2
  IF(F.GT.NT) GO TO 130
120 CONTINUE
  WRITE(6,499)
130 NC=L
  RETURN
499 FORMAT (10X4H NOP;
500 FORMAT (3110)
  END
  )

```

131
132

138

1280H266
1295H266
1290H266
1295H266
1300H266
1305H266
1310H266
1315H266
1320H266
1325H266
1330H266
1335H266
1340H266
1345H266
1350H266
1355H266
1360H266
1365H266
1370H266
1375H266
1380H266
1385H266
1390H266
1395H266
1400H266
1405H266
1410H266
1415H266
1420H266
1425H266
1430H266
1435H266
1440H266
1445H266
1450H266
1455H266
1460H266
1465H266
1470H266
1475H266
1480H266
1485H266
1490H266
9491
9492
1495H266
1500H266
1505H266
1510H266
1515H266
1520H266
1525H266
1530H266
1535H266
1540H266
1545H266

A-4 Transfer Function Solution by Recursion Equation "TRAFN"

This FORTRAN-IV subroutine extracts from the equations

$$\dot{\underline{x}} = \underline{A}\underline{x} + \underline{B}u$$

$$y = \underline{C}\underline{x}$$

The gain and roots of the polynomial

$$y/u = \frac{K(S + Z_1)(S + Z_2) \dots}{(S + P_1)(S + P_2) \dots}$$

The equations used to perform this process are listed in subsection 7.2.1. The performance of this subroutine is also discussed in this section. The call-statement is

CALL TRAFN (A, B, C, NS, NAR)

Input

- A = The N x N matrix.
- B = The N x 1 matrix.
- C = The 1 x N matrix.
- NS = N, the order of the system, ≤ 30
- NAR = The dimension of the square array containing A

Output

The numerator and denominator polynomials, the gain (K), and the poles (P_i) and zeros (Z_i) are printed out.

04/11/66

H266 TRAFN - EFN SOURCE STATEMENT - IFN(S) -

```

SUBROUTINE TRAFN(A,B,C,NS,NAR)
  DIMENSION A(NAR,NAR),H(NAR),C(NAR)
  DOUBLE PRECISION WOSP(30,30),Q(30,30),POLN(30),SP(30),DENP(30)
  DOUBLE PRECISION DA(30,30),DB(30),DC(30)
  DOUBLE PRECISION RL(32),CL(32),DL(32),WK(30),RI(30)
  DOUBLE PRECISION GAIN
  DENP(1)=1.0D0
  DO10 I=1,NS
    DR(I)=R(I)
    DC(I)=C(I)
    DO10 J=1,NS
      DA(I,J)=A(I,J)
10   O(I,J)=0.0D0
15   OIK(K)=1.0D0
      NSP1=NS+1
      D945M=1.0NSP1
      DO20 I=1,NS
        SP(I)=0.0D0
        DO20 K=1,NS
          SP(I)=SP(I)+Q(I,K)*DR(K)
20   POLN(M)=0.0D0
      DO25 K=1,NS
        POLN(M)=POLN(M)+DC(K)*SP(K)
25   POLN(M)=POLN(M)
      DO30 I=1,NS
        DO30 J=1,NS
          WOSP(I,J)=0.0D0
      DO30 K=1,NS
        WOSP(I,J)=WOSP(I,J)+DA(I,K)*Q(K,J)
30   WOSP(I,J)=WOSP(I,J)
      DP=0.0D0
      DO32 K=1,NS
        DP=DP+WOSP(K,K)
32   NP1=M+1
      FN=M
      DENP(NP1)=-DP/FN
      DO35 I=1,NS
        DO35 J=1,NS
          O(I,J)=WOSP(I,J)
35   OIK(K)=1.0NS
      DO40 K=1,NS
        OIK(K)=OIK(K)+DENP(NP1)
40   OIK(K)=OIK(K)
45   CONTINUE
      NALF=NS
      GAIN=POLN(NSP1)
      DO50 I=1,NS
        IF(POLN(I).NE.0.0D0) GO TO 55
50   CONTINUE
      GO TO 60
55   GAIN=POLN(I)
      NALF=I
      DO58 I=NALF,NSP1
        I2=I-NALF+1
58   POLN(I2)=POLN(I)/GAIN
60   CONTINUE
      NPOL=NS-NALF+1
      NNUM=NS-NALF

```

```

0010TRAF
0015TRAF
0020TRAF
0025TRAF
0026TRAF
0030TRAF
0032TRAF
0035TRAF
0040TRAF
0045TRAF
0050TRAF
0055TRAF
0060TRAF
0065TRAF
0070TRAF
0074TRAF
0075TRAF
0080TRAF
0085TRAF
0090TRAF
0095TRAF
0100TRAF
0105TRAF
0110TRAF
0115TRAF
0120TRAF
0125TRAF
0130TRAF
0135TRAF
0140TRAF
0145TRAF
0150TRAF
0155TRAF
0160TRAF
0165TRAF
0170TRAF
0175TRAF
0180TRAF
0185TRAF
0190TRAF
0195TRAF
0205TRAF
0210TRAF
0215TRAF
0220TRAF
0225TRAF
0230TRAF
0235TRAF
0240TRAF
0245TRAF
0250TRAF
0255TRAF
0260TRAF
0265TRAF
0270TRAF

```



```

H266      TRAFN      -      EFN      SOURCE STATEMENT      -      IFN(S)      -
C
      WRITE(6,75) POLN(NSP1)
      75 FORMAT(1H0,11HCO(N+1)H = ,F12.5)
      WRITE(6,80) GAIN
      80 FORMAT(1H0,7HGAIN = ,F12.5)
      WRITE(6,85)
      85 FORMAT(1H0,9X,20HNUMERATOR POLYNOMIAL)
      DO90I=1,NPOL
      90 WRITE(6,500) POLN(I)
      WRITE(6,500)
      CALL LIN (POLN,BL,CL,DL,WNUM,RR,RI,(FIND,IERR)
      WRITE(6,95) IFIND
      95 FORMAT(1H0,7HIFIND = ,F12.5)
      WRITE(6,100) IERR
      100 FORMAT(1H0,6HIERR = ,F12.5)
      WRITE(6,500)
      WRITE(6,105)
      105 FORMAT(1H0,9X,5HZEROS)
      DO110I=1,NNUM
      110 WRITE(6,500) RR(I),RI(I)
      CALL LIN(DENP,BL,CL,DL,NS,RR,KI,(FIND,IERR)
      WRITE(6,500)
      WRITE(6,115)
      115 FORMAT(1H0,9X,22HDENOMINATOR POLYNOMIAL)
      WRITE(6,95) IFIND
      WRITE(6,100) IERR
      DO120I=1,NSP1
      120 WRITE(6,500) OENP(I)
      WRITE(6,500)
      WRITE(6,125)
      125 FORMAT(1H0,9X,5HPULES)
      DO130I=1,NS
      130 WRITE(6,500) RR(I),RI(I)
      RETURN
      499 FORMAT(3110)
      500 FORMAT(1H0,E12.5,4X,E12.5)
      END

```

04/11/66

```

0271TRAF 117
0272TKAF
0275TRAF
0280TRAF 119
0285TRAF 120
0290TRAF
0295TRAF
0300TRAF
0305TRAF 124
030YTRAF 127
0310TRAF 128
0315TRAF 129
0320TRAF
0325TRAF 130
0330TRAF
0335TRAF 131
0340TRAF 132
0345TKAF
0350TRAF
0355TRAF 136
0360TRAF 141
0365TRAF 142
0370TRAF 143
0375TRAF
0380TRAF 144
0385TRAF 145
0320TRAF
0395TRAF 149
0400TRAF 152
0405TRAF 153
0410TRAF
0415TRAF
0420TRAF
0425TRAF 157
0430TRAF
0435TRAF
0440TRAF

```

A-5 Brockett's Method of Transfer Function Zero Derivation "Zeros"

This FORTRAN-IV subroutine takes as input the matrixes A, B, and C of the linear dynamical system transfer function described by

$$\dot{\underline{x}} = A\underline{x} + Bu$$

$$y = C\underline{x}$$

and generates a $N \times N$ matrix, $W\phi SP$, the eigenvalues of which contain the zeros of the transfer function

$$y/u = \frac{K(S + Z_1)(S + Z_2) \dots}{(S + P_1)(S + P_2) \dots}$$

It also generates the gain, K. The equations used to obtain this matrix are listed in subsection 7.2.2. The problems related to the use of this program are also discussed in this section.

The program is not self sufficient, but calls on an eigenvalue subroutine "Poles" to find the eigenvalues of the $W\phi SP$ -matrix.

The subroutine call statement is

CALL ZEROS (A, B, C, NS, NAR)

Input

A = The $N \times N$ matrix.

B = The $N \times 1$ matrix.

C = The $1 \times N$ matrix.

NS = N, the dimension of the system, ≤ 30

NAR = The dimension of the square array containing A

The subroutine first prints the gain K and then the α -term which is the difference between the number of zeros. Once the eigenvalues of $W\phi SP$ are computed this number of approximately zero eigenvalues must be discarded.

The subroutine calls on an eigenvalue subroutine "Poles" to print the eigenvalues of $W\phi SP$.

Listing follows:

05/06/66

H266 ZEROS - EFN SOURCE STATEMENT - IFN(S) -

```

SUBROUTINE ZEROS(A,B,C,NS,NAR)
DIMENSION A(NAR,NAR),B( 1),C( 1),SP1(30,30),SP2(30,30),SP3(42)
1,WOSP(30,30)
DOUBLE PRECISION SUM,QPR
FNS=FLOAT(INS)
ALF=1.0
DO 51 I=1,NS
DO 52 J=1,NS
5 SP1(I,J)=0.0
DO10K=1,NS
10 SP1(K,K)=1.0
15 DO20I=1,NS
DO20J=1,NS
SUM=0.000
DO 18 K=1,NS
18 SUM=SUM+A(I,K)*SP1(K,J)
20 SP2(I,J)=SUM
DO25I=1,NS
SUM = 0.000
DO 23 K=1,NS
23 SUM=SUM+SP1(I,K)*B(K)
25 SP3(I)=SUM
QPR=0.000
DO30K=1,NS
30 QPR=QPR+C(K)*SP3(K)
IF(ABS(QPR)-0.00001)33,33,40
33 DO35I=1,NS
DO35J=1,NS
35 SP1(I,J)=SP2(I,J)
ALF=ALF+1.0
IF(ALF-FNS)36,36,37
36 GO TO 15
37 WRITE (6,498)
GO TO 501
40 Q=1.0/QPR
WRITE(6,500) QPR
WRITE(6,500) ALF
DO55 I=1,NS
DO55 J=1,NS
55 SP1(I,J)=Q*B(I)*C(J)
DO60I=1,NS
DO60J=1,NS
SUM=A(I,J)
DO 58 K=1,NS
58 SUM=SUM-SP1(I,K)*SP2(K,J)
60 WOSP(I,J)=SUM
CALL POLES (WOSP,NS,30)
498 FORMAT (10X4HLOOP)
499 FORMAT (3110)
500 FORMAT (1H0,E12.5,6(4X,E12.5))
501 RETURN
END

```

1005H266
1010H266
1015H266

73

76
77

107

Appendix B
21-DIMENSION SYSTEM MATRIXES

PRECEDING PAGE BLANK NOT FILMED.

A MATRIX= F INVERSE X A PRIME

7/1/68 1-7

-0.47344E-22	0.14406E-02	0.00000E-38	0.17495E-00	0.75536E-03	0.28401E-00	0.12129E-02
0.00000E-38	0.00000E-38	0.10000E-01	0.00000E-38	0.00000E-38	0.00000E-38	0.00000E-38
-0.11128E-03	0.15800E-02	0.00000E-38	0.49792E-04	0.21607E-10	0.24656E-10	0.16880E-12
0.00000E-38	0.00000E-38	0.00000E-38	0.00000E-38	0.10000E-01	0.00000E-38	0.00000E-38
0.40745E-02	-0.40873E-00	0.00000E-38	-0.56632E-01	-0.24615E-01	-0.36380E-01	-0.22070E-03
0.00000E-38	0.00000E-38	0.00000E-38	0.00000E-38	0.00000E-38	0.00000E-38	0.10000E-01
0.82384E-03	-0.63516E-01	-0.00000E-38	-0.94293E-01	-0.14201E-03	-0.59295E-01	-0.25574E-01
0.00000E-38	0.00000E-38	0.00000E-38	0.00000E-38	0.00000E-38	0.00000E-38	0.00000E-38
0.88285E-02	-0.68058E-00	-0.00000E-38	-0.63635E-01	-0.52475E-03	-0.28701E-00	-0.76767E-03
0.00000E-38	0.00000E-38	0.00000E-38	0.00000E-38	0.00000E-38	0.00000E-38	0.00000E-38
-0.38793E-02	0.29910E-00	-0.00000E-38	0.13750E-00	0.72415E-03	-0.20004E-00	-0.68446E-03
0.00000E-38	0.00000E-38	0.00000E-38	0.00000E-38	0.00000E-38	0.00000E-38	0.00000E-38
-0.23322E-22	0.17481E-00	-0.00000E-38	0.99340E-01	0.67302E-03	-0.32858E-00	-0.13467E-02
0.00000E-38	0.00000E-38	0.00000E-38	0.00000E-38	0.00000E-38	0.00000E-38	0.00000E-38
-0.60485E-02	0.46637E-00	0.00000E-38	0.41151E-02	0.30844E-03	-0.17293E-00	-0.78176E-03
0.00000E-38	0.00000E-38	0.00000E-38	0.00000E-38	0.00000E-38	0.00000E-38	0.00000E-38
0.14340E-02	-0.11056E-00	0.00000E-38	-0.21591E-01	0.93300E-03	0.14991E-01	-0.83197E-04
0.00000E-38	0.00000E-38	0.00000E-38	0.00000E-38	0.00000E-38	0.00000E-38	0.00000E-38
0.00000E-38	0.00000E-38	0.00000E-38	0.00000E-38	0.00000E-38	0.00000E-38	0.00000E-38
0.00000E-38	0.00000E-38	0.00000E-38	0.00000E-38	0.00000E-38	0.00000E-38	0.00000E-38
0.00000E-38	0.00000E-38	0.00000E-38	0.00000E-38	0.00000E-38	0.00000E-38	0.00000E-38

PRECEDING PAGE BLANK NOT FILMED.

[illegible]

[illegible]

0.00000E-14	0.00000E-34	0.11550E 00	0.00000E-34	-0.14200E 00	0.00000E-34	0.10700E 00
0.00000E-14	0.00000E-34	0.00000E-34	0.16500E-01	0.00000E-34	0.66000E-01	0.00000E-34
-0.79151E 00	-0.00000E-02	-0.10000E 02	0.70244E-01	-0.13563E 02	-0.10015E 00	0.14036E 03

0.00000E-38	-0.83000E-02	0.00000E-38	0.00000E-38	0.00000E-38	0.00000E-38	-0.00000E-38
-0.56500E-01	0.00000E-38	-0.21700E 00	0.00000E-38	0.00000E-38	0.00000E-38	-0.00000E-38
0.26820E 00	-0.62473E 03	-0.50834E 00	0.28808E 02	0.00000E-38	0.13111E-01	-0.79306E-02

H MATKIX=(C + DA)

0.00000E-38	0.10000E 01	0.00000E-38	0.00000E-38	0.00000E-38	0.00000E-38	0.00000E-38
0.00000E-38	0.00000E-38	0.10000E 01	0.00000E-38	0.00000E-38	0.00000E-38	0.00000E-38
0.79306E-C2	-0.14637E C2	0.00000E-38	0.21251E 00	0.11927E-C2	-0.16695E 00	-0.54388E-03

A MATRIX=F INVERSE X A PRIME

-0.73822E-02	0.24413E 02	-0.00000E-38	0.37728E 00	0.13523E-02	0.63246E 00	0.22757E-02
0.00000E-38	0.00000E-38	0.10000E 01	0.00000E-38	0.00000E-38	0.00000E-38	0.00000E-38
-0.25822E-03	0.13089E 00	0.00000E-38	0.12147E-08	0.64336E-11	-0.21476E-08	-0.48252E-11
0.00000E-38	0.00000E-38	0.00000E-38	0.00000E-38	0.10000E 01	0.00000E-38	0.00000E-38
0.39192E-01	-0.19867E 02	0.00000E-38	-0.82635E 01	-0.30383E-01	0.10513E-01	-0.18506E-03
0.00000E-38	0.00000E-38	0.00000E-38	0.00000E-38	0.00000E-38	0.00000E-38	0.10000E 01
-0.60290E-02	0.30561E 01	0.00000E-38	-0.21732E 00	-0.11650E-03	-0.91253E 01	-0.32978E-01
0.00000E-38	0.00000E-38	0.00000E-38	0.00000E-38	0.00000E-38	0.00000E-38	0.00000E-38
-0.45133E-01	0.22878E 02	-0.00000E-38	-0.17073E 00	-0.90823E-03	-0.26713E 00	-0.49101E-03
0.00000E-38	0.00000E-38	0.00000E-38	0.00000E-38	0.00000E-38	0.00000E-38	0.00000E-38
-0.61139E-01	0.30991E 02	-0.00000E-38	0.25391E 00	0.11150E-02	-0.20665E 00	-0.46030E-03
0.00000E-38	0.00000E-38	0.00000E-38	0.00000E-38	0.00000E-38	0.00000E-38	0.00000E-38
-0.12045E-01	0.61056E 01	-0.00000E-38	0.21216E 00	0.12136E-02	-0.68230E 00	-0.21796E-02
0.00000E-38	0.00000E-38	0.00000E-38	0.00000E-38	0.00000E-38	0.00000E-38	0.00000E-38
-0.54979E-02	0.27869E 01	0.00000E-38	0.81296E-01	0.97091E-03	-0.87359E 00	-0.32711E-02
0.00000E-38	0.00000E-38	0.00000E-38	0.00000E-38	0.00000E-38	0.00000E-38	0.00000E-38
0.90893E-02	-0.46073E 01	0.00000E-38	-0.10394E-01	0.94348E-04	-0.11645E 00	-0.53900E-03
0.00000E-38	0.00000E-38	0.00000E-38	0.00000E-38	0.00000E-38	0.00000E-38	0.00000E-38
0.00000E-38	0.00000E-38	0.00000E-38	0.00000E-38	0.00000E-38	0.00000E-38	0.00000E-38
0.00000E-38	0.00000E-38	0.00000E-38	0.00000E-38	0.00000E-38	0.00000E-38	0.00000E-38
0.00000E-38	0.00000E-38	0.00000E-38	0.00000E-38	0.00000E-38	0.00000E-38	0.00000E-38
0.00000E-38	0.00000E-38	0.00000E-38	0.00000E-38	0.00000E-38	0.00000E-38	0.00000E-38

8

[illegible]

0.36958E+04	-0.24158E 01	-0.78769E-03	0.12467E 02	-0.00000E-38	-0.39336E-03	0.73822E-02
0.00000E-38	0.00000E-38	0.00000E-38	0.00000E-38	0.00000E-38	0.00000E-38	-0.00000E-38
0.10650E+10	0.62835E-07	0.58183E-10	-0.47250E 00	0.00000E-38	0.75274E-10	0.25822E-03
0.00000E-38	0.00000E-38	0.00000E-38	0.00000E-38	0.00000E-38	0.00000E-38	-0.00000E-38
0.27966E-01	0.29073E 02	0.22112E-01	-0.56016E 02	0.00000E-38	-0.12372E-01	-0.39192E-01
0.00000E-38	0.00000E-38	0.00000E-38	0.00000E-38	0.00000E-38	0.00000E-38	-0.00000E-38
-0.55488E-01	-0.93991E 02	-0.79805E-01	0.14323E 02	0.00000E-38	0.14941E-01	0.60290E-02
0.09090E-38	0.00000E-38	0.00000E-38	0.00000E-38	0.00000E-38	0.00000E-38	-0.00000E-38
0.69020E-01	0.15808E 03	0.12750E 00	-0.61911E 01	-0.00000E-38	-0.22401E-02	0.45133E-01
0.00000E-38	0.00000E-38	0.00000E-38	0.00000E-38	0.00000E-38	0.00000E-38	-0.00000E-38
0.18749E-02	0.52448E 01	0.50885E-02	0.17721E 02	-0.00000E-38	0.72723E-02	0.61139E-01
0.09090E-38	0.00000E-38	0.00000E-38	0.00000E-38	0.00000E-38	0.00000E-38	-0.00000E-38
-0.38974E-02	-0.64615E 01	-0.39978E-02	0.25700E 02	-0.00000E-38	0.11488E-01	0.12045E-01
0.10090E 01	0.09090E-38	0.00000E-38	0.00000E-38	0.00000E-38	0.00000E-38	-0.00000E-38
-0.10301E 00	-0.23389E 02	-0.17515E-01	0.29030E 02	0.00000E-38	0.13723E-01	0.54979E-02
0.09090E-38	0.00000E-38	0.10000E 01	0.00000E-38	0.00000E-38	0.00000E-38	-0.00000E-38
-0.21523E-02	-0.16064E 03	-0.12838E 00	0.46873E 01	0.00000E-38	0.22857E-02	-0.50893E-02
0.00000E-38	0.00000E-38	0.00000E-38	0.00000E-38	0.10000E 01	0.00000E-38	-0.00000E-38
0.00000E-38	0.00000E-38	0.00000E-38	0.00000E-38	0.00000E-38	0.10000E 01	-0.00000E-38
0.09090E-38	0.09090E-38	0.00000E-38	-0.31100E 05	-0.30590E 04	-0.23720E 02	-0.00000E-38
0.00000E-38	0.09090E-38	0.00000E-38	0.00000E-38	0.00000E-38	0.00000E-38	-0.11940E 00

H MATRIX=(C + DA)

0.00000E-38	0.10000E 01	0.00000E-38	0.00000E-38	0.00000E-38	0.00000E-38	0.00000E-38
0.00000E-38	0.00000E-38	0.10000E 01	0.00000E-38	0.00000E-38	0.00000E-38	0.00000E-38
-0.68461E-01	0.14032E 02	0.00000E-38	0.42600E 00	0.18553E-02	-0.15179E C0	-0.23738E-03

0.00000E-38	0.00000E-38	0.11818E 00	0.00000E-38	-0.12927E 00	0.00000E-38	0.70150E-01
0.00000E-38	0.00000E-38	0.00000E-38	0.13190E-01	0.00000E-38	0.69060E-01	0.00000E-38
-0.13376E 01	-0.40588E-02	-0.11749E 02	0.73551E-01	-0.21923E 02	-0.16040E 00	0.11334E 03

0.00000E-39	-0.52000E-02	0.00000E-38	0.00000E-38	0.00000E-38	0.00000E-38	-0.00000E-38
-0.31040E-01	0.00000E-38	-0.23626E 00	0.00000E-38	0.00000E-38	0.00000E-38	-0.00000E-38
0.14554E 07	-0.66647E 03	-0.53704E 00	0.29631E 02	0.00000E-38	0.11460E-01	0.68461E-01

-0.0000E-38	C.0000E-38	0.0000E-38	0.0000E-38	0.0000E-38	0.0000E-38
C.0000E-38	-0.0000E-38	0.0000E-38	-0.0000E-38	0.0000E-38	-C.0000E-38
C.0000E-38	C.0000E-38	C.0000E-38	C.0000E-38	C.0000E-38	C.0000E-38
0.0000E-38	C.0000E-38	0.0000E-38	0.0000E-38	0.0000E-38	0.0000E-38

[illegible]

A MATRIK X=F INVERSE X A PRIME

[illegible]

[illegible]

0.54969E-03	-0.28561E 02	-C.98148E-02	0.17363E 02	0.0000CE-38	-0.11093E-02	0.68446E-04
0.00000E-38	C.00000E-38	0.0000CE-38	0.0000CE-38	0.0000CE-38	0.0000CE-38	-0.00000E-38
-0.13627E-10	-C.15392E-C8	C.90401E-17	-0.21608E 01	-0.0000CE-38	C.17406E-10	-0.22440E-06
0.0000CE-38	C.0000CE-38	0.00000E-38	0.00000E-38	0.00000E-38	0.00000E-38	-0.00000E-38
0.76036E-01	0.16885E 02	-0.31292E-02	-0.38548E 03	-0.0000CE-38	-C.91797E-01	-C.10855E-03
0.0000CE-38	C.00000E-38	0.00000E-38	C.00000E-38	0.0000CE-38	0.00000E-38	-0.00000E-38
-0.37032E-01	-0.96742E 03	-0.39320E 00	-0.17833E 03	-C.0000CE-38	-0.23517E-01	0.44388E-03
0.0000CE-38	0.00000E-38	0.00000E-38	0.00000E-38	0.0000CE-38	C.00000E-38	-C.00000E-38
-0.82412E-02	0.45680E 03	C.18228E 00	0.25061E 02	-0.0000CE-38	C.21923E-C1	-0.26248E-03
C.00000E-38	C.00000E-38	0.00000E-38	0.00000E-38	0.0000CE-38	0.00000E-38	-C.00000E-38
-0.10357E-02	0.57932E 02	0.30657E-C1	0.17661E 03	0.00000E-38	C.67894E-01	-0.24468E-04
0.00000E-38	C.00000E-38	0.00000E-38	0.00000E-38	0.0000CE-38	C.00000E-38	-0.00000E-38
-0.10208E-02	0.39822E 02	0.20358E-01	0.10534E 03	0.0000CE-38	C.42448E-01	-0.25299E-04
0.1000CE 01	0.0000CE-38	0.00000E-38	0.00000E-38	0.0000CE-38	0.00000E-38	-C.00000E-38
-0.11718E 00	-C.89931E C0	0.35659E-03	0.16512E 02	-0.0000CE-38	0.70534E-02	C.51863E-04
0.0000CE-38	C.00000E-38	0.10000E 01	0.00000E-38	0.00000E-38	0.00000E-38	-C.00000E-38
0.96995E-04	-C.63969E 03	-0.25687E 00	C.10026E 02	-0.0000CE-38	0.47729E-C2	0.32579E-03
0.0000CE-38	C.00000E-38	0.00000E-38	0.00000E-38	0.1000CE 01	0.00000E-38	-0.00000E-38
0.0000CE-38	C.0000CE-38	0.00000E-38	0.00000E-38	0.00000E-38	C.10000E 01	-C.00000E-38
0.0000CE-38	C.00000E-38	C.00000E-38	-0.31100E 05	-0.3059CE 04	-C.23720E C2	-0.00000E-38
0.0000CE-38	0.00000E-38	0.00000E-38	0.0000CE-38	0.0000CE-38	0.00000E-38	-0.1194CE 00

H MATRIX=(C + DA)

0.00000E-38	0.10000E 01	0.00000E-38	0.00000E-38	0.00000E-38	0.00000E-38	0.00000E-38
0.00000E-38	0.00000E-38	0.10000E 01	0.00000E-38	0.00000E-38	0.00000E-38	0.00000E-38
-0.45222E-04	-0.34738E 02	0.00000E-38	0.99579E-01	0.29727E-03	0.13441E 00	0.39403E-03

0.00000E-38	0.00000E-38	0.43800E-01	0.00000E-38	-0.66000E-01	0.00000E-38	0.35500E-01
0.00000E-38	0.00000E-38	0.00000E-38	-0.44000E-02	0.00000E-38	0.39600E-01	0.00000E-38
-0.20487E 01	-0.36116E-02	-0.55270E 01	0.31056E-01	-0.25839E 02	-0.10124E 00	0.37404E 03

8 MATRIX

0.00000E-38	0.00000E-38	-0.00000E-38	0.00000E-38	-0.00000E-38	0.00000E-38	-0.00000E-38
0.00000E-38	-0.00000E-38	0.00000E-38	0.00000E-38	0.00000E-38	0.00000E-38	0.00000E-38
0.00000E-38	-0.00000E-38	0.00000E-38	0.00000E-38	0.00000E-38	0.00000E-38	0.00000E-38
0.31100E 05	0.00000E-38	0.00000E-38	-0.00000E-38	0.00000E-38	0.00000E-38	0.00000E-38

0.00000E-38	0.62230E 00	0.00000E-38	0.00000E-38	0.00000E-38	0.00000E-38	-0.00000E-38
0.96900E-01	0.00000E-38	-0.72900E-01	0.00000E-38	0.00000E-38	0.00000E-38	-0.00000E-38
0.35854E 00	-0.36905E 03	0.47739E 00	0.87389E 02	0.00000E-38	0.33560E-01	0.45222E-04